Contents

Preface **iii**

1 Introduction **1**
1.1 Issues in Control System Design 1
1.2 What Is in This Book 7

2 Norms for Signals and Systems **11**
2.1 Norms for Signals 11
2.2 Norms for Systems 13
2.3 Input-Output Relationships 15
2.4 Power Analysis (Optional) 16
2.5 Proofs for Tables 2.1 and 2.2 (Optional) 18
2.6 Computing by State-Space Methods (Optional) 21

3 Basic Concepts **27**
3.1 Basic Feedback Loop 27
3.2 Internal Stability 30
3.3 Asymptotic Tracking 33
3.4 Performance 35

4 Uncertainty and Robustness **39**
4.1 Plant Uncertainty 39
4.2 Robust Stability 43
4.3 Robust Performance 47
4.4 Robust Performance More Generally 51
4.5 Conclusion 52

5 Stabilization **57**
5.1 Controller Parametrization: Stable Plant 57
5.2 Coprime Factorization 59
5.3 Coprime Factorization by State-Space Methods (Optional) 63
5.4 Controller Parametrization: General Plant 64
5.5 Asymptotic Properties 66
5.6 Strong and Simultaneous Stabilization 68
5.7 Cart-Pendulum Example 73

6 Design Constraints **79**
6.1 Algebraic Constraints . . . 79
6.2 Analytic Constraints . . . 80

7 Loopshaping **93**
7.1 The Basic Technique of Loopshaping . . . 93
7.2 The Phase Formula (Optional) . . . 96
7.3 Examples . . . 100

8 Advanced Loopshaping **107**
8.1 Optimal Controllers . . . 107
8.2 Loopshaping with C . . . 108
8.3 Plants with RHP Poles and Zeros . . . 113
8.4 Shaping S, T, or Q . . . 125
8.5 Further Notions of Optimality . . . 128

9 Model Matching **139**
9.1 The Model-Matching Problem . . . 139
9.2 The Nevanlinna-Pick Problem . . . 140
9.3 Nevanlinna's Algorithm . . . 143
9.4 Solution of the Model-Matching Problem . . . 147
9.5 State-Space Solution (Optional) . . . 149

10 Design for Performance **153**
10.1 P^{-1} Stable . . . 153
10.2 P^{-1} Unstable . . . 158
10.3 Design Example: Flexible Beam . . . 159
10.4 2-Norm Minimization . . . 164

11 Stability Margin Optimization **169**
11.1 Optimal Robust Stability . . . 169
11.2 Conformal Mapping . . . 173
11.3 Gain Margin Optimization . . . 174
11.4 Phase Margin Optimization . . . 179

12 Design for Robust Performance **183**
12.1 The Modified Problem . . . 183
12.2 Spectral Factorization . . . 184
12.3 Solution of the Modified Problem . . . 185
12.4 Design Example: Flexible Beam Continued . . . 191

References **197**

Preface

Striking developments have taken place since 1980 in feedback control theory. The subject has become both more rigorous and more applicable. The rigor is not for its own sake, but rather that even in an engineering discipline rigor can lead to clarity and to methodical solutions to problems. The applicability is a consequence both of new problem formulations and new mathematical solutions to these problems. Moreover, computers and software have changed the way engineering design is done. These developments suggest a fresh presentation of the subject, one that exploits these new developments while emphasizing their connection with classical control.

Control systems are designed so that certain designated signals, such as tracking errors and actuator inputs, do not exceed pre-specified levels. Hindering the achievement of this goal are uncertainty about the plant to be controlled (the mathematical models that we use in representing real physical systems are idealizations) and errors in measuring signals (sensors can measure signals only to a certain accuracy). Despite the seemingly obvious requirement of bringing plant uncertainty explicitly into control problems, it was only in the early 1980s that control researchers re-established the link to the classical work of Bode and others by formulating a tractable mathematical notion of uncertainty in an input-output framework and developing rigorous mathematical techniques to cope with it. This book formulates a precise problem, called the *robust performance problem*, with the goal of achieving specified signal levels in the face of plant uncertainty.

The book is addressed to students in engineering who have had an undergraduate course in signals and systems, including an introduction to frequency-domain methods of analyzing feedback control systems, namely, Bode plots and the Nyquist criterion. A prior course on state-space theory would be advantageous for some optional sections, but is not necessary. To keep the development elementary, the systems are single-input/single-output and linear, operating in continuous time.

Chapters 1 to 7 are intended as the core for a one-semester senior course; they would need supplementing with additional examples. These chapters constitute a basic treatment of feedback design, containing a detailed formulation of the control design problem, the fundamental issue of performance/stability robustness tradeoff, and the graphical design technique of loopshaping, suitable for benign plants (stable, minimum phase). Chapters 8 to 12 are more advanced and are intended for a first graduate course. Chapter 8 is a bridge to the latter half of the book, extending the loopshaping technique and connecting it with notions of optimality. Chapters 9 to 12 treat controller design via optimization. The approach in these latter chapters is mathematical rather than graphical, using elementary tools involving interpolation by analytic functions. This mathematical approach is most useful for multivariable systems, where graphical techniques usually break down. Nevertheless, we believe the setting of single-input/single-output systems is where this new approach should be learned.

There are many people to whom we are grateful for their help in this book: Dale Enns for sharing his expertise in loopshaping; Raymond Kwong and Boyd Pearson for class testing the book; and Munther Dahleh, Ciprian Foias, and Karen Rudie for reading earlier drafts. Numerous

Caltech students also struggled with various versions of this material: Gary Balas, Carolyn Beck, Bobby Bodenheimer, and Roy Smith had particularly helpful suggestions. Finally, we would like to thank the AFOSR, ARO, NSERC, NSF, and ONR for partial financial support during the writing of this book.

Introduction

Without control systems there could be no manufacturing, no vehicles, no computers, no regulated environment—in short, no technology. Control systems are what make machines, in the broadest sense of the term, function as intended. Control systems are most often based on the principle of feedback, whereby the signal to be controlled is compared to a desired reference signal and the discrepancy used to compute corrective control action. The goal of this book is to present a theory of feedback control system design that captures the essential issues, can be applied to a wide range of practical problems, and is as simple as possible.

1.1 Issues in Control System Design

The process of designing a control system generally involves many steps. A typical scenario is as follows:

1. Study the system to be controlled and decide what types of sensors and actuators will be used and where they will be placed.
2. Model the resulting system to be controlled.
3. Simplify the model if necessary so that it is tractable.
4. Analyze the resulting model; determine its properties.
5. Decide on performance specifications.
6. Decide on the type of controller to be used.
7. Design a controller to meet the specs, if possible; if not, modify the specs or generalize the type of controller sought.
8. Simulate the resulting controlled system, either on a computer or in a pilot plant.
9. Repeat from step 1 if necessary.
10. Choose hardware and software and implement the controller.
11. Tune the controller on-line if necessary.

It must be kept in mind that a control engineer's role is not merely one of designing control systems for fixed plants, of simply "wrapping a little feedback" around an already fixed physical system. It also involves assisting in the choice and configuration of hardware by taking a system-wide view of performance. For this reason it is important that a theory of feedback not only lead to good designs when these are possible, but also indicate directly and unambiguously when the performance objectives cannot be met.

It is also important to realize at the outset that practical problems have uncertain, non-minimum-phase plants (*non-minimum-phase* means the existence of right half-plane zeros, so the inverse is unstable); that there are inevitably unmodeled dynamics that produce substantial uncertainty, usually at high frequency; and that sensor noise and input signal level constraints limit the achievable benefits of feedback. A theory that excludes some of these practical issues can still be useful in limited application domains. For example, many process control problems are so dominated by plant uncertainty and right half-plane zeros that sensor noise and input signal level constraints can be neglected. Some spacecraft problems, on the other hand, are so dominated by tradeoffs between sensor noise, disturbance rejection, and input signal level (e.g., fuel consumption) that plant uncertainty and non-minimum-phase effects are negligible. Nevertheless, any general theory should be able to treat all these issues explicitly and give quantitative and qualitative results about their impact on system performance.

In the present section we look at two issues involved in the design process: deciding on performance specifications and modeling. We begin with an example to illustrate these two issues.

Example A very interesting engineering system is the Keck astronomical telescope, currently under construction on Mauna Kea in Hawaii. When completed it will be the world's largest. The basic objective of the telescope is to collect and focus starlight using a large concave mirror. The shape of the mirror determines the quality of the observed image. The larger the mirror, the more light that can be collected, and hence the dimmer the star that can be observed. The diameter of the mirror on the Keck telescope will be 10 m. To make such a large, high-precision mirror out of a single piece of glass would be very difficult and costly. Instead, the mirror on the Keck telescope will be a mosaic of 36 hexagonal small mirrors. These 36 segments must then be aligned so that the composite mirror has the desired shape.

The control system to do this is illustrated in Figure 1.1. As shown, the mirror segments are subject to two types of forces: disturbance forces (described below) and forces from actuators. Behind each segment are three piston-type actuators, applying forces at three points on the segment to effect its orientation. In controlling the mirror's shape, it suffices to control the misalignment between adjacent mirror segments. In the gap between every two adjacent segments are (capacitor-type) sensors measuring local displacements between the two segments. These local displacements are stacked into the vector labeled y; this is what is to be controlled. For the mirror to have the ideal shape, these displacements should have certain ideal values that can be pre-computed; these are the components of the vector r. The controller must be designed so that in the closed-loop system y is held close to r despite the disturbance forces. Notice that the signals are vector valued. Such a system is *multivariable*.

Our uncertainty about the plant arises from disturbance sources:

- As the telescope turns to track a star, the direction of the force of gravity on the mirror changes.
- During the night, when astronomical observations are made, the ambient temperature changes.
- The telescope is susceptible to wind gusts.

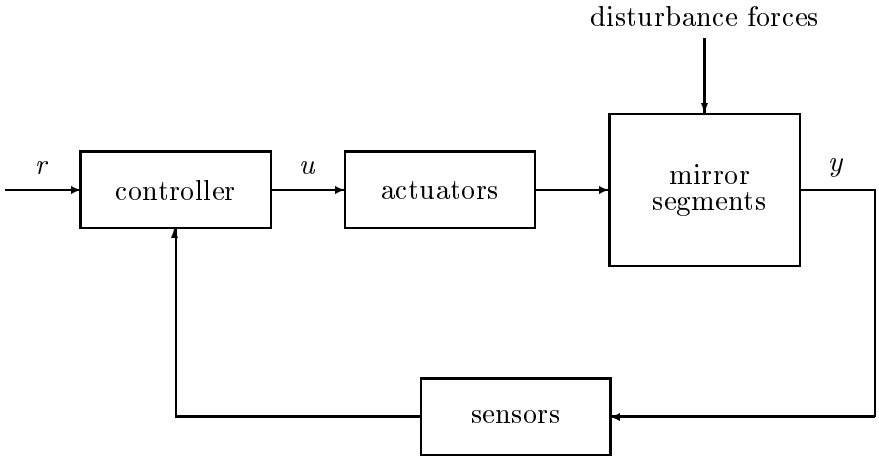

Figure 1.1: Block diagram of Keck telescope control system.

and from uncertain plant dynamics:

- The dynamic behavior of the components—mirror segments, actuators, sensors—cannot be modeled with infinite precision.

Now we continue with a discussion of the issues in general.

Control Objectives

Generally speaking, the objective in a control system is to make some output, say y, behave in a desired way by manipulating some input, say u. The simplest objective might be to keep y small (or close to some equilibrium point)—a *regulator problem*—or to keep $y - r$ small for r, a reference or command signal, in some set—a *servomechanism* or *servo problem*. Examples:

- On a commercial airplane the vertical acceleration should be less than a certain value for passenger comfort.
- In an audio amplifier the power of noise signals at the output must be sufficiently small for high fidelity.
- In papermaking the moisture content must be kept between prescribed values.

There might be the side constraint of keeping u itself small as well, because it might be constrained (e.g., the flow rate from a valve has a maximum value, determined when the valve is fully open) or it might be too expensive to use a large input. But what is small for a signal? It is natural to introduce norms for signals; then "y small" means "$\|y\|$ small." Which norm is appropriate depends on the particular application.

In summary, performance objectives of a control system naturally lead to the introduction of norms; then the specs are given as norm bounds on certain key signals of interest.

Models

Before discussing the issue of modeling a physical system it is important to distinguish among four different objects:

1. *Real physical system*: the one "out there."
2. *Ideal physical model*: obtained by schematically decomposing the real physical system into ideal building blocks; composed of resistors, masses, beams, kilns, isotropic media, Newtonian fluids, electrons, and so on.
3. *Ideal mathematical model*: obtained by applying natural laws to the ideal physical model; composed of nonlinear partial differential equations, and so on.
4. *Reduced mathematical model*: obtained from the ideal mathematical model by linearization, lumping, and so on; usually a rational transfer function.

Sometimes language makes a fuzzy distinction between the real physical system and the ideal physical model. For example, the word *resistor* applies to both the actual piece of ceramic and metal and the ideal object satisfying Ohm's law. Of course, the adjectives *real* and *ideal* could be used to disambiguate.

No mathematical system can precisely model a real physical system; there is always uncertainty. Uncertainty means that we cannot predict exactly what the output of a real physical system will be even if we know the input, so *we* are uncertain about the system. Uncertainty arises from two sources: unknown or unpredictable inputs (disturbance, noise, etc.) and unpredictable dynamics.

What should a model provide? It should predict the input-output response in such a way that we can use it to design a control system, and then be confident that the resulting design will work on the real physical system. Of course, this is not possible. A "leap of faith" will always be required on the part of the engineer. This cannot be eliminated, but it can be made more manageable with the use of effective modeling, analysis, and design techniques.

Mathematical Models in This Book

The models in this book are finite-dimensional, linear, and time-invariant. The main reason for this is that they are the simplest models for treating the fundamental issues in control system design. The resulting design techniques work remarkably well for a large class of engineering problems, partly because most systems are built to be as close to linear time-invariant as possible so that they are more easily controlled. Also, a good controller will keep the system in its linear regime. The uncertainty description is as simple as possible as well.

The basic form of the plant model in this book is

$$y = (P + \Delta)u + n.$$

Here y is the output, u the input, and P the nominal plant transfer function. The model uncertainty comes in two forms:

n: unknown noise or disturbance
Δ: unknown plant perturbation

Both n and Δ will be assumed to belong to sets, that is, some *a priori* information is assumed about n and Δ. Then every input u is capable of producing a *set* of outputs, namely, the set of all outputs $(P + \Delta)u + n$ as n and Δ range over their sets. Models capable of producing sets of outputs for a single input are said to be *nondeterministic*. There are two main ways of obtaining models, as described next.

Models from Science

The usual way of getting a model is by applying the laws of physics, chemistry, and so on. Consider the Keck telescope example. One can write down differential equations based on physical principles (e.g., Newton's laws) and making idealizing assumptions (e.g., the mirror segments are rigid). The coefficients in the differential equations will depend on physical constants, such as masses and physical dimensions. These can be measured. This method of applying physical laws and taking measurements is most successful in electromechanical systems, such as aerospace vehicles and robots. Some systems are difficult to model in this way, either because they are too complex or because their governing laws are unknown.

Models from Experimental Data

The second way of getting a model is by doing experiments on the physical system. Let's start with a simple thought experiment, one that captures many essential aspects of the relationships between physical systems and their models and the issues in obtaining models from experimental data. Consider a real physical system—the plant to be controlled—with one input, u, and one output, y. To design a control system for this plant, we must understand how u affects y.

The experiment runs like this. Suppose that the real physical system is in a rest state before an input u is applied (i.e., $u = y = 0$). Now apply some input signal u, resulting in some output signal y. Observe the pair (u, y). Repeat this experiment several times. Pretend that these data pairs are all we know about the real physical system. (This is the *black box* scenario. Usually, we know something about the internal workings of the system.)

After doing this experiment we will notice several things. First, the same input signal at different times produces different output signals. Second, if we hold $u = 0$, y will fluctuate in an unpredictable manner. Thus the real physical system produces just one output for any given input, so it itself is deterministic. However, we observers are uncertain because we cannot predict what that output will be.

Ideally, the model should *cover* the data in the sense that it should be capable of producing every experimentally observed input-output pair. (Of course, it would be better to cover not just the data observed in a finite number of experiments, but anything that can be produced by the real physical system. Obviously, this is impossible.) If nondeterminism that reasonably covers the range of expected data is not built into the model, we will not trust that designs based on such models will work on the real system.

In summary, for a useful theory of control design, plant models must be nondeterministic, having uncertainty built in explicitly.

Synthesis Problem

A synthesis problem is a theoretical problem, precise and unambiguous. Its purpose is primarily pedagogical: It gives us something clear to focus on for the purpose of study. The hope is that the principles learned from studying a formal synthesis problem will be useful when it comes to designing a real control system.

The most general block diagram of a control system is shown in Figure 1.2. The generalized plant consists of everything that is fixed at the start of the control design exercise: the plant, actuators that generate inputs to the plant, sensors measuring certain signals, analog-to-digital and digital-to-analog converters, and so on. The controller consists of the designable part: it may be an electric circuit, a programmable logic controller, a general-purpose computer, or some other

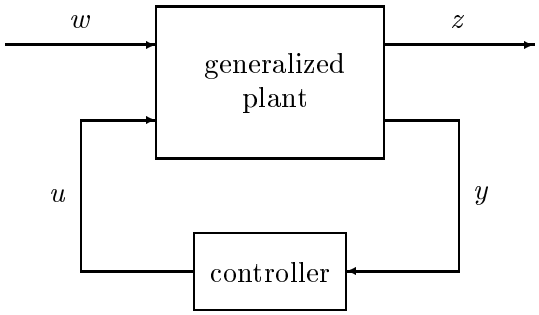

Figure 1.2: Most general control system.

such device. The signals w, z, y, and u are, in general, vector-valued functions of time. The components of w are all the exogenous inputs: references, disturbances, sensor noises, and so on. The components of z are all the signals we wish to control: tracking errors between reference signals and plant outputs, actuator signals whose values must be kept between certain limits, and so on. The vector y contains the outputs of all sensors. Finally, u contains all controlled inputs to the generalized plant. (Even open-loop control fits in; the generalized plant would be so defined that y is always constant.)

Very rarely is the exogenous input w a fixed, known signal. One of these rare instances is where a robot manipulator is required to trace out a definite path, as in welding. Usually, w is not fixed but belongs to a set that can be characterized to some degree. Some examples:

- In a thermostat-controlled temperature regulator for a house, the reference signal is always piecewise constant: at certain times during the day the thermostat is set to a new value. The temperature of the outside air is not piecewise constant but varies slowly within bounds.
- In a vehicle such as an airplane or ship the pilot's commands on the steering wheel, throttle, pedals, and so on come from a predictable set, and the gusts and wave motions have amplitudes and frequencies that can be bounded with some degree of confidence.
- The load power drawn on an electric power system has predictable characteristics.

Sometimes the designer does not attempt to model the exogenous inputs. Instead, she or he designs for a suitable response to a test input, such as a step, a sinusoid, or white noise. The designer may know from past experience how this correlates with actual performance in the field. Desired properties of z generally relate to how large it is according to various measures, as discussed above.

Finally, the output of the design exercise is a mathematical model of a controller. This must be implementable in hardware. If the controller you design is governed by a nonlinear partial differential equation, how are you going to implement it? A linear ordinary differential equation with constant coefficients, representing a finite-dimensional, time-invariant, linear system, can be simulated via an analog circuit or approximated by a digital computer, so this is the most common type of control law.

The synthesis problem can now be stated as follows: Given a set of generalized plants, a set of exogenous inputs, and an upper bound on the size of z, design an implementable controller to

achieve this bound. How the size of z is to be measured (e.g., power or maximum amplitude) depends on the context. This book focuses on an elementary version of this problem.

1.2 What Is in This Book

Since this book is for a first course on this subject, attention is restricted to systems whose models are single-input/single-output, finite-dimensional, linear, and time-invariant. Thus they have transfer functions that are rational in the Laplace variable s. The general layout of the book is that Chapters 2 to 4 and 6 are devoted to analysis of control systems, that is, the controller is already specified, and Chapters 5 and 7 to 12 to design.

Performance of a control system is specified in terms of the size of certain signals of interest. For example, the performance of a tracking system could be measured by the size of the error signal. Chapter 2, *Norms for Signals and Systems*, looks at several ways of defining norms for a signal $u(t)$; in particular, the 2-norm (associated with energy),

$$\left(\int_{-\infty}^{\infty} u(t)^2 dt \right)^{1/2},$$

the ∞-norm (maximum absolute value),

$$\max_t |u(t)|,$$

and the square root of the average power (actually, not quite a norm),

$$\left(\lim_{T \to \infty} \frac{1}{2T} \int_{-T}^{T} u(t)^2 dt \right)^{1/2}.$$

Also introduced are two norms for a system's transfer function $G(s)$: the 2-norm,

$$\|G\|_2 := \left(\frac{1}{2\pi} \int_{-\infty}^{\infty} |G(j\omega)|^2 d\omega \right)^{1/2},$$

and the ∞-norm,

$$\|G\|_\infty := \max_\omega |G(j\omega)|.$$

Notice that $\|G\|_\infty$ equals the peak amplitude on the Bode magnitude plot of G. Then two very useful tables are presented summarizing input-output norm relationships. For example, one table gives a bound on the 2-norm of the output knowing the 2-norm of the input and the ∞-norm of the transfer function. Such results are very useful in predicting, for example, the effect a disturbance will have on the output of a feedback system.

Chapters 3 and 4 are the most fundamental in the book. The system under consideration is shown in Figure 1.3, where P and C are the plant and controller transfer functions. The signals are as follows:

r	reference or command input
e	tracking error
u	control signal, controller output
d	plant disturbance
y	plant output
n	sensor noise

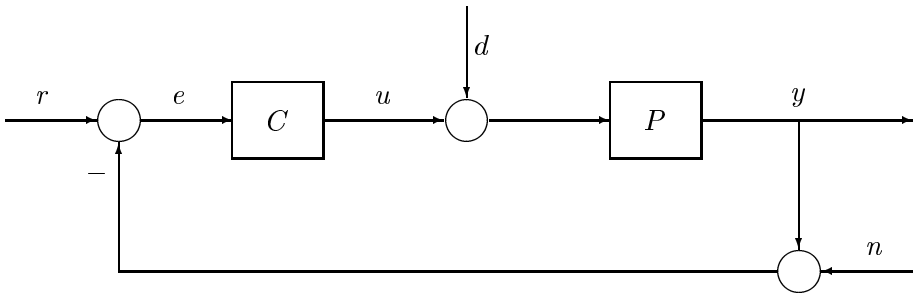

Figure 1.3: Single-loop feedback system.

In Chapter 3, *Basic Concepts*, internal stability is defined and characterized. Then the system is analyzed for its ability to track a *single* reference signal r—a step or a ramp—asymptotically as time increases. Finally, we look at tracking a *set* of reference signals. The transfer function from reference input r to tracking error e is denoted S, the *sensitivity function*. It is argued that a useful tracking performance criterion is $\|W_1 S\|_\infty < 1$, where W_1 is a transfer function which can be tuned by the control system designer.

Since no mathematical system can exactly model a physical system, we must be aware of how modeling errors might adversely affect the performance of a control system. Chapter 4, *Uncertainty and Robustness*, begins with a treatment of various models of plant uncertainty. The basic technique is to model the plant as belonging to a set $\mathcal{P}$. Such a set can be either *structured*—for example, there are a finite number of uncertain parameters—or *unstructured*—the frequency response lies in a set in the complex plane for every frequency. For us, unstructured is more important because it leads to a simple and useful design theory. In particular, multiplicative perturbation is chosen for detailed study, it being typical. In this uncertainty model there is a nominal plant P and the family $\mathcal{P}$ consists of all perturbed plants $\tilde{P}$ such that at each frequency ω the ratio $\tilde{P}(j\omega)/P(j\omega)$ lies in a disk in the complex plane with center 1. This notion of disk-like uncertainty is key; because of it the mathematical problems are tractable.

Generally speaking, the notion of robustness means that some characteristic of the feedback system holds for every plant in the set $\mathcal{P}$. A controller C provides *robust stability* if it provides internal stability for every plant in $\mathcal{P}$. Chapter 4 develops a test for robust stability for the multiplicative perturbation model, a test involving C and $\mathcal{P}$. The test is $\|W_2 T\|_\infty < 1$. Here T is the *complementary sensitivity function*, equal to $1 - S$ (or the transfer function from r to y), and W_2 is a transfer function whose magnitude at frequency ω equals the radius of the uncertainty disk at that frequency.

The final topic in Chapter 4 is robust performance, guaranteed tracking in the face of plant uncertainty. The main result is that the tracking performance spec $\|W_1 S\|_\infty < 1$ is satisfied for all plants in the multiplicative perturbation set if and only if the magnitude of $|W_1 S| + |W_2 T|$ is less than 1 for all frequencies, that is,

$$\| |W_1 S| + |W_2 T| \|_\infty < 1. \tag{1.1}$$

This is an analysis result: It tells exactly when some candidate controller provides robust performance.

Chapter 5, *Stabilization*, is the first on design. Most synthesis problems can be formulated like this: Given P, design C so that the feedback system (1) is internally stable, and (2) acquires some

additional desired property or properties, for example, the output y asymptotically tracks a step input r. The method of solution presented here is to parametrize all Cs for which (1) is true and then to find a parameter for which (2) holds. In this chapter such a parametrization is derived; it has the form

$$C = \frac{X + MQ}{Y - NQ},$$

where N, M, X, and Y are fixed stable proper transfer functions and Q is the parameter, an arbitrary stable proper transfer function. The usefulness of this parametrization derives from the fact that all closed-loop transfer functions are very simple functions of Q; for instance, the sensitivity function S, while a nonlinear function of C, equals simply $MY - MNQ$. This parametrization is then applied to three problems: achieving asymptotic performance specs, such as tracking a step; internal stabilization by a stable controller; and simultaneous stabilization of two plants by a common controller.

Before we see how to design control systems for the robust performance specification, it is important to understand the basic limitations on achievable performance: Why can't we achieve both arbitrarily good performance and stability robustness at the same time? In Chapter 6, *Design Constraints*, we study design constraints arising from two sources: from algebraic relationships that must hold among various transfer functions and from the fact that closed-loop transfer functions must be stable, that is, analytic in the right half-plane. The main conclusion is that feedback control design always involves a tradeoff between performance and stability robustness.

Chapter 7, *Loopshaping*, presents a graphical technique for designing a controller to achieve robust performance. This method is the most common in engineering practice. It is especially suitable for today's CAD packages in view of their graphics capabilities. The loop transfer function is $L := PC$. The idea is to shape the Bode magnitude plot of L so that (1.1) is achieved, at least approximately, and then to back-solve for C via $C = L/P$. When P or P^{-1} is not stable, L must contain Ps unstable poles and zeros (for internal stability of the feedback loop), an awkward constraint. For this reason, it is assumed in Chapter 7 that P and P^{-1} are both stable.

Thus Chapters 2 to 7 constitute a basic treatment of feedback design, containing a detailed formulation of the control design problem, the fundamental issue of performance/stability robustness tradeoff, and a graphical design technique suitable for benign plants (stable, minimum-phase). Chapters 8 to 12 are more advanced.

Chapter 8, *Advanced Loopshaping*, is a bridge between the two halves of the book; it extends the loopshaping technique and connects it with the notion of optimal designs. Loopshaping in Chapter 7 focuses on L, but other quantities, such as C, S, T, or the Q parameter in the stabilization results of Chapter 5, may also be "shaped" to achieve the same end. For many problems these alternatives are more convenient. Chapter 8 also offers some suggestions on how to extend loopshaping to handle right half-plane poles and zeros.

Optimal controllers are introduced in a formal way in Chapter 8. Several different notions of optimality are considered with an aim toward understanding in what way loopshaping controllers can be said to be optimal. It is shown that loopshaping controllers satisfy a very strong type of optimality, called *self-optimality*. The implication of this result is that when loopshaping is successful at finding an adequate controller, it cannot be improved upon uniformly.

Chapters 9 to 12 present a recently developed approach to the robust performance design problem. The approach is mathematical rather than graphical, using elementary tools involving interpolation by analytic functions. This mathematical approach is most useful for multivariable systems, where graphical techniques usually break down. Nevertheless, the setting of single-input/single-output systems is where this new approach should be learned. Besides, present-day software for

control design (e.g., MATLAB and Program CC) incorporate this approach.

Chapter 9, *Model Matching*, studies a hypothetical control problem called the model-matching problem: Given stable proper transfer functions T_1 and T_2, find a stable transfer function Q to minimize $\|T_1 - T_2Q\|_\infty$. The interpretation is this: T_1 is a model, T_2 is a plant, and Q is a cascade controller to be designed so that T_2Q approximates T_1. Thus $T_1 - T_2Q$ is the error transfer function. This problem is turned into a special interpolation problem: Given points $\{a_i\}$ in the right half-plane and values $\{b_i\}$, also complex numbers, find a stable transfer function G so that $\|G\|_\infty < 1$ and $G(a_i) = b_i$, that is, G interpolates the value b_i at the point a_i. When such a G exists and how to find one utilizes some beautiful mathematics due to Nevanlinna and Pick.

Chapter 10, *Design for Performance*, treats the problem of designing a controller to achieve the performance criterion $\|W_1S\|_\infty < 1$ alone, that is, with no plant uncertainty. When does such a controller exist, and how can it be computed? These questions are easy when the inverse of the plant transfer function is stable. When the inverse is unstable (i.e., P is non-minimum-phase), the questions are more interesting. The solutions presented in this chapter use model-matching theory. The procedure is applied to designing a controller for a flexible beam. The desired performance is given in terms of step response specs: overshoot and settling time. It is shown how to choose the weight W_1 to accommodate these time domain specs. Also treated in Chapter 10 is minimization of the 2-norm of some closed-loop transfer function, e.g., $\|W_1S\|_2$.

Next, in Chapter 11, *Stability Margin Optimization*, is considered the problem of designing a controller whose sole purpose is to maximize the stability margin, that is, performance is ignored. The maximum obtainable stability margin is a measure of how difficult the plant is to control. Three measures of stability margin are treated: the ∞-norm of a multiplicative perturbation, gain margin, and phase margin. It is shown that the problem of optimizing these stability margins can also be reduced to a model-matching problem.

Chapter 12, *Design for Robust Performance*, returns to the robust performance problem of designing a controller to achieve (1.1). Chapter 7 proposed loopshaping as a graphical method when P and P^{-1} are stable. Without these assumptions loopshaping can be awkward and the methodical procedure in this chapter can be used. Actually, (1.1) is too hard for mathematical analysis, so a compromise criterion is posed, namely,

$$\||W_1S|^2 + |W_2T|^2\|_\infty < 1/2. \tag{1.2}$$

Using a technique called spectral factorization, we can reduce this problem to a model-matching problem. As an illustration, the flexible beam example is reconsidered; besides step response specs on the tip deflection, a hard limit is placed on the plant input to prevent saturation of an amplifier.

Finally, some words about frequency-domain versus time-domain methods of design. Horowitz (1963) has long maintained that "frequency response methods have been found to be especially useful and transparent, enabling the designer to see the tradeoff between conflicting design factors." This point of view has gained much greater acceptance within the control community at large in recent years, although perhaps it would be better to stress the importance of input-output or operator-theoretic versus state-space methods, instead of frequency domain versus time domain. This book focuses almost exclusively on input-output methods, not because they are ultimately more fundamental than state-space methods, but simply for pedagogical reasons.

Notes and References

There are many books on feedback control systems. Particularly good ones are Bower and Schultheiss (1961) and Franklin et al. (1986). Regarding the Keck telescope, see Aubrun et al. (1987, 1988).

Norms for Signals and Systems

One way to describe the performance of a control system is in terms of the size of certain signals of interest. For example, the performance of a tracking system could be measured by the size of the error signal. This chapter looks at several ways of defining a signal's size (i.e., at several norms for signals). Which norm is appropriate depends on the situation at hand. Also introduced are norms for a system's transfer function. Then two very useful tables are developed summarizing input-output norm relationships.

2.1 Norms for Signals

We consider signals mapping $(-\infty, \infty)$ to $\mathbb{R}$. They are assumed to be piecewise continuous. Of course, a signal may be zero for $t < 0$ (i.e., it may start at time $t = 0$).

We are going to introduce several different norms for such signals. First, recall that a norm must have the following four properties:

(i) $\|u\| \geq 0$

(ii) $\|u\| = 0 \Leftrightarrow u(t) = 0, \qquad \forall t$

(iii) $\|au\| = |a|\|u\|, \qquad \forall a \in \mathbb{R}$

(iv) $\|u + v\| \leq \|u\| + \|v\|$

The last property is the familiar triangle inequality.

1-Norm The 1-norm of a signal $u(t)$ is the integral of its absolute value:

$$\|u\|_1 := \int_{-\infty}^{\infty} |u(t)|dt.$$

2-Norm The 2-norm of $u(t)$ is

$$\|u\|_2 := \left(\int_{-\infty}^{\infty} u(t)^2 dt\right)^{1/2}.$$

For example, suppose that u is the current through a 1 Ω resistor. Then the instantaneous power equals $u(t)^2$ and the total energy equals the integral of this, namely, $\|u\|_2^2$. We shall generalize this

interpretation: The *instantaneous power* of a signal $u(t)$ is defined to be $u(t)^2$ and its *energy* is defined to be the square of its 2-norm.

∞-Norm The ∞-norm of a signal is the least upper bound of its absolute value:

$$\|u\|_\infty := \sup_t |u(t)|.$$

For example, the ∞-norm of

$$(1 - \mathrm{e}^{-t})1(t)$$

equals 1. Here $1(t)$ denotes the unit step function.

Power Signals The *average power* of u is the average over time of its instantaneous power:

$$\lim_{T\to\infty} \frac{1}{2T} \int_{-T}^{T} u(t)^2 dt.$$

The signal u will be called a *power signal* if this limit exists, and then the squareroot of the average power will be denoted $pow(u)$:

$$pow(u) := \left(\lim_{T\to\infty} \frac{1}{2T} \int_{-T}^{T} u(t)^2 dt \right)^{1/2}.$$

Note that a nonzero signal can have zero average power, so *pow* is not a norm. It does, however, have properties (i), (iii), and (iv).

Now we ask the question: Does finiteness of one norm imply finiteness of any others? There are some easy answers:

1. If $\|u\|_2 < \infty$, then u is a power signal with $pow(u) = 0$.

   Proof Assuming that u has finite 2-norm, we get

   $$\frac{1}{2T} \int_{-T}^{T} u(t)^2 dt \le \frac{1}{2T} \|u\|_2^2.$$

   But the right-hand side tends to zero as $T \to \infty$. ■

2. If u is a power signal and $\|u\|_\infty < \infty$, then $pow(u) \le \|u\|_\infty$.

   Proof We have

   $$\frac{1}{2T} \int_{-T}^{T} u(t)^2 dt \le \|u\|_\infty^2 \frac{1}{2T} \int_{-T}^{T} dt = \|u\|_\infty^2.$$

   Let T tend to ∞. ■

3. If $\|u\|_1 < \infty$ and $\|u\|_\infty < \infty$, then $\|u\|_2 \le (\|u\|_\infty \|u\|_1)^{1/2}$, and hence $\|u\|_2 < \infty$.

   Proof

   $$\int_{-\infty}^{\infty} u(t)^2 dt = \int_{-\infty}^{\infty} |u(t)||u(t)| dt \le \|u\|_\infty \|u\|_1 \ ■$$

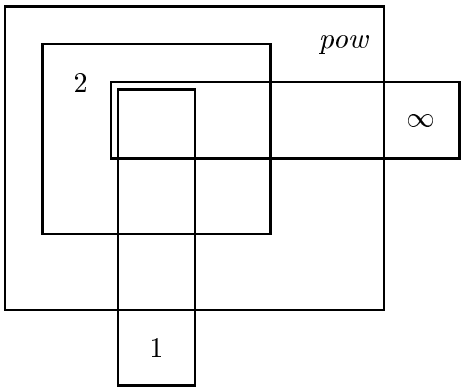

Figure 2.1: Set inclusions.

A Venn diagram summarizing the set inclusions is shown in Figure 2.1. Note that the set labeled "*pow*" contains all power signals for which *pow* is finite; the set labeled "1" contains all signals of finite 1-norm; and so on. It is instructive to get examples of functions in all the components of this diagram (Exercise 2). For example, consider

$$u_1(t) = \begin{cases} 0, & \text{if } t \leq 0 \\ 1/\sqrt{t}, & \text{if } 0 < t \leq 1 \\ 0, & \text{if } t > 1. \end{cases}$$

This has finite 1-norm:

$$\|u_1\|_1 = \int_0^1 \frac{1}{\sqrt{t}} dt = 2.$$

Its 2-norm is infinite because the integral of $1/t$ is divergent over the interval $[0, 1]$. For the same reason, u_1 is not a power signal. Finally, u_1 is not bounded, so $\|u_1\|_\infty$ is infinite. Therefore, u_1 lives in the bottom component in the diagram.

2.2 Norms for Systems

We consider systems that are linear, time-invariant, causal, and (usually) finite-dimensional. In the time domain an input-output model for such a system has the form of a convolution equation,

$$y = G * u,$$

that is,

$$y(t) = \int_{-\infty}^{\infty} G(t - \tau)u(\tau)d\tau.$$

Causality means that $G(t) = 0$ for $t < 0$. Let $\hat{G}(s)$ denote the transfer function, the Laplace transform of G. Then $\hat{G}$ is rational (by finite-dimensionality) with real coefficients. We say that $\hat{G}$ is *stable* if it is analytic in the closed right half-plane (Re $s \geq 0$), *proper* if $\hat{G}(j\infty)$ is finite (degree of denominator $\geq$ degree of numerator), *strictly proper* if $\hat{G}(j\infty) = 0$ (degree of denominator $>$ degree of numerator), and *biproper* if $\hat{G}$ and $\hat{G}^{-1}$ are both proper (degree of denominator = degree of numerator).

We introduce two norms for the transfer function $\hat{G}$.

2-Norm

$$\|\hat{G}\|_2 := \left(\frac{1}{2\pi}\int_{-\infty}^{\infty}|\hat{G}(j\omega)|^2 d\omega\right)^{1/2}$$

∞-Norm

$$\|\hat{G}\|_\infty := \sup_\omega |\hat{G}(j\omega)|$$

Note that if $\hat{G}$ is stable, then by Parseval's theorem

$$\|\hat{G}\|_2 = \left(\frac{1}{2\pi}\int_{-\infty}^{\infty}|\hat{G}(j\omega)|^2 d\omega\right)^{1/2} = \left(\int_{-\infty}^{\infty}|G(t)|^2 dt\right)^{1/2}.$$

The ∞-norm of $\hat{G}$ equals the distance in the complex plane from the origin to the farthest point on the Nyquist plot of $\hat{G}$. It also appears as the peak value on the Bode magnitude plot of $\hat{G}$. An important property of the ∞-norm is that it is submultiplicative:

$$\|\hat{G}\hat{H}\|_\infty \le \|\hat{G}\|_\infty \|\hat{H}\|_\infty.$$

It is easy to tell when these two norms are finite.

Lemma 1 *The 2-norm of $\hat{G}$ is finite iff $\hat{G}$ is strictly proper and has no poles on the imaginary axis; the ∞-norm is finite iff $\hat{G}$ is proper and has no poles on the imaginary axis.*

Proof Assume that $\hat{G}$ is strictly proper, with no poles on the imaginary axis. Then the Bode magnitude plot rolls off at high frequency. It is not hard to see that the plot of $c/(\tau s+1)$ dominates that of $\hat{G}$ for sufficiently large positive c and sufficiently small positive τ, that is,

$$|c/(\tau j\omega + 1)| \ge |\hat{G}(j\omega)|, \qquad \forall\omega.$$

But $c/(\tau s+1)$ has finite 2-norm; its 2-norm equals $c/\sqrt{2\tau}$ (how to do this computation is shown below). Hence $\hat{G}$ has finite 2-norm.

The rest of the proof follows similar lines. ■

How to Compute the 2-Norm

Suppose that $\hat{G}$ is strictly proper and has no poles on the imaginary axis (so its 2-norm is finite). We have

$$\begin{aligned}\|\hat{G}\|_2^2 &= \frac{1}{2\pi}\int_{-\infty}^{\infty}|\hat{G}(j\omega)|^2 d\omega \\ &= \frac{1}{2\pi j}\int_{-j\infty}^{j\infty}\hat{G}(-s)\hat{G}(s)ds \\ &= \frac{1}{2\pi j}\oint \hat{G}(-s)\hat{G}(s)ds.\end{aligned}$$

The last integral is a contour integral up the imaginary axis, then around an infinite semicircle in the left half-plane; the contribution to the integral from this semicircle equals zero because $\hat{G}$ is

strictly proper. By the residue theorem, $\|\hat{G}\|_2^2$ equals the sum of the residues of $\hat{G}(-s)\hat{G}(s)$ at its poles in the left half-plane.

Example 1 Take $\hat{G}(s) = 1/(\tau s + 1)$, $\tau > 0$. The left half-plane pole of $\hat{G}(-s)\hat{G}(s)$ is at $s = -1/\tau$. The residue at this pole equals

$$\lim_{s \to -1/\tau} \left(s + \frac{1}{\tau} \right) \frac{1}{-\tau s + 1} \frac{1}{\tau s + 1} = \frac{1}{2\tau}.$$

Hence $\|\hat{G}\|_2 = 1/\sqrt{2\tau}$.

How to Compute the ∞-Norm
This requires a search. Set up a fine grid of frequency points,

$$\{\omega_1, \ldots, \omega_N\}.$$

Then an estimate for $\|\hat{G}\|_\infty$ is

$$\max_{1 \le k \le N} |\hat{G}(j\omega_k)|.$$

Alternatively, one could find where $|\hat{G}(j\omega)|$ is maximum by solving the equation

$$\frac{d|\hat{G}|^2}{d\omega}(j\omega) = 0.$$

This derivative can be computed in closed form because $\hat{G}$ is rational. It then remains to compute the roots of a polynomial.

Example 2 Consider

$$\hat{G}(s) = \frac{as + 1}{bs + 1}$$

with $a, b > 0$. Look at the Bode magnitude plot: For $a \ge b$ it is increasing (high-pass); else, it is decreasing (low-pass). Thus

$$\|\hat{G}\|_\infty = \begin{cases} a/b, & a \ge b \\ 1, & a < b. \end{cases}$$

2.3 Input-Output Relationships

The question of interest in this section is: If we know how big the input is, how big is the output going to be? Consider a linear system with input u, output y, and transfer function $\hat{G}$, assumed stable and strictly proper. The results are summarized in two tables below. Suppose that u is the unit impulse, δ. Then the 2-norm of y equals the 2-norm of G, which by Parseval's theorem equals the 2-norm of $\hat{G}$; this gives entry (1,1) in Table 2.1. The rest of the first column is for the ∞-norm and *pow*, and the second column is for a sinusoidal input. The ∞ in the (1,2) entry is true as long as $\hat{G}(j\omega) \neq 0$.

	$u(t) = \delta(t)$	$u(t) = \sin(\omega t)$
$\|y\|_2$	$\|\hat{G}\|_2$	∞
$\|y\|_\infty$	$\|G\|_\infty$	$\|\hat{G}(j\omega)\|$
$pow(y)$	0	$\frac{1}{\sqrt{2}}\|\hat{G}(j\omega)\|$

Table 2.1: Output norms and *pow* for two inputs

Now suppose that u is not a fixed signal but that it can be any signal of 2-norm ≤ 1. It turns out that the least upper bound on the 2-norm of the output, that is,

$$\sup\{\|y\|_2 : \|u\|_2 \leq 1\},$$

which we can call the 2-norm/2-norm *system gain*, equals the ∞-norm of $\hat{G}$; this provides entry (1,1) in Table 2.2. The other entries are the other system gains. The ∞ in the various entries is true as long as $\hat{G} \not\equiv 0$, that is, as long as there is some ω for which $\hat{G}(j\omega) \neq 0$.

	$\|u\|_2$	$\|u\|_\infty$	$pow(u)$
$\|y\|_2$	$\|\hat{G}\|_\infty$	∞	∞
$\|y\|_\infty$	$\|\hat{G}\|_2$	$\|G\|_1$	∞
$pow(y)$	0	$\leq \|\hat{G}\|_\infty$	$\|\hat{G}\|_\infty$

Table 2.2: System Gains

A typical application of these tables is as follows. Suppose that our control analysis or design problem involves, among other things, a requirement of disturbance attenuation: The controlled system has a disturbance input, say u, whose effect on the plant output, say y, should be small. Let G denote the impulse response from u to y. The controlled system will be required to be stable, so the transfer function $\hat{G}$ will be stable. Typically, it will be strictly proper, too (or at least proper). The tables tell us how much u affects y according to various measures. For example, if u is known to be a sinusoid of fixed frequency (maybe u comes from a power source at 60 Hz), then the second column of Table 2.1 gives the relative size of y according to the three measures. More commonly, the disturbance signal will not be known *a priori*, so Table 2.2 will be more relevant.

Notice that the ∞-norm of the transfer function appears in several entries in the tables. This norm is therefore an important measure for system performance.

Example A system with transfer function $1/(10s+1)$ has a disturbance input $d(t)$ known to have the energy bound $\|d\|_2 \leq 0.4$. Suppose that we want to find the best estimate of the ∞-norm of the output $y(t)$. Table 2.2 says that the 2-norm/∞-norm gain equals the 2-norm of the transfer function, which equals $1/\sqrt{20}$. Thus

$$\|y\|_\infty \leq \frac{0.4}{\sqrt{20}}.$$

The next two sections concern the proofs of the tables and are therefore optional.

2.4 Power Analysis (Optional)

For a power signal u define the *autocorrelation function*

$$R_u(\tau) := \lim_{T\to\infty} \frac{1}{2T} \int_{-T}^{T} u(t)u(t+\tau)dt,$$

that is, $R_u(\tau)$ is the average value of the product $u(t)u(t+\tau)$. Observe that

$$R_u(0) = pow(u)^2 \geq 0.$$

We must restrict our definition of a power signal to those signals for which the above limit exists for all values of τ, not just $\tau = 0$. For such signals we have the additional property that

$$|R_u(\tau)| \leq R_u(0).$$

Proof The Cauchy-Schwarz inequality implies that

$$\left| \int_{-T}^{T} u(t)v(t)dt \right| \leq \left(\int_{-T}^{T} u(t)^2 dt \right)^{1/2} \left(\int_{-T}^{T} v(t)^2 dt \right)^{1/2}.$$

Set $v(t) = u(t+\tau)$ and multiply by $1/(2T)$ to get

$$\left| \frac{1}{2T} \int_{-T}^{T} u(t)u(t+\tau)dt \right| \leq \left(\frac{1}{2T} \int_{-T}^{T} u(t)^2 dt \right)^{1/2} \left(\frac{1}{2T} \int_{-T}^{T} u(t+\tau)^2 dt \right)^{1/2}.$$

Now let $T \to \infty$ to get the desired result. ■

Let S_u denote the Fourier transform of R_u. Thus

$$\begin{aligned} S_u(j\omega) &= \int_{-\infty}^{\infty} R_u(\tau) \mathrm{e}^{-j\omega\tau} d\tau, \\ R_u(\tau) &= \frac{1}{2\pi} \int_{-\infty}^{\infty} S_u(j\omega) \mathrm{e}^{j\omega\tau} d\omega, \\ pow(u)^2 &= R_u(0) = \frac{1}{2\pi} \int_{-\infty}^{\infty} S_u(j\omega) d\omega. \end{aligned}$$

From the last equation we interpret $S_u(j\omega)/2\pi$ as power density. The function S_u is called the *power spectral density* of the signal u.

Now consider two power signals, u and v. Their *cross-correlation function* is

$$R_{uv}(\tau) := \lim_{T\to\infty} \frac{1}{2T} \int_{-T}^{T} u(t)v(t+\tau)dt$$

and S_{uv}, the Fourier transform, is called their *cross-power spectral density function.*

We now derive some useful facts concerning a linear system with transfer function $\hat{G}$, assumed stable and proper, and its input u and output y.

1. $R_{uy} = G * R_u$

Proof Since

$$y(t) = \int_{-\infty}^{\infty} G(\alpha)u(t-\alpha)d\alpha \tag{2.1}$$

we have

$$u(t)y(t+\tau) = \int_{-\infty}^{\infty} G(\alpha)u(t)u(t+\tau-\alpha)d\alpha.$$

Thus the average value of $u(t)y(t+\tau)$ equals

$$\int_{-\infty}^{\infty} G(\alpha)R_u(\tau-\alpha)d\alpha. \blacksquare$$

2. $R_y = G * G_{\text{rev}} * R_u$ where $G_{\text{rev}}(t) := G(-t)$

Proof Using (2.1) we get

$$y(t)y(t+\tau) = \int_{-\infty}^{\infty} G(\alpha)y(t)u(t+\tau-\alpha)d\alpha,$$

so the average value of $y(t)y(t+\tau)$ equals

$$\int_{-\infty}^{\infty} G(\alpha)R_{yu}(\tau-\alpha)d\alpha$$

(i.e., $R_y = G * R_{yu}$). Similarly, you can check that $R_{yu} = G_{\text{rev}} * R_u$. $\blacksquare$

3. $S_y(j\omega) = |\hat{G}(j\omega)|^2 S_u(j\omega)$

Proof From the previous fact we have

$$S_y(j\omega) = \hat{G}(j\omega)\hat{G}_{\text{rev}}(j\omega)S_u(j\omega),$$

so it remains to show that the Fourier transform of G_{rev} equals the complex-conjugate of $\hat{G}(j\omega)$. This is easy. $\blacksquare$

2.5 Proofs for Tables 2.1 and 2.2 (Optional)

Table 2.1

Entry (1,1) If $u = \delta$, then $y = G$, so $\|y\|_2 = \|G\|_2$. But by Parseval's theorem, $\|G\|_2 = \|\hat{G}\|_2$.

Entry (2,1) Again, since $y = G$.

Entry (3,1)

$$\begin{aligned} pow(y)^2 &= \lim \frac{1}{2T}\int_0^T G(t)^2 dt \\ &\leq \lim \frac{1}{2T}\int_0^\infty G(t)^2 dt \\ &= \lim \frac{1}{2T}\|G\|_2^2 \\ &= 0 \end{aligned}$$

Entry (1,2) With the input $u(t) = \sin(\omega t)$, the output is

$$y(t) = |\hat{G}(j\omega)|\sin[\omega t + \arg \hat{G}(j\omega)]. \tag{2.2}$$

The 2-norm of this signal is infinite as long as $\hat{G}(j\omega) \neq 0$, that is, the system's transfer function does not have a zero at the frequency of excitation.

Entry (2,2) The amplitude of the sinusoid (2.2) equals $|\hat{G}(j\omega)|$.

Entry (3,2) Let $\phi := \arg \hat{G}(j\omega)$. Then

$$\begin{aligned} pow(y)^2 &= \lim \frac{1}{2T} \int_{-T}^{T} |\hat{G}(j\omega)|^2 \sin^2(\omega t + \phi) dt \\ &= |\hat{G}(j\omega)|^2 \lim \frac{1}{2T} \int_{-T}^{T} \sin^2(\omega t + \phi) dt \\ &= |\hat{G}(j\omega)|^2 \lim \frac{1}{2\omega T} \int_{-\omega T+\phi}^{\omega T+\phi} \sin^2(\theta) d\theta \\ &= |\hat{G}(j\omega)|^2 \frac{1}{\pi} \int_{0}^{\pi} \sin^2(\theta) d\theta \\ &= \frac{1}{2} |\hat{G}(j\omega)|^2. \end{aligned}$$

Table 2.2

Entry (1,1) First we see that $\|\hat{G}\|_\infty$ is an upper bound on the 2-norm/2-norm system gain:

$$\begin{aligned} \|y\|_2^2 &= \|\hat{y}\|_2^2 \\ &= \frac{1}{2\pi} \int_{-\infty}^{\infty} |\hat{G}(j\omega)|^2 |\hat{u}(j\omega)|^2 d\omega \\ &\leq \|\hat{G}\|_\infty^2 \frac{1}{2\pi} \int_{-\infty}^{\infty} |\hat{u}(j\omega)|^2 d\omega \\ &= \|\hat{G}\|_\infty^2 \|\hat{u}\|_2^2 \\ &= \|\hat{G}\|_\infty^2 \|u\|_2^2. \end{aligned}$$

To show that $\|\hat{G}\|_\infty$ is the least upper bound, first choose a frequency ω_o where $|\hat{G}(j\omega)|$ is maximum, that is,

$$|\hat{G}(j\omega_o)| = \|\hat{G}\|_\infty.$$

Now choose the input u so that

$$|\hat{u}(j\omega)| = \begin{cases} c, & \text{if } |\omega - \omega_o| < \epsilon \text{ or } |\omega + \omega_o| < \epsilon \\ 0, & \text{otherwise,} \end{cases}$$

where ϵ is a small positive number and c is chosen so that u has unit 2-norm (i.e., $c = \sqrt{\pi/2\epsilon}$). Then

$$\begin{aligned} \|\hat{y}\|_2^2 &\approx \frac{1}{2\pi} \left[|\hat{G}(-j\omega_o)|^2 \pi + |\hat{G}(j\omega_o)|^2 \pi \right] \\ &= |\hat{G}(j\omega_o)|^2 \\ &= \|\hat{G}\|_\infty^2. \end{aligned}$$

Entry (2,1) This is an application of the Cauchy-Schwarz inequality:

$$\begin{aligned} |y(t)| &= \left| \int_{-\infty}^{\infty} G(t-\tau)u(\tau)d\tau \right| \\ &\leq \left(\int_{-\infty}^{\infty} G(t-\tau)^2 d\tau \right)^{1/2} \left(\int_{-\infty}^{\infty} u(\tau)^2 d\tau \right)^{1/2} \\ &= \|G\|_2 \|u\|_2 \\ &= \|\hat{G}\|_2 \|u\|_2. \end{aligned}$$

Hence

$$\|y\|_\infty \leq \|\hat{G}\|_2 \|u\|_2.$$

To show that $\|\hat{G}\|_2$ is the least upper bound, apply the input

$$u(t) = G(-t)/\|G\|_2.$$

Then $\|u\|_2 = 1$ and $|y(0)| = \|G\|_2$, so $\|y\|_\infty \geq \|G\|_2$.

Entry (3,1) If $\|u\|_2 \leq 1$, then the 2-norm of y is finite [as in entry (1,1)], so $pow(y) = 0$.

Entry (1,2) Apply a sinusoidal input of unit amplitude and frequency ω such that $j\omega$ is not a zero of $\hat{G}$. Then $\|u\|_\infty = 1$, but $\|y\|_2 = \infty$.

Entry (2,2) First, $\|G\|_1$ is an upper bound on the ∞-norm/∞-norm system gain:

$$\begin{aligned} |y(t)| &= \left| \int_{-\infty}^{\infty} G(\tau)u(t-\tau)d\tau \right| \\ &\leq \int_{-\infty}^{\infty} |G(\tau)u(t-\tau)|\, d\tau \\ &\leq \int_{-\infty}^{\infty} |G(\tau)|\, d\tau \|u\|_\infty \\ &= \|G\|_1 \|u\|_\infty. \end{aligned}$$

That $\|G\|_1$ is the least upper bound can be seen as follows. Fix t and set

$$u(t-\tau) := \operatorname{sgn}(G(\tau)), \qquad \forall \tau.$$

Then $\|u\|_\infty = 1$ and

$$\begin{aligned} y(t) &= \int_{-\infty}^{\infty} G(\tau)u(t-\tau)d\tau \\ &= \int_{-\infty}^{\infty} |G(\tau)| d\tau \\ &= \|G\|_1. \end{aligned}$$

So $\|y\|_\infty \geq \|G\|_1$.

Entry (3,2) If u is a power signal and $\|u\|_\infty \leq 1$, then $pow(u) \leq 1$, so

$$\sup\{pow(y) : \|u\|_\infty \leq 1\} \leq \sup\{pow(y) : pow(u) \leq 1\}.$$

We will see in entry (3,3) that the latter supremum equals $\|\hat{G}\|_\infty$.

Entry (1,3) If u is a power signal, then from the preceding section,

$$S_y(j\omega) = |\hat{G}(j\omega)|^2 S_u(j\omega),$$

so

$$pow(y)^2 = \frac{1}{2\pi}\int_{-\infty}^{\infty} |\hat{G}(j\omega)|^2 S_u(j\omega)d\omega. \tag{2.3}$$

Unless $|\hat{G}(j\omega)|^2 S_u(j\omega)$ equals zero for all ω, $pow(y)$ is positive, in which case its 2-norm is infinite.

Entry (2,3) This case is not so important, so a complete proof is omitted. The main idea is this: If $pow(u) \leq 1$, then $pow(y)$ is finite but $\|y\|_\infty$ is not necessarily (see u_8 in Exercise 2). So for a proof of this entry, one should construct an input with $pow(u) \leq 1$, but such that $\|y\|_\infty = \infty$.

Entry (3,3) From (2.3) we get immediately that

$$pow(y) \leq \|\hat{G}\|_\infty pow(u).$$

To achieve equality, suppose that

$$|\hat{G}(j\omega_o)| = \|\hat{G}\|_\infty$$

and let the input be

$$u(t) = \sqrt{2}\sin(\omega_o t).$$

Then $R_u(\tau) = \cos(\omega_o \tau)$, so

$$pow(u) = R_u(0) = 1.$$

Also,

$$S_u(j\omega) = \pi\left[\delta(\omega - \omega_o) + \delta(\omega + \omega_o)\right],$$

so from (2.3)

$$\begin{aligned} pow(y)^2 &= \frac{1}{2}|\hat{G}(j\omega_o)|^2 + \frac{1}{2}|\hat{G}(-j\omega_o)|^2 \\ &= |\hat{G}(j\omega_o)|^2 \\ &= \|\hat{G}\|_\infty^2. \end{aligned}$$

2.6 Computing by State-Space Methods (Optional)

This book is on classical control, which is set in the frequency domain. Current widespread practice, however, is to do computations using state-space methods. The purpose of this optional section is to illustrate how this is done for the problem of computing the 2-norm and ∞-norm of a transfer function. The derivation of the procedures is brief.

Consider a state-space model of the form

$$\begin{aligned} \dot{x}(t) &= Ax(t) + Bu(t), \\ y(t) &= Cx(t). \end{aligned}$$

Here $u(t)$ is the input signal and $y(t)$ the output signal, both scalar-valued. In contrast, $x(t)$ is a vector-valued function with, say, n components. The dot in $\dot{x}$ means take the derivative of each component. Then A, B, C are real matrices of sizes

$$n \times n, \quad n \times 1, \quad 1 \times n.$$

The equations are assumed to hold for $t \geq 0$. Take Laplace transforms with zero initial conditions on x:

$$\begin{aligned} s\hat{x}(s) &= A\hat{x}(s) + B\hat{u}(s), \\ \hat{y}(s) &= C\hat{x}(s). \end{aligned}$$

Now eliminate $\hat{x}(s)$ to get

$$\hat{y}(s) = C(sI - A)^{-1}B\hat{u}(s).$$

We conclude that the transfer function from $\hat{u}$ to $\hat{y}$ is

$$\hat{G}(s) = C(sI - A)^{-1}B.$$

This transfer function is strictly proper. [Try an example: start with some A, B, C with $n = 2$, and compute $\hat{G}(s)$.]

Going the other way, from a strictly proper transfer function to a state-space model, is more profound, but it is true that for every strictly proper transfer function $\hat{G}(s)$ there exist (A, B, C) such that

$$\hat{G}(s) = C(sI - A)^{-1}B.$$

From the representation

$$\hat{G}(s) = \frac{1}{\det(sI - A)} C \operatorname{adj}(sI - A)B$$

it should be clear that the poles of $\hat{G}(s)$ are included in the eigenvalues of A. We say that A is *stable* if all its eigenvalues lie in $\operatorname{Re} s < 0$, in which case $\hat{G}$ is a stable transfer function.

Now start with the representation

$$\hat{G}(s) = C(sI - A)^{-1}B$$

with A stable. We want to compute $\|\hat{G}\|_2$ and $\|\hat{G}\|_\infty$ from the data (A, B, C).

The 2-Norm

Define the matrix exponential

$$\mathrm{e}^{tA} := I + tA + \frac{t^2}{2!}A^2 + \cdots$$

just as if A were a scalar (convergence can be proved). Let a prime denote transpose and define the matrix

$$L := \int_0^\infty \mathrm{e}^{tA} BB' \mathrm{e}^{tA'} \, dt$$

(the integral converges because A is stable). Then L satisfies the equation

$$AL + LA' + BB' = 0.$$

Proof Integrate both sides of the equation

$$\frac{d}{dt}\mathrm{e}^{tA}BB'\mathrm{e}^{tA'} = A\mathrm{e}^{tA}BB'\mathrm{e}^{tA'} + \mathrm{e}^{tA}BB'\mathrm{e}^{tA'}A'$$

from 0 to ∞, noting that $\exp(tA)$ converges to 0 because A is stable, to get

$$-BB' = AL + LA'. \blacksquare$$

In terms of L a simple formula for the 2-norm of $\hat{G}$ is

$$\|\hat{G}\|_2 = (CLC')^{1/2}.$$

Proof The impulse response function is

$$G(t) = C\mathrm{e}^{tA}B, \quad t > 0.$$

Calling on Parseval we get

$$\begin{aligned} \|\hat{G}\|_2^2 &= \|G\|_2^2 \\ &= \int_0^\infty C\mathrm{e}^{tA}BB'\mathrm{e}^{tA'}C'dt \\ &= C\int_0^\infty \mathrm{e}^{tA}BB'\mathrm{e}^{tA'}dtC' \\ &= CLC'. \blacksquare \end{aligned}$$

So a procedure to compute the 2-norm is as follows:

Step 1 Solve the equation

$$AL + LA' + BB' = 0$$

for the matrix L.

Step 2

$$\|\hat{G}\|_2 = (CLC')^{1/2}$$

The ∞-Norm

Computing the ∞-norm is harder; we shall have to be content with a search procedure. Define the $2n \times 2n$ matrix

$$H := \begin{bmatrix} A & BB' \\ -C'C & -A' \end{bmatrix}.$$

Theorem 1 $\|\hat{G}\|_\infty < 1$ *iff* H *has no eigenvalues on the imaginary axis.*

Proof The proof of this theorem is a bit involved, so only sufficiency is considered, and it is only sketched.

It is not too hard to derive that

$$1/[1 - \hat{G}(-s)\hat{G}(s)] = 1 + \begin{bmatrix} 0 & B' \end{bmatrix}(sI - H)^{-1}\begin{bmatrix} B \\ 0 \end{bmatrix}.$$

Thus the poles of $[1 - \hat{G}(-s)\hat{G}(s)]^{-1}$ are contained in the eigenvalues of H.

Assume that H has no eigenvalues on the imaginary axis. Then $[1 - \hat{G}(-s)\hat{G}(s)]^{-1}$ has no poles there, so $1 - \hat{G}(-s)\hat{G}(s)$ has no zeros there, that is,

$$|\hat{G}(j\omega)| \neq 1, \quad \forall\omega.$$

Since $\hat{G}$ is strictly proper, this implies that

$$|\hat{G}(j\omega)| < 1, \quad \forall\omega$$

(i.e., $\|\hat{G}\|_\infty < 1$). ■

The theorem suggests this way to compute an ∞-norm: Select a positive number γ; test if $\|\hat{G}\|_\infty < \gamma$ (i.e., if $\|\gamma^{-1}\hat{G}\|_\infty < 1$) by calculating the eigenvalues of the appropriate matrix; increase or decrease γ accordingly; repeat. A bisection search is quite efficient: Get upper and lower bounds for $\|\hat{G}\|_\infty$; try γ midway between these bounds; continue.

Exercises

1. Suppose that $u(t)$ is a continuous signal whose derivative $\dot{u}(t)$ is continuous too. Which of the following qualifies as a norm for u?

$$\sup_t |\dot{u}(t)|$$

$$|u(0)| + \sup_t |\dot{u}(t)|$$

$$\max\{\sup_t |u(t)|, \sup_t |\dot{u}(t)|\}$$

$$\sup_t |u(t)| + \sup_t |\dot{u}(t)|$$

2. Consider the Venn diagram in Figure 2.1. Show that the functions u_1 to u_9, defined below, are located in the diagram as shown in Figure 2.2. All the functions are zero for $t < 0$.

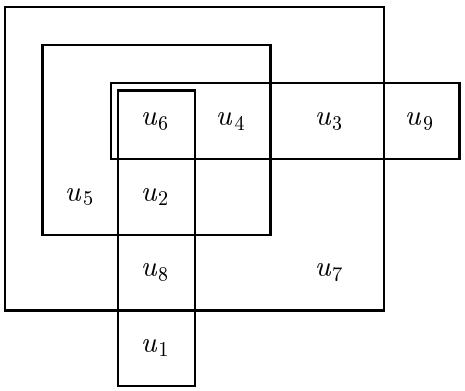

Figure 2.2: Figure for Exercise 2.

$$
\begin{aligned}
u_1(t) &= \begin{cases} 1/\sqrt{t}, & \text{if } t \le 1 \\ 0, & \text{if } t > 1 \end{cases} \\
u_2(t) &= \begin{cases} 1/t^{1/4}, & \text{if } t \le 1 \\ 0, & \text{if } t > 1 \end{cases} \\
u_3(t) &= 1 \\
u_4(t) &= 1/(1+t) \\
u_5(t) &= u_2(t) + u_4(t) \\
u_6(t) &= 0 \\
u_7(t) &= u_2(t) + 1
\end{aligned}
$$

For u_8, set

$$v_k(t) = \begin{cases} k, & \text{if } k < t < k + k^{-3} \\ 0, & \text{otherwise} \end{cases}$$

and then

$$u_8(t) = \sum_1^\infty v_k(t).$$

Finally, let u_9 equal 1 in the intervals

$$[2^{2k}, 2^{2k+1}], \quad k = 0, 1, 2, \ldots$$

and zero elsewhere.

3. Suppose that $\hat{G}(s)$ is a real-rational, stable transfer function with $\hat{G}^{-1}$ stable, too (i.e., neither poles nor zeros in Re $s \ge 0$). True or false: The Bode phase plot, $\angle\hat{G}(j\omega)$ versus ω, can be uniquely constructed from the Bode magnitude plot, $|\hat{G}(j\omega)|$ versus ω. (Answer: false!)

4. Recall that the transfer function for a pure timedelay of τ time units is

$$\hat{D}(s) := \mathrm{e}^{-s\tau}.$$

Say that a norm $\|\ \|$ on transfer functions is *time-delay invariant* if for every transfer function $\hat{G}$ (such that $\|\hat{G}\| < \infty$) and every $\tau > 0$,

$$\|\hat{D}\hat{G}\| = \|\hat{G}\|.$$

Is the 2-norm or ∞-norm time-delay invariant?

5. Compute the 1-norm of the impulse response corresponding to the transfer function

$$\frac{1}{\tau s + 1}, \quad \tau > 0.$$

6. For $\hat{G}$ stable and strictly proper, show that $\|G\|_1 < \infty$ and find an inequality relating $\|\hat{G}\|_\infty$ and $\|G\|_1$.

7. This concerns entry (2,2) in Table 2.2. The given entry assumes that $\hat{G}$ is stable and strictly proper. When $\hat{G}$ is stable but only proper, it can be expressed as

$$\hat{G}(s) = c + \hat{G}_1(s)$$

with c constant and $\hat{G}_1$ stable and strictly proper. Show that the correct (2,2)-entry is

$$|c| + \|G_1\|_1.$$

8. Show that entries (2,2) and (3,2) in Table 2.1 and entries (1,1), (3,2), and (3,3) in Table 2.2 hold when $\hat{G}$ is stable and proper (instead of strictly proper).

9. Let $\hat{G}(s)$ be a strictly proper stable transfer function and $G(t)$ its inverse Laplace transform. Let $u(t)$ be a signal of finite 1-norm. True or false:

$$\|G * u\|_1 \leq \|G\|_1 \|u\|_1 ?$$

10. Consider a system with transfer function

$$\frac{\omega_n^2}{s^2 + 2\zeta\omega_n s + \omega_n^2}, \quad \zeta, \omega_n > 0,$$

and input

$$u(t) = \sin 0.1t, \quad -\infty < t < \infty.$$

Compute *pow* of the output.

11. Consider a system with transfer function

$$\frac{s+2}{4s+1}$$

and input u and output y. Compute

$$\sup_{\|u\|_\infty = 1} \|y\|_\infty$$

and find an input achieving this supremum.

12. For a linear system with input $u(t)$ and output $y(t)$, prove that

$$\sup_{\|u\| \leq 1} \|y\| = \sup_{\|u\| = 1} \|y\|$$

where the norm is, say, the 2-norm.

13. Show that the 2-norm for transfer functions is not submultiplicative.

14. Write a MATLAB program to compute the ∞-norm of a transfer function using the grid method. Test your program on the function

$$\frac{1}{s^2 + 10^{-6}s + 1}$$

and compare your answer to the exact solution computed by hand using the derivative method.

Notes and References

The material in this chapter belongs to the field of mathematics called functional analysis. Tools from functional analysis were introduced into the subject of feedback control around 1960 by G. Zames and I. Sandberg. Some references are Desoer and Vidyasagar (1975), Holtzman (1970), Mees (1981), and Willems (1971). The state-space procedure for the ∞-norm is from Boyd et al. (1989).

Basic Concepts

This chapter and the next are the most fundamental. We concentrate on the single-loop feedback system. Stability of this system is defined and characterized. Then the system is analyzed for its ability to track certain signals (i.e., steps and ramps) asymptotically as time increases. Finally, tracking is addressed as a performance specification. Uncertainty is postponed until the next chapter.

Now a word about notation. In the preceding chapter we used signals in the time and frequency domains; the notation was $u(t)$ for a function of time and $\hat{u}(s)$ for its Laplace transform. When the context is solely the frequency domain, it is convenient to drop the hat and write $u(s)$; similarly for an impulse response $G(t)$ and the corresponding transfer function $\hat{G}(s)$.

3.1 Basic Feedback Loop

The most elementary feedback control system has three components: a plant (the object to be controlled, no matter what it is, is always called the *plant*), a sensor to measure the output of the plant, and a controller to generate the plant's input. Usually, actuators are lumped in with the plant. We begin with the block diagram in Figure 3.1. Notice that each of the three components

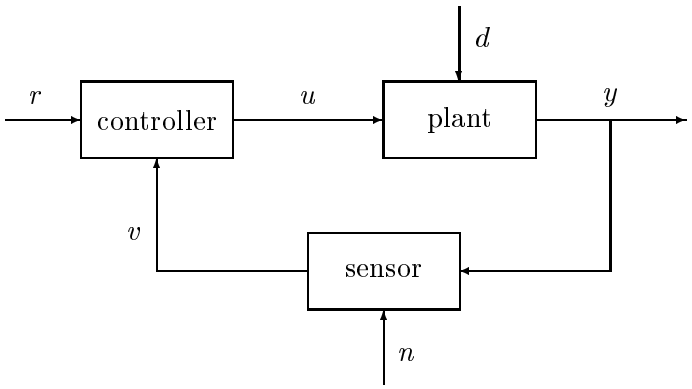

Figure 3.1: Elementary control system.

has two inputs, one internal to the system and one coming from outside, and one output. These signals have the following interpretations:

r	reference or command input
v	sensor output
u	actuating signal, plant input
d	external disturbance
y	plant output and measured signal
n	sensor noise

The three signals coming from outside—r, d, and n—are called *exogenous inputs*.

In what follows we shall consider a variety of performance objectives, but they can be summarized by saying that y should approximate some prespecified function of r, and it should do so in the presence of the disturbance d, sensor noise n, with uncertainty in the plant. We may also want to limit the size of u. Frequently, it makes more sense to describe the performance objective in terms of the measurement v rather than y, since often the only knowledge of y is obtained from v.

The analysis to follow is done in the frequency domain. To simplify notation, hats are omitted from Laplace transforms.

Each of the three components in Figure 3.1 is assumed to be linear, so its output is a linear function of its input, in this case a two-dimensional vector. For example, the plant equation has the form

$$y = P \begin{pmatrix} d \\ u \end{pmatrix}.$$

Partitioning the 1×2 transfer matrix P as

$$P = \begin{bmatrix} P_1 & P_2 \end{bmatrix},$$

we get

$$y = P_1 d + P_2 u.$$

We shall take an even more specialized viewpoint and suppose that the outputs of the three components are linear functions of the sums (or difference) of their inputs; that is, the plant, sensor, and controller equations are taken to be of the form

$$\begin{aligned} y &= P(d+u), \\ v &= F(y+n), \\ u &= C(r-v). \end{aligned}$$

The minus sign in the last equation is a matter of tradition. The block diagram for these equations is in Figure 3.2. Our convention is that plus signs at summing junctions are omitted.

This section ends with the notion of *well-posedness*. This means that in Figure 3.2 all closed-loop transfer functions exist, that is, all transfer functions from the three exogenous inputs to all internal signals, namely, u, y, v, and the outputs of the summing junctions. Label the outputs of the summing junctions as in Figure 3.3. For well-posedness it suffices to look at the nine transfer functions from r, d, n to x_1, x_2, x_3. (The other transfer functions are obtainable from these.) Write the equations at the summing junctions:

$$\begin{aligned} x_1 &= r - Fx_3, \\ x_2 &= d + Cx_1, \\ x_3 &= n + Px_2. \end{aligned}$$

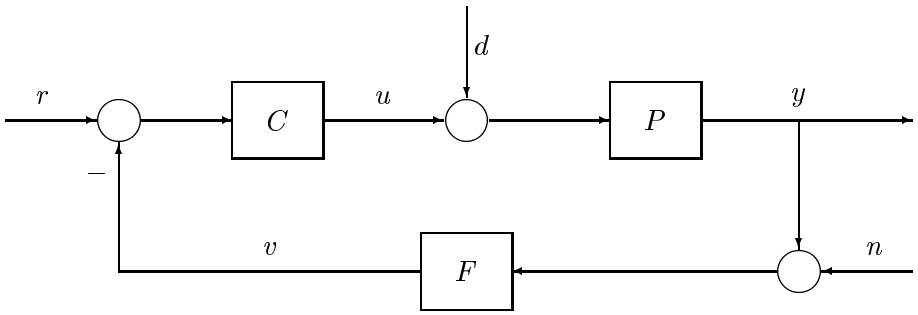

Figure 3.2: Basic feedback loop.

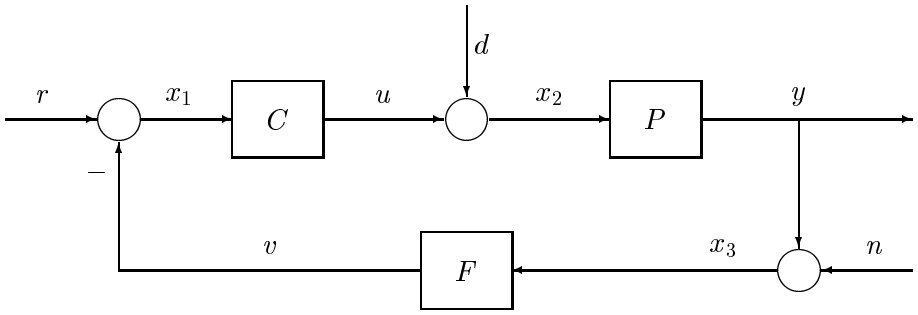

Figure 3.3: Basic feedback loop.

In matrix form these are

$$\begin{bmatrix} 1 & 0 & F \\ -C & 1 & 0 \\ 0 & -P & 1 \end{bmatrix} \begin{pmatrix} x_1 \\ x_2 \\ x_3 \end{pmatrix} = \begin{pmatrix} r \\ d \\ n \end{pmatrix}.$$

Thus, the system is well-posed iff the above 3×3 matrix is nonsingular, that is, the determinant $1 + PCF$ is not identically equal to zero. [For instance, the system with $P(s) = 1$, $C(s) = 1$, $F(s) = -1$ is not well-posed.] Then the nine transfer functions are obtained from the equation

$$\begin{pmatrix} x_1 \\ x_2 \\ x_3 \end{pmatrix} = \begin{bmatrix} 1 & 0 & F \\ -C & 1 & 0 \\ 0 & -P & 1 \end{bmatrix}^{-1} \begin{pmatrix} r \\ d \\ n \end{pmatrix},$$

that is,

$$\begin{pmatrix} x_1 \\ x_2 \\ x_3 \end{pmatrix} = \frac{1}{1+PCF} \begin{bmatrix} 1 & -PF & -F \\ C & 1 & -CF \\ PC & P & 1 \end{bmatrix} \begin{pmatrix} r \\ d \\ n \end{pmatrix}. \tag{3.1}$$

A stronger notion of well-posedness that makes sense when P, C, and F are proper is that the nine transfer functions above are proper. A necessary and sufficient condition for this is that $1 + PCF$ not be strictly proper [i.e., $PCF(\infty) \neq -1$].

One might argue that the transfer functions of all physical systems are strictly proper: If a sinusoid of ever-increasing frequency is applied to a (linear, time-invariant) system, the amplitude

of the output will go to zero. This is somewhat misleading because a real system will cease to behave linearly as the frequency of the input increases. Furthermore, our transfer functions will be used to parametrize an uncertainty set, and as we shall see, it may be convenient to allow some of them to be only proper. A proportional-integral-derivative controller is very common in practice, especially in chemical engineering. It has the form

$$k_1 + \frac{k_2}{s} + k_3 s.$$

This is not proper, but it can be approximated over any desired frequency range by a proper one, for example,

$$k_1 + \frac{k_2}{s} + \frac{k_3 s}{\tau s + 1}.$$

Notice that the feedback system is automatically well-posed, in the stronger sense, if P, C, and F are proper and one is strictly proper. For most of the book, we shall make the following *standing assumption*, under which the nine transfer functions in (3.1) are proper:

$$P \text{ is strictly proper, } C \text{ and } F \text{ are proper.}$$

However, at times it will be convenient to require only that P be proper. In this case we shall always assume that $|PCF| < 1$ at $\omega = \infty$, which ensures that $1 + PCF$ is not strictly proper. Given that no model, no matter how complex, can approximate a real system at sufficiently high frequencies, we should be very uncomfortable if $|PCF| > 1$ at $\omega = \infty$, because such a controller would almost surely be unstable if implemented on a real system.

3.2 Internal Stability

Consider a system with input u, output y, and transfer function $\hat{G}$, assumed stable and proper. We can write

$$\hat{G} = G_0 + \hat{G}_1,$$

where G_0 is a constant and $\hat{G}_1$ is strictly proper.

$$\text{Example: } \frac{s}{s+1} = 1 - \frac{1}{s+1}.$$

In the time domain the equation is

$$y(t) = G_0 u(t) + \int_{-\infty}^{\infty} G_1(t-\tau) u(\tau)\, d\tau.$$

If $|u(t)| \leq c$ for all t, then

$$|y(t)| \leq |G_0| c + \int_{-\infty}^{\infty} |G_1(\tau)|\, d\tau c.$$

The right-hand side is finite. Thus the output is bounded whenever the input is bounded. [This argument is the basis for entry (2,2) in Table 2.2.]

If the nine transfer functions in (3.1) are stable, then the feedback system is said to be *internally stable*. As a consequence, if the exogenous inputs are bounded in magnitude, so too are x_1, x_2, and x_3, and hence u, y, and v. So internal stability guarantees bounded internal signals for all bounded exogenous signals.

The idea behind this definition of internal stability is that it is not enough to look only at input-output transfer functions, such as from r to y, for example. This transfer function could be stable, so that y is bounded when r is, and yet an internal signal could be unbounded, probably causing internal damage to the physical system.

For the remainder of this section hats are dropped.

Example In Figure 3.3 take

$$C(s) = \frac{s-1}{s+1}, \quad P(s) = \frac{1}{s^2-1}, \quad F(s) = 1.$$

Check that the transfer function from r to y is stable, but that from d to y is not. The feedback system is therefore not internally stable. As we will see later, this offense is caused by the cancellation of the controller zero and the plant pole at the point $s = 1$.

We shall develop a test for internal stability which is easier than examining nine transfer functions. Write P, C, and F as ratios of coprime polynomials (i.e., polynomials with no common factors):

$$P = \frac{N_P}{M_P}, \quad C = \frac{N_C}{M_C}, \quad F = \frac{N_F}{M_F}.$$

The *characteristic polynomial* of the feedback system is the one formed by taking the product of the three numerators plus the product of the three denominators:

$$N_P N_C N_F + M_P M_C M_F.$$

The *closed-loop poles* are the zeros of the characteristic polynomial.

Theorem 1 *The feedback system is internally stable iff there are no closed-loop poles in* $\mathrm{Re}\, s \geq 0$.

Proof For simplicity assume that $F = 1$; the proof in the general case is similar, but a bit messier.

From (3.1) we have

$$\begin{pmatrix} x_1 \\ x_2 \\ x_3 \end{pmatrix} = \frac{1}{1+PC} \begin{bmatrix} 1 & -P & -1 \\ C & 1 & -C \\ PC & P & 1 \end{bmatrix} \begin{pmatrix} r \\ d \\ n \end{pmatrix}.$$

Substitute in the ratios and clear fractions to get

$$\begin{pmatrix} x_1 \\ x_2 \\ x_3 \end{pmatrix} = \frac{1}{N_P N_C + M_P M_C} \begin{bmatrix} M_P M_C & -N_P M_C & -M_P M_C \\ M_P N_C & M_P M_C & -M_P N_C \\ N_P N_C & N_P M_C & M_P M_C \end{bmatrix} \begin{pmatrix} r \\ d \\ n \end{pmatrix}. \tag{3.2}$$

Note that the characteristic polynomial equals $N_P N_C + M_P M_C$. Sufficiency is now evident; the feedback system is internally stable if the characteristic polynomial has no zeros in $\mathrm{Re}\, s \geq 0$.

Necessity involves a subtle point. Suppose that the feedback system is internally stable. Then all nine transfer functions in (3.2) are stable, that is, they have no poles in $\mathrm{Re}\, s \geq 0$. But we cannot immediately conclude that the polynomial $N_P N_C + M_P M_C$ has no zeros in $\mathrm{Re}\, s \geq 0$ because this polynomial may conceivably have a right half-plane zero which is also a zero of all nine numerators in (3.2), and hence is canceled to form nine stable transfer functions. However, the characteristic polynomial has no zero which is also a zero of all nine numerators, $M_P M_C$, $N_P M_C$, and so on.

Proof of this statement is left as an exercise. (It follows from the fact that we took coprime factors to start with, that is, N_P and M_P are coprime, as are the other numerator-denominator pairs.) ■

By Theorem 1 internal stability can be determined simply by checking the zeros of a polynomial. There is another test that provides additional insight.

Theorem 2 *The feedback system is internally stable iff the following two conditions hold:*

(a) The transfer function $1 + PCF$ *has no zeros in* $Res \geq 0$.

(b) There is no pole-zero cancellation in $Res \geq 0$ *when the product* PCF *is formed.*

Proof Recall that the feedback system is internally stable iff all nine transfer functions

$$\frac{1}{1+PCF}\begin{bmatrix} 1 & -PF & -F \\ C & 1 & -CF \\ PC & P & 1 \end{bmatrix}$$

are stable.

($\Rightarrow$) Assume that the feedback system is internally stable. Then in particular $(1 + PCF)^{-1}$ is stable (i.e., it has no poles in Re$s \geq 0$). Hence $1 + PCF$ has no zeros there. This proves (a).

To prove (b), write P, C, F as ratios of coprime polynomials:

$$P = \frac{N_P}{M_P}, \quad C = \frac{N_C}{M_C}, \quad F = \frac{N_F}{M_F}.$$

By Theorem 1 the characteristic polynomial

$$N_P N_C N_F + M_P M_C M_F$$

has no zeros in Re$s \geq 0$. Thus the pair (N_P, M_C) have no common zero in Re$s \geq 0$, and similarly for the other numerator-denominator pairs.

($\Leftarrow$) Assume (a) and (b). Factor P, C, F as above, and let s_0 be a zero of the characteristic polynomial, that is,

$$(N_P N_C N_F + M_P M_C M_F)(s_0) = 0.$$

We must show that Re$s_0 < 0$; this will prove internal stability by Theorem 1. Suppose to the contrary that Re$s_0 \geq 0$. If

$$(M_P M_C M_F)(s_0) = 0,$$

then

$$(N_P N_C N_F)(s_0) = 0.$$

But this violates (b). Thus

$$(M_P M_C M_F)(s_0) \neq 0,$$

so we can divide by it above to get

$$1 + \frac{N_P N_C N_F}{M_P M_C M_F}(s_0) = 0,$$

that is,

$$1 + (PCF)(s_0) = 0,$$

which violates (a). ■

Finally, let us recall for later use the Nyquist stability criterion. It can be derived from Theorem 2 and the principle of the argument. Begin with the curve $\mathcal{D}$ in the complex plane: It starts at the origin, goes up the imaginary axis, turns into the right half-plane following a semicircle of infinite radius, and comes up the negative imaginary axis to the origin again:

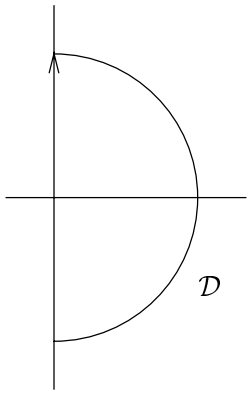

As a point s makes one circuit around this curve, the point $P(s)C(s)F(s)$ traces out a curve called the *Nyquist plot* of PCF. If PCF has a pole on the imaginary axis, then $\mathcal{D}$ must have a small indentation to avoid it.

Nyquist Criterion *Construct the Nyquist plot of PCF, indenting to the left around poles on the imaginary axis. Let n denote the total number of poles of P, C, and F in Res ≥ 0. Then the feedback system is internally stable iff the Nyquist plot does not pass through the point -1 and encircles it exactly n times counterclockwise.*

3.3 Asymptotic Tracking

In this section we look at a typical performance specification, perfect asymptotic tracking of a reference signal. Both time domain and frequency domain occur, so the notation distinction is required.

For the remainder of this chapter we specialize to the *unity-feedback* case, $\hat{F} = 1$, so the block diagram is as in Figure 3.4. Here e is the tracking error; with $n = d = 0$, e equals the reference input (ideal response), r, minus the plant output (actual response), y.

We wish to study this system's capability of tracking certain test inputs asymptotically as time tends to infinity. The two test inputs are the step

$$r(t) = \begin{cases} c, & \text{if } t \geq 0 \\ 0, & \text{if } t < 0 \end{cases}$$

and the ramp

$$r(t) = \begin{cases} ct, & \text{if } t \geq 0 \\ 0, & \text{if } t < 0 \end{cases}$$

(c is a nonzero real number). As an application of the former think of the temperature-control thermostat in a room; when you change the setting on the thermostat (step input), you would like

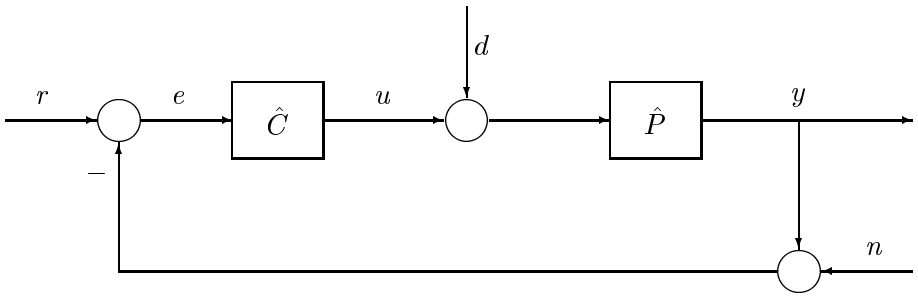

Figure 3.4: Unity-feedback loop.

the room temperature eventually to change to the new setting (of course, you would like the change to occur within a reasonable time). A situation with a ramp input is a radar dish designed to track orbiting satellites. A satellite moving in a circular orbit at constant angular velocity sweeps out an angle that is approximately a linear function of time (i.e., a ramp).

Define the *loop transfer function* $\hat{L} := \hat{P}\hat{C}$. The transfer function from reference input r to tracking error e is

$$\hat{S} := \frac{1}{1+\hat{L}},$$

called the *sensitivity function*—more on this in the next section. The ability of the system to track steps and ramps asymptotically depends on the number of zeros of $\hat{S}$ at $s = 0$.

Theorem 3 *Assume that the feedback system is internally stable and $n = d = 0$.*

(a) If r is a step, then $e(t) \longrightarrow 0$ as $t \longrightarrow \infty$ iff $\hat{S}$ has at least one zero at the origin.

(b) If r is a ramp, then $e(t) \longrightarrow 0$ as $t \longrightarrow \infty$ iff $\hat{S}$ has at least two zeros at the origin.

The proof is an application of the *final-value theorem*: If $\hat{y}(s)$ is a rational Laplace transform that has no poles in $\mathrm{Re}\, s \geq 0$ except possibly a simple pole at $s = 0$, then $\lim_{t\to\infty} y(t)$ exists and it equals $\lim_{s\to 0} s\hat{y}(s)$.

Proof (a) The Laplace transform of the foregoing step is $\hat{r}(s) = c/s$. The transfer function from r to e equals $\hat{S}$, so

$$\hat{e}(s) = \hat{S}(s)\frac{c}{s}.$$

Since the feedback system is internally stable, $\hat{S}$ is a stable transfer function. It follows from the final-value theorem that $e(t)$ does indeed converge as $t \longrightarrow \infty$, and its limit is the residue of the function $\hat{e}(s)$ at the pole $s = 0$:

$$e(\infty) = \hat{S}(0)c.$$

The right-hand side equals zero iff $\hat{S}(0) = 0$.

(b) Similarly with $\hat{r}(s) = c/s^2$. ■

Note that $\hat{S}$ has a zero at $s = 0$ iff $\hat{L}$ has a pole there. Thus, from the theorem we see that if the feedback system is internally stable and either $\hat{P}$ or $\hat{C}$ has a pole at the origin (i.e., an inherent integrator), then the output $y(t)$ will asymptotically track any step input r.

Example To see how this works, take the simplest possible example,

$$\hat{P}(s) = \frac{1}{s}, \quad \hat{C}(s) = 1.$$

Then the transfer function from r to e equals

$$\frac{1}{1 + s^{-1}} = \frac{s}{s+1}.$$

So the open-loop pole at $s = 0$ becomes a closed-loop zero of the error transfer function; then this zero cancels the pole of $\hat{r}(s)$, resulting in no unstable poles in $\hat{e}(s)$. Similar remarks apply for a ramp input.

Theorem 3 is a special case of an elementary principle: For perfect asymptotic tracking, the loop transfer function $\hat{L}$ must contain an internal model of the unstable poles of $\hat{r}$.

A similar analysis can be done for the situation where $r = n = 0$ and d is a sinusoid, say $d(t) = \sin(\omega t)1(t)$ (1 is the unit step). You can show this: If the feedback system is internally stable, then $y(t) \longrightarrow 0$ as $t \longrightarrow \infty$ iff either $\hat{P}$ has a zero at $s = j\omega$ or $\hat{C}$ has a pole at $s = j\omega$ (Exercise 3).

3.4 Performance

In this section we again look at tracking a reference signal, but whereas in the preceding section we considered perfect asymptotic tracking of a *single* signal, we will now consider a *set* of reference signals and a bound on the steady-state error. This performance objective will be quantified in terms of a weighted norm bound.

As before, let L denote the loop transfer function, $L := PC$. The transfer function from reference input r to tracking error e is

$$S := \frac{1}{1+L},$$

called the *sensitivity function*. In the analysis to follow, it will always be assumed that the feedback system is internally stable, so S is a stable, proper transfer function. Observe that since L is strictly proper (since P is), $S(j\infty) = 1$.

The name *sensitivity function* comes from the following idea. Let T denote the transfer function from r to y:

$$T = \frac{PC}{1+PC}.$$

One way to quantify how sensitive T is to variations in P is to take the limiting ratio of a relative perturbation in T (i.e., $\Delta T/T$) to a relative perturbation in P (i.e., $\Delta P/P$). Thinking of P as a variable and T as a function of it, we get

$$\lim_{\Delta P \to 0} \frac{\Delta T/T}{\Delta P/P} = \frac{dT}{dP}\frac{P}{T}.$$

The right-hand side is easily evaluated to be S. In this way, S is the sensitivity of the closed-loop transfer function T to an infinitesimal perturbation in P.

Now we have to decide on a performance specification, a measure of goodness of tracking. This decision depends on two things: what we know about r and what measure we choose to assign to the tracking error. Usually, r is not known in advance—few control systems are designed for one

and only one input. Rather, a set of possible rs will be known or at least postulated for the purpose of design.

Let's first consider sinusoidal inputs. Suppose that r can be any sinusoid of amplitude ≤ 1 and we want e to have amplitude $< \epsilon$. Then the performance specification can be expressed succinctly as

$$\|S\|_\infty < \epsilon.$$

Here we used Table 2.1: the maximum amplitude of e equals the ∞-norm of the transfer function. Or if we define the (trivial, in this case) weighting function $W_1(s) = 1/\epsilon$, then the performance specification is $\|W_1 S\|_\infty < 1$.

The situation becomes more realistic and more interesting with a frequency-dependent weighting function. Assume that $W_1(s)$ is real-rational; you will see below that only the magnitude of $W_1(j\omega)$ is relevant, so any poles or zeros in $\mathrm{Re}s > 0$ can be reflected into the left half-plane without changing the magnitude. Let us consider four scenarios giving rise to an ∞-norm bound on $W_1 S$. The first three require W_1 to be stable.

1. Suppose that the family of reference inputs is all signals of the form $r = W_1 r_{pf}$, where r_{pf}, a pre-filtered input, is any sinusoid of amplitude ≤ 1. Thus the set of rs consists of sinusoids with frequency-dependent amplitudes. Then the maximum amplitude of e equals $\|W_1 S\|_\infty$.

2. Recall from Chapter 2 that
$$\|r\|_2^2 = \frac{1}{2\pi} \int_{-\infty}^{\infty} |r(j\omega)|^2 \, d\omega$$
and that $\|r\|_2^2$ is a measure of the energy of r. Thus we may think of $|r(j\omega)|^2$ as *energy spectral density*, or energy spectrum. Suppose that the set of all rs is
$$\{r : r = W_1 r_{pf}, \|r_{pf}\|_2 \leq 1\},$$
that is,
$$\left\{ r : \frac{1}{2\pi} \int_{-\infty}^{\infty} |r(j\omega)/W_1(j\omega)|^2 \, d\omega \leq 1 \right\}.$$
Thus, r has an energy constraint and its energy spectrum is weighted by $1/|W_1(j\omega)|^2$. For example, if W_1 were a bandpass filter, the energy spectrum of r would be confined to the passband. More generally, W_1 could be used to shape the energy spectrum of the expected class of reference inputs. Now suppose that the tracking error measure is the 2-norm of e. Then from Table 2.2,
$$\sup_r \|e\|_2 = \sup\{\|S W_1 r_{pf}\|_2 : \|r_{pf}\|_2 \leq 1\} = \|W_1 S\|_\infty,$$
so $\|W_1 S\|_\infty < 1$ means that $\|e\|_2 < 1$ for all rs in the set above .

3. This scenario is like the preceding one except for signals of finite power. We see from Table 2.2 that $\|W_1 S\|_\infty$ equals the supremum of $pow(e)$ over all r_{pf} with $pow(r_{pf}) \leq 1$. So W_1 could be used to shape the power spectrum of the expected class of rs.

4. In several applications, for example aircraft flight-control design, designers have acquired through experience desired shapes for the Bode magnitude plot of S. In particular, suppose that good performance is known to be achieved if the plot of $|S(j\omega)|$ lies under some curve. We could rewrite this as
$$|S(j\omega)| < |W_1(j\omega)|^{-1}, \quad \forall \omega,$$
or in other words, $\|W_1 S\|_\infty < 1$.

There is a nice graphical interpretation of the norm bound $\|W_1 S\|_\infty < 1$. Note that

$$\begin{aligned} \|W_1 S\|_\infty < 1 &\Leftrightarrow \left| \frac{W_1(j\omega)}{1 + L(j\omega)} \right| < 1, \quad \forall \omega \\ &\Leftrightarrow |W_1(j\omega)| < |1 + L(j\omega)|, \quad \forall \omega. \end{aligned}$$

The last inequality says that at every frequency, the point $L(j\omega)$ on the Nyquist plot lies outside the disk of center -1, radius $|W_1(j\omega)|$ (Figure 3.5).

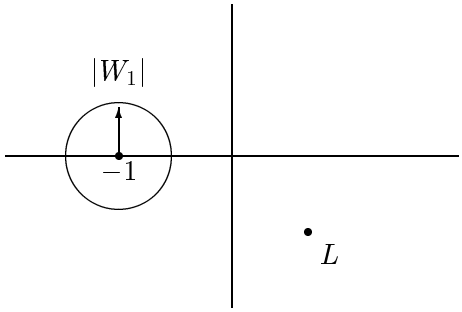

Figure 3.5: Performance specification graphically.

Other performance problems could be posed by focusing on the response to the other two exogenous inputs, d and n. Note that the transfer functions from d, n to e, u are given by

$$\begin{bmatrix} e \\ u \end{bmatrix} = - \begin{bmatrix} PS & S \\ T & CS \end{bmatrix} \begin{bmatrix} d \\ n \end{bmatrix},$$

where

$$T := 1 - S = \frac{PC}{1 + PC},$$

called the *complementary sensitivity function*.

Various performance specifications could be made using weighted versions of the transfer functions above. Note that a performance spec with weight W on PS is equivalent to the weight WP on S. Similarly, a weight W on $CS = T/P$ is equivalent to the weight W/P on T. Thus performance specs that involve e result in weights on S and performance specs on u result in weights on T. Essentially all problems in this book boil down to weighting S or T or some combination, and the tradeoff between making S small and making T small is the main issue in design.

Exercises

1. Consider the unity-feedback system $[F(s) = 1]$. The definition of internal stability is that all nine closed-loop transfer functions should be stable. In the unity-feedback case, it actually suffices to check only two of the nine. Which two?

2. In this problem and the next, there is a mixture of the time and frequency domains, so the $\hat{}$ -convention is in force.

   Let

   $$\hat{P}(s) = \frac{1}{10s + 1}, \quad \hat{C}(s) = k, \quad \hat{F}(s) = 1.$$

Find the least positive gain k so that the following are all true:

(a) The feedback system is internally stable.

(b) $|e(\infty)| \leq 0.1$ when $r(t)$ is the unit step and $n = d = 0$.

(c) $\|y\|_\infty \leq 0.1$ for all $d(t)$ such that $\|d\|_2 \leq 1$ when $r = n = 0$.

3. For the setup in Figure 3.4, take $r = n = 0$, $d(t) = \sin(\omega t)1(t)$. Prove that if the feedback system is internally stable, then $y(t) \to 0$ as $t \to \infty$ iff either $\hat{P}$ has a zero at $s = j\omega$ or $\hat{C}$ has a pole at $s = j\omega$.

4. Consider the feedback system with plant P and sensor F. Assume that P is strictly proper and F is proper. Find conditions on P and F for the existence of a proper controller so that

   The feedback system is internally stable.

   $y(t) - r(t) \to 0$ when r is a unit step.

   $y(t) \to 0$ when d is a sinusoid of frequency 100 rad/s.

Notes and References

The material in Sections 3.1 to 3.3 is quite standard. However, Section 3.4 reflects the more recent viewpoint of Zames (1981), who formulated the problem of optimizing $W_1 S$ with respect to the ∞-norm, stressing the role of the weight W_1. Additional motivation for this problem is offered in Zames and Francis (1983).

Uncertainty and Robustness

No mathematical system can exactly model a physical system. For this reason we must be aware of how modeling errors might adversely affect the performance of a control system. This chapter begins with a treatment of various models of plant uncertainty. Then robust stability, stability in the face of plant uncertainty, is studied using the small-gain theorem. The final topic is robust performance, guaranteed tracking in the face of plant uncertainty.

4.1 Plant Uncertainty

The basic technique is to model the plant as belonging to a set $\mathcal{P}$. The reasons for doing this were presented in Chapter 1. Such a set can be either *structured* or *unstructured*.

For an example of a structured set consider the plant model

$$\frac{1}{s^2 + as + 1}.$$

This is a standard second-order transfer function with natural frequency 1 rad/s and damping ratio $a/2$—it could represent, for example, a mass-spring-damper setup or an R-L-C circuit. Suppose that the constant a is known only to the extent that it lies in some interval $[a_{\min}, a_{\max}]$. Then the plant belongs to the structured set

$$\mathcal{P} = \left\{ \frac{1}{s^2 + as + 1} : a_{\min} \leq a \leq a_{\max} \right\}.$$

Thus one type of structured set is parametrized by a finite number of scalar parameters (one parameter, a, in this example). Another type of structured uncertainty is a discrete set of plants, not necessarily parametrized explicitly.

For us, unstructured sets are more important, for two reasons. First, we believe that all models used in feedback design should include some unstructured uncertainty to cover unmodeled dynamics, particularly at high frequency. Other types of uncertainty, though important, may or may not arise naturally in a given problem. Second, for a specific type of unstructured uncertainty, disk uncertainty, we can develop simple, general analysis methods. Thus the basic starting point for an unstructured set is that of disk-like uncertainty. In what follows, multiplicative disk uncertainty is chosen for detailed study. This is only one type of unstructured perturbation. The important point is that we use disk uncertainty instead of a more complicated description. We do this because it greatly simplifies our analysis and lets us say some fairly precise things. The price we pay is conservativeness.

Multiplicative Perturbation

Suppose that the nominal plant transfer function is P and consider perturbed plant transfer functions of the form $\tilde{P} = (1 + \Delta W_2)P$. Here W_2 is a fixed stable transfer function, the weight, and Δ is a variable stable transfer function satisfying $\|\Delta\|_\infty < 1$. Furthermore, it is assumed that no unstable poles of P are canceled in forming $\tilde{P}$. (Thus, P and $\tilde{P}$ have the same unstable poles.) Such a perturbation Δ is said to be *allowable*.

The idea behind this uncertainty model is that ΔW_2 is the normalized plant perturbation away from 1:

$$\frac{\tilde{P}}{P} - 1 = \Delta W_2.$$

Hence if $\|\Delta\|_\infty \leq 1$, then

$$\left| \frac{\tilde{P}(j\omega)}{P(j\omega)} - 1 \right| \leq |W_2(j\omega)|, \qquad \forall \omega,$$

so $|W_2(j\omega)|$ provides the uncertainty profile. This inequality describes a disk in the complex plane: At each frequency the point $\tilde{P}/P$ lies in the disk with center 1, radius $|W_2|$. Typically, $|W_2(j\omega)|$ is a (roughly) increasing function of ω: Uncertainty increases with increasing frequency. The main purpose of Δ is to account for phase uncertainty and to act as a scaling factor on the magnitude of the perturbation (i.e., $|\Delta|$ varies between 0 and 1).

Thus, this uncertainty model is characterized by a nominal plant P together with a weighting function W_2. How does one get the weighting function W_2 in practice? This is illustrated by a few examples.

Example 1 Suppose that the plant is stable and its transfer function is arrived at by means of frequency-response experiments: Magnitude and phase are measured at a number of frequencies, $\omega_i, i = 1, \ldots, m$, and this experiment is repeated several, say n, times. Let the magnitude-phase measurement for frequency ω_i and experiment k be denoted (M_{ik}, ϕ_{ik}). Based on these data select nominal magnitude-phase pairs (M_i, ϕ_i) for each frequency ω_i, and fit a nominal transfer function $P(s)$ to these data. Then fit a weighting function $W_2(s)$ so that

$$\left| \frac{M_{ik} \mathrm{e}^{j\phi_{ik}}}{M_i \mathrm{e}^{j\phi_i}} - 1 \right| \leq |W_2(j\omega_i)|, \quad i = 1, \ldots, m; \ k = 1, \ldots, n.$$

Example 2 Assume that the nominal plant transfer function is a double integrator:

$$P(s) = \frac{1}{s^2}.$$

For example, a dc motor with negligible viscous damping could have such a transfer function. You can think of other physical systems with only inertia, no damping. Suppose that a more detailed model has a time delay, yielding the transfer function

$$\tilde{P}(s) = \mathrm{e}^{-\tau s} \frac{1}{s^2},$$

and suppose that the time delay is known only to the extent that it lies in the interval $0 \leq \tau \leq 0.1$. This time-delay factor $\exp(-\tau s)$ can be treated as a multiplicative perturbation of the nominal plant by embedding $\tilde{P}$ in the family

$$\{(1 + \Delta W_2)P : \|\Delta\|_\infty \leq 1\}.$$

To do this, the weight W_2 should be chosen so that the normalized perturbation satisfies

$$\left| \frac{\tilde{P}(j\omega)}{P(j\omega)} - 1 \right| \leq |W_2(j\omega)|, \quad \forall \omega, \tau,$$

that is,

$$\left| \mathrm{e}^{-\tau j\omega} - 1 \right| \leq |W_2(j\omega)|, \quad \forall \omega, \tau.$$

A little time with Bode magnitude plots shows that a suitable first-order weight is

$$W_2(s) = \frac{0.21s}{0.1s + 1}.$$

Figure 4.1 is the Bode magnitude plot of this W_2 and $\exp(-\tau s) - 1$ for $\tau = 0.1$, the worst value.

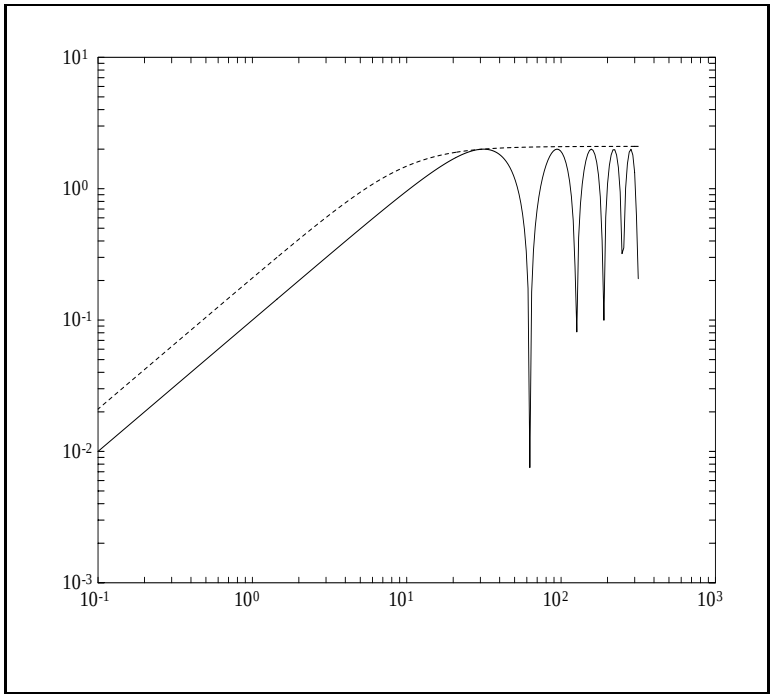

Figure 4.1: Bode plots of W_2 (dash) and $\exp(-0.1s) - 1$ (solid).

To get a feeling for how conservative this is, compare at a few frequencies ω the actual uncertainty set

$$\left\{ \frac{\tilde{P}(j\omega)}{P(j\omega)} : 0 \leq \tau \leq 0.1 \right\} = \left\{ \mathrm{e}^{-\tau j\omega} : 0 \leq \tau \leq 0.1 \right\}$$

with the covering disk

$$\{s : |s - 1| \leq |W_2(j\omega)|\}.$$

Example 3 Suppose that the plant transfer function is

$$\tilde{P}(s) = \frac{k}{s - 2},$$

where the gain k is uncertain but is known to lie in the interval $[0.1, 10]$. This plant too can be embedded in a family consisting of multiplicative perturbations of a nominal plant

$$P(s) = \frac{k_0}{s-2}.$$

The weight W_2 must satisfy

$$\left| \frac{\tilde{P}(j\omega)}{P(j\omega)} - 1 \right| \leq |W_2(j\omega)|, \quad \forall \omega, k,$$

that is,

$$\max_{0.1 \leq k \leq 10} \left| \frac{k}{k_0} - 1 \right| \leq |W_2(j\omega)|, \quad \forall \omega.$$

The left-hand side is minimized by $k_0 = 5.05$, for which the left-hand side equals $4.95/5.05$. In this way we get the nominal plant

$$P(s) = \frac{5.05}{s-2}$$

and constant weight $W_2(s) = 4.95/5.05$.

The multiplicative perturbation model is not suitable for every application because the disk covering the uncertainty set is sometimes too coarse an approximation. In this case a controller designed for the multiplicative uncertainty model would probably be too conservative for the original uncertainty model.

The discussion above illustrates an important point. In modeling a plant we may arrive at a certain plant set. This set may be too awkward to cope with mathematically, so we may embed it in a larger set that is easier to handle. Conceivably, the achievable performance for the larger set may not be as good as the achievable performance for the smaller; that is, there may exist—even though we cannot find it—a controller that is better for the smaller set than the controller we design for the larger set. In this sense the latter controller is *conservative* for the smaller set.

In this book we stick with plant uncertainty that is disk-like. It will be conservative for some problems, but the payoff is that we obtain some very nice theoretical results. The resulting theory is remarkably practical as well.

Other Perturbations

Other uncertainty models are possible besides multiplicative perturbations, as illustrated by the following example.

Example 4 As at the start of this section, consider the family of plant transfer functions

$$\frac{1}{s^2 + as + 1}, \quad 0.4 \leq a \leq 0.8.$$

Thus

$$a = 0.6 + 0.2\Delta, \quad -1 \leq \Delta \leq 1,$$

so the family can be expressed as

$$\frac{P(s)}{1 + \Delta W_2(s) P(s)}, \quad -1 \leq \Delta \leq 1,$$

where

$$P(s) := \frac{1}{s^2 + 0.6s + 1}, \quad W_2(s) := 0.2s.$$

Note that P is the nominal plant transfer function for the value $a = 0.6$, the midpoint of the interval. The block diagram corresponding to this representation of the plant is shown in Figure 4.2. Thus

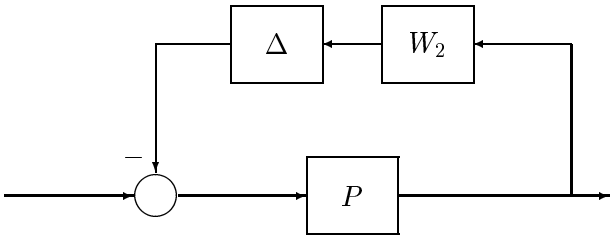

Figure 4.2: Example 4.

the original plant has been represented as a feedback uncertainty around a nominal plant.

The following list summarizes the common uncertainty models:

$$(1 + \Delta W_2)P$$
$$P + \Delta W_2$$
$$P/(1 + \Delta W_2 P)$$
$$P/(1 + \Delta W_2)$$

Appropriate assumptions would be made on Δ and W_2 in each case. Typically, we can relax the assumption that Δ be stable; but then the theorems to follow would be harder to prove.

4.2 Robust Stability

The notion of robustness can be described as follows. Suppose that the plant transfer function P belongs to a set $\mathcal{P}$, as in the preceding section. Consider some characteristic of the feedback system, for example, that it is internally stable. A controller C is *robust* with respect to this characteristic if this characteristic holds for every plant in $\mathcal{P}$. The notion of robustness therefore requires a controller, a set of plants, and some characteristic of the system. For us, the two most important variations of this notion are robust stability, treated in this section, and robust performance, treated in the next.

A controller C provides *robust stability* if it provides internal stability for every plant in $\mathcal{P}$. We might like to have a test for robust stability, a test involving C and $\mathcal{P}$. Or if $\mathcal{P}$ has an associated size, the maximum size such that C stabilizes all of $\mathcal{P}$ might be a useful notion of stability margin.

The Nyquist plot gives information about stability margin. Note that the distance from the critical point -1 to the nearest point on the Nyquist plot of L equals $1/\|S\|_\infty$:

$$\begin{aligned} \text{distance from -1 to Nyquist plot} &= \inf_\omega |-1 - L(j\omega)| \\ &= \inf_\omega |1 + L(j\omega)| \\ &= \left[\sup_\omega \frac{1}{|1 + L(j\omega)|}\right]^{-1} \end{aligned}$$

$$= \|S\|_\infty^{-1}.$$

Thus if $\|S\|_\infty \gg 1$, the Nyquist plot comes close to the critical point, and the feedback system is nearly unstable. However, as a measure of stability margin this distance is not entirely adequate because it contains no frequency information. More precisely, if the nominal plant P is perturbed to $\tilde{P}$, having the same number of unstable poles as has P and satisfying the inequality

$$|\tilde{P}(j\omega)C(j\omega) - P(j\omega)C(j\omega)| < \|S\|_\infty^{-1}, \quad \forall\omega,$$

then internal stability is preserved (the number of encirclements of the critical point by the Nyquist plot does not change). But this is usually very conservative; for instance, larger perturbations could be allowed at frequencies where $P(j\omega)C(j\omega)$ is far from the critical point.

Better stability margins are obtained by taking explicit frequency-dependent perturbation models: for example, the multiplicative perturbation model, $\tilde{P} = (1 + \Delta W_2)P$. Fix a positive number β and consider the family of plants

$$\{\tilde{P} : \Delta \text{ is stable and } \|\Delta\|_\infty \leq \beta\}.$$

Now a controller C that achieves internal stability for the nominal plant P will stabilize this entire family if β is small enough. Denote by β_{sup} the least upper bound on β such that C achieves internal stability for the entire family. Then β_{sup} is a stability margin (with respect to this uncertainty model). Analogous stability margins could be defined for the other uncertainty models.

We turn now to two classical measures of stability margin, gain and phase margin. Assume that the feedback system is internally stable with plant P and controller C. Now perturb the plant to kP, with k a positive real number. The *upper gain margin*, denoted $k_{\max}$, is the first value of k greater than 1 when the feedback system is not internally stable; that is, $k_{\max}$ is the maximum number such that internal stability holds for $1 \leq k < k_{\max}$. If there is no such number, then set $k_{\max} := \infty$. Similarly, the *lower gain margin*, $k_{\min}$, is the least nonnegative number such that internal stability holds for $k_{\min} < k \leq 1$. These two numbers can be read off the Nyquist plot of L; for example, $-1/k_{\max}$ is the point where the Nyquist plot intersects the segment $(-1, 0)$ of the real axis, the closest point to -1 if there are several points of intersection.

Now perturb the plant to $\mathrm{e}^{-j\phi}P$, with ϕ a positive real number. The *phase margin*, $\phi_{\max}$, is the maximum number (usually expressed in degrees) such that internal stability holds for $0 \leq \phi < \phi_{\max}$. You can see that $\phi_{\max}$ is the angle through which the Nyquist plot must be rotated until it passes through the critical point, -1; or, in radians, $\phi_{\max}$ equals the arc length along the unit circle from the Nyquist plot to the critical point.

Thus gain and phase margins measure the distance from the critical point to the Nyquist plot in certain specific directions. Gain and phase margins have traditionally been important measures of stability robustness: if either is small, the system is close to instability. Notice, however, that the gain and phase margins can be relatively large and yet the Nyquist plot of L can pass close to the critical point; that is, *simultaneous* small changes in gain and phase could cause internal instability. We return to these margins in Chapter 11.

Now we look at a typical robust stability test, one for the multiplicative perturbation model. Assume that the nominal feedback system (i.e., with $\Delta = 0$) is internally stable for controller C. Bring in again the complementary sensitivity function

$$T = 1 - S = \frac{L}{1+L} = \frac{PC}{1+PC}.$$

Theorem 1 *(Multiplicative uncertainty model) C provides robust stability iff $\|W_2T\|_\infty < 1$.*

Proof ($\Leftarrow$) Assume that $\|W_2T\|_\infty < 1$. Construct the Nyquist plot of L, indenting $\mathcal{D}$ to the left around poles on the imaginary axis. Since the nominal feedback system is internally stable, we know this from the Nyquist criterion: The Nyquist plot of L does not pass through -1 and its number of counterclockwise encirclements equals the number of poles of P in Re$s \geq 0$ plus the number of poles of C in Re$s \geq 0$.

Fix an allowable Δ. Construct the Nyquist plot of $\tilde{P}C = (1 + \Delta W_2)L$. No additional indentations are required since ΔW_2 introduces no additional imaginary axis poles. We have to show that the Nyquist plot of $(1 + \Delta W_2)L$ does not pass through -1 and its number of counterclockwise encirclements equals the number of poles of $(1 + \Delta W_2)P$ in Re $s \geq 0$ plus the number of poles of C in Re $s \geq 0$; equivalently, the Nyquist plot of $(1 + \Delta W_2)L$ does not pass through -1 and encircles it exactly as many times as does the Nyquist plot of L. We must show, in other words, that the perturbation does not change the number of encirclements.

The key equation is

$$1 + (1 + \Delta W_2)L = (1 + L)(1 + \Delta W_2 T). \tag{4.1}$$

Since

$$\|\Delta W_2 T\|_\infty \leq \|W_2 T\|_\infty < 1,$$

the point $1 + \Delta W_2 T$ always lies in some closed disk with center 1, radius < 1, for all points s on $\mathcal{D}$. Thus from (4.1), as s goes once around $\mathcal{D}$, the net change in the angle of $1 + (1 + \Delta W_2)L$ equals the net change in the angle of $1 + L$. This gives the desired result.

($\Rightarrow$) Suppose that $\|W_2T\|_\infty \geq 1$. We will construct an allowable Δ that destabilizes the feedback system. Since T is strictly proper, at some frequency ω,

$$|W_2(j\omega)T(j\omega)| = 1. \tag{4.2}$$

Suppose that $\omega = 0$. Then $W_2(0)T(0)$ is a real number, either $+1$ or -1. If $\Delta = -W_2(0)T(0)$, then Δ is allowable and

$$1 + \Delta W_2(0)T(0) = 0.$$

From (4.1) the Nyquist plot of $(1 + \Delta W_2)L$ passes through the critical point, so the perturbed feedback system is not internally stable.

If $\omega > 0$, constructing an admissible Δ takes a little more work; the details are omitted. ■

The theorem can be used effectively to find the stability margin $\beta_{\sup}$ defined previously. The simple scaling technique

$$\begin{aligned} \{\tilde{P} = (1 + \Delta W_2)P : \|\Delta\|_\infty \leq \beta\} &= \{\tilde{P} = (1 + \beta^{-1}\Delta\beta W_2)P : \|\beta^{-1}\Delta\|_\infty \leq 1\} \\ &= \{\tilde{P} = (1 + \Delta_1 \beta W_2)P : \|\Delta_1\|_\infty \leq 1\} \end{aligned}$$

together with the theorem shows that

$$\beta_{\sup} = \sup\{\beta : \|\beta W_2 T\|_\infty < 1\} = 1/\|W_2 T\|_\infty.$$

The condition $\|W_2T\|_\infty < 1$ also has a nice graphical interpretation. Note that

$$\begin{aligned} \|W_2T\|_\infty < 1 &\Leftrightarrow \left|\frac{W_2(j\omega)L(j\omega)}{1 + L(j\omega)}\right| < 1, \quad \forall\omega \\ &\Leftrightarrow |W_2(j\omega)L(j\omega)| < |1 + L(j\omega)|, \quad \forall\omega. \end{aligned}$$

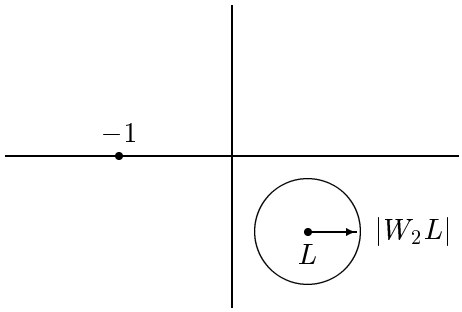

Figure 4.3: Robust stability graphically.

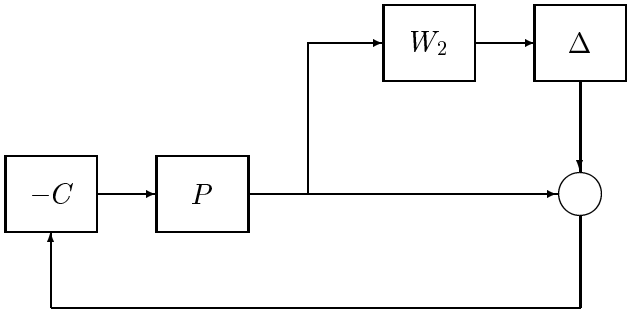

Figure 4.4: Perturbed feedback system.

The last inequality says that at every frequency, the critical point, -1, lies outside the disk of center $L(j\omega)$, radius $|W_2(j\omega)L(j\omega)|$ (Figure 4.3).

There is a simple way to see the relevance of the condition $\|W_2T\|_\infty < 1$. First, draw the block diagram of the perturbed feedback system, but ignoring inputs (Figure 4.4). The transfer function from the output of Δ around to the input of Δ equals $-W_2T$, so the block diagram collapses to the configuration shown in Figure 4.5. The maximum loop gain in Figure 4.5 equals $\|-\Delta W_2T\|_\infty$,

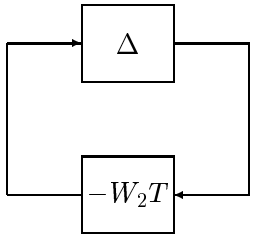

Figure 4.5: Collapsed block diagram.

which is < 1 for all allowable Δs iff the small-gain condition $\|W_2T\|_\infty < 1$ holds.

The foregoing discussion is related to the *small-gain theorem*, a special case of which is this: If L is stable and $\|L\|_\infty < 1$, then $(1+L)^{-1}$ is stable too. An easy proof uses the Nyquist criterion.

Summary of Robust Stability Tests

Table 4.1 summarizes the robust stability tests for the other uncertainty models.

Perturbation	Condition
$(1+\Delta W_2)P$	$\|W_2T\|_\infty < 1$
$P+\Delta W_2$	$\|W_2CS\|_\infty < 1$
$P/(1+\Delta W_2P)$	$\|W_2PS\|_\infty < 1$
$P/(1+\Delta W_2)$	$\|W_2S\|_\infty < 1$

Table 4.1

Note that we get the same four transfer functions—T, CS, PS, S—as we did in Section 3.4. This should not be too surprising since (up to sign) these are the only closed-loop transfer functions for a unity feedback SISO system.

4.3 Robust Performance

Now we look into performance of the perturbed plant. Suppose that the plant transfer function belongs to a set $\mathcal{P}$. The general notion of *robust performance* is that internal stability and performance, of a specified type, should hold for all plants in $\mathcal{P}$. Again we focus on multiplicative perturbations.

Recall that when the nominal feedback system is internally stable, the *nominal performance* condition is $\|W_1S\|_\infty < 1$ and the *robust stability* condition is $\|W_2T\|_\infty < 1$. If P is perturbed to $(1+\Delta W_2)P$, S is perturbed to

$$\frac{1}{1+(1+\Delta W_2)L} = \frac{S}{1+\Delta W_2T}.$$

Clearly, the *robust performance* condition should therefore be

$$\|W_2T\|_\infty < 1 \text{ and } \left\| \frac{W_1S}{1+\Delta W_2T} \right\|_\infty < 1, \quad \forall \Delta.$$

Here Δ must be allowable. The next theorem gives a test for robust performance in terms of the function

$$s \mapsto |W_1(s)S(s)| + |W_2(s)T(s)|,$$

which is denoted $|W_1S| + |W_2T|$.

Theorem 2 *A necessary and sufficient condition for robust performance is*

$$\| |W_1S| + |W_2T| \|_\infty < 1. \tag{4.3}$$

Proof ($\Leftarrow$) Assume (4.3), or equivalently,

$$\|W_2T\|_\infty \text{ and } \left\| \frac{W_1S}{1-|W_2T|} \right\|_\infty < 1. \tag{4.4}$$

Fix Δ. In what follows, functions are evaluated at an arbitrary point $j\omega$, but this is suppressed to simplify notation. We have

$$1 = |1 + \Delta W_2 T - \Delta W_2 T| \leq |1 + \Delta W_2 T| + |W_2 T|$$

and therefore

$$1 - |W_2 T| \leq |1 + \Delta W_2 T|.$$

This implies that

$$\left\| \frac{W_1 S}{1 - |W_2 T|} \right\|_\infty \geq \left\| \frac{W_1 S}{1 + \Delta W_2 T} \right\|_\infty .$$

This and (4.4) yield

$$\left\| \frac{W_1 S}{1 + \Delta W_2 T} \right\|_\infty < 1.$$

($\Rightarrow$) Assume that

$$\|W_2 T\|_\infty < 1 \text{ and } \left\| \frac{W_1 S}{1 + \Delta W_2 T} \right\|_\infty < 1, \quad \forall \Delta. \tag{4.5}$$

Pick a frequency ω where

$$\frac{|W_1 S|}{1 - |W_2 T|}$$

is maximum. Now pick Δ so that

$$1 - |W_2 T| = |1 + \Delta W_2 T|.$$

The idea here is that $\Delta(j\omega)$ should rotate $W_2(j\omega)T(j\omega)$ so that $\Delta(j\omega)W_2(j\omega)T(j\omega)$ is negative real. The details of how to construct such an allowable Δ are omitted. Now we have

$$\begin{aligned} \left\| \frac{W_1 S}{1 - |W_2 T|} \right\|_\infty &= \frac{|W_1 S|}{1 - |W_2 T|} \\ &= \frac{|W_1 S|}{|1 + \Delta W_2 T|} \\ &\leq \left\| \frac{W_1 S}{1 + \Delta W_2 T} \right\|_\infty . \end{aligned}$$

So from this and (4.5) there follows (4.4). ■

Test (4.3) also has a nice graphical interpretation. For each frequency ω, construct two closed disks: one with center -1, radius $|W_1(j\omega)|$; the other with center $L(j\omega)$, radius $|W_2(j\omega)L(j\omega)|$. Then (4.3) holds iff for each ω these two disks are disjoint (Figure 4.6).

The robust performance condition says that the robust performance level 1 is achieved. More generally, let's say that robust performance level α is achieved if

$$\|W_2 T\|_\infty < 1 \text{ and } \left\| \frac{W_1 S}{1 + \Delta W_2 T} \right\|_\infty < \alpha, \quad \forall \Delta.$$

Noting that at every frequency

$$\max_{|\Delta| \leq 1} \left| \frac{W_1 S}{1 + \Delta W_2 T} \right| = \frac{|W_1 S|}{1 - |W_2 T|}$$

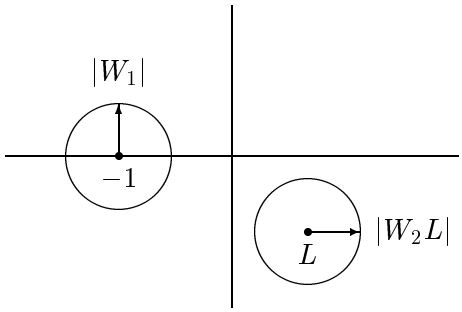

Figure 4.6: Robust performance graphically.

we get that the minimum α equals

$$\left\| \frac{W_1 S}{1 - |W_2 T|} \right\|_\infty . \tag{4.6}$$

Alternatively, we may wish to know how large the uncertainty can be while the robust performance condition holds. To do this, we scale the uncertainty level, that is, we allow Δ to satisfy $\|\Delta\|_\infty < \beta$. Application of Theorem 1 shows that internal stability is robust iff $\|\beta W_2 T\|_\infty < 1$. Let's say that the uncertainty level β is permissible if

$$\|\beta W_2 T\|_\infty < 1 \text{ and } \left\| \frac{W_1 S}{1 + \Delta W_2 T} \right\|_\infty < 1, \quad \forall \Delta.$$

Again, noting that

$$\max_{|\Delta| \le 1} \left| \frac{W_1 S}{1 + \beta \Delta W_2 T} \right| = \frac{|W_1 S|}{1 - \beta |W_2 T|},$$

we get that the maximum β equals

$$\left\| \frac{W_2 T}{1 - |W_1 S|} \right\|_\infty^{-1} .$$

Now we turn briefly to some related problems.

Robust Stability for Multiple Perturbations

Suppose that a nominal plant P is perturbed to

$$\tilde{P} = P \frac{1 + \Delta_2 W_2}{1 + \Delta_1 W_1}$$

with W_1, W_2 both stable and Δ_1, Δ_2 both admissible. The robust stability condition is

$$\| |W_1 S| + |W_2 T| \|_\infty < 1,$$

which is just the robust performance condition in Theorem 2. A sketch of the proof goes like this: From the fourth entry in Table 4.1, for fixed Δ_2 the robust stability condition for varying Δ_1 is

$$\left\| W_1 \frac{1}{1 + (1 + \Delta_2 W_2) L} \right\|_\infty < 1.$$

Then from Theorem 2 this holds for all admissible Δ_2 iff

$$\| |W_1 S| + |W_2 T| \|_\infty < 1.$$

This illustrates a more general point: Robust performance with one perturbation is equivalent to robust stability with two perturbations, provided that performance is in terms of the ∞-norm and the second perturbation is chosen appropriately.

Robust Command Response

Consider the block diagram shown in Figure 4.7. Shown are a plant P and two controller compo-

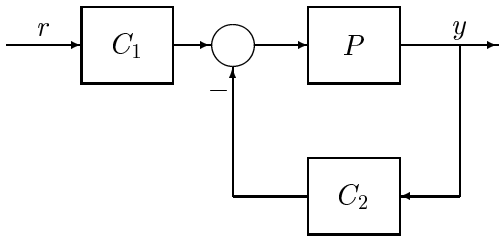

Figure 4.7: Two-degree-of-freedom controller.

nents, C_1 and C_2. This is known as a two-degree-of-freedom controller because the plant input is allowed to be a function of the two signals r and y independently, not just $r - y$. We will not go into details about such controllers or about the appropriate definition of internal stability.

Define

$$S := \frac{1}{1 + PC_2}, \quad T := 1 - S.$$

Then the transfer function from r to y, denoted T_{yr}, is

$$T_{yr} = PSC_1.$$

Let M be a transfer function representing a model that we want the foregoing system to emulate. Denote by e the difference between y and the output of M. The error transfer function, that from r to e, is

$$T_{er} = T_{yr} - M = PSC_1 - M.$$

The ideal choice for C_1, the one making $T_{er} = 0$, would therefore be

$$C_1 = \frac{M}{PS}.$$

This choice may violate the internal stability constraint, but let's suppose that in order to continue that it does not (this places some limitations on M).

Consider now a multiplicative perturbation of the plant: P becomes $\tilde{P} = (1 + \Delta W_2)P$, Δ admissible. Then T_{er} becomes

$$\begin{aligned} \tilde{T}_{er} &= \frac{\tilde{P}C_1}{1 + \tilde{P}C_2} - M \\ &= \frac{\tilde{P}}{1 + \tilde{P}C_2}\frac{M}{PS} - M \\ &= \frac{\Delta W_2 MS}{1 + \Delta W_2 T} \text{ (after some algebra).} \end{aligned}$$

Defining $W_1 := W_2 M$, we find that the maximum ∞-norm of the error transfer function, over all admissible Δ, is

$$\max_{\Delta} \|\tilde{T}_{ec}\|_\infty = \left\| \frac{W_1 S}{1 - |W_2 T|} \right\|_\infty .$$

The right-hand side we have already seen in (4.6).

Note that we convert the problem of making the closed-loop response from r to y match some desired response by subtracting off that desired response and forming an error signal e which we seek to keep small. In some treatments of the command response problem, the performance specification is taken to be: make $|T_{yr}|$ close to a desired model. The problem with this specification is that two transfer functions can be close in magnitude but differ substantially in phase. Surprisingly, this can occur even when both transfer functions are minimum phase. The interested reader may want to investigate this further using the gain-phase relation developed in Chapter 7.

4.4 Robust Performance More Generally

Theorem 2 gives the robust performance test under the following conditions:

Perturbation model:	$(1 + \Delta W_2)P$
Nominal performance condition:	$\|W_1 S\|_\infty < 1$

Table 4.2 gives tests for the four uncertainty models and two nominal performance conditions.

	Nominal Performance Condition	
Perturbation	$\|W_1 S\|_\infty < 1$	$\|W_1 T\|_\infty < 1$
$(1 + \Delta W_2)P$	$\|\|W_1 S\| + \|W_2 T\|\|_\infty < 1$	messy
$P + W_2 \Delta$	$\|\|W_1 S\| + \|W_2 C S\|\|_\infty < 1$	messy
$P/(1 + \Delta W_2 P)$	messy	$\|\|W_1 T\| + \|W_2 P S\|\|_\infty < 1$
$P/(1 + \Delta W_2)$	messy	$\|\|W_1 T\| + \|W_2 S\|\|_\infty < 1$

Table 4.2

The entries marked *messy* are just that. The difficulty is the way in which Δ enters. For example, consider the case where

Perturbation model:	$(1 + \Delta W_2)P$
Nominal performance condition:	$\|W_1 T\|_\infty < 1$

The perturbed T is

$$\frac{(1 + \Delta W_2)PC}{1 + (1 + \Delta W_2)PC} = \frac{(1 + \Delta W_2)T}{1 + \Delta W_2 T},$$

so the perturbed performance condition is equivalent to

$$|W_1(1 + \Delta W_2)T| < |1 + \Delta W_2 T|, \quad \forall \omega.$$

Now for each fixed ω

$$|W_1(1 + \Delta W_2)T| \leq |W_1 T|(1 + |W_2|)$$

and

$$1 - |W_2T| \le |1 + \Delta W_2T|.$$

So a sufficient condition for robust performance is

$$\left\| \frac{W_1T(1 + |W_2|)}{1 - |W_2T|} \right\|_\infty < 1.$$

4.5 Conclusion

The nominal feedback system is assumed to be internally stable. Then the *nominal performance* condition is $\|W_1S\|_\infty < 1$ and the *robust stability* condition (with respect to multiplicative perturbations) is $\|W_2T\|_\infty < 1$.

The condition for simultaneously achieving nominal performance and robust stability is

$$\| \max\,(|W_1S|, |W_2T|)\|_\infty < 1. \tag{4.7}$$

The *robust performance* condition is

$$\|W_2T\|_\infty < 1 \text{ and } \left\| \frac{W_1S}{1 + \Delta W_2T} \right\|_\infty < 1, \quad \forall \Delta$$

and the test for this is

$$\||W_1S| + |W_2T|\|_\infty < 1. \tag{4.8}$$

Since

$$\max\,(|W_1S|, |W_2T|) \le |W_1S| + |W_2T| \le 2 \max\,(|W_1S|, |W_2T|) \tag{4.9}$$

conditions (4.7) and (4.8) are not too far apart. For instance, if nominal performance and robust stability are obtained with a safety factor of 2, that is,

$$\|W_1S\|_\infty < 1/2, \quad \|W_2T\|_\infty < 1/2,$$

then robust performance is automatically obtained.

A compromise condition, which we shall treat in Chapters 8 and 12, is

$$\|(|W_1S|^2 + |W_2T|^2)^{1/2}\|_\infty < 1. \tag{4.10}$$

Simple plane geometry shows that

$$\max\,(|W_1S|, |W_2T|) \le (|W_1S|^2 + |W_2T|^2)^{1/2} \le |W_1S| + |W_2T| \tag{4.11}$$

and

$$\frac{1}{\sqrt{2}}(|W_1S| + |W_2T|) \le (|W_1S|^2 + |W_2T|^2)^{1/2} \le \sqrt{2} \max\,(|W_1S|, |W_2T|). \tag{4.12}$$

Thus (4.10) is a reasonable approximation to both (4.7) and (4.8).

To elaborate on this point, let's consider

$$x = \begin{pmatrix} x_1 \\ x_2 \end{pmatrix} = \begin{pmatrix} |W_1S| \\ |W_2T| \end{pmatrix}$$

as a vector in $\mathbb{R}^2$. Then (4.7), (4.8), and (4.10) correspond, respectively, to the three different norms

$$\max\,(|x_1|, |x_2|), \quad |x_1| + |x_2|, \quad (|x_1|^2 + |x_2|^2)^{1/2}.$$

The third is the Euclidean norm and is the most tractable. The point being made here is that choice of these spatial norms is not crucial: The tradeoffs between $|W_1S|$ and $|W_2T|$ inherent in control problems mean that although the norms may differ by as much as a factor of 2, the actual solutions one gets by using the different norms are not very different.

Exercises

1. Consider a unity-feedback system. True or false: If a controller internally stabilizes two plants, they have the same number of poles in Re$s \geq 0$.

2. Unity-feedback problem. Let $P_\alpha(s)$ be a plant depending on a real parameter α. Suppose that the poles of P_α move continuously as α varies over the interval $[0, 1]$. True or false: If a controller internally stabilizes P_α for every α in $[0, 1]$, then P_α has the same number of poles in Re $s \geq 0$ for every α in $[0, 1]$.

3. For the unity-feedback system with $P(s) = k/s$, does there exist a proper controller $C(s)$ such that the feedback system is internally stable for both $k = +1$ and $k = -1$?

4. Suppose that
$$P(s) = \frac{\omega_n^2}{s(s + 2\zeta\omega_n)}, \quad C(s) = 1$$
with $\omega_n, \zeta > 0$. Note that the characteristic polynomial is the standard second-order one. Find the phase margin as a function of ζ. Sketch the graph of this function.

5. Consider the unity-feedback system with
$$P(s) = \frac{1}{(s + 1)(s + \alpha)}, \quad C(s) = \frac{1}{s}.$$
For what range of α (a real number) is the feedback system internally stable? Find the upper and lower gain margins as functions of α.

6. This problem studies robust stability for real parameter variations. Consider the unity-feedback system with $C(s) = 10$ and plant
$$\frac{1}{s - a},$$
where a is real.

   (a) Find the range of a for the feedback system to be internally stable.

   (b) For $a = 0$ the plant is $P(s) = 1/s$. Regarding a as a perturbation, we can write the plant as
$$\tilde{P} = \frac{P}{1 + \Delta W_2 P}$$
with $W_2(s) = -a$. Then $\tilde{P}$ equals the true plant when $\Delta(s) = 1$. Apply robust stability theory to see when the feedback system with plant $\tilde{P}$ is internally stable for all $\|\Delta\|_\infty \leq 1$. You will get a smaller range for a than in part (a).

   (c) Repeat with the nominal plant $P(s) = 1/(s + 100)$.

7. This problem concerns robust stability of the unity-feedback system. Suppose that P and C are nominal transfer functions for which the feedback system is internally stable. Instead of allowing perturbations in just P, this problem allows perturbations in C too. Suppose that P may be perturbed to
$$(1 + \Delta_1 W)P$$

and C may be perturbed to

$$(1 + \Delta_2 V)C.$$

The transfer functions W and V are fixed, while Δ_1 and Δ_2 are variable transfer functions having ∞-norms no greater than 1. Making appropriate additional assumptions, find a sufficient condition, depending only on the four functions P, C, W, V, for robust stability. Prove sufficiency. (A weak sufficient condition is the goal; for example, the condition $W = V = 0$ would be too strong.)

8. Assume that the nominal plant transfer function is a double integrator,

$$P(s) = \frac{1}{s^2}.$$

The performance requirement is that the plant output should track reference inputs over the frequency range $[0, 1]$. The performance weight W_1 could therefore be chosen so that its magnitude is constant over this frequency range and then rolls off at higher frequencies. A common choice for W_1 is a Butterworth filter, which is maximally flat over its bandwidth. Choose a third-order Butterworth filter for W_1 with cutoff frequency 1 rad/s. Take the weight W_2 to be

$$W_2(s) = \frac{0.21s}{0.1s + 1}.$$

(a) Design a proper C to achieve internal stability for the nominal plant.

(b) Check the robust stability condition $\|W_2 T\|_\infty < 1$. If this does not hold, redesign C until it does. It is not necessary to get a C that yields good performance.

(c) Compute the robust performance level α for your controller from (4.6).

9. Consider the class of perturbed plants of the form

$$\frac{P}{1 + \Delta W_2 P},$$

where W_2 is a fixed stable weighting function with $W_2 P$ strictly proper and Δ is a variable stable transfer function with $\|\Delta\|_\infty \leq 1$. Assume that C is a controller achieving internal stability for P. Prove that C provides internal stability for the perturbed plant if $\|W_2 PS\|_\infty < 1$.

10. Suppose that the plant transfer function is

$$\tilde{P}(s) = [1 + \Delta(s) W_2(s)]\, P(s),$$

where

$$W_2(s) = \frac{2}{s + 10}, \quad P(s) = \frac{1}{s - 1},$$

and the stable perturbation Δ satisfies $\|\Delta\|_\infty \leq 2$. Suppose that the controller is the pure gain $C(s) = k$. We want the feedback system to be internally stable for all such perturbations. Determine over what range of k this is true.

Notes and References

The basis for this chapter is Doyle and Stein (1981). This paper emphasized the importance of explicit uncertainty models such as multiplicative and additive. Theorem 1 is stated in that paper, but a complete proof is due to Chen and Desoer (1982). The sufficiency part of this theorem is a version of the small-gain theorem, due to Sandberg and Zames [see, e.g., Desoer and Vidyasagar (1975)].

Stabilization

In this chapter we study the unity-feedback system with block diagram shown in Figure 5.1. Here

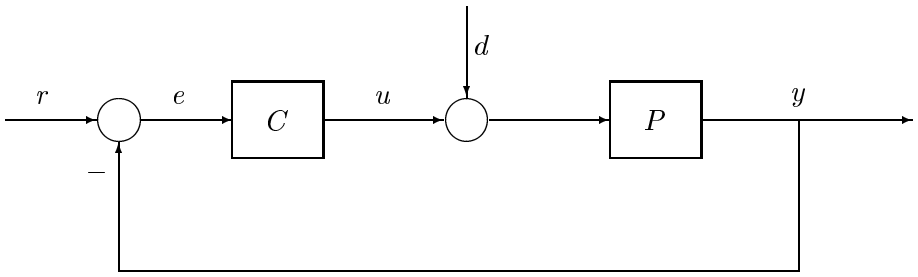

Figure 5.1: Unity-feedback system.

P is strictly proper and C is proper.

Most synthesis problems can be formulated in this way: Given P, design C so that the feedback system (1) is internally stable, and (2) acquires some additional desired property; for example, the output y asymptotically tracks a step input r. The method of solution is to parametrize all Cs for which (1) is true, and then to see if there exists a parameter for which (2) holds. In this chapter such a parametrization is derived and then applied to two problems: achieving asymptotic performance specs and internal stabilization by a stable controller.

5.1 Controller Parametrization: Stable Plant

In this section we assume that P is already stable, and we parametrize all Cs for which the feedback system is internally stable. Introduce the symbol $\mathcal{S}$ for the family of all stable, proper, real-rational functions. Notice that $\mathcal{S}$ is closed under addition and multiplication: If $F, G \in \mathcal{S}$, then $F + G, FG \in \mathcal{S}$. Also, $1 \in \mathcal{S}$. (Thus $\mathcal{S}$ is a commutative ring with identity.)

Theorem 1 *Assume that $P \in \mathcal{S}$. The set of all Cs for which the feedback system is internally stable equals*

$$\left\{ \frac{Q}{1 - PQ} : Q \in \mathcal{S} \right\}.$$

Proof ($\subset$) Suppose that C achieves internal stability. Let Q denote the transfer function from r to u, that is,

$$Q := \frac{C}{1+PC}.$$

Then $Q \in \mathcal{S}$ and

$$C = \frac{Q}{1-PQ}.$$

($\supset$) Conversely, suppose that $Q \in \mathcal{S}$ and define

$$C := \frac{Q}{1-PQ}. \tag{5.1}$$

According to the definition in Section 3.2, the feedback system is internally stable iff the nine transfer functions

$$\frac{1}{1+PC}\begin{bmatrix} 1 & -P & -1 \\ C & 1 & -C \\ PC & P & 1 \end{bmatrix}$$

all are stable and proper. After substitution from (5.1) and clearing of fractions, this matrix becomes

$$\begin{bmatrix} 1-PQ & -P(1-PQ) & -(1-PQ) \\ Q & 1-PQ & -Q \\ PQ & P(1-PQ) & 1-PQ \end{bmatrix}.$$

Clearly, these nine entries belong to $\mathcal{S}$. ■

Note that all nine transfer functions above are affine functions of the free parameter Q; that is, each is of the form $T_1 + T_2 Q$ for some T_1, T_2 in $\mathcal{S}$. In particular the sensitivity and complementary sensitivity functions are

$$\begin{aligned} S &= 1-PQ, \\ T &= PQ. \end{aligned}$$

Let us look at a simple application. Suppose that we want to find a C so that the feedback system is internally stable and y asymptotically tracks a step r (when $d = 0$). Parametrize C as in the theorem. Then y asymptotically tracks a step iff the transfer function from r to e (i.e., S) has a zero at $s = 0$, that is,

$$P(0)Q(0) = 1.$$

This equation has a solution Q in $\mathcal{S}$ iff $P(0) \neq 0$. Conclusion: The problem has a solution iff $P(0) \neq 0$; when this holds, the set of all solutions is

$$\left\{ C = \frac{Q}{1-PQ} : Q \in \mathcal{S}, Q(0) = \frac{1}{P(0)} \right\}.$$

Observe that Q inverts P at dc. Also, you can check that a controller of the latter form has a pole at $s = 0$, as it must by Theorem 3 of Chapter 3.

Example For the plant

$$P(s) = \frac{1}{(s+1)(s+2)}$$

suppose that it is desired to find an internally stabilizing controller so that y asymptotically tracks a ramp r. Parametrize C as in the theorem. The transfer function S from r to e must have (at least) two zeros at $s = 0$, where r has two poles. Let us take

$$Q(s) = \frac{as + b}{s + 1}.$$

This belongs to $\mathcal{S}$ and has two variables, a and b, for the assignment of the two zeros of S. We have

$$\begin{aligned} S(s) &= 1 - \frac{as + b}{(s + 1)^2(s + 2)} \\ &= \frac{s^3 + 4s^2 + (5 - a)s + (2 - b)}{(s + 1)^2(s + 2)}, \end{aligned}$$

so we should take $a = 5, b = 2$. This gives

$$\begin{aligned} Q(s) &= \frac{5s + 2}{s + 1}, \\ C(s) &= \frac{(5s + 2)(s + 1)(s + 2)}{s^2(s + 4)}. \end{aligned}$$

The controller is internally stabilizing and has two poles at $s = 0$.

5.2 Coprime Factorization

Now suppose that P is not stable and we want to find an internally stabilizing C. We might try as follows. Write P as the ratio of coprime polynomials,

$$P = \frac{N}{M}.$$

By Euclid's algorithm (reviewed below) we can get two other polynomials X, Y satisfying the equation

$$NX + MY = 1.$$

Remembering Theorem 3.1 (the feedback system is internally stable iff the characteristic polynomial has no zeros in Re $s \geq 0$), we might try to make the left-hand side equal to the characteristic polynomial by setting

$$C = \frac{X}{Y}.$$

The trouble is that Y may be 0; even if not, this C may not be proper.

Example 1 For $P(s) = 1/s$, we can take $N(s) = 1$, $M(s) = s$. One solution to the equation $NX + MY = 1$ is $X(s) = 1$, $Y(s) = 0$, for which X/Y is undefined. Another solution is $X(s) = -s + 1$, $Y(s) = 1$, for which X/Y is not proper.

The remedy is to arrange that N, M, X, Y are all elements of $\mathcal{S}$ instead of polynomials. Two functions N and M in $\mathcal{S}$ are *coprime* if there exist two other functions X and Y also in $\mathcal{S}$ and satisfying the equation

$$NX + MY = 1.$$

Notice that for this equation to hold, N and M can have no common zeros in Re$s \geq 0$ nor at the point $s = \infty$—if there were such a point s_0, there would follow

$$0 = N(s_0)X(s_0) + M(s_0)Y(s_0) \neq 1.$$

It can be proved that this condition is also sufficient for coprimeness.

Let G be a real-rational transfer function. A representation of the form

$$G = \frac{N}{M}, \qquad N, M \in \mathcal{S},$$

where N and M are coprime, is called a *coprime factorization* of G over $\mathcal{S}$. The purpose of this section is to present a method for the construction of four functions in $\mathcal{S}$ satisfying the two equations

$$G = \frac{N}{M}, \qquad NX + MY = 1.$$

The construction of N and M is easy.

Example 2 Take $G(s) = 1/(s-1)$. To write $G = N/M$ with N and M in $\mathcal{S}$, simply divide the numerator and denominator polynomials, 1 and $s-1$, by a common polynomial with no zeros in Re$s \geq 0$, say $(s+1)^k$:

$$\frac{1}{s-1} = \frac{N(s)}{M(s)}, \quad N(s) = \frac{1}{(s+1)^k}, \quad M(s) = \frac{s-1}{(s+1)^k}.$$

If the integer k is greater than 1, then N and M are not coprime—they have a common zero at $s = \infty$. So

$$N(s) = \frac{1}{s+1}, \quad M(s) = \frac{s-1}{s+1}$$

suffice.

More generally, to get N and M we could divide the numerator and denominator polynomials of G by $(s+1)^k$, where k equals the maximum of their degrees. What is not so easy is to get the other two functions, X and Y, and this is why we need Euclid's algorithm.

Euclid's algorithm computes the greatest common divisor of two given polynomials, say $n(\lambda)$ and $m(\lambda)$. When n and m are coprime, the algorithm can be used to compute polynomials $x(\lambda)$, $y(\lambda)$ satisfying

$$nx + my = 1.$$

Procedure A: Euclid's Algorithm

Input: polynomials n, m

Initialize: If it is not true that degree $(n) \geq$ degree (m), interchange n and m.

Step 1 Divide m into n to get quotient q_1 and remainder r_1:

$$n = mq_1 + r_1,$$

$$\text{degree } r_1 < \text{ degree } m.$$

Step 2 Divide r_1 into m to get quotient q_2 and remainder r_2:

$$m = r_1 q_2 + r_2,$$

$$\text{degree } r_2 < \text{ degree } r_1.$$

Step 3 Divide r_2 into r_1:

$$r_1 = r_2 q_3 + r_3,$$

$$\text{degree } r_3 < \text{ degree } r_2.$$

Continue.

Stop at Step k when r_k is a nonzero constant.

Then x, y are obtained as illustrated by the following example for $k = 3$. The equations are

$$n = mq_1 + r_1,$$

$$m = r_1 q_2 + r_2,$$

$$r_1 = r_2 q_3 + r_3,$$

that is,

$$\begin{bmatrix} 1 & 0 & 0 \\ q_2 & 1 & 0 \\ -1 & q_3 & 1 \end{bmatrix} \begin{bmatrix} r_1 \\ r_2 \\ r_3 \end{bmatrix} = \begin{bmatrix} 1 & -q_1 \\ 0 & 1 \\ 0 & 0 \end{bmatrix} \begin{bmatrix} n \\ m \end{bmatrix}.$$

Solve for r_3 by, say, Gaussian elimination:

$$r_3 = (1 + q_2 q_3)n + [-q_3 - q_1(1 + q_2 q_3)]m.$$

Set

$$\begin{aligned} x &= \frac{1}{r_3}(1 + q_2 q_3), \\ y &= \frac{1}{r_3}[-q_3 - q_1(1 + q_2 q_3)]. \end{aligned}$$

Example 3 The algorithm for $n(\lambda) = \lambda^2$, $m(\lambda) = 6\lambda^2 - 5\lambda + 1$ goes like this:

$$\begin{aligned} q_1(\lambda) &= \frac{1}{6}, \\ r_1(\lambda) &= \frac{5}{6}\lambda - \frac{1}{6}, \\ q_2(\lambda) &= \frac{36}{5}\lambda - \frac{114}{25}, \\ r_2(\lambda) &= \frac{6}{25}. \end{aligned}$$

Since r_2 is a nonzero constant, we stop after Step 2. Then the equations are

$$\begin{aligned} n &= mq_1 + r_1, \\ m &= r_1 q_2 + r_2, \end{aligned}$$

yielding

$$r_2 = (1 + q_1 q_2)m - q_2 n.$$

So we should take

$$x = -\frac{q_2}{r_2}, \quad y = \frac{1 + q_1 q_2}{r_2},$$

that is,

$$x(\lambda) = -30\lambda + 19, \quad y(\lambda) = 5\lambda + 1.$$

Next is a procedure for doing a coprime factorization of G. The main idea is to transform variables, $s \to \lambda$, so that polynomials in λ yield functions in $\mathcal{S}$.

Procedure B

Input: G

Step 1 If G is stable, set $N = G$, $M = 1$, $X = 0$, $Y = 1$, and stop; else, continue.

Step 2 Transform $G(s)$ to $\tilde{G}(\lambda)$ under the mapping $s = (1 - \lambda)/\lambda$. Write $\tilde{G}$ as a ratio of coprime polynomials:

$$\tilde{G}(\lambda) = \frac{n(\lambda)}{m(\lambda)}.$$

Step 3 Using Euclid's algorithm, find polynomials $x(\lambda)$, $y(\lambda)$ such that

$$nx + my = 1.$$

Step 4 Transform $n(\lambda)$, $m(\lambda)$, $x(\lambda)$, $y(\lambda)$ to $N(s)$, $M(s)$, $X(s)$, $Y(s)$ under the mapping $\lambda = 1/(s + 1)$.

The mapping used in this procedure is not unique; the only requirement is that polynomials n, and so on, map to N, and so on, in $\mathcal{S}$.

Example 4 For

$$G(s) = \frac{1}{(s-1)(s-2)}$$

the algorithm gives

$$\begin{aligned}
\tilde{G}(\lambda) &= \frac{\lambda^2}{6\lambda^2 - 5\lambda + 1}, \\
n(\lambda) &= \lambda^2, \\
m(\lambda) &= 6\lambda^2 - 5\lambda + 1, \\
x(\lambda) &= -30\lambda + 19, \\
y(\lambda) &= 5\lambda + 1 \quad \text{(from Example 3)}, \\
N(s) &= \frac{1}{(s+1)^2},
\end{aligned}$$

$$\begin{aligned} M(s) &= \frac{(s-1)(s-2)}{(s+1)^2}, \\ X(s) &= \frac{19s-11}{s+1}, \\ Y(s) &= \frac{s+6}{s+1}. \end{aligned}$$

5.3 Coprime Factorization by State-Space Methods (Optional)

This optional section presents a state-space procedure for computing a coprime factorization over $\mathcal{S}$ of a proper G. This procedure is more efficient than the polynomial method in the preceding section.

We start with a new data structure. Suppose that A, B, C, D are real matrices of dimensions

$$n \times n, \quad n \times 1, \quad 1 \times n, \quad 1 \times 1.$$

The transfer function going along with this quartet is

$$D + C(sI - A)^{-1}B.$$

Note that the constant D equals the value of the transfer function at $s = \infty$; if the transfer function is strictly proper, then $D = 0$. It is convenient to write

$$\left[\begin{array}{c|c} A & B \\ \hline C & D \end{array}\right]$$

instead of

$$D + C(sI - A)^{-1}B.$$

Beginning with a realization of G,

$$G(s) = \left[\begin{array}{c|c} A & B \\ \hline C & D \end{array}\right],$$

the goal is to get state-space realizations for four functions N, M, X, Y, all in $\mathcal{S}$, such that

$$G = \frac{N}{M}, \quad NX + MY = 1.$$

First, we look at how to get N and M. If the input and output of G are denoted u and y, respectively, then the state model of G is

$$\begin{aligned} \dot{x} &= Ax + Bu, & (5.2) \\ y &= Cx + Du. & (5.3) \end{aligned}$$

Choose a real matrix F, $1 \times n$, such that $A + BF$ is stable (i.e., all eigenvalues in $\mathrm{Re}\, s < 0$). Now define the signal $v := u - Fx$. Then from (5.2) and (5.3) we get

$$\begin{aligned} \dot{x} &= (A + BF)x + Bv, \\ u &= Fx + v, \\ y &= (C + DF)x + Dv. \end{aligned}$$

Evidently from these equations, the transfer function from v to u is

$$M(s) := \left[\begin{array}{c|c} A+BF & B \\ \hline F & 1 \end{array}\right], \tag{5.4}$$

and that from v to y is

$$N(s) := \left[\begin{array}{c|c} A+BF & B \\ \hline C+DF & D \end{array}\right]. \tag{5.5}$$

Therefore,

$$u = Mv, \quad y = Nv,$$

so that $y = NM^{-1}u$, that is, $G = N/M$. Clearly, N and M are proper, and they are stable because $A+BF$ is. Thus $N, M \in \mathcal{S}$. Suggestion: Test the formulas above for the simplest case, $G(s) = 1/s$ ($A = 0$, $B = 1$, $C = 1$, $D = 0$).

The theory behind the formulas for X and Y is beyond the scope of this book. The procedure is to choose a real matrix H, $n \times 1$, so that $A + HC$ is stable, and then set

$$X(s) := \left[\begin{array}{c|c} A+HC & H \\ \hline F & 0 \end{array}\right], \tag{5.6}$$

$$Y(s) := \left[\begin{array}{c|c} A+HC & -B-HD \\ \hline F & 1 \end{array}\right]. \tag{5.7}$$

In summary, the procedure to do a coprime factorization of G is this:

Step 1 Get a realization (A, B, C, D) of G.

Step 2 Compute matrices F and H so that $A + BF$ and $A + HC$ are stable.

Step 3 Using formulas (5.4) to (5.7), compute the four functions N, M, X, Y.

5.4 Controller Parametrization: General Plant

The transfer function P is no longer assumed to be stable. Let $P = N/M$ be a coprime factorization over $\mathcal{S}$ and let X, Y be two functions in $\mathcal{S}$ satisfying the equation

$$NX + MY = 1. \tag{5.8}$$

Theorem 2 *The set of all Cs for which the feedback system is internally stable equals*

$$\left\{ \frac{X+MQ}{Y-NQ} : Q \in \mathcal{S} \right\}.$$

It is useful to note that Theorem 2 reduces to Theorem 1 when $P \in \mathcal{S}$. To see this, recall from Section 5.2 (Step 1 of Procedure B) that we can take

$$N = P, \quad M = 1, \quad X = 0, \quad Y = 1$$

when $P \in \mathcal{S}$. Then

$$\frac{X+MQ}{Y-NQ} = \frac{Q}{1-PQ}.$$

The proof of Theorem 2 requires a preliminary result.

Lemma 1 *Let $C = N_C/M_C$ be a coprime factorization over $\mathcal{S}$. Then the feedback system is internally stable iff*

$$(NN_C + MM_C)^{-1} \in \mathcal{S}.$$

The proof of this lemma is almost identical to the proof of Theorem 3.1, and so is omitted.

Proof of Theorem 2 ($\supset$) Suppose that $Q \in \mathcal{S}$ and

$$C := \frac{X + MQ}{Y - NQ}.$$

To show that the feedback system is internally stable, define

$$N_C := X + MQ, \qquad M_C := Y - NQ.$$

Then from the equation

$$NX + MY = 1$$

it follows that

$$NN_C + MM_C = 1.$$

Therefore, $C = N_C/M_C$ is a coprime factorization, and from Lemma 1 the feedback system is internally stable.

($\subset$) Conversely, let C be any controller achieving internal stability. We must find a Q in $\mathcal{S}$ such that

$$C = \frac{X + MQ}{Y - NQ}.$$

Let $C = N_C/M_C$ be a coprime factorization over $\mathcal{S}$ and define

$$V := (NN_C + MM_C)^{-1}$$

so that

$$NN_CV + MM_CV = 1. \tag{5.9}$$

By Lemma 1, $V \in \mathcal{S}$. Let Q be the solution of

$$M_CV = Y - NQ. \tag{5.10}$$

Substitute (5.10) into (5.9) to get

$$NN_CV + M(Y - NQ) = 1. \tag{5.11}$$

Also, add and subtract NMQ in (5.8) to give

$$N(X + MQ) + M(Y - NQ) = 1. \tag{5.12}$$

Comparing (5.11) and (5.12), we see that

$$N_CV = X + MQ. \tag{5.13}$$

Now (5.10) and (5.13) give

$$C = \frac{N_CV}{M_CV} = \frac{X + MQ}{Y - NQ}.$$

It remains to show that $Q \in \mathcal{S}$. Multiply (5.10) by X and (5.13) by Y, then subtract and switch sides:

$$(NX + MY)Q = YN_CV - XM_CV.$$

But the left-hand side equals Q by (5.8), while the right-hand side belongs to $\mathcal{S}$. So we are done. ■

Theorem 2 gives an automatic way to stabilize a plant.

Example Let

$$P(s) = \frac{1}{(s-1)(s-2)}.$$

Apply Procedure B to get

$$\begin{aligned} N(s) &= \frac{1}{(s+1)^2}, \\ M(s) &= \frac{(s-1)(s-2)}{(s+1)^2}, \\ X(s) &= \frac{19s-11}{s+1}, \\ Y(s) &= \frac{s+6}{s+1}. \end{aligned}$$

According to the theorem, the controller

$$C(s) = \frac{X(s)}{Y(s)} = \frac{19s-11}{s+6}$$

achieves internal stability.

As before, when P was stable, all closed-loop transfer functions are affine functions of Q if C is parametrized as in the theorem statement. For example, the sensitivity and complementary sensitivity functions are

$$\begin{aligned} S &= M(Y - NQ), \\ T &= N(X + MQ). \end{aligned}$$

Finally, it is sometimes useful to note that Lemma 1 suggests another way to solve the equation $NX + MY = 1$ given coprime N and M. First, find a controller C achieving internal stability for $P = N/M$—this might be easier than solving for X and Y. Next, write a coprime factorization of C: $C = N_C/M_C$. Then Lemma 1 says that

$$V := NN_C + MM_C$$

is invertible in $\mathcal{S}$. Finally, set $X = N_CV^{-1}$ and $Y = M_CV^{-1}$.

5.5 Asymptotic Properties

How to find a C to achieve internal stability and asymptotic properties simultaneously is perhaps best shown by an example.

Let

$$P(s) = \frac{1}{(s-1)(s-2)}.$$

The problem is to find a proper C so that

1. The feedback system is internally stable.
2. The final value of y equals 1 when r is a unit step and $d = 0$.
3. The final value of y equals zero when d is a sinusoid of 10 rad/s and $r = 0$.

The first step is to parametrize all stabilizing Cs. Suitable N, M, X, Y are given in the example of the preceding section. From Theorem 2 C must have the form

$$C = \frac{X + MQ}{Y - NQ} \tag{5.14}$$

for some Q in $\mathcal{S}$ in order to satisfy (1). For such C the transfer function from r to y equals $N(X + MQ)$. By the final-value theorem (2) holds iff

$$N(0)[X(0) + M(0)Q(0)] = 1. \tag{5.15}$$

Similarly, the transfer function from d to y equals $N(Y - NQ)$, so (3) holds iff

$$N(10j)[Y(10j) - N(10j)Q(10j)] = 0. \tag{5.16}$$

So the problem reduces to the purely algebraic one of finding a function Q in $\mathcal{S}$ satisfying (5.15) and (5.16), which reduce to

$$\begin{aligned} Q(0) &= 6, \qquad (5.17)\\ Q(10j) &= (6 + 10j)(1 + 10j) = -94 + 70j. \end{aligned}$$

This last equation is really two real equations:

$$\begin{aligned} \text{Re } Q(10j) &= -94, \qquad (5.18)\\ \text{Im } Q(10j) &= 70. \qquad (5.19) \end{aligned}$$

So we must find a function Q in $\mathcal{S}$ satisfying (5.17), (5.18), and (5.19).

A method that will certainly work is to let Q be a polynomial in $(s+1)^{-1}$ with enough variable coefficients. This guarantees that $Q \in \mathcal{S}$. Since we need to satisfy three equations, we should allow three coefficients. So take Q in the form

$$Q(s) = x_1 + x_2 \frac{1}{s+1} + x_3 \frac{1}{(s+1)^2}.$$

The three equations (5.17)-(5.19) lead to one of the form $Ax = b$, where

$$x = \begin{pmatrix} x_1 \\ x_2 \\ x_3 \end{pmatrix}.$$

Solve for x. In this case the solution is

$$x_1 = -79, \quad x_2 = -723, \quad x_3 = 808.$$

This gives

$$Q(s) = \frac{-79s^2 - 881s + 6}{(s+1)^2}.$$

Finally, we get C from (5.14):

$$C(s) = \frac{-60s^4 - 598s^3 + 2515s^2 - 1794s + 1}{s(s^2 + 100)(s + 9)}.$$

In summary, the procedure consists of four steps:

1. Parametrize all internally stabilizing controllers.
2. Reduce the asymptotic specs to interpolation constraints on the parameter.
3. Find (if possible) a parameter to satisfy these constraints.
4. Back-substitute to get the controller.

5.6 Strong and Simultaneous Stabilization

Practicing control engineers are reluctant to use unstable controllers, especially if the plant itself is stable. System integrity is the motivation: For example, if a sensor or actuator fails, or is deliberately turned off during start-up or shutdown, and the feedback loop opens, overall stability is maintained if both plant and controller individually are stable. If the plant itself is unstable, the argument against using an unstable controller is less compelling. However, knowledge of when a plant is or is not stabilizable with a stable controller is useful for another problem, namely, simultaneous stabilization, meaning stabilization of several plants by the same controller.

The issue of simultaneous stabilization arises when a plant is subject to a discrete change, such as when a component burns out. Simultaneous stabilization of two plants can also be viewed as an example of a problem involving highly structured uncertainty. A set of plants with exactly two elements is the most extreme example of highly structured uncertainty, standing at the opposite end of the spectrum from the unstructured disk-like uncertainty, which is the type of uncertainty focused on in this book.

Say that a plant is *strongly stabilizable* if internal stabilization can be achieved with C itself a stable transfer function. We start with an example of a plant that is not strongly stabilizable.

Example 1 Consider the plant transfer function

$$P(s) = \frac{s-1}{s(s-2)}.$$

Every C achieving internal stability is itself unstable. To prove this, start with a coprime factorization of P:

$$\begin{aligned} N(s) &= \frac{s-1}{(s+1)^2}, \\ M(s) &= \frac{s(s-2)}{(s+1)^2}, \\ X(s) &= \frac{14s-1}{s+1}, \\ Y(s) &= \frac{s-9}{s+1}. \end{aligned}$$

According to Theorem 2, all stabilizing controllers have the form

$$C = \frac{X+MQ}{Y-NQ}$$

for some Q in $\mathcal{S}$. Since $X+MQ$ and $Y-NQ$ too are coprime—they satisfy the equation

$$N(X+MQ) + M(Y-NQ) = 1$$

—they have no common zero in Re$s \geq 0$. So to show that all such Cs are unstable, it suffices to show that $Y - NQ$ has a zero in Re$s \geq 0$ for every Q in $\mathcal{S}$. Now

$$N(1) = 0, \quad N(\infty) = 0,$$

so for every Q in $\mathcal{S}$

$$\begin{aligned} (Y - NQ)(1) &= Y(1) \\ &= -4, \\ (Y - NQ)(\infty) &= Y(\infty) \\ &= 1. \end{aligned}$$

Notice that the two numbers on the right-hand side have opposite sign. Thus as s moves along the positive real axis, the function $(Y - NQ)(s)$ changes sign. By continuity, it must equal zero at some such point, that is, $Y - NQ$ has a real zero somewhere on the positive real axis.

The poles and zeros of P must share a certain property in order for P to be strongly stabilizable. In the following theorem, the point at $s = \infty$ is included among the real zeros of P.

Theorem 3 *P is strongly stabilizable iff it has an even number of real poles between every pair of real zeros in Re$s \geq 0$.*

To illustrate, continue with the example above. The zeros, including the point at infinity, are at $s = 1, \infty$. Between this pair is a single pole, at $s = 2$. This plant therefore fails the test.

As another example, consider

$$P(s) = \frac{(s-1)^2(s^2 - s + 1)}{(s-2)^2(s+1)^3}.$$

On the positive real axis, including ∞, P has three zeros, two at $s = 1$ and one at $s = \infty$. It has two other zeros in Re$s \geq 0$, which, not being real, are irrelevant. In counting poles between pairs of zeros we only have to consider distinct zeros (there are no poles between coincident zeros). Between zeros at $s = 1, \infty$ lie two poles, at $s = 2$. So this P is strongly stabilizable.

Proof of Theorem 3, Necessity The proof is just as in Example 1. Assume that the pole-zero test fails. To show that every stabilizing controller is unstable, start with a coprime factorization of P,

$$P = \frac{N}{M}, \quad NX + MY = 1,$$

and some stabilizing controller,

$$C = \frac{X + MQ}{Y - NQ}, \quad Q \in \mathcal{S}.$$

It suffices to show that $Y - NQ$ has a zero in Re$s \geq 0$.

By assumption, there is some pair of real zeros of N in Re$s \geq 0$, at $s = \sigma_1, \sigma_2$, say, with an odd number of zeros of M in between. It follows that $M(\sigma_1)$ and $M(\sigma_2)$ have opposite sign; then so do $Y(\sigma_1)$ and $Y(\sigma_2)$, since $MY = 1$ at the right half-plane zeros of N. Hence the function $Y - NQ$ has a real zero somewhere between $s = \sigma_1$ and $s = \sigma_2$. ■

The proof of sufficiency is first illustrated by means of an example.

Example 2 Take the plant transfer function

$$P(s) = \frac{s-1}{(s-2)^2}.$$

This has two poles, at $s = 2$, between the two zeros at $s = 1, \infty$, so P is strongly stabilizable. To get a stable, stabilizing C, we should get a Q in $\mathcal{S}$ such that the inverse of $U := Y - NQ$ belongs to $\mathcal{S}$. Equivalently, we should get a U in $\mathcal{S}$ such that $U^{-1} \in \mathcal{S}$ and $U = Y$ at the two zeros of N, namely, $s = 1, \infty$. For this P we have

$$N(s) = \frac{s-1}{(s+1)^2}, \quad M(s) = \frac{(s-2)^2}{(s+1)^2}.$$

Now

$$Y(1) = \frac{1}{M(1)} = 4, \quad Y(\infty) = \frac{1}{M(\infty)} = 1.$$

So the problem reduces to constructing a U in $\mathcal{S}$ such that

$$U^{-1} \in \mathcal{S}, \quad U(1) = 4, \quad U(\infty) = 1.$$

The latter problem can be solved in two steps. First, get a U_1 in $\mathcal{S}$ such that

$$U_1^{-1} \in \mathcal{S}, \quad U_1(1) = 4.$$

The easiest choice is the constant $U_1(s) = 4$. Now we look for U of the form

$$U = (1 + aF)^l U_1,$$

where a is a constant, l an integer, and $F \in \mathcal{S}$. To guarantee that $U(1) = U_1(1)$ we should arrange that $F(1) = 0$, for example,

$$F(s) = \frac{s-1}{s+1}.$$

Then for $U(\infty) = 1$ we need $(1 + a)^l 4 = 1$, that is,

$$a = \left(\frac{1}{4}\right)^{1/l} - 1, \tag{5.20}$$

and for $U^{-1} \in \mathcal{S}$ it suffices to have $\|aF\|_\infty < 1$ (i.e., $|a| < 1/\|F\|_\infty = 1$). So suitable l and a can be obtained by first choosing l large enough that

$$\left| \left(\frac{1}{4}\right)^{1/l} - 1 \right| < 1$$

and then getting a from (5.20), for example, $l = 1, a = -3/4$. This gives

$$U(s) = \left(1 - \frac{3}{4}\frac{s-1}{s+1}\right) 4 = \frac{s+7}{s+1}.$$

Finally, U, M, N uniquely determine C, as follows:

$$U = Y - NQ \Longrightarrow Q = \frac{Y-U}{N} \Longrightarrow C = \frac{X+MQ}{Y-NQ} = \frac{1-MU}{NU}.$$

For this example we get $C(s) = 27/(s+7)$. Notice that we did not actually have to construct X and Y.

Now for the constructive procedure that proves sufficiency in Theorem 3. The general procedure is fairly involved, so a simplifying assumption will be made that Ps unstable poles and zeros (including ∞) are all real and distinct. (Of course, Theorem 3 holds without this assumption.)

Procedure

Step 0 Write $P = N/M$ with N, M coprime. Arrange the non-negative real zeros of N as follows:

$$0 \le \sigma_1 < \sigma_2 < \cdots < \sigma_m = \infty.$$

Define $r_i := 1/M(\sigma_i)$, $i = 1, \ldots, m$. Then P is strongly stabilizable iff $r_1, \ldots, r_m$ all have the same sign. If this is true, continue.

Step 1 Set $U_1(s) = r_1$.

Continue. Assume that U_k has been constructed to satisfy

$$U_k, U_k^{-1} \in \mathcal{S}, \quad U_k(\sigma_i) = r_i, \quad i = 1, \ldots, k.$$

Step $k+1$ Choose F in $\mathcal{S}$ to have zeros at $s = \sigma_1, \ldots, \sigma_k$. Choose $l \ge 1$ and a so that

$$[1 + aF(\sigma_{k+1})]^l U_k(\sigma_{k+1}) = r_{k+1},$$

$$|a| < \frac{1}{\|F\|_\infty}.$$

Set $U_{k+1} = (1+aF)^l U_k$.

Continue to Step m.

Step $m+1$ Set $U = U_m$ and $C = (1 - MU)/(NU)$.

Now we return to the problem of simultaneous stabilization and see that it can be reduced to one of strong stabilization. Two plants P_1 and P_2 are *simultaneously stabilizable* if internal stability is achievable for both by a common controller. Bring in coprime factorizations:

$$P_i = \frac{N_i}{M_i}, \quad N_i X_i + M_i Y_i = 1, \quad i = 1, 2$$

and define

$$N = N_2 M_1 - N_1 M_2, \quad M = N_2 X_1 + M_2 Y_1, \quad P = \frac{N}{M}.$$

For example, if P_1 is already stable, we may take

$$N_1 = P_1, \quad M_1 = 1, \quad X_1 = 0, \quad Y_1 = 1,$$

in which case

$$N = N_2 - P_1 M_2, \quad M = M_2,$$

so $P = P_2 - P_1$.

Theorem 4 *P_1 and P_2 are simultaneously stabilizable iff P is strongly stabilizable.*

Proof The controllers stabilizing P_i are

$$\frac{X_i + M_i Q_i}{Y_i - N_i Q_i}, \quad Q_i \in \mathcal{S}.$$

Thus P_1 and P_2 are simultaneously stabilizable iff there exist Q_1, Q_2 in $\mathcal{S}$ such that

$$\frac{X_1 + M_1 Q_1}{Y_1 - N_1 Q_1} = \frac{X_2 + M_2 Q_2}{Y_2 - N_2 Q_2}.$$

Since these two fractions both have coprime factors, this equation holds iff there exists U in $\mathcal{S}$ such that

$$\begin{aligned} U^{-1} &\in \mathcal{S}, \\ X_1 + M_1 Q_1 &= U(X_2 + M_2 Q_2), \\ Y_1 - N_1 Q_1 &= U(Y_2 - N_2 Q_2). \end{aligned}$$

To simplify the bookkeeping, write these last two equations in matrix form:

$$\begin{bmatrix} 1 & Q_1 \end{bmatrix} \begin{bmatrix} X_1 & Y_1 \\ M_1 & -N_1 \end{bmatrix} = U \begin{bmatrix} 1 & Q_2 \end{bmatrix} \begin{bmatrix} X_2 & Y_2 \\ M_2 & -N_2 \end{bmatrix}.$$

Postmultiply this equation by

$$\begin{bmatrix} N_2 & Y_2 \\ M_2 & -X_2 \end{bmatrix}$$

to get

$$\begin{bmatrix} 1 & Q_1 \end{bmatrix} \begin{bmatrix} X_1 & Y_1 \\ M_1 & -N_1 \end{bmatrix} \begin{bmatrix} N_2 & Y_2 \\ M_2 & -X_2 \end{bmatrix} = U \begin{bmatrix} 1 & Q_2 \end{bmatrix}.$$

Now the first column of the matrix

$$\begin{bmatrix} X_1 & Y_1 \\ M_1 & -N_1 \end{bmatrix} \begin{bmatrix} N_2 & Y_2 \\ M_2 & -X_2 \end{bmatrix}$$

is

$$\begin{bmatrix} M \\ N \end{bmatrix};$$

denote the second column by

$$\begin{bmatrix} X \\ Y \end{bmatrix}.$$

Then the previous matrix equation is equivalent to the two equations

$$\begin{aligned} M + N Q_1 &= U, \\ X + Y Q_1 &= U Q_2. \end{aligned}$$

To recap, P_1 and P_2 are simultaneously stabilizable iff there exist Q_1, Q_2, U in $\mathcal{S}$ such that

$$\begin{aligned} U^{-1} &\in \mathcal{S}, \\ M + N Q_1 &= U, \\ X + Y Q_1 &= U Q_2. \end{aligned}$$

Clearly, this is equivalent to the condition, there exist Q_1, U in $\mathcal{S}$ such that

$$\begin{aligned} U^{-1} &\in \mathcal{S}, \\ M + NQ_1 &= U \end{aligned}$$

[because we can get Q_2 via $(X + YQ_1)/U$]. But it can be checked that N and M are coprime. Thus from Lemma 1 the previous condition is equivalent to, P can be stabilized by some stable controller, namely, Q_1. ■

Example 3 Consider

$$P_1(s) = \frac{1}{s+1}, \quad P_2(s) = \frac{as+b}{(s+1)(s-1)},$$

where a and b are real constants with $a \neq 1$. Since P_1 is stable, we have

$$P(s) = P_2(s) - P_1(s) = -\frac{(1-a)s - (1+b)}{(s+1)(s-1)}.$$

This has zeros at

$$s = \frac{1+b}{1-a}, \infty$$

and a simple unstable pole at $s = 1$. So P is strongly stabilizable, or P_1 and P_2 are simultaneously stabilizable, iff either the zero $(1+b)/(1-a)$ is negative or it lies to the right of the unstable pole, that is,

$$\text{either } \frac{1+b}{1-a} < 0 \quad \text{or} \quad \frac{1+b}{1-a} > 1.$$

Simultaneous stabilization for more than two plants is still an unsolved problem.

5.7 Cart-Pendulum Example

An interesting stabilization problem is afforded by the cart-pendulum example, a common toy control system. The setup is shown in Figure 5.2. The system consists of a cart of mass M that slides in one dimension x on a horizontal surface, with a ball of mass m at the end of a rigid massless pendulum of length l. The cart and ball are treated as point masses, with the pivot at the center of the cart. There is assumed to be no friction and no air resistance. Shown as inputs are a horizontal force u on the cart and a force d on the ball perpendicular to the pendulum. The other signals shown are the angle θ and the position of the ball $y = x + l\sin\theta$.

Elementary dynamics yields the following equations of motion:

$$(M+m)\ddot{x} + ml(\ddot{\theta}\cos\theta - \dot{\theta}^2\sin\theta) = u + d\cos\theta, \tag{5.21}$$

$$m\left(\ddot{x}\cos\theta + l\ddot{\theta} - g\sin\theta\right) = d. \tag{5.22}$$

These are nonlinear equations which can be linearized about an equilibrium position, of which there are two: $(x, \theta) = (0, 0)$ and $(x, \theta) = (0, \pi)$ (i.e., the pendulum either up or down).

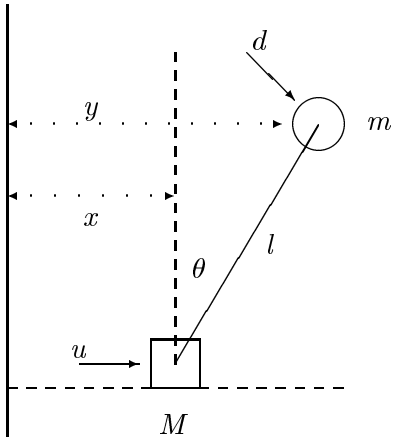

Figure 5.2: Cart-pendulum example.

Linearization About Pendulum Up

The two linearized equations are

$$\begin{aligned}(M+m)\ddot{x} + ml\ddot{\theta} &= u + d,\\ \ddot{x} + l\ddot{\theta} - g\theta &= \frac{1}{m}d.\end{aligned}$$

Take Laplace transforms to get

$$\begin{bmatrix} (M+m)s^2 & mls^2 \\ s^2 & ls^2 - g \end{bmatrix} \begin{bmatrix} \hat{x} \\ \hat{\theta} \end{bmatrix} = \begin{bmatrix} \hat{u} + \hat{d} \\ \frac{1}{m}\hat{d} \end{bmatrix}.$$

Thus

$$\begin{bmatrix} \hat{x} \\ \hat{\theta} \end{bmatrix} = \frac{1}{D(s)} \begin{bmatrix} ls^2 - g & -g \\ -s^2 & \frac{M}{m}s^2 \end{bmatrix} \begin{bmatrix} \hat{u} \\ \hat{d} \end{bmatrix},$$

where

$$D(s) = s^2[Mls^2 - (M+m)g].$$

Finally,

$$\hat{y} = \hat{x} + l\hat{\theta} = \frac{1}{D(s)} \begin{bmatrix} -g & \frac{M}{m}ls^2 g \end{bmatrix} \begin{bmatrix} \hat{u} \\ \hat{d} \end{bmatrix}.$$

In particular, the transfer functions from u to x and y are, respectively,

$$\frac{ls^2 - g}{D(s)}, \quad \frac{-g}{D(s)}.$$

These are both unstable, having right half-plane poles at

$$s = 0,\ 0,\ \sqrt{\frac{(M+m)g}{Ml}}.$$

Also, the transfer function from u to x has a right half-plane zero at $s = \sqrt{g/l}$.

Linearization About Pendulum Down

Replacing θ by $\pi + \theta$ in equations (5.21) and (5.22) and linearizing, we get

$$\begin{aligned} (M+m)\ddot{x} - ml\ddot{\theta} &= u - d, \\ -\ddot{x} + l\ddot{\theta} + g\theta &= \frac{1}{m}d, \end{aligned}$$

so

$$\begin{bmatrix} \hat{x} \\ \hat{\theta} \end{bmatrix} = \frac{1}{D(s)} \begin{bmatrix} ls^2 + g & -g \\ s^2 & \frac{M}{m}s^2 \end{bmatrix} \begin{bmatrix} \hat{u} \\ \hat{d} \end{bmatrix},$$

and

$$\hat{y} = \hat{x} - l\hat{\theta} = \frac{1}{D(s)} \begin{bmatrix} g & -\frac{M}{m}ls^2 g \end{bmatrix} \begin{bmatrix} \hat{u} \\ \hat{d} \end{bmatrix},$$

where

$$D(s) = s^2[Mls^2 + (M+m)g].$$

The transfer functions from u to x and y are now, respectively,

$$\frac{ls^2 + g}{D(s)}, \quad \frac{g}{D(s)}.$$

Let us look at the problem of stabilizing the u-to-x transfer function with the pendulum in the up position. The transfer function is

$$\frac{ls^2 - g}{s^2[Mls^2 - (M+m)g]}.$$

Since this has an unstable pole, namely,

$$\sqrt{\frac{(M+m)g}{Ml}},$$

between two real zeros at $s = \sqrt{g/l}, \infty$, from the preceding section this transfer function is not strongly stabilizable. Having no finite zeros, the u-to-y transfer function is, however.

Is the cart-pendulum stabilizable if we measure x and control d? First of all, what does this mean? The cart-pendulum as configured is really a multivariable system: It has two inputs, u and d, and two outputs, x and θ (y is a linear combination of these two). So really there are four loops we could close: from x to u and d and from θ to u and d. Let us contemplate closing just from x to d. We would like all closed-loop transfer functions to be stable, for example, u-to-θ, x-to-θ, and so on. Is this possible?

(This analysis applies only to the linearized system. Since there are poles on the imaginary axis, the stability of the linear system does not determine even the local stability of the nonlinear system.)

We shall return to this example in the next chapter.

Exercises

1. Compute a coprime factorization over $\mathcal{S}$ of
$$G(s) = \frac{s^3}{s^2 - s + 1}.$$

2. For
$$P(s) = \frac{3}{s - 4}$$
compute a controller C so that the feedback system is internally stable and the tracking error e goes to 0 when r is a ramp and $d = 0$.

3. For
$$P(s) = \frac{1}{s(s^2 + 0.2s + 1)}$$
find an internally stabilizing C so that the final value of $r - y$ equals zero when r is a unit ramp and d is a sinusoid of frequency 2 rad/s.

4. Suppose that $P(s) = 1/s$ and $C = Q/(1 - PQ)$, where Q is a proper real-rational function. Characterize those functions Q for which the feedback system is internally stable.

5. Suppose that N, M are coprime functions in $\mathcal{S}$. Prove that if $NM^{-1} \in \mathcal{S}$, then $M^{-1} \in \mathcal{S}$. Is this true without the coprimeness assumption?

6. The problem is to find an internally stabilizing C so that e tends to zero asymptotically when r is a step and $d = 0$. When is the problem solvable? Characterize all solutions. (Do not assume P is stable.)

7. Let
$$P(s) = \frac{s}{(s - 1)(10s + 1)}.$$
Find a C to achieve internal stability. What are the closed-loop poles? What is the dc gain from d to y?

8. For formulas (5.4) to (5.7), verify that $NX + MY = 1$.

9. Consider the feedback system with plant P and controller C. Assume internal stability. Consider a coprime factorization of P over $\mathcal{S}$, $P = N/M$. Suppose that P is perturbed to
$$P = \frac{N + \Delta_1}{M + \Delta_2},$$
where
$$\begin{aligned} \Delta_1, \Delta_2 &\in \mathcal{S}, \\ \|\Delta_1\|_\infty, \|\Delta_2\|_\infty &\leq \gamma. \end{aligned}$$
Find a bound on γ for robust stability.

10. Compute a stable, stabilizing controller for
$$P(s) = \frac{(s - 1)(s^2 + s + 1)}{(s - 2)(s - 3)(s + 1)^2}.$$

11. Study simultaneous stabilization of the cart-pendulum system in the up and down configurations.

Notes and References

The idea behind Theorem 1 is due to Newton et al. (1957). They observed that while the transfer function from r to y is nonlinear in C, it is linear in Q, the transfer function from r to u. So they proposed to design Q to achieve desired performance and then obtain C by back-substitution. Theorem 1 itself is due to Zames (1981). The controller parametrization in Theorem 1 is used in the field of process control, where it is called *internal model control* [because the controller $C = Q/(1 - PQ)$ contains a model of the plant P] (Morari and Zafiriou, 1989).

The original form of Theorem 2 is due independently to Youla et al. (1976) and Kucera (1979). Its present form is due to Desoer et al. (1980), who saw the advantage of doing coprime factorization over $\mathcal{S}$ instead of the ring of polynomials. This idea in turn is due to Vidyasagar (1972). State-space formulas for coprime factorization were first derived by Khargonekar and Sontag (1982). The formulas in Section 5.3 are from Nett et al. 1984. Section 5.5 is adapted from Francis and Vidyasagar (1983). The algebraic point of view has been explored in detail by Desoer and co-workers (e.g., Desoer and Gustafson, 1984) and by Vidyasagar (1985). The notion of strong stabilization and Theorem 3 are due to Youla et al. (1974). Simultaneous stabilization was first treated by Saeks and Murray (1982). The simple proofs of Theorems 3 and 4 given here are borrowed from Vidyasagar (1985). The controller parametrization of Theorem 2 has been exploited in a CAD method for controller design (Boyd et al., 1988).

Design Constraints

Before we see how to design control systems for the robust performance specification, it is useful to determine the basic limitations on achievable performance. In this chapter we study design constraints arising from two sources: from algebraic relationships that must hold among various transfer functions; from the fact that closed-loop transfer functions must be stable (i.e., analytic in the right half-plane). It is assumed throughout this chapter that the feedback system is internally stable.

6.1 Algebraic Constraints

There are three items in this section.

1. The identity $S + T = 1$ always holds. This is an immediate consequence of the definitions of S and T. So in particular, $|S(j\omega)|$ and $|T(j\omega)|$ cannot both be less than $1/2$ at the same frequency ω.

2. A necessary condition for robust performance is that the weighting functions satisfy

$$\min\{|W_1(j\omega)|, |W_2(j\omega)|\} < 1, \quad \forall\omega.$$

Proof Fix ω and assume that $|W_1| \leq |W_2|$ (the argument $j\omega$ is suppressed). Then

$$\begin{aligned} |W_1| &= |W_1(S+T)| \\ &\leq |W_1S| + |W_1T| \\ &\leq |W_1S| + |W_2T|. \end{aligned}$$

So robust performance (see Theorem 4.2), that is,

$$\||W_1S| + |W_2T|\|_\infty < 1,$$

implies that $|W_1| < 1$, and hence

$$\min\{|W_1|, |W_2|\} < 1.$$

The same conclusion can be drawn when $|W_2| \leq |W_1|$. ■

So at every frequency either $|W_1|$ or $|W_2|$ must be less than 1. Typically, $|W_1(j\omega)|$ is monotonically decreasing—for good tracking of low-frequency signals—and $|W_2(j\omega)|$ is monotonically increasing—uncertainty increases with increasing frequency.

3. If p is a pole of L in $\mathrm{Re}s \geq 0$ and z is a zero of L in the same half-plane, then

$$S(p) = 0, \quad S(z) = 1, \tag{6.1}$$

$$T(p) = 1, \quad T(z) = 0. \tag{6.2}$$

These interpolation constraints are immediate from the definitions of S and T. For example,

$$S(p) = \frac{1}{1 + L(p)} = \frac{1}{\infty} = 0.$$

6.2 Analytic Constraints

In this section we derive some constraints concerning achievable performance obtained from analytic function theory. The first subsection presents some mathematical preliminaries.

Preliminaries

We begin with the following fundamental facts concerning complex functions: the maximum modulus theorem, Cauchy's theorem, and Cauchy's integral formula. These are stated here for convenience.

Maximum Modulus Theorem *Suppose that Ω is a region (nonempty, open, connected set) in the complex plane and F is a function that is analytic in Ω. Suppose that F is not equal to a constant. Then $|F|$ does not attain its maximum value at an interior point of Ω.*

A simple application of this theorem, with Ω equal to the open right half-plane, shows that for F in $\mathcal{S}$

$$\|F\|_\infty = \sup_{\mathrm{Re}s>0} |F(s)|.$$

Cauchy's Theorem *Suppose that Ω is a bounded open set with connected complement and $\mathcal{D}$ is a non-self-intersecting closed contour in Ω. If F is analytic in Ω, then*

$$\oint_{\mathcal{D}} F(s)ds = 0.$$

Cauchy's Integral Formula *Suppose that F is analytic on a non-self-intersecting closed contour $\mathcal{D}$ and in its interior Ω. Let s_0 be a point in Ω. Then*

$$F(s_0) = \frac{1}{2\pi j} \oint_{\mathcal{D}} \frac{F(s)}{s - s_0} ds.$$

We shall also need the Poisson integral formula, which says that the value of a bounded analytic function at a point in the right half-plane is completely determined by the coordinates of the point together with the values of the function on the imaginary axis.

Lemma 1 *Let F be analytic and of bounded magnitude in $\mathrm{Re}s \geq 0$ and let $s_0 = \sigma_0 + j\omega_0$ be a point in the complex plane with $\sigma_0 > 0$. Then*

$$F(s_0) = \frac{1}{\pi} \int_{-\infty}^{\infty} F(j\omega) \frac{\sigma_0}{\sigma_0^2 + (\omega - \omega_0)^2} d\omega.$$

Proof Construct the Nyquist contour $\mathcal{D}$ in the complex plane taking the radius, r, large enough so that the point s_0 is encircled by $\mathcal{D}$.

Cauchy's integral formula gives

$$F(s_0) = \frac{1}{2\pi j} \oint_{\mathcal{D}} \frac{F(s)}{s - s_0} ds.$$

Also, since $-\overline{s}_0$ is not encircled by $\mathcal{D}$, Cauchy's theorem gives

$$0 = \frac{1}{2\pi j} \oint_{\mathcal{D}} \frac{F(s)}{s + \overline{s}_0} ds.$$

Subtract these two equations to get

$$F(s_0) = \frac{1}{2\pi j} \oint_{\mathcal{D}} F(s) \frac{\overline{s}_0 + s_0}{(s - s_0)(s + \overline{s}_0)} ds.$$

Thus

$$F(s_0) = I_1 + I_2,$$

where

$$\begin{aligned} I_1 &:= \frac{1}{\pi} \int_{-r}^{r} F(j\omega) \frac{\sigma_0}{(s_0 - j\omega)(\overline{s}_0 + j\omega)} d\omega \\ &= \frac{1}{\pi} \int_{-r}^{r} F(j\omega) \frac{\sigma_0}{\sigma_0^2 + (\omega - \omega_0)^2} d\omega, \\ I_2 &:= \frac{1}{\pi j} \int_{-\pi/2}^{\pi/2} F(r\mathrm{e}^{j\theta}) \frac{\sigma_0}{(r\mathrm{e}^{j\theta} - s_0)(r\mathrm{e}^{j\theta} + \overline{s}_0)} r j \mathrm{e}^{j\theta} d\theta. \end{aligned}$$

As $r \to \infty$

$$I_1 \to \frac{1}{\pi} \int_{-\infty}^{\infty} F(j\omega) \frac{\sigma_0}{\sigma_0^2 + (\omega - \omega_0)^2} d\omega.$$

So it remains to show that $I_2 \to 0$ as $r \to \infty$.

We have

$$I_2 \leq \frac{\sigma_0}{\pi} \|F\|_\infty \frac{1}{r} \int_{-\pi/2}^{\pi/2} \frac{1}{|\mathrm{e}^{j\theta} - s_0 r^{-1}||\mathrm{e}^{j\theta} + \overline{s}_0 r^{-1}|} d\theta.$$

The integral

$$\int_{-\pi/2}^{\pi/2} \frac{1}{|\mathrm{e}^{j\theta} - s_0 r^{-1}||\mathrm{e}^{j\theta} + \overline{s}_0 r^{-1}|} d\theta$$

converges as $r \to \infty$. Thus

$$I_2 \leq \text{constant } \times \frac{1}{r},$$

which gives the desired result. ■

Bounds on the Weights W_1 and W_2

Suppose that the loop transfer function L has a zero z in $\mathrm{Re} s \geq 0$. Then

$$\|W_1 S\|_\infty \geq |W_1(z)|. \tag{6.3}$$

This is a direct consequence of the maximum modulus theorem and (6.1):

$$|W_1(z)| = |W_1(z)S(z)| \leq \sup_{\mathrm{Re} s \geq 0} |W_1(s)S(s)| = \|W_1 S\|_\infty.$$

So a necessary condition that the performance criterion $\|W_1 S\|_\infty < 1$ be achievable is that the weight satisfy $|W_1(z)| < 1$. In words, the magnitude of the weight at a right half-plane zero of P or C must be less than 1.

Similarly, suppose that L has a pole p in $\mathrm{Re} s \geq 0$. Then

$$\|W_2 T\|_\infty \geq |W_2(p)|, \tag{6.4}$$

so a necessary condition for the robust stability criterion $\|W_2 T\|_\infty < 1$ is that the weight W_2 satisfy $|W_2(p)| < 1$.

All-Pass and Minimum-Phase Transfer Functions

Two types of transfer functions play a critical role in the rest of this book: all-pass and minimum-phase. A function in $\mathcal{S}$ is *all-pass* if its magnitude equals 1 at all points on the imaginary axis. The terminology comes from the fact that a filter with an all-pass transfer function passes without attenuation input sinusoids of all frequencies. It is not difficult to show that such a function has pole-zero symmetry about the imaginary axis in the sense that a point s_0 is a zero iff its reflection, $-\overline{s}_0$, is a pole. Consequently, the function being stable, all its zeros lie in the right half-plane. Thus an all-pass function is, up to sign, the product of factors of the form

$$\frac{s - s_0}{s + \overline{s}_0}, \qquad \mathrm{Re} s_0 > 0.$$

Examples of all-pass functions are

$$1, \quad \frac{s-1}{s+1}, \quad \frac{s^2 - s + 2}{s^2 + s + 2}.$$

A function in $\mathcal{S}$ is *minimum-phase* if it has no zeros in $\mathrm{Re} s > 0$. This terminology can be explained as follows. Let G be a minimum-phase transfer function. There are many other transfer functions having the same magnitude as G, for example FG where F is all-pass. But all these other transfer functions have greater phase. Thus, of all the transfer functions having Gs magnitude, the one with the minimum phase is G. Examples of minimum-phase functions are

$$1, \quad \frac{1}{s+1}, \quad \frac{s}{s+1}, \quad \frac{s+2}{s^2 + s + 1}.$$

It is a useful fact that every function in $\mathcal{S}$ can be written as the product of two such factors: for example

$$\frac{4(s-2)}{s^2 + s + 1} = \left(\frac{s-2}{s+2}\right)\left(\frac{4(s+2)}{s^2 + s + 1}\right).$$

Lemma 2 *For each function G in $\mathcal{S}$ there exist an all-pass function G_{ap} and a minimum-phase function G_{mp} such that $G = G_{ap}G_{mp}$. The factors are unique up to sign.*

Proof Let G_{ap} be the product of all factors of the form

$$\frac{s - s_0}{s + \overline{s}_0},$$

where s_0 ranges over all zeros of G in $\mathrm{Re}s > 0$, counting multiplicities, and then define

$$G_{mp} = \frac{G}{G_{ap}}.$$

The proof of uniqueness is left as an exercise. ■

For technical reasons we assume for the remainder of this section that L has no poles on the imaginary axis. Factor the sensitivity function as

$$S = S_{ap}S_{mp}.$$

Then S_{mp} has no zeros on the imaginary axis (such zeros would be poles of L) and S_{mp} is not strictly proper (since S is not). Thus $S_{mp}^{-1} \in \mathcal{S}$.

As a simple example of the use of all-pass functions, suppose that P has a zero at z with $z > 0$, a pole at p with $p > 0$; also, suppose that C has neither poles nor zeros in the closed right half-plane. Then

$$S_{ap}(s) = \frac{s - p}{s + p}, \quad T_{ap}(s) = \frac{s - z}{s + z}.$$

It follows from the preceding section that $S(z) = 1$, and hence

$$S_{mp}(z) = S_{ap}(z)^{-1} = \frac{z + p}{z - p}.$$

Similarly,

$$T_{mp}(p) = T_{ap}(p)^{-1} = \frac{p + z}{p - z}.$$

Then

$$\|W_1S\|_\infty = \|W_1S_{mp}\|_\infty \geq |W_1(z)S_{mp}(z)| = \left|W_1(z)\frac{z + p}{z - p}\right|$$

and

$$\|W_2T\|_\infty \geq \left|W_2(p)\frac{p + z}{p - z}\right|.$$

Thus, if there are a pole and zero close to each other in the right half-plane, they can greatly amplify the effect that either would have alone.

Example These inequalities are effectively illustrated with the cart-pendulum example of Section 5.7. Let $P(s)$ be the u-to-x transfer function for the up position of the pendulum, that is,

$$P(s) = \frac{ls^2 - g}{s^2[Mls^2 - (M + m)g]}.$$

Define the ratio $r := m/M$ of pendulum mass to cart mass. The zero and pole of P in $\mathrm{Re}s > 0$ are

$$z = \sqrt{\frac{g}{l}}, \quad p = z\sqrt{1+r}.$$

Note that for r fixed, a larger value of l means a smaller value of p, and this in turn means that the system is easier to stabilize (the time constant is slower). The foregoing two inequalities on $\|W_1 S\|_\infty$ and $\|W_2 T\|_\infty$ apply. Since the cart-pendulum is a stabilization task, let us focus on

$$\|W_2 T\|_\infty \geq \left| W_2(p) \frac{p+z}{p-z} \right|. \tag{6.5}$$

The robust stabilization problem becomes harder the larger the value of the right-hand side of (6.5). The scaling factor in this inequality is

$$\frac{p+z}{p-z} = \frac{\sqrt{1+r}+1}{\sqrt{1+r}-1}. \tag{6.6}$$

This quantity is always greater than 1, and it approaches 1 only when r approaches ∞, that is, only when the pendulum mass is much larger than the cart mass. There is a tradeoff, however, in that a large value of r means a large value of p, the unstable pole; for a typical W_2 (high-pass) this in turn means a relatively large value of $|W_2(p)|$ in (6.5). So at least for small uncertainty, the worst-case scenario is a short pendulum with a small mass m relative to the cart mass M.

In contrast, the u-to-y transfer function has no zeros, so the constraint there is simply

$$\|W_2 T\|_\infty \geq |W_2(p)|.$$

If robust stabilization were the only objective, we could achieve equality by careful selection of the controller. Note that for this case there is no apparent tradeoff in making m/M large. The difference between the two cases, measuring x and measuring y, again highlights the important fact that sensor location can have a significant effect on the difficulty of controlling a system or on the ultimate achievable performance.

Some simple experiments can be done to illustrate the points made in this example. Obtain several sticks of various lengths and try to balance them in the palm of your hand. You will notice that it is easier to balance longer sticks, because the dynamics are slower and p above is smaller. It is also easier to balance the sticks if you look at the top of the stick (measuring y) rather than at the bottom (measuring x). In fact, even for a stick that is easily balanced when looking at the top, it will be impossible to balance it while looking only at the bottom. There is also feedback from the forces that your hand feels, but this is similar to measuring x.

The interested reader may repeat the analysis for the down position of the pendulum. At this point it is useful to include the following lemma which will be used subsequently.

Lemma 3 *For every point $s_0 = \sigma_0 + j\omega_0$ with $\sigma_0 > 0$,*

$$\log |S_{mp}(s_0)| = \frac{1}{\pi} \int_{-\infty}^{\infty} \log |S(j\omega)| \frac{\sigma_0}{\sigma_0^2 + (\omega - \omega_0)^2} d\omega.$$

Proof Set $F(s) := \ln S_{mp}(s)$. Then F is analytic and of bounded magnitude in Re$s \geq 0$. (This follows from the properties $S_{mp}, S_{mp}^{-1} \in \mathcal{S}$; the idea is that since S_{mp} has no poles or zeros in the right half-plane, $\ln S_{mp}$ is well-behaved there.) Apply Lemma 1 to get

$$F(s_0) = \frac{1}{\pi}\int_{-\infty}^{\infty} F(j\omega)\frac{\sigma_0}{\sigma_0^2 + (\omega - \omega_0)^2}d\omega.$$

Now take real parts of both sides:

$$\mathrm{Re}F(s_0) = \frac{1}{\pi}\int_{-\infty}^{\infty} \mathrm{Re}F(j\omega)\frac{\sigma_0}{\sigma_0^2 + (\omega - \omega_0)^2}d\omega. \tag{6.7}$$

But

$$S_{mp} = \mathrm{e}^F = \mathrm{e}^{\mathrm{Re}F}\mathrm{e}^{j\mathrm{Im}F},$$

so

$$|S_{mp}| = \mathrm{e}^{\mathrm{Re}F},$$

that is,

$$\ln|S_{mp}| = \mathrm{Re}F.$$

Thus from (6.7)

$$\ln|S_{mp}(s_0)| = \frac{1}{\pi}\int_{-\infty}^{\infty} \ln|S_{mp}(j\omega)|\frac{\sigma_0}{\sigma_0^2 + (\omega - \omega_0)^2}d\omega,$$

or since $|S| = |S_{mp}|$ on the imaginary axis,

$$\ln|S_{mp}(s_0)| = \frac{1}{\pi}\int_{-\infty}^{\infty} \ln|S(j\omega)|\frac{\sigma_0}{\sigma_0^2 + (\omega - \omega_0)^2}d\omega.$$

Finally, since $\log x = \log \mathrm{e} \ln x$, the result follows upon multiplying the last equation by $\log \mathrm{e}$. ■

The Waterbed Effect

Consider a tracking problem where the reference signals have their energy spectra concentrated in a known frequency range, say $[\omega_1, \omega_2]$. This is the idealized situation where W_1 is a bandpass filter. Let M_1 denote the maximum magnitude of S on this frequency band,

$$M_1 := \max_{\omega_1 \leq \omega \leq \omega_2} |S(j\omega)|,$$

and let M_2 denote the maximum magnitude over all frequencies, that is, $\|S\|_\infty$. Then good tracking capability is characterized by the inequality $M_1 \ll 1$. On the other hand, we cannot permit M_2 to be too large: Remember (Section 4.2) that $1/M_2$ equals the distance from the critical point to the Nyquist plot of L, so large M_2 means small stability margin (a typical upper bound for M_2 is 2). Notice that M_2 must be at least 1 because this is the value of S at infinite frequency. So the question arises: Can we have M_1 very small and M_2 not too large? Or does it happen that very small M_1 necessarily means very large M_2? The latter situation might be compared to a waterbed: As $|S|$ is pushed down on one frequency range, it pops up somewhere else. It turns out that non-minimum-phase plants exhibit the waterbed effect.

Theorem 1 *Suppose that P has a zero at z with Re$z > 0$. Then there exist positive constants c_1 and c_2, depending only on ω_1, ω_2, and z, such that*

$$c_1 \log M_1 + c_2 \log M_2 \geq \log|S_{ap}(z)^{-1}| \geq 0.$$

Proof Since z is a zero of P, it follows from the preceding section that $S(z) = 1$, and hence $S_{mp}(z) = S_{ap}(z)^{-1}$. Apply Lemma 3 with

$$s_0 = z = \sigma_0 + j\omega_0$$

to get

$$\log|S_{ap}(z)^{-1}| = \frac{1}{\pi}\int_{-\infty}^{\infty} \log|S(j\omega)| \frac{\sigma_0}{\sigma_0^2 + (\omega - \omega_0)^2} d\omega.$$

Thus

$$\log|S_{ap}(z)^{-1}| \leq c_1 \log M_1 + c_2 \log M_2,$$

where c_1 is defined to be the integral of

$$\frac{1}{\pi}\frac{\sigma_0}{\sigma_0^2 + (\omega - \omega_0)^2}$$

over the set

$$[-\omega_2, -\omega_1] \cup [\omega_1, \omega_2]$$

and c_2 equals the same integral but over the complementary set.

It remains to observe that $|S_{ap}(z)| \leq 1$ by the maximum modulus theorem, so

$$\log|S_{ap}(z)^{-1}| \geq 0. \blacksquare$$

Example As an illustration of the theorem consider the plant transfer function

$$P(s) = \frac{s-1}{(s+1)(s-p)},$$

where $p > 0$, $p \neq 1$. As observed in the preceding section, S must interpolate zero at the unstable poles of P, so $S(p) = 0$. Thus the all-pass factor of S must contain the factor

$$\frac{s-p}{s+p}.$$

that is,

$$S_{ap}(s) = \frac{s-p}{s+p} G(s)$$

for some all-pass function G. Since $|G(1)| \leq 1$ (maximum modulus theorem), there follows

$$|S_{ap}(1)| \leq \left|\frac{1-p}{1+p}\right|.$$

So the theorem gives

$$c_1 \log M_1 + c_2 \log M_2 \geq \log\left|\frac{1+p}{1-p}\right|.$$

Note that the right-hand side is very large if p is close to 1. This example illustrates again a general fact: The waterbed effect is amplified if the plant has a pole and a zero close together in the right half-plane. We would expect such a plant to be very difficult to control.

It is emphasized that the waterbed effect applies to non-minimum-phase plants only. In fact, the following can be proved (Section 10.1): If P has no zeros in $\mathrm{Re}\, s > 0$ nor on the imaginary axis

in the frequency range $[\omega_1, \omega_2]$, then for every $\epsilon > 0$ and $\delta > 1$ there exists a controller C so that the feedback system is internally stable, $M_1 < \epsilon$, and $M_2 < \delta$. As a very easy example, take

$$P(s) = \frac{1}{s+1}.$$

The controller $C(s) = k$ is internally stabilizing for all $k > 0$, and then

$$S(s) = \frac{s+1}{s+1+k}.$$

So $\|S\|_\infty = 1$ and, for every $\epsilon > 0$ and ω_2, if k is large enough, then

$$|S(j\omega)| < \epsilon, \quad \forall \omega \leq \omega_2.$$

The Area Formula

Herein is derived a formula for the area bounded by the graph of $|S(j\omega)|$ (log scale) plotted as a function of ω (linear scale). The formula is valid when the relative degree of L is large enough. *Relative degree* equals degree of denominator minus degree of numerator.

Let $\{p_i\}$ denote the set of poles of L in $\mathrm{Re} s > 0$.

Theorem 2 *Assume that the relative degree of L is at least 2. Then*

$$\int_0^\infty \log|S(j\omega)| d\omega = \pi(\log \mathrm{e})(\sum \mathrm{Re} p_i).$$

Proof In Lemma 3 take $\omega_0 = 0$ to get

$$\log|S_{mp}(\sigma_0)| = \frac{1}{\pi}\int_{-\infty}^\infty \log|S(j\omega)| \frac{\sigma_0}{\sigma_0^2 + \omega^2} d\omega,$$

or equivalently,

$$\int_0^\infty \log|S(j\omega)| \frac{\sigma_0}{\sigma_0^2 + \omega^2} d\omega = \frac{\pi}{2}\log|S_{mp}(\sigma_0)|.$$

Multiply by σ_0:

$$\int_0^\infty \log|S(j\omega)| \frac{\sigma_0^2}{\sigma_0^2 + \omega^2} d\omega = \frac{\pi}{2}\sigma_0 \log|S_{mp}(\sigma_0)|.$$

It can be shown that the left-hand side converges to

$$\int_0^\infty \log|S(j\omega)| d\omega$$

as $\sigma_0 \to \infty$. [The idea is that for very large σ_0 the function

$$\frac{\sigma_0^2}{\sigma_0^2 + \omega^2}$$

equals nearly 1 up to large values of ω. On the other hand, $\log|S(j\omega)|$ tends to zero as ω tends to ∞.] So it remains to show that

$$\lim_{\sigma \to \infty} \frac{\sigma}{2}\log|S_{mp}(\sigma)| = (\log \mathrm{e})(\sum \mathrm{Re} p_i). \tag{6.8}$$

We can write

$$S = S_{ap} S_{mp},$$

where

$$S_{ap}(s) = \prod_i \frac{s - p_i}{s + \overline{p}_i}.$$

It is claimed that

$$\lim_{\sigma \to \infty} \sigma \ln S(\sigma) = 0.$$

To see this, note that since L has relative degree at least 2 we can write

$$L(\sigma) \approx \frac{c}{\sigma^k} \text{ as } \sigma \to \infty$$

for some constant c and some integer $k \geq 2$. Thus as $\sigma \to \infty$

$$\sigma \ln S(\sigma) = -\sigma \ln[1 + L(\sigma)] \approx -\sigma \ln \left(1 + \frac{c}{\sigma^k}\right).$$

Now use the Maclaurin's series

$$\ln(1 + x) = x - \frac{x^2}{2} + \cdots \tag{6.9}$$

to get

$$\sigma \ln S(\sigma) \approx -\sigma \left(\frac{c}{\sigma^k} - \cdots\right).$$

The right-hand side converges to zero as σ tends to ∞. This proves the claim.

In view of the claim, to prove (6.8) it remains to show that

$$\lim_{\sigma \to \infty} \frac{\sigma}{2} \ln \left|[S_{ap}(\sigma)^{-1}]\right| = \sum \text{Re} p_i. \tag{6.10}$$

Now

$$\ln(S_{ap}(\sigma)^{-1}) = \ln \prod_i \frac{\sigma + \overline{p}_i}{\sigma - p_i} = \sum_i \ln \frac{\sigma + \overline{p}_i}{\sigma - p_i},$$

so to prove (6.10) it suffices to prove

$$\lim_{\sigma \to \infty} \frac{\sigma}{2} \ln \left|\frac{\sigma + \overline{p}_i}{\sigma - p_i}\right| = \text{Re} p_i. \tag{6.11}$$

Let $p_i = x + jy$ and use (6.9) again as follows:

$$\begin{aligned}
\frac{\sigma}{2} \ln \left|\frac{\sigma + \overline{p}_i}{\sigma - p_i}\right| &= \frac{\sigma}{2} \ln \left|\frac{1 + \overline{p}_i \sigma^{-1}}{1 - p_i \sigma^{-1}}\right| \\
&= \frac{\sigma}{4} \ln \frac{(1 + x\sigma^{-1})^2 + (y\sigma^{-1})^2}{(1 - x\sigma^{-1})^2 + (y\sigma^{-1})^2} \\
&= \frac{\sigma}{4} \left\{\ln[(1 + x\sigma^{-1})^2 + (y\sigma^{-1})^2] - \ln[(1 - x\sigma^{-1})^2 + (y\sigma^{-1})^2]\right\} \\
&= \frac{\sigma}{4} \left\{2\frac{x}{\sigma} + 2\frac{x}{\sigma} + \cdots\right\} \\
&= x + \cdots \\
&= \text{Re} p_i + \cdots.
\end{aligned}$$

Letting $\sigma \to \infty$ gives (6.11). ■

Example Take the plant and controller

$$P(s) = \frac{1}{(s-1)(s+2)}, \quad C(s) = 10.$$

The feedback system is internally stable and L has relative degree 2. The plot of $|S(j\omega)|$, log scale, versus ω, linear scale, is shown in Figure 6.1. The area below the line $|S| = 1$ is negative, the area

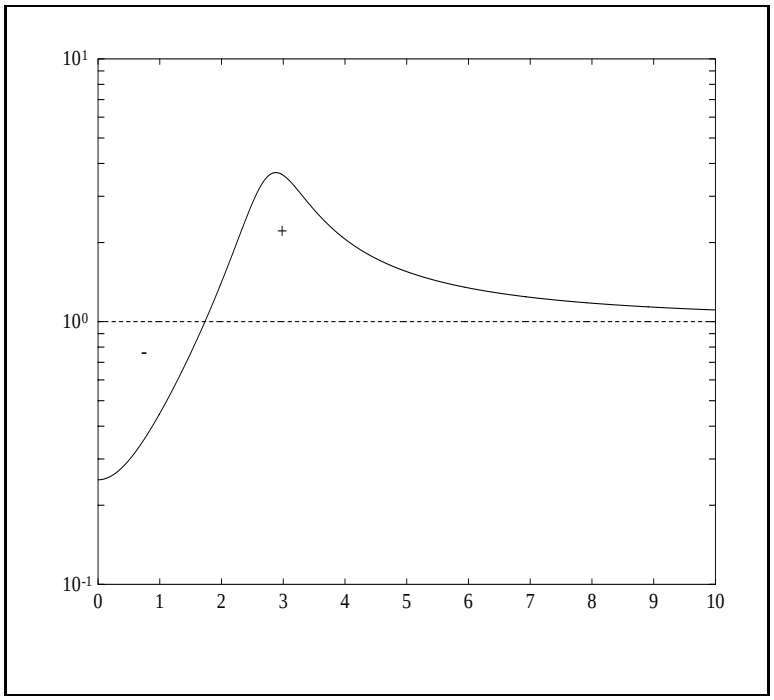

Figure 6.1: $|S(j\omega)|$, log scale, versus ω, linear scale.

above, positive. The theorem says that the net area is positive, equaling

$$\pi(\log \mathrm{e})(\sum \mathrm{Re} p_i) = \pi(\log \mathrm{e}).$$

So the negative area, required for good tracking over some frequency range, must unavoidably be accompanied by some positive area.

The waterbed effect applies to non-minimum-phase systems, whereas the area formula applies in general (except for the relative degree assumption). In particular, the area formula does not itself imply a peaking phenomenon, only an area conservation. However, one can infer a type of peaking phenomenon from the area formula when another constraint is imposed, namely, controller bandwidth, or more precisely, the bandwidth of the loop transfer function PC. For example, suppose that the constraint is

$$|PC| < \frac{1}{\omega^2}, \quad \forall \omega \geq \omega_1,$$

where $\omega_1 > 1$. This is one way of saying that the loop bandwidth is constrained to be $\leq \omega_1$. Then for $\omega \geq \omega_1$

$$|S| \leq \frac{1}{1-|PC|} < \frac{1}{1-\omega^{-2}} = \frac{\omega^2}{\omega^2 - 1}.$$

Hence

$$\int_{\omega_1}^{\infty} \log|S(j\omega)|d\omega \leq \int_{\omega_1}^{\infty} \log\frac{\omega^2}{\omega^2-1}d\omega.$$

The latter integral—denote it by I—is finite. This is proved by the following computation:

$$\begin{aligned} I &= \frac{1}{\ln 10}\int_{\omega_1}^{\infty} \ln\frac{1}{1-\omega^{-2}}d\omega \\ &= -\frac{1}{\ln 10}\int_{\omega_1}^{\infty} \ln(1-\omega^{-2})d\omega \\ &= \frac{1}{\ln 10}\int_{\omega_1}^{\infty} \left(\omega^{-2}+\frac{1}{2}\omega^{-4}+\frac{1}{3}\omega^{-6}+\cdots\right)d\omega \\ &= \frac{1}{\ln 10}\left(\omega_1^{-1}+\frac{1}{2\times 3}\omega_1^{-3}+\frac{1}{3\times 5}\omega_1^{-5}+\cdots\right) \\ &< \infty. \end{aligned}$$

Hence the possible positive area over the interval $[\omega_1, \infty)$ is limited. Thus if $|S|$ is made smaller and smaller over some subinterval of $[0, \omega_1]$, incurring a larger and larger debt of negative area, then $|S|$ must necessarily become larger and larger somewhere else in $[0, \omega_1]$. Roughly speaking, with a loop bandwidth constraint the waterbed effect applies even to minimum-phase plants.

Exercises

1. Prove the statement about uniqueness in Lemma 2.

2. True or false: For every $\delta > 1$ there exists an internally stabilizing controller such that $\|T\|_\infty < \delta$.

3. Regarding inequality (6.3), the implication is that good tracking is impossible if P has a right half-plane zero where $|W_1|$ is not small. This problem is an attempt to see this phenomenon more precisely by studying $|W_1(z)|$ as a function of z for a typical weighting function. Take W_1 to be a third-order Butterworth filter with cutoff frequency 1 rad/s. Plot

   $$|W_1(0.1+j\omega)| \quad \text{versus} \quad \omega$$

   for ω going from 0 up to where $|W_1| < 0.01$. Repeat for abscissae of 1 and 10.

4. Let

   $$P(s) = 4\frac{s-2}{(s+1)^2}.$$

   Suppose that C is an internally stabilizing controller such that

   $$\|S\|_\infty = 1.5.$$

   Give a positive lower bound for

   $$\max_{0\leq\omega\leq 0.1} |S(j\omega)|.$$

5. Define $\epsilon := \|W_1 S\|_\infty$ and $\delta := \|CS\|_\infty$. So ϵ is a measure of tracking performance, while δ measures control effort; note that CS equals the transfer function from reference input r to plant input. In a design we would like $\epsilon < 1$ and δ not too large. Derive the following inequality, showing that ϵ and δ cannot both be very small in general: For every point s_0 with $\mathrm{Re} s_0 \geq 0$,
$$|W_1(s_0)| \leq \epsilon + |W_1(s_0)P(s_0)|\delta.$$

6. Let ω be a frequency such that $j\omega$ is not a pole of P. Suppose that
$$\epsilon := |S(j\omega)| < 1.$$
Derive a lower bound for $|C(j\omega)|$ that blows up as $\epsilon \to 0$. Conclusion: Good tracking at a particular frequency requires large controller gain at this frequency.

7. Suppose that the plant transfer function is
$$P(s) = \frac{1}{s^2 - s + 4}.$$
We want the controller C to achieve the following:

   internal stability,
   $|S(j\omega)| \leq \epsilon$ for $0 \leq \omega < 0.1$,
   $|S(j\omega)| \leq 2$ for $0.1 \leq \omega < 5$,
   $|S(j\omega)| \leq 1$ for $5 \leq \omega < \infty$.

   Find a (positive) lower bound on the achievable ϵ.

Notes and References

This chapter is in the spirit of Bode's book (Bode, 1945) on feedback amplifiers. Bode showed that electronic amplifiers must have certain inherent properties simply by virtue of the fact that stable network functions are analytic, and hence have certain strong properties. Bode's work was generalized to control systems by Bower and Schultheiss (1961) and Horowitz (1963).

The interpolation conditions (6.1) and (6.2) were obtained by Raggazini and Franklin (1958). These constraints on S and T are essentially equivalent to the controller parametrization in Theorem 5.2. Inequality (6.3) was noted, for example, by Zames and Francis (1983). The waterbed effect, Theorem 1, was proved by Francis and Zames (1984), but the derivation here is due to Freudenberg and Looze (1985). The area formula, Theorem 2, was proved by Bode (1945) in case L is stable, and by Freudenberg and Looze (1985) in the general case. An excellent discussion of performance limitations may be found in Freudenberg and Looze (1988).

Loopshaping

This chapter presents a graphical technique for designing a controller to achieve robust performance for a plant that is stable and minimum-phase.

7.1 The Basic Technique of Loopshaping

Recall from Section 4.3 that the robust performance problem is to design a proper controller C so that the feedback system for the nominal plant is internally stable and the inequality

$$\||W_1 S| + |W_2 T|\|_\infty < 1 \tag{7.1}$$

is satisfied. Thus the problem input data are P, W_1, and W_2; a solution of the problem is a controller C achieving robust performance.

We saw in Chapter 6 that the robust performance problem is not always solvable—the tracking objective may be too stringent for the nominal plant and its associated uncertainty model. Unfortunately, constructive (necessary and sufficient) conditions on P, W_1, and W_2 for the robust performance problem to be solvable are unknown.

In this chapter we look at a graphical method that is likely to provide a solution when one exists. The idea is to construct the loop transfer function L to achieve (7.1) approximately, and then to get C via $C = L/P$. The underlying constraints are internal stability of the nominal feedback system and properness of C, so that L is not freely assignable. When P or P^{-1} is not stable, L must contain P's unstable poles and zeros (Theorem 3.2), an awkward constraint. For this reason, we assume in this chapter that P and P^{-1} are both stable.

In terms of W_1, W_2, and L the robust performance inequality is

$$\Gamma(j\omega) := \left|\frac{W_1(j\omega)}{1+L(j\omega)}\right| + \left|\frac{W_2(j\omega)L(j\omega)}{1+L(j\omega)}\right| < 1. \tag{7.2}$$

This must hold for all ω. The idea in loopshaping is to get conditions on L for (7.2) to hold, at least approximately. It is convenient to drop the argument $j\omega$.

We are interested in alternative conditions under which (7.2) holds. Recall from Section 6.1 that a necessary condition is

$$\min\{|W_1|, |W_2|\} < 1,$$

so we will assume this throughout. Thus at each frequency, either $|W_1| < 1$ or $|W_2| < 1$. We will consider these two cases separately and derive conditions comparable to (7.2).

We begin by noting the following inequalities, which follow from the definition of Γ:

$$(|W_1| - |W_2|)|S| + |W_2| \le \Gamma \le (|W_1| + |W_2|)|S| + |W_2|, \tag{7.3}$$

$$(|W_2| - |W_1|)|T| + |W_1| \le \Gamma \le (|W_2| + |W_1|)|T| + |W_1|, \tag{7.4}$$

$$\frac{|W_1| + |W_2L|}{1 + |L|} \le \Gamma \le \frac{|W_1| + |W_2L|}{|1 - |L||}. \tag{7.5}$$

- Suppose that $|W_2| < 1$. Then from (7.3)

$$\Gamma < 1 \iff \frac{|W_1| + |W_2|}{1 - |W_2|}|S| < 1, \tag{7.6}$$

$$\Gamma < 1 \implies \frac{|W_1| - |W_2|}{1 - |W_2|}|S| < 1. \tag{7.7}$$

  Or, in terms of L, from (7.5)

$$\Gamma < 1 \iff |L| > \frac{|W_1| + 1}{1 - |W_2|}, \tag{7.8}$$

$$\Gamma < 1 \implies |L| > \frac{|W_1| - 1}{1 - |W_2|}. \tag{7.9}$$

  When $|W_1| \gg 1$, the conditions on the right-hand sides of (7.6) and (7.7) approach each other, as do those in (7.8) and (7.9), and we may approximate the condition $\Gamma < 1$ by

$$\frac{|W_1|}{1 - |W_2|}|S| < 1 \tag{7.10}$$

  or

$$|L| > \frac{|W_1|}{1 - |W_2|}. \tag{7.11}$$

  Notice that (7.10) is like the nominal performance condition $|W_1S| < 1$ except that the weight W_1 is increased by dividing it by $1 - |W_2|$: Robust performance is achieved by nominal performance with a larger weight.

- Now suppose that $|W_1| < 1$. We may proceed similarly to obtain from (7.4)

$$\Gamma < 1 \iff \frac{|W_2| + |W_1|}{1 - |W_1|}|T| < 1,$$

$$\Gamma < 1 \implies \frac{|W_2| - |W_1|}{1 - |W_1|}|T| < 1$$

  or from (7.5)

$$\Gamma < 1 \iff |L| < \frac{1 - |W_1|}{|W_2| + 1},$$

$$\Gamma < 1 \implies |L| < \frac{1 - |W_1|}{|W_2| - 1}.$$

When $|W_2| \gg 1$, we may approximate the condition $\Gamma < 1$ by

$$\frac{|W_2|}{1-|W_1|}|T| < 1 \tag{7.12}$$

or

$$|L| < \frac{1-|W_1|}{|W_2|}. \tag{7.13}$$

Inequality (7.12) says that robust performance is achieved by robust stability with a larger weight.

The discussion above is summarized as follows:

$\|W_1\| \gg 1 > \|W_2\|$	$\|L\| > \dfrac{\|W_1\|}{1-\|W_2\|}$
$\|W_1\| < 1 \ll \|W_2\|$	$\|L\| < \dfrac{1-\|W_1\|}{\|W_2\|}$

For example, the first row says that over frequencies where $|W_1| \gg 1 > |W_2|$ the loopshape should satisfy

$$|L| > \frac{|W_1|}{1-|W_2|}.$$

Let's take the typical situation where $|W_1(j\omega)|$ is a decreasing function of ω and $|W_2(j\omega)|$ is an increasing function of ω. Typically, at low frequency

$$|W_1| > 1 > |W_2|$$

and at high frequency

$$|W_1| < 1 < |W_2|.$$

A loopshaping design goes very roughly like this:

1. Plot two curves on log-log scale, magnitude versus frequency: first, the graph of

   $$\frac{|W_1|}{1-|W_2|}$$

   over the low-frequency range where $|W_1| > 1 > |W_2|$; second, the graph of

   $$\frac{1-|W_1|}{|W_2|}$$

   over the high-frequency range where $|W_1| < 1 < |W_2|$.

2. On this plot fit another curve which is going to be the graph of $|L|$: At low frequency let it lie above the first curve and also be $\gg 1$; at high frequency let it lie below the second curve and also be $\ll 1$; at very high frequency let it roll off at least as fast as does $|P|$ (so C is proper); do a smooth transition from low to high frequency, keeping the slope as gentle as possible near crossover, the frequency where the magnitude equals 1 (the reason for this is described below).

3. Get a stable, minimum-phase transfer function L whose Bode magnitude plot is the curve just constructed, normalizing so that $L(0) > 0$.

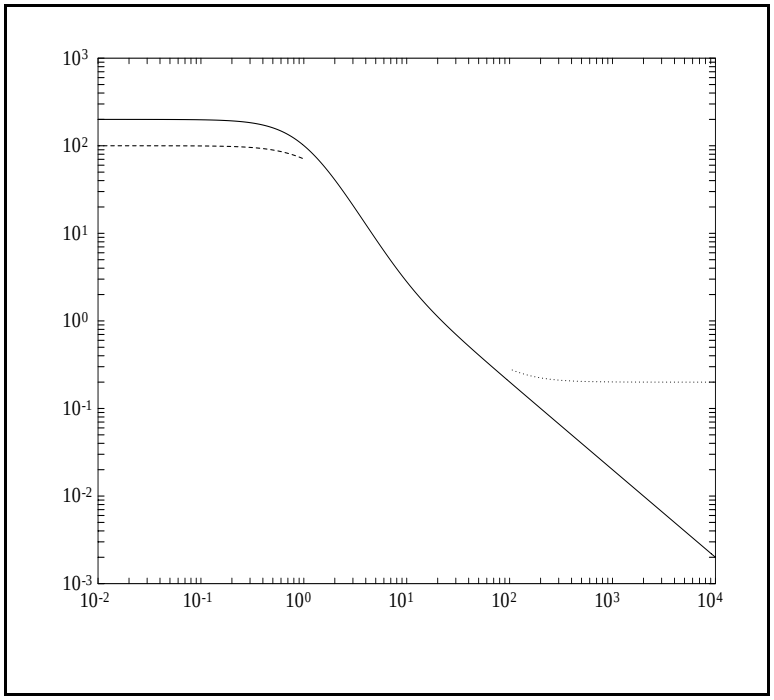

Figure 7.1: Bode plots of $|L|$ (solid), $|W_1|/(1-|W_2|)$ (dash), and $(1-|W_1|)/|W_2|$ (dot).

Typical curves are as in Figure 7.1. Such a curve for $|L|$ will satisfy (7.11) and (7.13), and hence (7.2) at low and high frequencies. But (7.2) will not necessarily hold at intermediate frequencies. Even worse, L may not result in nominal internal stability. If $L(0) > 0$ and $|L|$ is as just pictured (i.e., a decreasing function), then the angle of L starts out at zero and decreases (this follows from the phase formula to be derived in the next section). So the Nyquist plot of L starts out on the positive real axis and begins to move clockwise. By the Nyquist criterion, nominal internal stability will hold iff the angle of L at crossover is greater than 180° (i.e., crossover occurs in the third or fourth quadrant). But the greater the slope of $|L|$ near crossover, the smaller the angle of L (proved in the next section). So internal instability is unavoidable if $|L|$ drops off too rapidly through crossover, and hence in our loopshaping we must maintain a gentle slope; a rule of thumb is that the magnitude of the slope should not be more than 2. After doing the three steps above we must validate the design by checking that internal stability and (7.2) both hold. If not, we must go back and try again. Loopshaping therefore is a craft requiring experience for mastery.

7.2 The Phase Formula (Optional)

It is a fundamental fact that if L is stable and minimum-phase and normalized so that $L(0) > 0$, then its magnitude Bode plot uniquely determines its phase plot. The normalization is necessary, for

$$\frac{1}{s+1} \text{ and } \frac{-1}{s+1}$$

are stable, minimum-phase, and have the same magnitude plot, but they have different phase plots. Our goal in this section is a formula for $\angle L$ in terms of $|L|$.

Assume that L is proper, L and L^{-1} are analytic in $\mathrm{Re}\, s \geq 0$, and $L(0) > 0$. Define $G := \ln L$.

Then

$$\mathrm{Re}G = \ln|L|, \quad \mathrm{Im}G = \angle L,$$

and G has the following three properties:

1. G is analytic in some right half-plane containing the imaginary axis. Instead of a formal proof, one way to see why this is true is to look at the derivative of G:

$$G' = \frac{L'}{L}.$$

   Since L is analytic in the right half-plane, so is L'. Then since L has no zeros in the right half-plane, G' exists at all points in the right half-plane, and hence at points a bit to the left of the imaginary axis.

2. $\mathrm{Re}G(j\omega)$ is an even function of ω and $\mathrm{Im}G(j\omega)$ is an odd function of ω.

3. $s^{-1}G(s)$ tends to zero uniformly on semicircles in the right half-plane as the radius tends to infinity, that is,

$$\lim_{R\to\infty} \sup_{-\pi/2\le\theta\le\pi/2} \left| \frac{G(Re^{j\theta})}{Re^{j\theta}} \right| = 0.$$

Proof Since

$$G(Re^{j\theta}) = \ln|L(Re^{j\theta})| + j\angle L(Re^{j\theta})$$

and $\angle L(Re^{j\theta})$ is bounded as $R \to \infty$, we have

$$\left| \frac{G(Re^{j\theta})}{Re^{j\theta}} \right| \to \frac{|\ln|L(Re^{j\theta})||}{R}.$$

Now L is proper, so for some c and $k \ge 0$,

$$L(s) \approx \frac{c}{s^k} \text{ as } |s| \to \infty.$$

Thus

$$\begin{aligned} \left| \frac{G(Re^{j\theta})}{Re^{j\theta}} \right| &\to \frac{|\ln|c/R^k||}{R} \\ &= \frac{|\ln|c| - k\ln|R||}{R} \\ &\to k\frac{\ln R}{R} \\ &\to 0. \blacksquare \end{aligned}$$

Next, we obtain an expression for the imaginary part of G in terms of its real part.

Lemma 1 *For each frequency* ω_0

$$\mathrm{Im}\ G(j\omega_0) = \frac{2\omega_0}{\pi} \int_0^\infty \frac{\mathrm{Re}G(j\omega) - \mathrm{Re}G(j\omega_0)}{\omega^2 - \omega_0^2} d\omega.$$

Proof Define the function

$$\begin{aligned} F(s) &:= \frac{G(s) - \mathrm{Re}G(j\omega_0)}{s - j\omega_0} - \frac{G(s) - \mathrm{Re}G(j\omega_0)}{s + j\omega_0} \\ &= 2j\omega_0 \frac{G(s) - \mathrm{Re}G(j\omega_0)}{s^2 + \omega_0^2}. \end{aligned} \tag{7.14}$$

Then F is analytic in the right half-plane and on the imaginary axis, except for poles at $\pm j\omega_0$. Bring in the usual Nyquist contour: Go up the imaginary axis, indenting to the right at the points $-j\omega_0$ and $j\omega_0$ along semicircles of radius r, then close the contour by a large semicircle of radius R in the right half-plane. The integral of F around this contour equals zero (Cauchy's theorem). This integral equals the sum of six separate integrals corresponding to the three intervals on the imaginary axis, the two smaller semicircles, and the larger semicircle. Let I_1 denote the sum of the three integrals along the intervals on the imaginary axis, I_2 the integral around the lower small semicircle, I_3 around the upper small semicircle, and I_4 around the large semicircle. We show that

$$\lim_{R\to\infty, r\to 0} I_1 = 2\omega_0 \int_{-\infty}^{\infty} \frac{\mathrm{Re}G(j\omega) - \mathrm{Re}G(j\omega_0)}{\omega^2 - \omega_0^2} d\omega, \tag{7.15}$$

$$\lim_{r\to 0} I_2 = -\pi \mathrm{Im}\ G(j\omega_0), \tag{7.16}$$

$$\lim_{r\to 0} I_3 = -\pi \mathrm{Im}\ G(j\omega_0), \tag{7.17}$$

$$\lim_{R\to\infty} I_4 = 0. \tag{7.18}$$

The lemma follows immediately from these four equations and the fact that $\mathrm{Re}G(j\omega)$ is even.

First,

$$I_1 = \int jF(j\omega)d\omega,$$

where the integral is over the set

$$[-R, -\omega_0 - r] \cup [-\omega_0 + r, \omega_0 - r] \cup [\omega_0 + r, R]. \tag{7.19}$$

As $R \to \infty$ and $r \to 0$, this set becomes the interval $(-\infty, \infty)$. Also, from (7.14)

$$jF(j\omega) = 2\omega_0 \frac{G(j\omega) - \mathrm{Re}G(j\omega_0)}{\omega^2 - \omega_0^2}.$$

Since

$$\frac{\mathrm{Im}\ G(j\omega)}{\omega^2 - \omega_0^2}$$

is an odd function, its integral over set (7.19) equals zero, and we therefore get (7.15).

Second,

$$\begin{aligned} I_2 &= \int_{-\pi/2}^{\pi/2} \frac{G(-j\omega_0 + re^{j\theta}) - \mathrm{Re}G(j\omega_0)}{-j\omega_0 + re^{j\theta} - j\omega_0} jre^{j\theta} d\theta \\ &\quad - \int_{-\pi/2}^{\pi/2} \frac{G(-j\omega_0 + re^{j\theta}) - \mathrm{Re}G(j\omega_0)}{-j\omega_0 + re^{j\theta} + j\omega_0} jre^{j\theta} d\theta. \end{aligned}$$

As $r \to 0$, the first integral tends to 0 while the second tends to

$$[G(-j\omega_0) - \mathrm{Re}G(j\omega_0)]j \int_{-\pi/2}^{\pi/2} d\theta = \pi \mathrm{Im}\ G(j\omega_0).$$

This proves (7.16). Verification of (7.17) is similar.

Finally,

$$I_4 = -\int_{-\pi/2}^{\pi/2} F(R\mathrm{e}^{j\theta}) j R\mathrm{e}^{j\theta} d\theta,$$

so

$$|I_4| \leq \sup_{-\frac{\pi}{2} \leq \theta \leq \frac{\pi}{2}} \left| \frac{2\omega_0 [G(R\mathrm{e}^{j\theta}) - \mathrm{Re}G(j\omega_0)]}{(R\mathrm{e}^{j\theta})^2 + \omega_0^2} \right| R\pi.$$

Thus

$$|I_4| \to \text{ (const) } \sup_\theta \frac{|G(R\mathrm{e}^{j\theta})|}{R} \to 0.$$

This proves (7.18). ■

Rewriting the formula in the lemma in terms of L we get

$$\angle L(j\omega_0) = \frac{2\omega_0}{\pi} \int_0^\infty \frac{\ln|L(j\omega)| - \ln|L(j\omega_0)|}{\omega^2 - \omega_0^2} d\omega. \tag{7.20}$$

This is now manipulated to get the phase formula.

Theorem 1 *For every frequency* ω_0

$$\angle L(j\omega_0) = \frac{1}{\pi} \int_{-\infty}^\infty \frac{d\ln|L|}{d\nu} \ln\coth\frac{|\nu|}{2} d\nu,$$

where the integration variable $\nu = \ln(\omega/\omega_0)$.

Proof Change variables of integration in (7.20) to get

$$\angle L(j\omega_0) = \frac{1}{\pi} \int_{-\infty}^\infty \frac{\ln|L| - \ln|L(j\omega_0)|}{\sinh\nu} d\nu.$$

Note that in this integral $\ln|L|$ is really $\ln|L(j\omega_0 \mathrm{e}^\nu)|$ considered as a function of ν. Now integrate by parts, from $-\infty$ to 0 and from 0 to ∞:

$$\begin{aligned}
\angle L(j\omega_0) \quad = \quad & -\frac{1}{\pi}\left[(\ln|L| - \ln|L(j\omega_0)|)\ln\coth\frac{\nu}{2}\right]_0^\infty \\
& + \frac{1}{\pi}\int_0^\infty \frac{d\ln|L|}{d\nu} \ln\coth\frac{\nu}{2} d\nu \\
& + \frac{1}{\pi}[(\ln|L| - \ln|L(j\omega_0)|)\ln\coth\frac{-\nu}{2}]_0^\infty \\
& + \frac{1}{\pi}\int_{-\infty}^0 \frac{d\ln|L|}{d\nu} \ln\coth\frac{-\nu}{2} d\nu.
\end{aligned}$$

The first and third terms sum to zero. ■

Example Suppose that $\ln|L|$ has constant slope,

$$\frac{d\ln|L|}{d\nu} = -c.$$

Then

$$\angle L(j\omega_0) = -\frac{c}{\pi}\int_{-\infty}^{\infty} \ln\coth\frac{|\nu|}{2}d\nu = -\frac{c\pi}{2};$$

that is, the phase shift is constant at $-90c$ degrees.

In the phase formula, the slope function $d\ln|L|/d\nu$ is weighted by the function

$$\ln\coth\frac{|\nu|}{2} = \ln\left|\frac{\omega+\omega_0}{\omega-\omega_0}\right|.$$

This function is symmetric about $\omega = \omega_0$ (ln scale on the horizontal axis), positive, infinite at $\omega = \omega_0$, increasing from $\omega = 0$ to $\omega = \omega_0$, and decreasing from $\omega = \omega_0$ to $\omega = \infty$. In this way, the values of $d\ln|L|/d\nu$ are more heavily weighted near $\omega = \omega_0$. We conclude, roughly speaking, that the steeper the graph of $|L|$ near the frequency ω_0, the smaller the value of $\angle L$.

7.3 Examples

This section presents three simple examples of loopshaping.

Example 1 In principle the only information we need to know about P right now is its relative degree, degree of denominator minus degree of numerator. This determines the high-frequency slope on its Bode magnitude plot. We have to let L have at least equal relative degree or else C will not be proper. Assume that the relative degree of P equals 1. The actual plant transfer function enters into the picture only at the very end when we get C from L via $C = L/P$.

Take the weighting function W_2 to be

$$W_2(s) = \frac{s+1}{20(0.01s+1)}.$$

See Figure 7.2 for the Bode magnitude plot. Remember (Section 4.2) that $|W_2(j\omega)|$ is an upper bound on the magnitude of the relative plant perturbation at frequency ω. For this example, $|W_2|$ starts at 0.05 and increases monotonically up to 5, crossing 1 at 20 rad/s.

Let the performance objective be to track sinusoidal reference signals over the frequency range from 0 to 1 rad/s. Let's not say at the start what maximum tracking error we will tolerate; rather, let's see what tracking error is incurred for a couple of loopshapes. Ideally, we would take W_1 to have constant magnitude over the frequency range $[0, 1]$ and zero magnitude beyond. Such a magnitude characteristic cannot come from a rational function. Nevertheless, you can check that Theorem 4.2 continues to be valid for such W_1; that is, if the nominal feedback system is internally stable, then

$$\|W_2T\|_\infty < 1 \text{ and } \left\|\frac{W_1S}{1+\Delta W_2T}\right\|_\infty < 1, \quad \forall\Delta$$

iff

$$\||W_1S| + |W_2T|\|_\infty < 1.$$

With this justification, we can take

$$|W_1(j\omega)| = \begin{cases} a, & \text{if } 0 \le \omega \le 1 \\ 0, & \text{else,} \end{cases}$$

where a is as yet unspecified.

Let's first try a first-order, low-pass loop transfer function, that is, of the form

$$L(s) = \frac{b}{cs+1}.$$

It is reasonable to take $c = 1$ so that $|L|$ starts rolling off near the upper end of the operating band $[0, 1]$. We want b as large as possible for good tracking. The largest value of b so that

$$|L| \leq \frac{1 - |W_1|}{|W_2|} = \frac{1}{|W_2|}, \quad \omega \geq 20$$

is 20. So we have

$$L(s) = \frac{20}{s+1}.$$

See Figure 7.2. For this L the nominal feedback system is internally stable.

It remains to check what robust performance level we have achieved. For this we choose the largest value of a so that

$$|L| \geq \frac{a}{1 - |W_2|}, \quad \omega \leq 1.$$

The function

$$\frac{a}{1 - |W_2(j\omega)|}$$

is increasing over the range $[0, 1]$, while $|L(j\omega)|$ is decreasing. So a can be got by solving

$$|L(j1)| = \frac{a}{1 - |W_2(j1)|}.$$

This gives $a = 13.15$.

Now to verify robust performance, graph the function

$$|W_1(j\omega)S(j\omega)| + |W_2(j\omega)T(j\omega)|$$

(Figure 7.2). Its maximum value is about 0.92. Since this is less than 1, robust performance is verified. (We could also have determined as in Section 4.3 the largest a for which the robust performance condition holds.)

Let's recap. For the performance weight

$$|W_1(j\omega)| = \begin{cases} 13.15, & \text{if } 0 \leq \omega \leq 1 \\ 0, & \text{else,} \end{cases}$$

we can take $L(s) = 20/(s+1)$ to achieve robust performance. The tracking error is then $\leq 1/13.15 = 7.6\%$.

Suppose that a 7.6% tracking error is too large. To reduce the error make $|L|$ larger over the frequency range $[0, 1]$. For example, we could try

$$L(s) = \frac{s+10}{s+1}\frac{20}{s+1}.$$

The new factor, $(s+10)/(s+1)$, has magnitude nearly 10 over $[0, 1]$ and rolls off to about 1 above 10 rad/s. See Figure 7.3. Again, the nominal feedback system is internally stable. If we take W_1 as before and compute a again we get $a = 93.46$. The robust performance inequality is checked graphically (Figure 7.3). Now the tracking error is $\leq 1/93.46 = 1.07\%$.

The problem above is quite easy because $|W_2|$ is small on the operating band $[0, 1]$; the requirements of performance and robust stability are only weakly competitive.

Example 2 This example examines the pitch rate control of an aircraft. The signals are

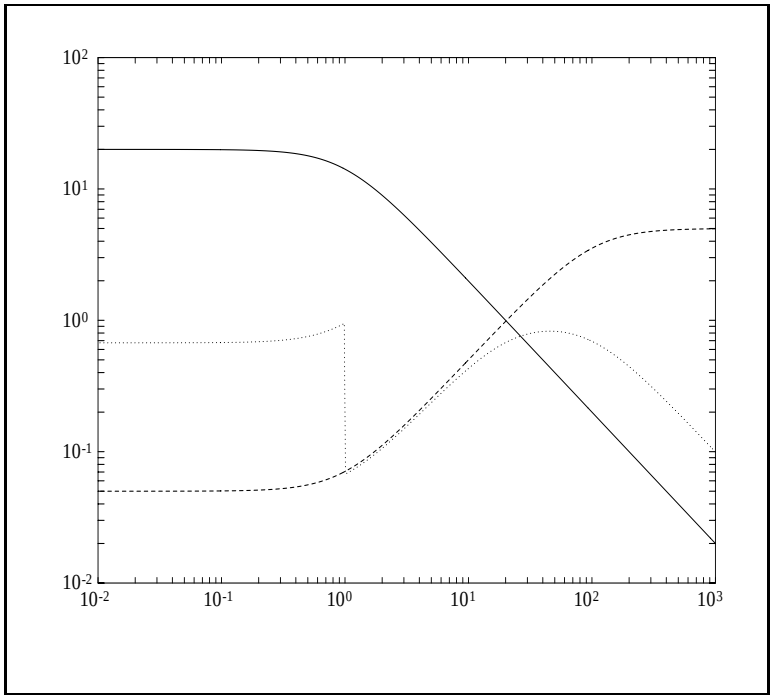

Figure 7.2: Bode plots of $|L|$ (solid), $|W_2|$ (dash), and $|W_1S| + |W_2T|$ (dot).

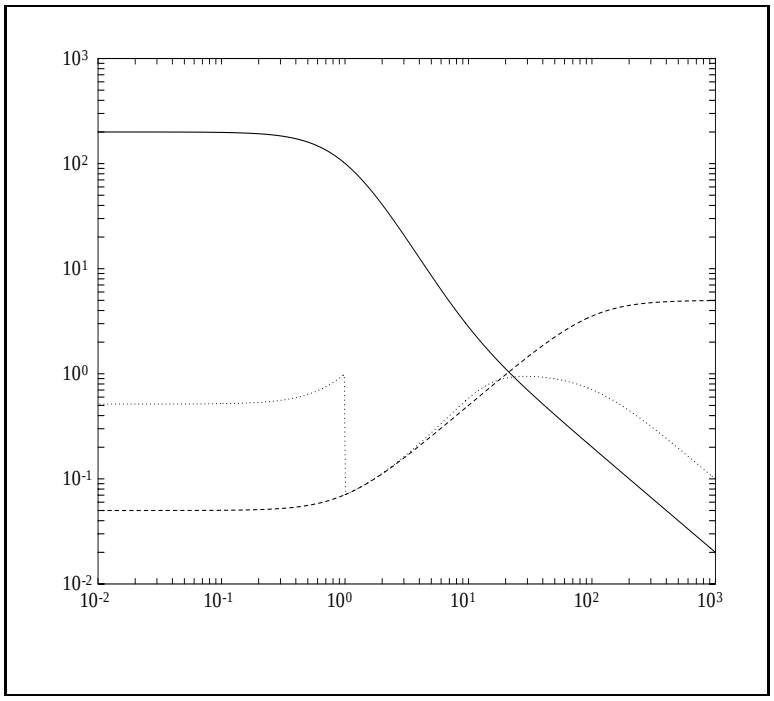

Figure 7.3: Bode plots of $|L|$ (solid), $|W_2|$ (dash), and $|W_1S| + |W_2T|$ (dot).

r pitch rate command (by pilot)

u elevator deflection

y pitch rate of the aircraft

Suppose that the first approximation of the plant is

$$P(s) = \frac{s+1}{s^2 + 2 \times 0.7 \times 5s + 5^2}.$$

This would model the rigid motion of the aircraft (i.e., ignoring bending). The natural frequency is 5 rad/s and the damping ratio 0.7.

Again, rather than specify a performance weight W_1, common practice is to specify a desired loopshape. The simplest decent loop transfer function is

$$L(s) = \frac{\omega_c}{s},$$

where ω_c, a positive constant, is the crossover frequency, where $|L| = 1$. The loopshape $|L(j\omega)|$ versus ω is a straight line (log-log scale) of slope -1.

This is the simplest loopshape having the following features:

1. Good tracking and disturbance rejection (i.e., $|S|$ small) at low frequency.
2. Good robustness (i.e., $|T|$ small) at high frequency.
3. Internal stability.

In principle, the larger ω_c, the better the performance, for then $|S|$ is smaller over a wider frequency range; note that

$$S(s) = \frac{s}{s+\omega_c}.$$

For such L with $\omega_c = 10$, the controller is

$$C(s) = 10\frac{s^2 + 2 \times 0.7 \times s + 5^2}{s(s+1)}.$$

In actuality, there is a limitation on how large ω_c can be because of high-frequency uncertainty: remember that we modeled only the rigid body, whereas the actual aircraft is flexible and has bending modes just as a flexible beam has. Suppose that the first bending mode (the fundamental) is known to be at approximately 45 rad/s. If we included this mode in the transfer function P, there would be a pole in the left half-plane near the point $s = 45j$ on the imaginary axis. This would mean in turn that $|P(j\omega)|$ would be relatively large around $\omega = 45$. For the controller above, the loopshape could then take the form in Figure 7.4. Since the magnitude is greater than 1 at 45 rad/s, the feedback system is potentially unstable, depending on the phase at 45 rad/s.

The typical way to accommodate such uncertainty is to ensure for the nominal plant model that $|L|$ is sufficiently small, starting at the frequency where appreciable uncertainty begins. For example, we might demand that

$$|L(j\omega)| \leq 0.5, \quad \forall \omega \geq 45.$$

(We have implicitly just defined a weight W_2.) The largest value of ω_c satisfying this condition is $\omega_c = 45/2$.

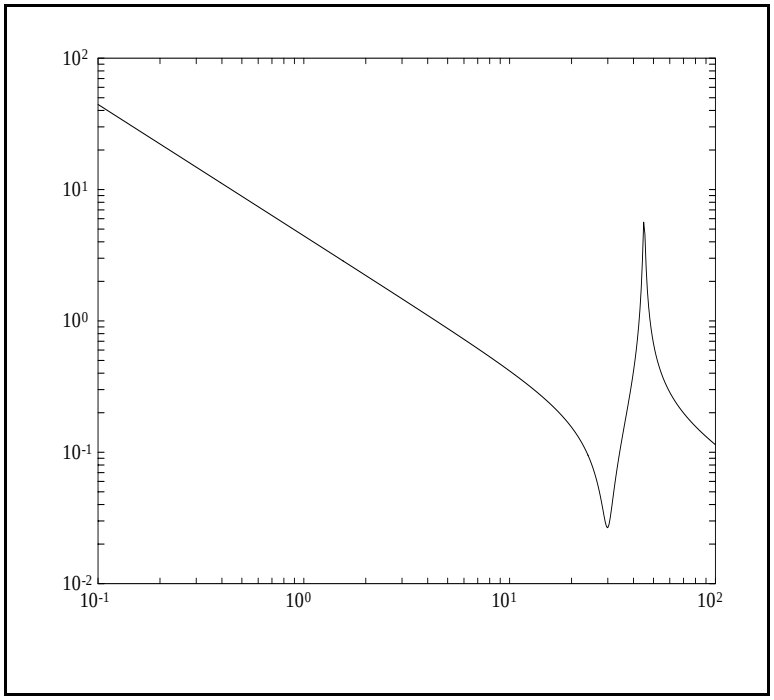

Figure 7.4: Loopshape, Example 2.

Example 3 Consider the plant transfer function

$$P(s) = \frac{s+1}{s^2 + 2 \times 0.7 \times 5s + 5^2} \; \frac{s^2 + 2 \times 0.05 \times 30s + 30^2}{s^2 + 2 \times 0.01 \times 45s + 45^2}.$$

This is an extension of the model of Example 2, with the first bending mode at 45 rad/s included. This mode is very lightly damped, with damping ratio 0.01. This frequency and damping ratio will have associated uncertainty, typically 2 to 3%. Also included in P is an additional pair of lightly damped zeros. The magnitude Bode plot of P is in Figure 7.5. Suppose that the desired loop transfer function is again $L(s) = \omega_c/s$. This would require that $C = L/P$ have the factor

$$s^2 + 2 \times 0.01 \times 45s + 45^2$$

in its numerator, that is, C would be like a notch filter with a very deep notch. But since, as stated above, the numbers 45 and 0.01 are uncertain, a more prudent approach is to have a shallower notch by setting L to be, say,

$$L(s) = \frac{\omega_c}{s} \; \frac{s^2 + 2 \times 0.03 \times 45s + 45^2}{s^2 + 2 \times 0.01 \times 45s + 45^2}.$$

With the same rationale as in Example 2, we now maximize ω_c such that

$$|L(j\omega)| \leq 0.5, \quad \forall \omega \geq 45.$$

This yields $\omega_c \approx 8$ and the loopshape in Figure 7.6. The controller is

$$C(s) = 8 \frac{s^2 + 2 \times 0.7 \times 5s + 5^2}{s(s+1)} \; \frac{s^2 + 2 \times 0.03 \times 45s + 45^2}{s^2 + 2 \times 0.05 \times 30s + 30^2}.$$

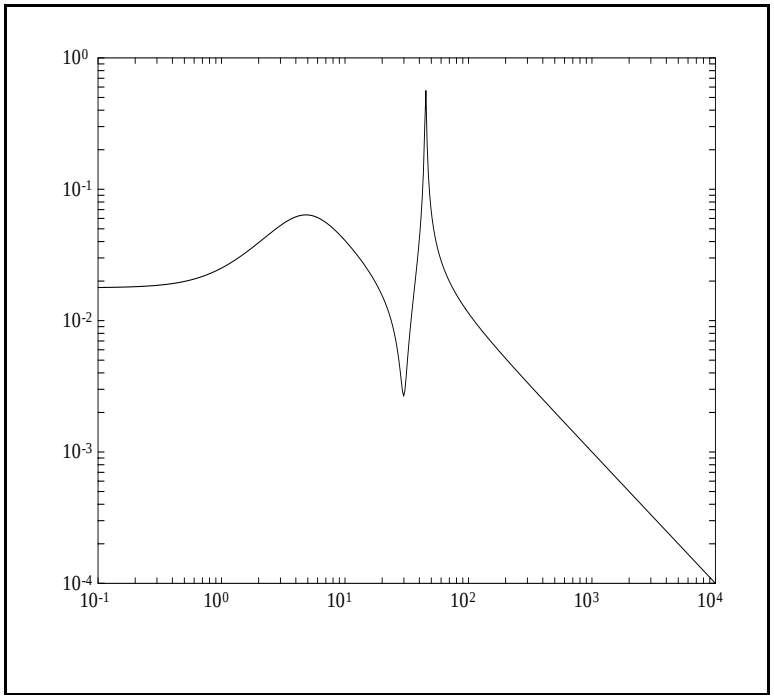

Figure 7.5: Bode plot of $|P|$, Example 3.

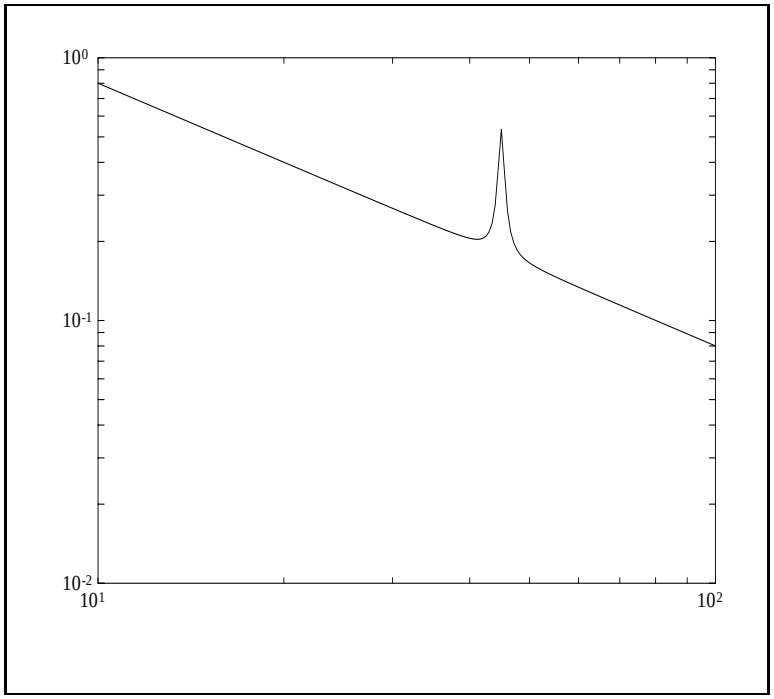

Figure 7.6: Loopshape, Example 3.

Exercises

1. This problem concerns the plant in Example 2 in Section 4.1—the double integrator with an uncertain time delay. Take
$$P(s) = \frac{1}{(s+0.01)^2}.$$
(This is supposed to be a stable approximation to the double integrator.) The time delay was accommodated by embedding the plant in a multiplicative perturbation with weight
$$W_2(s) = \frac{0.1s}{0.05s+1}.$$
To get good tracking over the frequency range $[0,1]$, a typical choice for W_1 would be a Butterworth filter with cutoff of 1 rad/s. To get at most 10% tracking error on the operating band, we would take the gain of the filter to be 10. A third-order such filter is
$$W_1(s) = \frac{10}{s^3+2s^2+2s+1}.$$
For these data, design a controller to achieve robust performance.

2. Repeat the design in Example 1, Section 7.3, but with
$$W_2(s) = \frac{10s+1}{20(0.01s+1)}.$$
This is more difficult because $|W_2|$ is fairly substantial on the operating band. See what performance level a you can achieve.

3. Consider the plant transfer function
$$P(s) = \frac{-s+16}{(s-6)(s+11)}.$$
This is unstable and non-minimum-phase, and loopshaping is consequently difficult for it. But try the loop transfer function
$$L(s) = \frac{\omega_c}{s}\,\frac{-s+16}{16}\,\frac{s+6}{s-6}\,\frac{1}{0.001s+1}.$$
This contains the unstable pole and zero of P, as it must for internal stability; it has relative degree 1, as it must for C to be proper; and it equals approximately $-\omega_c/s$ for low frequency. Compute ω_c to minimize $\|S\|_\infty$. Compute the resulting magnitude Bode plot of S and T.

Notes and References

The technique of loopshaping was developed by Bode for the design of feedback amplifiers (Bode, 1945), and subsequently Bower and Schultheiss (1961) and Horowitz (1963) adapted it for the design of control systems. The latter two references concentrate on particularly simple loopshaping techniques, namely, lead and lag compensation. Loopshaping and the root-locus method are the primary ones used today in practice for single-loop feedback systems. The phase formula is due to Bode. Exercise 3 is based on a simplified analysis of the X-29 experimental airplane (Enns 1986).

Advanced Loopshaping

In Chapter 7 we saw how to convert performance specifications on S and T into specifications on the loop transfer function L. For a stable, minimum-phase plant and L having at least the same relative degree as P, the controller was obtained from $C = L/P$. In this chapter we discuss extensions to this basic idea by doing loopshaping directly with C or other quantities and by considering plants with right half-plane (RHP) poles or zeros. Finally, we introduce several optimal control problems and explore in what sense loopshaping designs can be said to be optimal. Our aim is to extend and deepen our understanding of loopshaping, to provide an introduction to optimal design, and to establish some connections between the two approaches. Much of this chapter is closely related to what has traditionally been called classical control, particularly the work of Bode.

8.1 Optimal Controllers

Recall from Section 4.5 that in general the norm

$$\|(|W_1 S|^2 + |W_2 T|^2)^{1/2}\|_\infty$$

is a reasonable performance measure, a compromise norm for the robust performance problem. Throughout this chapter we consider problems where P, W_1, and W_2 are fixed but C is variable, so it is convenient to indicate the functional dependence of this norm on C by defining

$$\psi(C) := \|(|W_1 S|^2 + |W_2 T|^2)^{1/2}\|_\infty. \tag{8.1}$$

Throughout this chapter we refer to the *optimal* C, the controller that minimizes ψ, for the purpose of comparing it to controllers obtained via other methods in order to help evaluate their effectiveness. A procedure for determining the optimal C given P and weights W_1 and W_2 is developed in Chapter 12.

We shall treat the unity-feedback loop of Figure 8.1. Suppose that we focus on the response of e and u to the two inputs d and n (r has the same effect as n), and recall that the transfer functions from d and n to e and u are given as follows:

$$\begin{bmatrix} e \\ u \end{bmatrix} = -\begin{bmatrix} PS & S \\ T & CS \end{bmatrix} \begin{bmatrix} d \\ n \end{bmatrix}.$$

If we introduce weights W_e on e, W_u on u, W_d on d, and W_n on n, then we could make our performance specification to keep the matrix

$$\begin{bmatrix} W_e & 0 \\ 0 & W_u \end{bmatrix} \begin{bmatrix} PS & S \\ T & CS \end{bmatrix} \begin{bmatrix} W_d & 0 \\ 0 & W_n \end{bmatrix} = \begin{bmatrix} W_e S \\ W_u CS \end{bmatrix} \begin{bmatrix} W_d P & W_n \end{bmatrix}$$

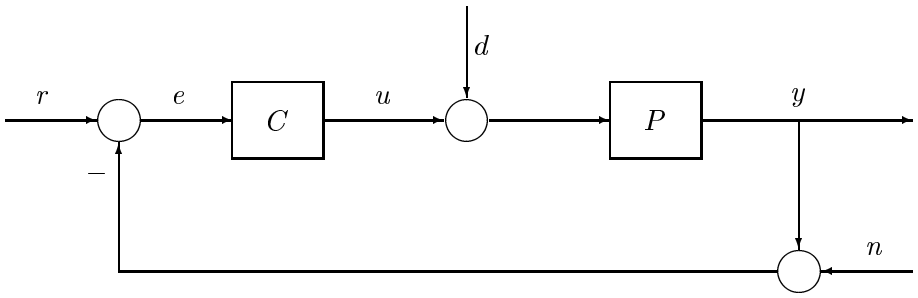

Figure 8.1: Unity-feedback loop.

small in some sense. A convenient specification is

$$\left\| (|W_e S|^2 + |W_u C S|^2)^{1/2} (|W_d P|^2 + |W_n|^2)^{1/2} \right\|_\infty < 1,$$

which is equivalent to

$$\left\| (|W_1 S|^2 + |W_2 T|^2)^{1/2} \right\|_\infty < 1,$$

where

$$|W_1| = |W_e|(|W_d P|^2 + |W_n|^2)^{1/2}, \qquad |W_2| = |W_u|(|W_n|^2 |P|^{-2} + |W_d|^2)^{1/2}. \tag{8.2}$$

Thus this problem fits the type of performance specification in (8.1).

We will use this setup throughout this chapter, as it makes a useful "standard" problem for a number of reasons. First, it leads to some very interesting control problems, even when simple constant weights are used. Second, there is a rich theory available for this problem, although it will only be hinted at in this chapter. Third, it is easy to motivate problems in this framework that greatly stretch the loopshaping methods. Finally, despite its simplicity, the problem setup is easy to relate to what might arise in many practical situations.

8.2 Loopshaping with C

The loopshaping procedure developed in Chapter 7 involved converting performance specifications on S and T into specifications on the loop transfer function L, and then constructing an L to satisfy the resulting specifications and have reasonable crossover characteristics. Assuming that the plant had neither RHP poles nor zeros, and that L had at least the same relative degree as P, the controller was obtained from $C = L/P$. In this section we consider a slightly different approach that focuses more directly on C. Rather than construct L without regard to P, we could begin with a very simple controller, say $C = 1$, and compare the resulting L with the specification. It is often easy then to add simple dynamics to C to meet the specification.

In some instances it is more convenient to do loopshaping directly in terms of C rather than L. This will typically occur when the weights on S and T share substantial dynamics with P, as in (8.2). If we put a constant weight of 1 on d and n and a constant weight of 0.5 on u and e, then the weights from (8.2) become

$$W_e = W_u = 0.5, \qquad W_d = W_n = 1, \tag{8.3}$$

$$|W_1| = 0.5(|P|^2 + 1)^{1/2}, \qquad |W_2| = 0.5(|P|^{-2} + 1)^{1/2}. \tag{8.4}$$

With W_1 and W_2 so defined, for the performance specification to be met the loopshape will usually be very similar to P, so that the controller C will have $|C| \approx 1$. We can get some insight into why this is so by interpreting the weights in terms of the requirements they place on $|C|$ as follows.

For $L = PC$

$$|W_1 S|^2 = 0.25\frac{|P|^2 + 1}{|L + 1|^2}, \qquad |W_2 T|^2 = 0.25\frac{|P|^{-2} + 1}{|L^{-1} + 1|^2},$$

and

$$\frac{|W_2 T|}{|W_1 S|} = |C|.$$

Assuming that $\psi(C) < 1$, at frequencies for which $|P| \gg 1$ we have that

$$|W_1| \approx 0.5|P|, \qquad |W_2| \approx 0.5, \qquad |W_1 S| \approx 0.5\frac{|T|}{|C|}, \qquad |W_2 T| \approx 0.5|T|,$$

and when $|P| \ll 1$,

$$|W_1| \approx 0.5, \qquad |W_2| \approx 0.5\frac{1}{|P|}, \qquad |W_1 S| \approx 0.5|S|, \qquad |W_2 T| \approx 0.5|CS|.$$

The crossover region can occur wherever $|P| \approx 1$. When $|P| = 1$, we have

$$|W_1| = |W_2| = \frac{\sqrt{2}}{2}.$$

Viewing this as a standard loopshaping problem, we would expect that $|L| \approx |P|$ and $|C| = 1$.

Example 1 Consider P given by

$$P(s) = \frac{0.5}{s} + \sum_{i=1}^{4} \frac{0.2s}{s^2 + 2\zeta_i\omega_i s + \omega_i^2},$$

where $\omega_1 = 0.2$, $\omega_2 = 0.5$, $\omega_3 = 2$, $\omega_4 = 10$, $\zeta_i = 0.02$. The Bode magnitude plot of P is shown in Figure 8.2, and the resulting weights W_1 and W_2 on S and T are shown in Figure 8.3.

The complicated weights would appear to make this a tricky loopshaping problem, but in fact the controller $C = 1$ meets the specification. The quantity

$$(|W_1 S|^2 + |W_2 T|^2)^{1/2} \tag{8.5}$$

for $C = 1$ is plotted in Figure 8.4. The optimal ψ for this problem is approximately 0.69, so $C = 1$ is very close to optimal.

This example illustrates the point that loopshaping directly using C can often be much simpler than loopshaping with L and solving for C. While the example is somewhat contrived, similar things can happen quite naturally. In particular, this example exhibits some characteristics of plants that arise in the control of flexible structures.

Example 2 We will now use the same setup but with a slightly simpler plant P which we will motivate with a simple mechanical analog of a two-mode flexible structure (Figure 8.5). Shown is a one-dimensional rigid beam of mass M, length $2l$, and moment of inertia I connected to a

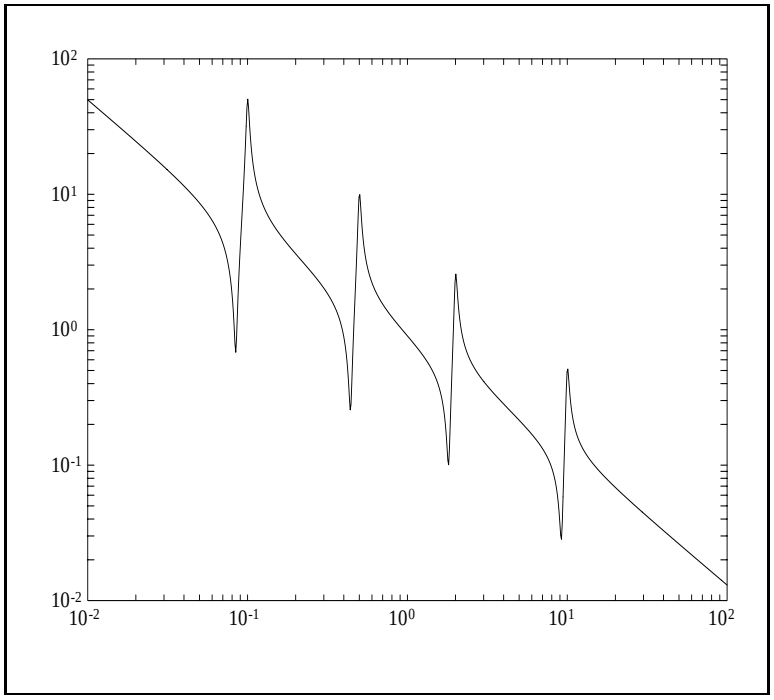

Figure 8.2: Bode plot of $|P|$.

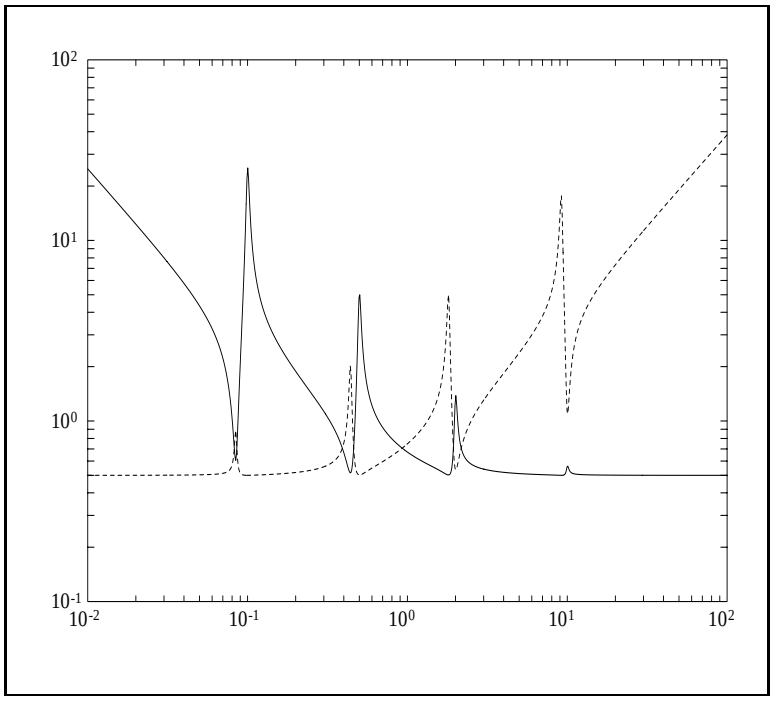

Figure 8.3: Bode plots of $|W_1|$ (solid) and $|W_2|$ (dash).

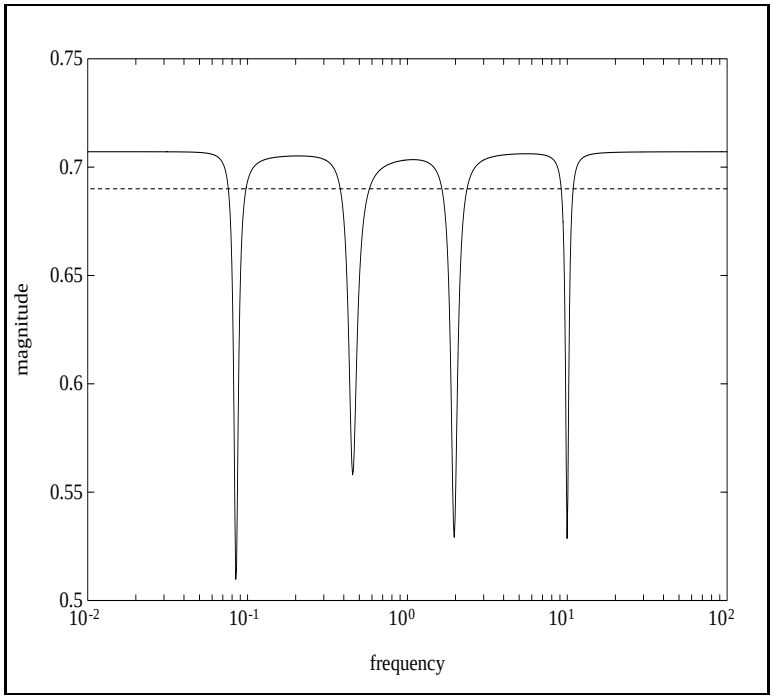

Figure 8.4: $(|W_1S|^2 + |W_2T|^2)^{1/2}$ for $C = 1$ (solid) and optimal C (dash).

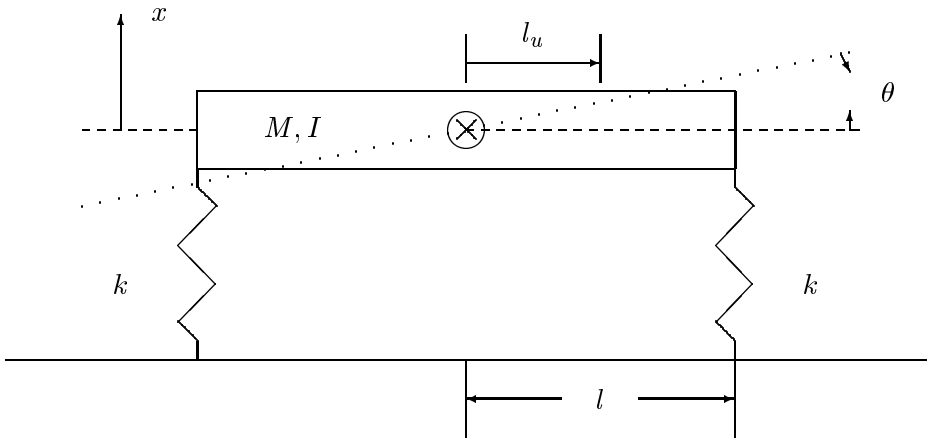

Figure 8.5: Mechanical structure, Example 2.

fixed base by two springs, each with spring constant k. We assume that the beam undergoes small vertical deflections x of the center of mass and small rotations θ about the center of mass. If we apply a vertical force u at position l_u from the center of mass, the linearized equations of motion are

$$\begin{aligned} M\ddot{x} + 2kx &= u, \\ I\ddot{\theta} + 2kl^2\theta &= l_u u. \end{aligned}$$

Taking $M = 2$, $I = 0.5$, $l = 2$, $k = 0.25$, and $l_u = 1$, we get that the transfer functions from u to x and θ are respectively

$$\frac{0.5}{s^2 + 0.5^2}, \qquad \frac{2}{s^2 + 2^2}.$$

We will now measure $y := \dot{x} \pm \dot{\theta}$, the vertical velocity of the beam at the position ± 1 from the center of mass. For $+1$, the measurement is at the same location as the force input u; this is called *collocated*. In the -1 case the measurement is at the other side of the beam, *noncollocated*. The resulting transfer function from u to y is then

$$P(s) = \frac{0.5s}{s^2 + 0.5^2} \pm \frac{2s}{s^2 + 2^2} = \frac{(2 \pm 0.5)s(1 \pm s^2)}{(s^2 + 0.5^2)(s^2 + 2^2)}. \tag{8.6}$$

A plot of $|P|$ is shown in Figure 8.6. The collocated system has zeros at $\pm j$ and the noncollocated

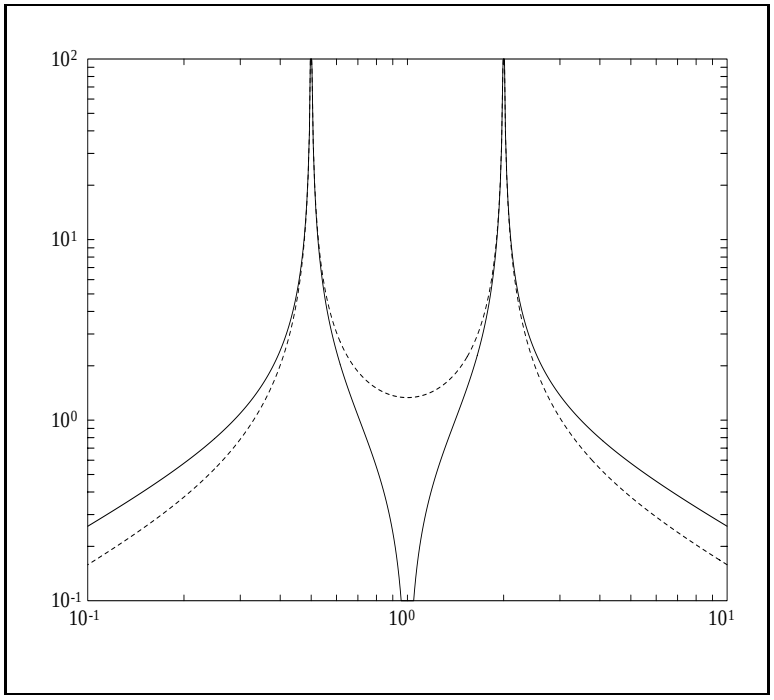

Figure 8.6: Bode plots of $|P|$ for $+$ (solid) and $-$ (dash).

system has zeros at ± 1. As expected, we shall see that the noncollocated system is more difficult to control. For the collocated case it turns out that the optimal controller for the weights (8.3) is exactly $C = 1$, which is again much simpler than the resulting loopshape. It also turns out that this result holds for all positive values of M, I, l, l_u, and k, excluding those for which the

system is not mechanically possible. In each case, the optimal controller is $C = 1$ and the optimal $\psi = \sqrt{2}/2 \approx 0.707$. A proof of this, along with a discussion of the noncollocated case, is given in the last section of this chapter.

It is interesting to note that both examples above have multiple crossover frequencies, that is, several distinct frequencies at which $|L| = 1$. By contrast, most previous examples had only one crossover frequency. Indeed, most problems considered in classical control texts have a single crossover, and this might be considered typical. There are, however, certain application domains, such as the control of flexible structures, where multiple crossovers are common. It turns out that such systems have some interesting characteristics which may appear counterintuitive to readers unfamiliar with them. These issues will be explored more fully in the last section of this chapter.

It is not unusual for a reasonable controller to be much simpler than the resulting loopshape even when the problem setup is different from the one considered in the examples above. It often makes sense to begin the loopshaping design process with L equal to some constant times P and then add dynamic elements to try to get the right loopshape.

Example 3 As a slightly different example, consider the same setup as in Example 1 but with

$$P(s) = \frac{1}{s+1} + \frac{0.1s}{s^2 + 2\zeta\omega_1 s + \omega_1^2},$$

where $\zeta = 0.02$ and $\omega_1 = 0.5$. Suppose also that the weight on the error e is

$$W_e(s) = 0.5\frac{s+0.5}{s+0.01},$$

with $W_u = 0.5$ and $W_d = W_n = 1$ as before. This gives us the performance objective as in (8.1), (8.2), and (8.4) except that now

$$|W_1| = |W_e|(|P|^2 + 1)^{1/2}, \qquad |W_2| = 0.5(|P|^{-2} + 1)^{1/2}.$$

The Bode magnitude plot of P is shown in Figure 8.7 and the resulting weights W_1 and W_2 on S and T are shown in Figure 8.8.

If we compare the loopshaping constraints in Figure 8.9 with the Bode plot of P in Figure 8.7 we see immediately that $C = 1$ will not work because there is not enough gain at low frequency. Adding the simple lag compensator

$$C(s) = \frac{s+1}{s+0.01}$$

gives the loopshape shown in Figure 8.9 and $(|W_1S|^2 + |W_2T|^2)^{1/2}$ as shown in Figure 8.10. Figure 8.10 also shows the optimal level for this problem. The simple controller found here is very close to optimal.

8.3 Plants with RHP Poles and Zeros

Plants with RHP Zeros

Suppose that we begin a loopshaping problem with a plant P_0, controller C_0, and loop transfer function $L_0 = P_0C_0$ with neither RHP poles nor zeros and a single crossover. Now consider the effect of adding a single RHP zero at $s = z$ to the plant by multiplying by the all-pass function

$$P_z(s) = \frac{z-s}{z+s},$$

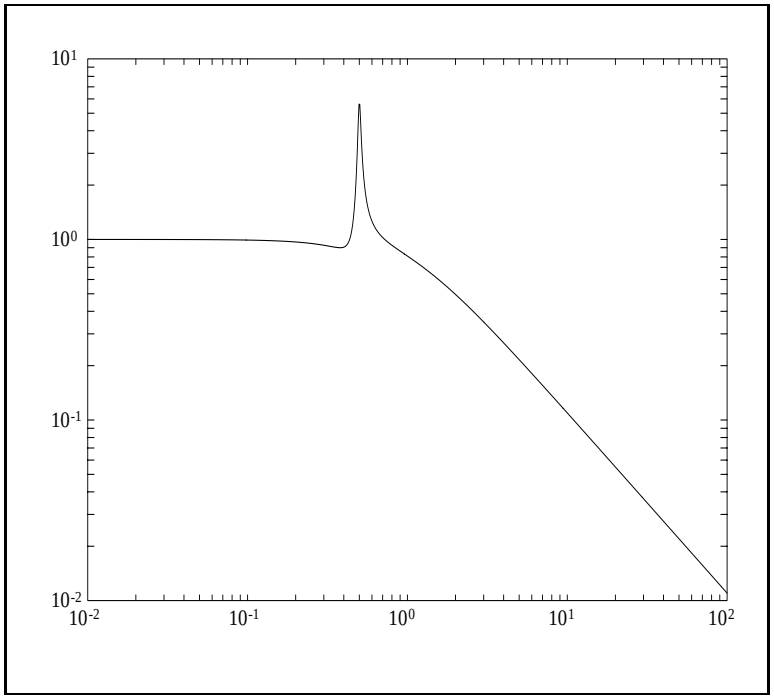

Figure 8.7: Bode plot of $|P|$.

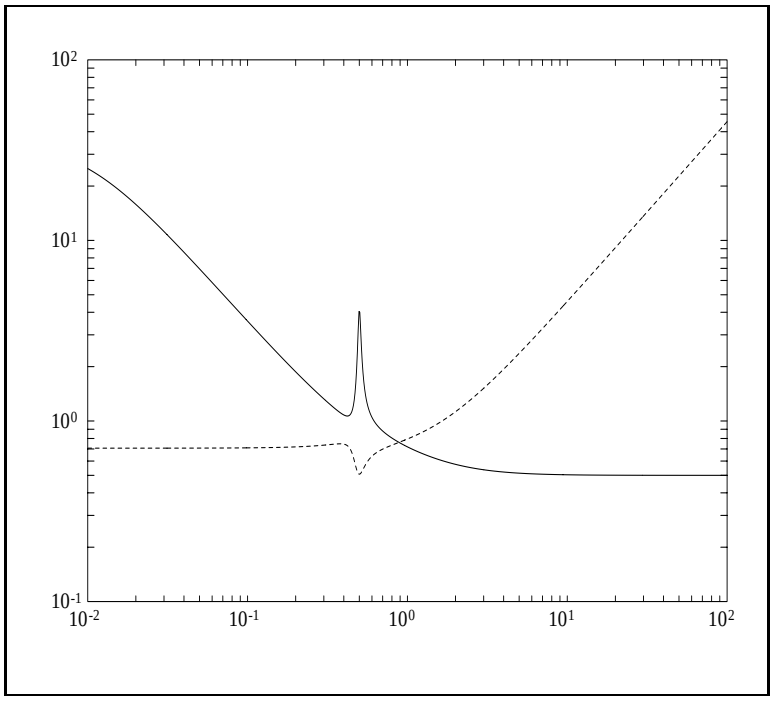

Figure 8.8: Bode plots of $|W_1|$ (solid) and $|W_2|$ (dash).

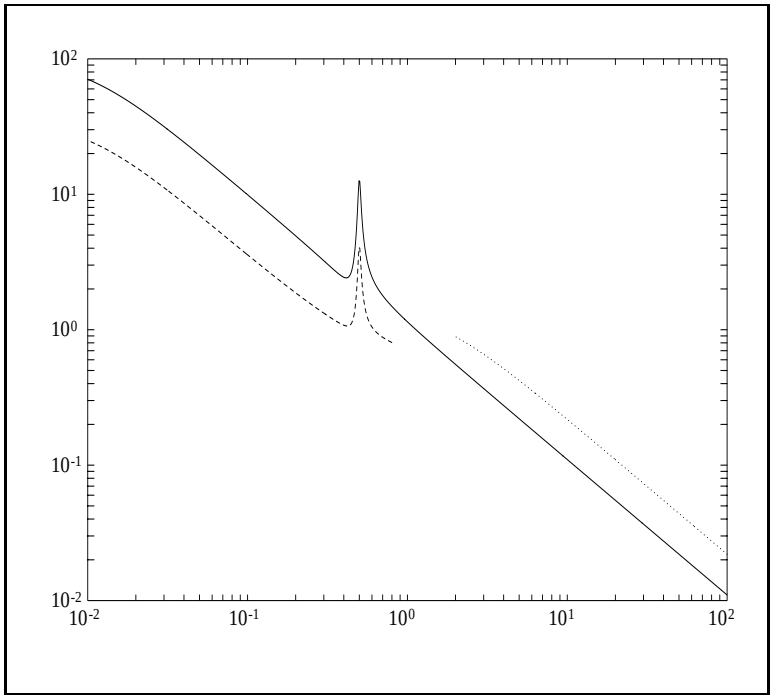

Figure 8.9: Loopshaping constraints and $|L|$ (solid) for $C = (s+1)/(s+0.01)$.

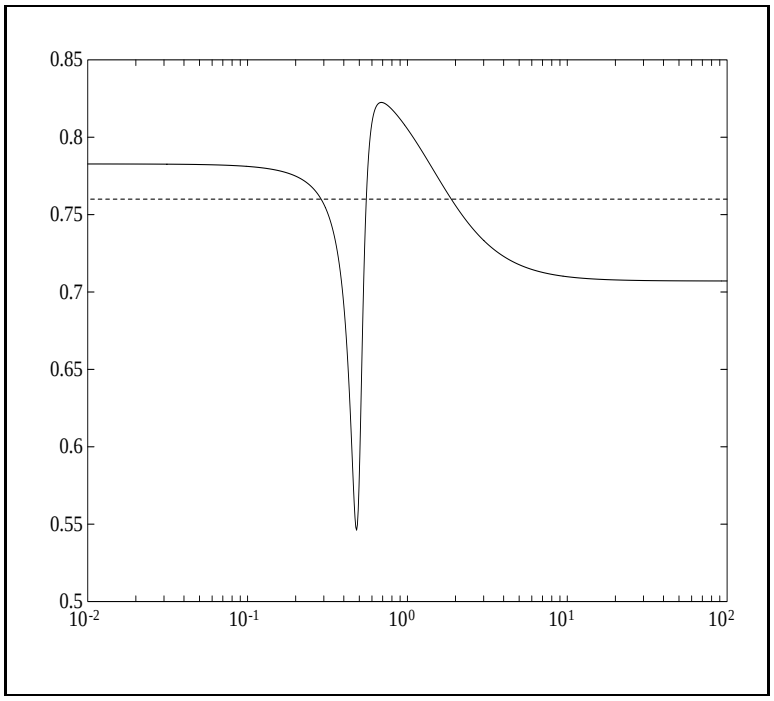

Figure 8.10: $(|W_1S|^2 + |W_2T|^2)^{1/2}$ for $C = (s+1)/(s+0.01)$ (solid) and optimal C (dash).

where the sign of P_z is chosen so that $P_z(0) = 1$. This also adds the same factor to the loop transfer function, which becomes

$$L(s) = L_0(s)\frac{z-s}{z+s}.$$

From the results of Chapter 6 we would expect problems unless z is larger than the crossover frequency: Recall that

$$\|W_1 S\|_\infty \geq |W_1(z)|,$$

so that $|W_1|$ must not be large at z.

We may also consider the effect of the RHP zero in terms of the gain-phase relations from Section 7.2. The phase at crossover will be the original phase of L_0 plus the phase of P_z:

$$\begin{aligned} \angle L(j\omega) &= \angle L_0(j\omega) + \angle P_z(j\omega), \\ \angle P_z(j\omega) &= 2\angle(-j\omega + z). \end{aligned}$$

The phase from P_z is negative and can be substantial as ω approaches z, with $\angle P_z(jz) = -\pi/2$. Again, we see that if z approaches the crossover frequency, the additional phase will degrade the closed-loop system performance or even lead to instability. Thus RHP zeros make the problem worse for systems with one crossover. As an example, let the initial loopshape be $L_0(s) = 1/s$ with L as above. The crossover frequency is $\omega = 1$ and the closed-loop system is stable if $z > 1$ and unstable if $z \leq 1$.

If P_z has a complex pair of RHP zeros, then

$$P_z(s) = \frac{\omega_z^2 - 2\zeta_z\omega_z s + s^2}{\omega_z^2 + 2\zeta_z\omega_z s + s^2}$$

and

$$\angle P_z(j\omega) = 2\angle(-2\zeta_z\omega_z j\omega + \omega_z^2 - \omega^2).$$

Observe that for lightly damped zeros where ζ_z is small, the phase changes abruptly near $\omega = \omega_z$. Otherwise, the same remarks apply here as in the case of one RHP zero. The simplest strategy to adopt in doing loopshaping designs for systems with RHP zeros is to proceed as usual while keeping track of the extra phase.

It would seem from this discussion that RHP zeros are always undesirable, that we would always avoid them if possible, and that we would never deliberately introduce them in our controllers. It is clearly true that all other things being equal, there is no advantage in having RHP zeros in the plant, because we could always add them in the controller if they were desirable. The issue of using RHP zeros in the controller is more subtle. Basically, they are clearly undesirable when there is only one crossover, but may be useful when there are multiple crossovers. This issue will be considered more fully in later sections on optimality.

Plants with RHP Poles

The problems created by RHP poles are similar to those created by RHP zeros, but there are important differences. Suppose that we begin again with a loopshaping problem with a plant P_0, controller C_0, and loop transfer function $L_0 = P_0C_0$ with neither RHP poles nor zeros and a single crossover. Now consider the effect of adding a single RHP pole at $s = p$ to the plant by multiplying it by the all-pass function

$$P_p(s) = \frac{s+p}{s-p}.$$

This also adds the same factor to the loop transfer function L. The sign of P_p is chosen so that $P_p(0) = -1$. For p small, this gives the right number of encirclements for L to give closed-loop stability. Now we expect that we will have problems unless p is *smaller* than the crossover frequency: Recall that

$$\|W_2 T\|_\infty \geq |W_2(p)|,$$

so that $|W_2|$ must not be large at p.

We may also consider the effect of the RHP pole in terms of the gain-phase relations. The phase at crossover will be the original phase of L_0 plus the phase of P_p:

$$\begin{aligned} \angle L(j\omega) &= \angle L_0(j\omega) + \angle P_p(j\omega), \\ \angle P_p(j\omega) &= 2\angle(j\omega + p). \end{aligned}$$

We may illustrate this with the same example. Let the initial loopshape be $L_0(s) = 1/s$ with L as above. The crossover frequency is $\omega = 1$ and the closed-loop system is stable if $p < 1$ and unstable if $p \geq 1$. Similar effects hold when there is more than one RHP pole.

All things being equal, we would prefer to avoid RHP poles in our plants. Even though they can be stabilized by feedback, there is a price to pay in terms of closed-loop performance. Recall that there are times when we must add RHP poles in our compensator just to stabilize the system. Are there other times when we would want to add RHP poles? Clearly no if we have only one crossover, but if there are multiple crossovers it might be advantageous. This will be discussed in a later section on optimality.

Including RHP Poles and Zeros in Uncertainty Description

A somewhat more formal strategy for handling RHP poles and zeros is to include them in the uncertainty description as follows. Suppose that we have a RHP zero at z. Then we can factor P as

$$P(s) = P_0(s)\frac{z-s}{z+s} = P_0(s)\left(1 + \frac{-2s}{z+s}\right)$$

and cover this with a multiplicative perturbation to get

$$P = P_0\left(1 + W_z\Delta\right), \qquad W_z(s) = \frac{2s}{z+s}.$$

A somewhat tighter cover is given by

$$\begin{aligned} P(s) &= P_0(s)\left(\frac{z}{z+s} - \frac{s}{z+s}\right) \\ &= P_0(s)\frac{z}{z+s}\left[1 + W_z(s)\Delta(s)\right], \\ W_z(s) &= \frac{s}{z}. \end{aligned}$$

Robust stability for uncertainty in this form would involve a test on $\|W_z T\|_\infty$.

Why would we want to do this? If we put all the RHP zeros into the plant uncertainty, then we can use any design technique for plants with no RHP zeros, provided that we account for the extra uncertainty. Basically, one makes sure that T is small enough where necessary. The way we have covered the RHP zero above makes the model have little uncertainty at low frequencies and considerable uncertainty at high frequencies. The transition occurs at frequencies near z. It is also

easy to cover the all-pass part with an uncertainty that is large at low frequencies and small at high frequencies.

We can model RHP poles similarly. Care must be taken, however, because RHP poles don't naturally go into multiplicative uncertainty. Suppose that we have a RHP pole at p. Then we can factor P as

$$P(s) = P_0(s)\frac{s+p}{s-p} = P_0(s)\left(1+\frac{-2p}{s+p}\right)^{-1}$$

and cover this with a perturbation to get

$$P = P_0\frac{1}{1+W_p\Delta}, \qquad W_p(s) = \frac{2p}{s+p}.$$

This introduces an additional weight on S. A somewhat tighter cover is given by

$$\begin{aligned} P(s) &= P_0(s)\left(\frac{s}{s+p}-\frac{p}{s+p}\right)^{-1} \\ &= P_0(s)\frac{s+p}{s}\frac{1}{1+W_p(s)\Delta(s)}, \\ W_p(s) &= \frac{p}{s}. \end{aligned}$$

How conservative is this covering method? For most problems with a single crossover and for which the performance objectives are achievable, this approach will work well. Basically, we need to make sure that S is small enough where there are RHP poles and T is small enough where there are RHP zeros. There are more complicated problems, particularly those involving multiple crossovers, where the impact of RHP poles and zeros might be quite different. This issue will be considered again in the final section of this chapter.

Examples

We will now consider several examples that illustrate loopshaping for systems with RHP zeros and poles.

Example 1 Consider

$$P(s) = P_0(s)\frac{z-s}{z+s}, \quad P_0(s) = \frac{1}{s}.$$

As in Section 8.2,

$$|W_1| = 0.5(|P|^2+1)^{1/2}, \qquad |W_2| = 0.5(|P|^{-2}+1)^{1/2}, \tag{8.7}$$

or

$$W_1(s) = 0.5\left(1+\frac{1}{s}\right), \qquad W_2(s) = 0.5(s+1). \tag{8.8}$$

The obvious controller for P_0 is $C = 1$, which is also optimal with $|W_1S| = |W_2T| = 0.5$ and $\psi(C) = \sqrt{2}/2$. This simple controller will work fine for $z \gg 1$, but deteriorates as z approaches 1 and does not stabilize for $z \leq 1$ because of the additional phase lag caused by the all-pass factor. Recall that for any controller

$$\|W_1S\|_\infty \geq |W_1(z)| = 0.5\left(1+\frac{1}{z}\right),$$

but it is possible to improve substantially on $C = 1$ as z gets close to 1.

We will now focus on $z = 2$. For $C = 1$ the loopshape constraints and the loopshape $L = CP$ are shown in Figure 8.11. The closed-loop performance is shown in Figure 8.12. Note that $\psi(C) > 2$, with both $|W_1 S|$ and $|W_2 T|$ exceeding the specification at low and high frequencies, with a large peak in the middle. This is due to too much phase lag in L at crossover ($\omega = 1$). Recall from the gain-phase formula in Section 7.2 that we may improve the phase at crossover by reducing the low-frequency gain, reducing the crossover frequency, and increasing the high-frequency gain. A simple controller that does this is of the form

$$C(s) = \frac{k(s+2)}{(s+2k^2)}, \quad k > 1. \tag{8.9}$$

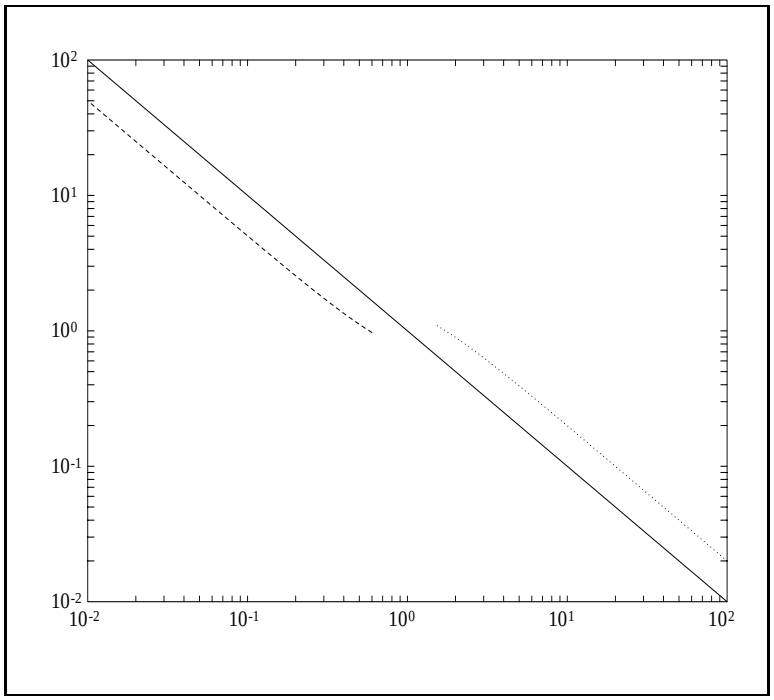

Figure 8.11: Loopshaping constraints (dash and dot) and $|L|$ (solid) for $C = 1$.

It turns out that the optimal C has $k = 1.78$, which yields an optimal $\psi(C) = 1.02$. A value of k very close to optimal is also easily arrived at by a little trial and error. The loopshape for the optimal C is shown in Figure 8.13 and the closed-loop performance is shown in Figure 8.14. The controller reduces the low-frequency gain and the crossover frequency and raises the high-frequency gain of L, as expected.

Next we will try an alternative design by covering the RHP zero with uncertainty and then loopshaping with the resulting minimum-phase nominal plant. For general z write

$$P(s) = \frac{1}{s}\left(\frac{z}{z+s} - \frac{s}{z+s}\right) = P_0(s)\left[1 + W_z(s)\Delta(s)\right],$$

where

$$P_0(s) = \frac{1}{s}\frac{z}{z+s}, \qquad W_z(s) = \frac{s}{z}. \tag{8.10}$$

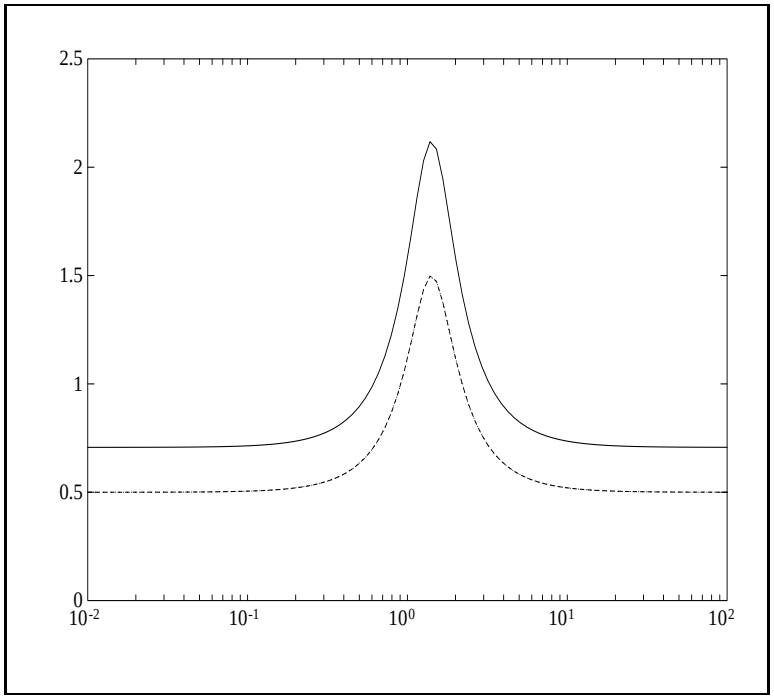

Figure 8.12: $(|W_1S|^2 + |W_2T|^2)^{1/2}$ (solid), $|W_1S|$ and $|W_2T|$ (both dash) for $C = 1$.

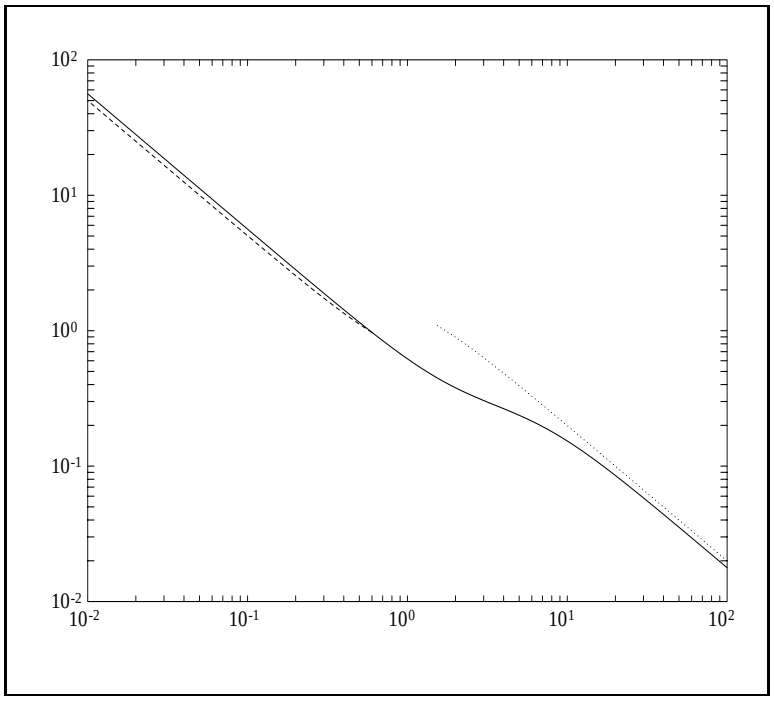

Figure 8.13: Loopshaping constraints (dash and dot) and $|L|$ (solid) for optimal C.

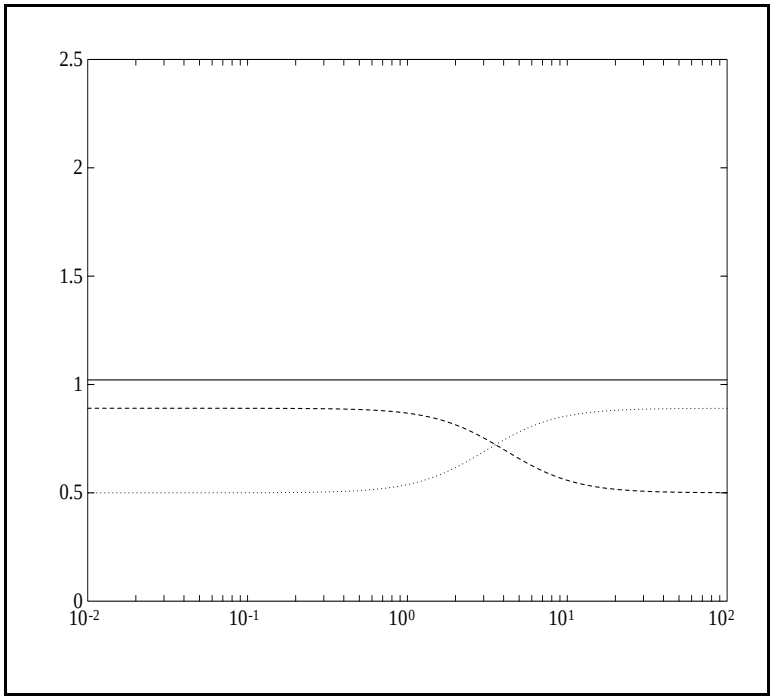

Figure 8.14: $(|W_1S|^2 + |W_2T|^2)^{1/2}$ (solid), $|W_1S|$ (dash), and $|W_2T|$ (dot), optimal C.

We now have two weights on T: W_2 and W_z. We need to find a weight that covers both of these. A reasonable approximation is

$$|W_{\text{tot}}| = |W_2| + |W_z| + |W_2||W_z|.$$

It is routine to show that

$$\left| \frac{(1 + \Delta W_z)W_2T}{1 + \Delta W_zT} \right| \leq \frac{|W_2T|(1 + |W_z|)}{1 - |W_zT|}$$

and

$$\frac{|W_2T|(1 + |W_z|)}{1 - |W_zT|} < 1 \quad \text{iff} \quad |W_{\text{tot}}T| < 1,$$

so using W_{tot} is a safe, but possibly conservative approximation. As an alternative way of thinking about this in terms of uncertainty descriptions, note that

$$\{(1 + |W_2|\Delta_1)(1 + |W_z|\Delta_2) : |\Delta_1| \leq 1, |\Delta_2| \leq 1\} \subset \{1 + |W_{\text{tot}}|\Delta : |\Delta| \leq 1\}.$$

If $z \gg 1$, this additional "uncertainty" will be negligible and the controller $C = 1$ will be fine.

Again, for the case $z = 2$ the plot for $|W_{\text{tot}}|$ is shown in Figure 8.15, together with plots of $|W_2|$ and $|W_z|$. To help us understand how conservative we have been by these approximations, we can compare

$$(|W_1S|^2 + |W_2T|^2)^{1/2} \tag{8.11}$$

for P with RHP zero at $s = 2$ with

$$\left[|W_1S|^2 + (1 + |W_z|)^2|W_2T|^2\right]^{1/2} \frac{1}{1 - |W_zT|} \tag{8.12}$$

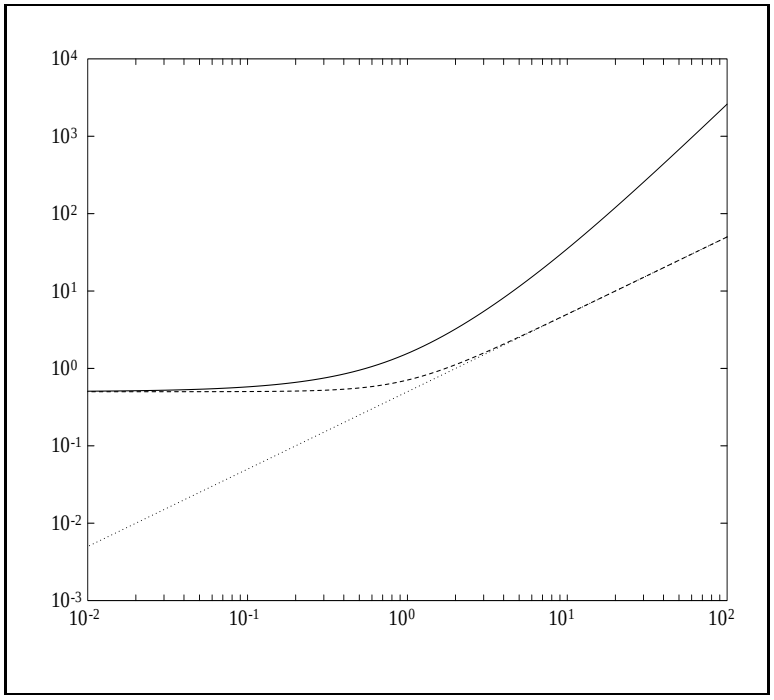

Figure 8.15: $|W_2|$ (dash), $|W_z|$ (dot), and $|W_{\rm tot}|$ (solid).

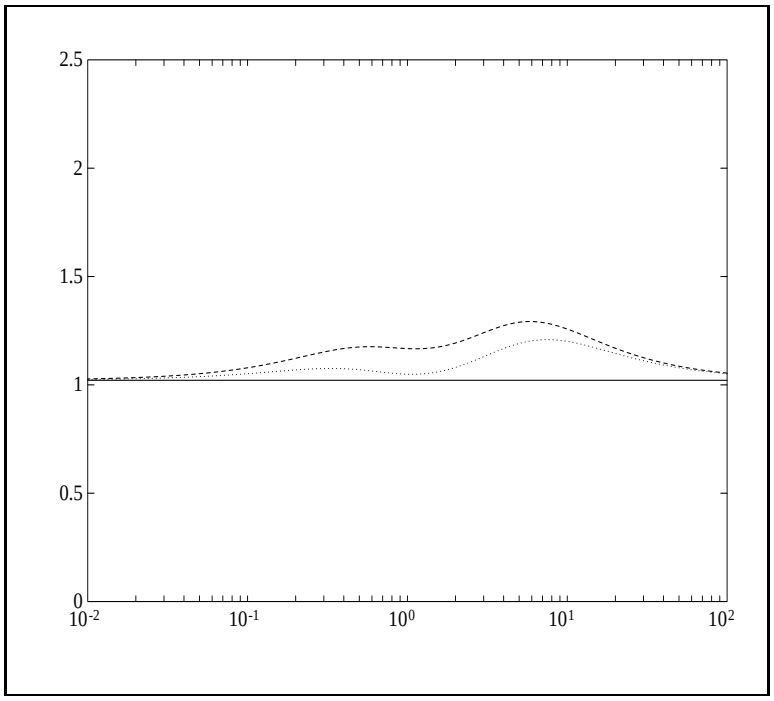

Figure 8.16: Plots of (8.11) (solid), (8.12) (dash), and (8.13) (dot).

and

$$(|W_1 S|^2 + |W_{\rm tot} T|^2)^{1/2}, \tag{8.13}$$

where in (8.12) and (8.13) we use the plant P_0 from (8.10). By construction, we have that (8.11) $\leq$ (8.12), but (8.13) is not necessarily an upper bound for (8.11). All three quantities are plotted in Figure 8.16.

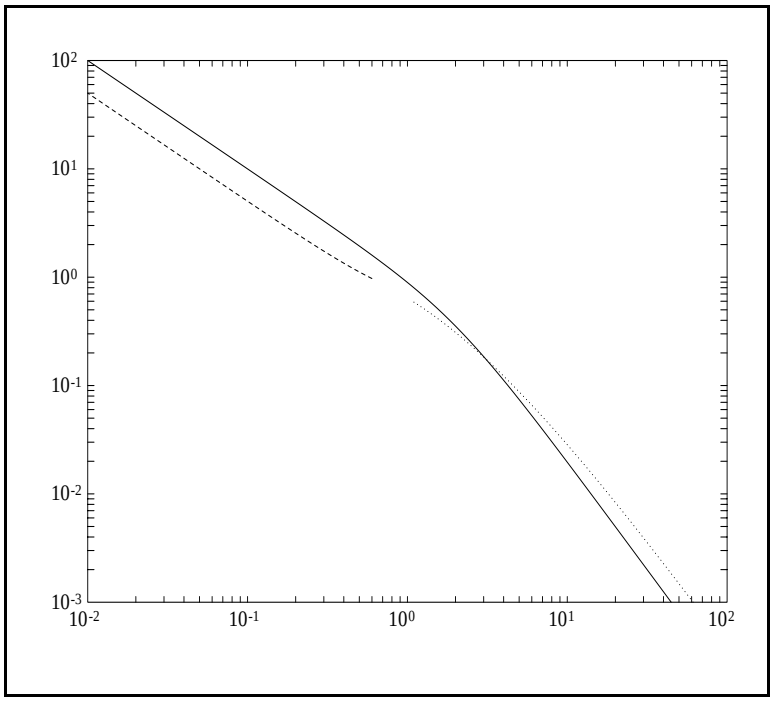

Figure 8.17: Loopshaping constraints (dash and dot) and $|L|$ (solid), $C = 1$.

For $P = P_0$ and $C = 1$, the loopshape $L = CP$ is shown in Figure 8.17, along with the loopshaping constraints. As before, there is too much phase lag in the crossover region, which is verified in Figure 8.18. As before, we may improve the phase at crossover by reducing the low-frequency gain, reducing the crossover frequency, and increasing the high-frequency gain. The optimal controller should once again be adequate, as is verified in Figures 8.19 and 8.20.

This example illustrates how the simple loopshaping ideas from this chapter and the preceding one can be extended to handle plants with RHP zeros.

Example 2 Now consider the problem of stabilizing the plant

$$P(s) = \frac{\alpha s - 1}{\alpha - s}, \qquad \alpha \in (0, 1). \tag{8.14}$$

It is easily checked that a constant controller $C = k$ stabilizes this system iff $k \in (\alpha, 1/\alpha)$. We may compare this with the conclusions we would arrive at if we were to cover the RHP zero and pole with uncertainty about a nominally stable, minimum-phase plant. For example, we may write

$$\frac{\alpha s - 1}{\alpha - s} = \frac{1}{s}\left(\frac{1 + \alpha s \Delta_1(s)}{1 + \alpha/s \Delta_2(s)}\right). \tag{8.15}$$

We can pose this in the standard form of $\psi(C)$ in (8.1) with plant $P(s) = 1/s$ and weights $W_1(s) = \alpha/s$ and $W_2(s) = \alpha s$. If we now consider loopshaping for this problem, we will meet this

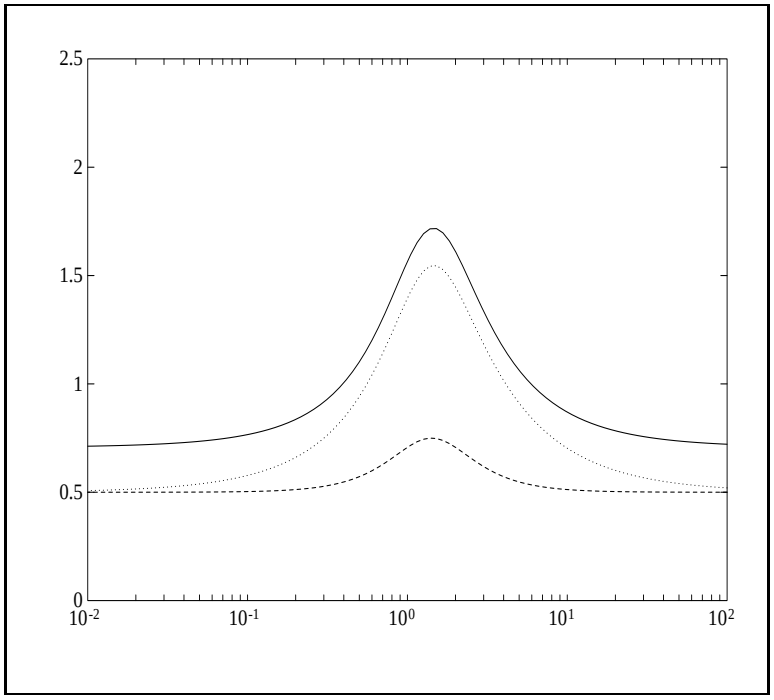

Figure 8.18: $(|W_1S|^2 + |W_{\rm tot}T|^2)^{1/2}$ (solid), $|W_1S|$ (dash), and $|W_{\rm tot}T|$ (dot), $C = 1$.

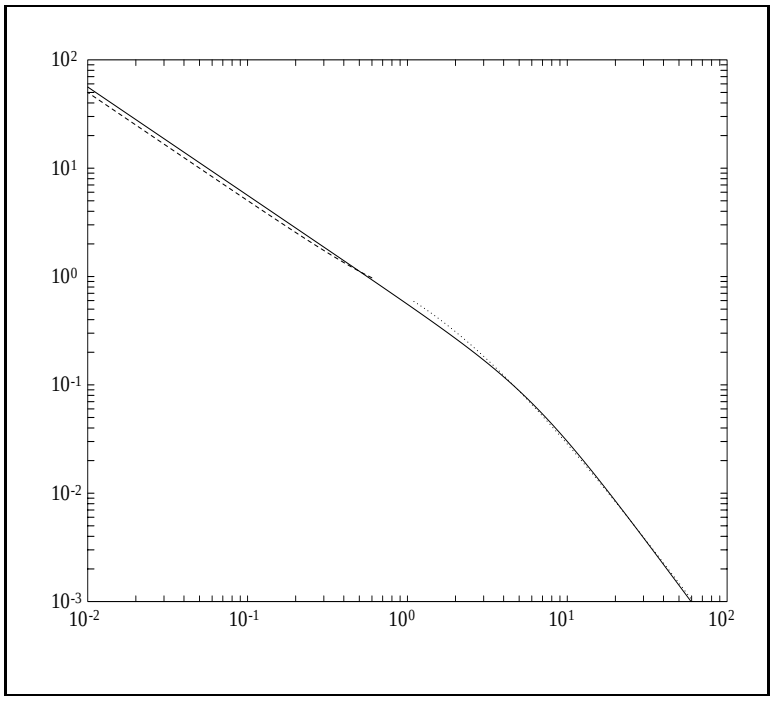

Figure 8.19: Loopshaping constraints (dash and dot) and $|L|$ (solid) for optimal C.

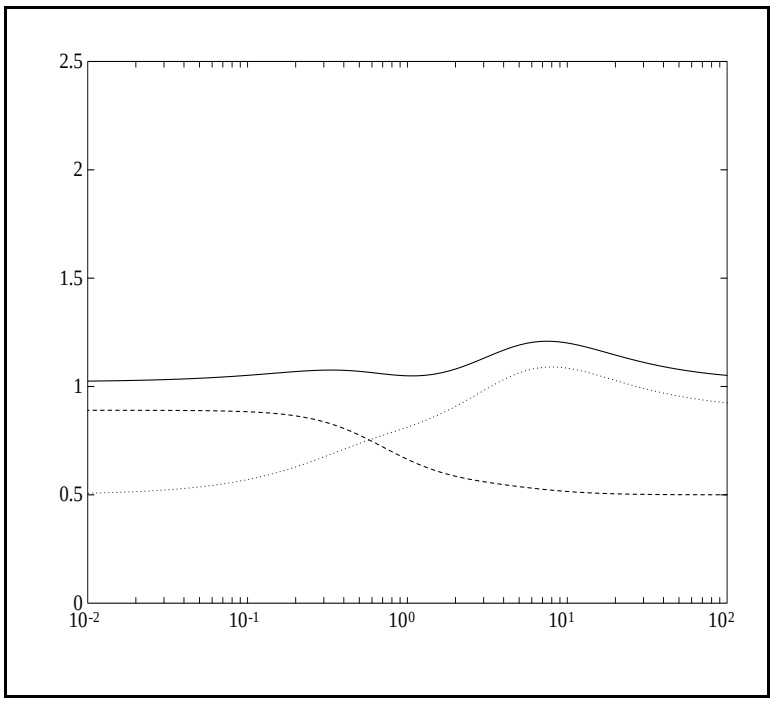

Figure 8.20: $(|W_1S|^2 + |W_{\rm tot}T|^2)^{1/2}$ (solid), $|W_1S|$ (dash), and $|W_{\rm tot}T|$ (dot), optimal C.

specification with a constant controller $C = k$ roughly if $k \in (\alpha, 1/\alpha)$, as before. Thus for this problem with both a RHP pole and zero, the approximation of covering the RHP pole and zero with uncertainty produces very little conservatism.

8.4 Shaping S, T, or Q

It is possible to do designs directly in terms of S and T rather than translate the specifications into constraints on the loopshape. This is especially useful when P is either stable or minimum-phase, or both. Then the stability constraints on S and T are particularly simple. For example, if there are only RHP zeros, these must appear in T, but T is otherwise unconstrained. The performance objective due to weights on T can be directly handled by the choice of T, but S is not as easy. Since $S = 1 - T$, we can make S small by making T close to 1. Although this can sometimes be a bit awkward, it is often the case that by looking at T and S directly in addition to L, we can arrive at a design more quickly.

Another alternative to loopshaping is to use Q, appearing in the parametrization of all stabilizing controllers. To summarize this, recall (Section 5.1) that if we have a stable P, we can parametrize the set of all stabilizing controllers as

$$C = \frac{Q}{1 - PQ},$$

where Q is any stable transfer function. In terms of this free parameter Q, we have that $S = 1 - PQ$ and $T = PQ$. As Q approaches $1/P$, then S approaches 0 and C approaches ∞. Thus for minimum-phase P, we can make S arbitrarily small, as expected. For non-minimum-phase P, recall that we can factor $P = P_{ap}P_{mp}$ where P_{ap} is all-pass and P_{mp} is minimum-phase. We can approximately invert the minimum-phase part by letting $Q = F/P_{mp}$, where F is a low-pass filter so that Q

is proper. We can then shape the low-pass F to trade off between S and T. This approach is essentially shaping T since $T = FP_{ap}$.

Example Take

$$P(s) = \frac{1}{s}\left(\frac{2-s}{2+s}\right). \tag{8.16}$$

Consider directly shaping T and look at tradeoffs between S and T and the limitations imposed by the RHP zero at $s = 2$. For internal stability we must have $T(2) = 0$ and $T(0) = 1$, so we can parametrize a family of allowable Ts with

$$\begin{aligned} T(s) &= \left(\frac{2-s}{2+s}\right)\frac{1}{1+\tau s}, \\ S(s) &= 1 - T(s) \\ &= \frac{s}{s+2}\left(\frac{\tau s + 2\tau + 2}{\tau s + 1}\right). \end{aligned}$$

This gives

$$\begin{aligned} L(s) &= \frac{T(s)}{S(s)} \\ &= \frac{2-s}{s(\tau s + 2\tau + 2)}, \\ C(s) &= \frac{s+2}{\tau s + 2\tau + 2}. \end{aligned}$$

For this parametrization, $1/\tau$ is roughly the closed-loop bandwidth, so we are pushing the bandwidth up by making τ small. This is shown in Figures 8.21 and 8.22, where S, T, and L are plotted for $\tau = 0.01$, 0.1, 1, 10, and 100. There are negligible changes in S, T, and L at low frequency as τ is decreased from 0.1 to 0.01, although the high-frequency characteristics change substantially. This illustrates another way the limits are imposed by RHP zeros.

If we take limits as $\tau \to 0$, we get

$$T \to \frac{2-s}{2+s}, \quad S \to \frac{2s}{s+2}, \quad L \to \frac{2-s}{2s}, \quad C \to \frac{2+s}{2}. \tag{8.17}$$

Thus even at the expense of an infinite bandwidth controller, we cannot get disturbance rejection much above $\omega = 1$. Recall that if we take the weight

$$W_1(s) = \frac{s+2}{2s},$$

then for any stabilizing controller

$$\|W_1 S\|_\infty \geq \left.\frac{s+2}{2s}\right|_{s=2} = 1,$$

so the S in (8.17) cannot be uniformly improved on. For very low bandwidths (i.e., for $\tau \gg 1$ and $\omega \ll 1$), the RHP zero has negligible impact as

$$T \approx \frac{1}{\tau s + 1}, \quad S \approx \frac{\tau s}{\tau s + 1}, \quad L \approx \frac{1}{\tau s}, \quad C \approx \frac{1}{\tau}.$$

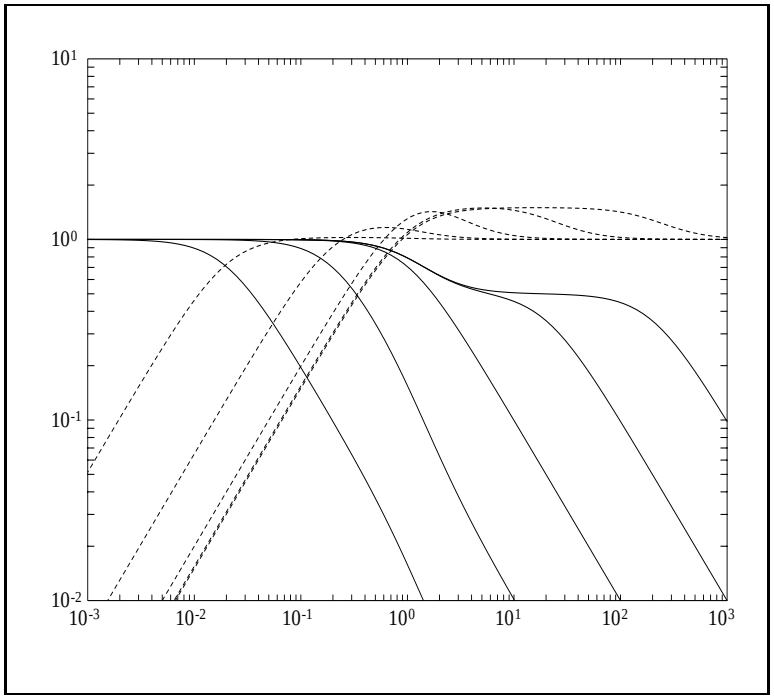

Figure 8.21: $|T|$ (solid) and $|S|$ (dash) for $0.01 \leq \tau \leq 100$.

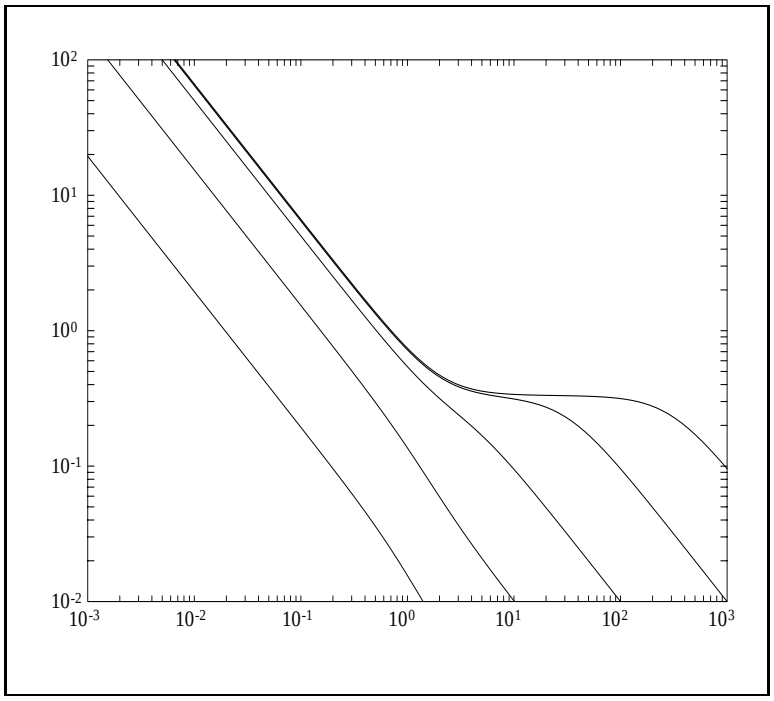

Figure 8.22: $|L|$ for $0.01 \leq \tau \leq 100$.

This example illustrates how we may easily explore the tradeoffs between S and T for P with RHP zeros by putting the zeros in T and then exploring a one-parameter family of T and hence S. Similar tradeoffs may be explored for plants with RHP poles by parametrizing a family of S. For plants with both RHP poles and zeros, it is necessary to use the more complicated parametrization developed in Chapter 5.

8.5 Further Notions of Optimality

Each of the design methods presented so far—shaping L, S, T, or Q—gives the designer something handy to manipulate to obtain a controller. In each case, the resulting controller will have to be examined in the closed-loop system to see if it is satisfactory—every controller results in some tradeoff between S and T, and the designer must decide if that tradeoff makes sense for a particular problem. However, some controllers are intrinsically poor. In particular, we would like to avoid design techniques that yield controllers that can be *uniformly* improved upon, that is, where both $|S|$ and $|T|$ can be reduced at every frequency. Such controllers clearly do a poor job on the tradeoff between S and T.

In this section we define several notions of optimality which we will use to help understand the notion of an intrinsically poor controller. In what follows, all controllers are assumed to be internally stabilizing and all weights are assumed to be stable and not identically zero; C_o is a fixed controller, and S_o and T_o its corresponding sensitivity and complementary sensitivity functions; C is some generic, variable controller and S and T its corresponding functions.

The first type of optimality we will consider is Pareto optimality. A controller C_o is *Pareto* (Par.) *optimal* if there is no C such that at every frequency $|S| < |S_o|$ and $|T| < |T_o|$; equivalently, for every C, at some frequency either $|S| \geq |S_o|$ or $|T| \geq |T_o|$. A controller C_o is *strongly Pareto* (str. Par.) *optimal* if there is no $C \neq C_o$ such that at every frequency $|S| \leq |S_o|$ and $|T| \leq |T_o|$; equivalently, for every $C \neq C_o$, at some frequency either $|S| > |S_o|$ or $|T| > |T_o|$. The class of strongly Pareto optimal controllers is quite large: some of them give good S and T tradeoffs, some do not. But controllers that are not strongly Pareto optimal, that is, are outside this class, are evidently poor because they can be improved uniformly.

Our primary objective in this section and the next is to show that loopshaping generally yields strongly Pareto optimal controllers. Unfortunately, we must take a circuitous route to establish this, introducing several intermediate notions of optimality. There are added benefits, however, in that these additional notions of optimality have some independent interest, and we shall see that optimal controllers, the subject of Chapter 12, are also Pareto optimal.

We have argued that the norm

$$\|(|W_1 S|^2 + |W_2 T|^2)^{1/2}\|_\infty$$

is a reasonable performance measure, a compromise norm for the robust performance problem. Recall that for fixed P with C variable, we defined

$$\psi(C) := \|(|W_1 S|^2 + |W_2 T|^2)^{1/2}\|_\infty.$$

Using $\psi(C)$, we can define two additional notions of optimality, together with strengthened versions involving uniqueness that are analogous to strongly Pareto optimal.

1. For given weights W_1 and W_2, C_o is *optimal* if $\psi(C_o) \leq \psi(C)$ for every C, and *uniquely optimal* if $\psi(C_o) < \psi(C)$ for every $C \neq C_o$.

2. C_o is *potentially* (pot.) *optimal* if there exist weights W_1, W_2 such that C_o is optimal for these weights and *potentially uniquely* (pot. uni.) *optimal* if there exist weights W_1, W_2 such that C_o is uniquely optimal for these weights.

These notions, along with Pareto optimal, are related according to the Venn diagram shown in Figure 8.23, which is easily verified. Potentially uniquely optimal is the strongest of the four notions.

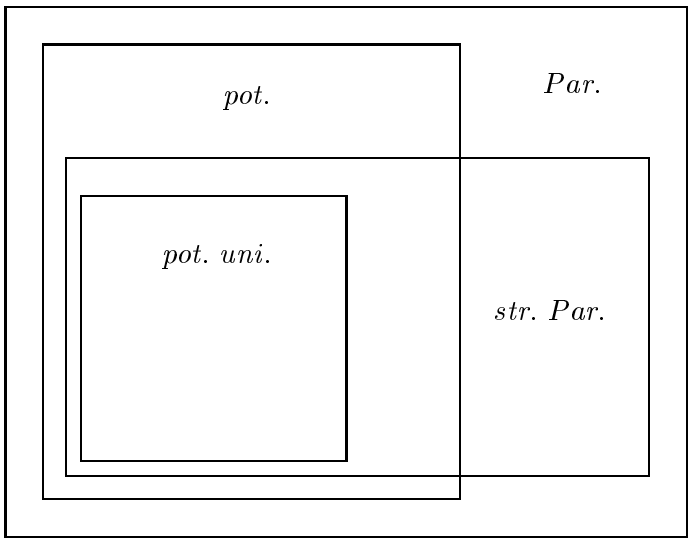

Figure 8.23: Notions of optimality.

Self-Optimality

In this subsection an even stronger type of optimality is introduced whose significance is due to three features:

1. It is easy to characterize.
2. Loopshaping generally produces controllers with this type of optimality.
3. It implies all the notions above, and in particular, strong Pareto optimality.

Fix a controller C_o, define $L_o := PC_o$, and define weights as follows: W_1^{-1} is the minimum-phase factor of S_o and W_2^{-1} is the minimum-phase factor of T_o. Thus the weights are defined in terms of the controller itself. Observe that W_2^{-1} may be strictly proper, and that both W_1^{-1} and W_2^{-1} may have zeros on the imaginary axis. Thus the weights W_1 and W_2 may not be bounded on the imaginary axis. Since $W_1 S_o$ equals the all-pass factor of S_o, it has constant magnitude 1 on the imaginary axis. Similarly for $W_2 T_o$. Thus

$$|W_1 S_o|^2 + |W_2 T_o|^2 = 2, \quad \forall \omega.$$

Given W_1 and W_2 so defined, C_o is called *self-optimal* if it is optimal with respect to these weights. Similarly, it is *uniquely self-optimal* if it is uniquely optimal with respect to these weights.

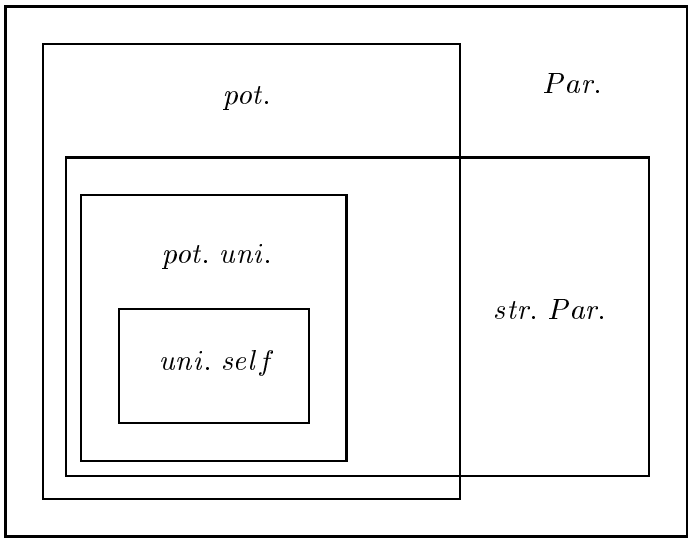

Figure 8.24: Notions of optimality.

It will be shown below that for almost all controllers, a self-optimal controller is uniquely self-optimal. The Venn diagram, including uniquely self-optimal is shown in Figure 8.24.

It is convenient to introduce the following notation. For a transfer function G having no poles on the imaginary axis, let

$$\begin{aligned} \#p(G) &:= \text{number of open RHP poles of } G, \\ \#z(G) &:= \text{number of open RHP zeros of } G, \\ \#i(G) &:= \text{number of imaginary axis zeros of } G. \end{aligned}$$

The main result is as follows.

Theorem 1 *If $\#i(L_o - 1) = 0$, C_o is self-optimal iff C_o is uniquely self-optimal iff*

$$\#z(L_o - 1) > \#p(C_o) + \#z(C_o). \tag{8.18}$$

We are restricting attention to the case $\#i(L_o - 1) = 0$ primarily for technical reasons, as it simplifies the development with a negligible loss of generality. Note that $\#i(L_o - 1) = 0$ iff $L_o(j\omega) \neq 1, \quad \forall\omega$. This would hold for almost all controllers, because if $\#i(L_o - 1) \neq 0$, then a small change, say by a constant gain, in L_o would make $\#i(L_o - 1) = 0$. It can easily be shown that if $\#i(L_o - 1) \geq 1$, then C_o is always self-optimal, but characterizing uniquely self-optimal is more difficult.

Observe from the principle of the argument that in terms of the Nyquist plot of L_o,

$$\begin{aligned} \#z(L_o - 1) &= \#p(L_o - 1) + (\text{no. clockwise enc. of } +1) \\ &= \#p(L_o) + (\text{no. clockwise enc. of } +1) \\ &= \#p(P) + \#p(C_o) + (\text{no. clockwise enc. of } +1). \end{aligned}$$

So condition (8.18) is equivalent to

$$\#p(P) + (\text{no. clockwise enc. of } +1) > \#z(C_o).$$

A typical loopshaping controller for a stable plant will have $\#z(C_o) = 0$ and

$$(\text{no. clockwise enc. of } +1) > 0,$$

and will thus be self-optimal.

Example For a simple illustration, suppose that

$$P(s) = \frac{s+1}{100s+1}.$$

The controller $C_o(s) = 10$ yields

$$L_o(s) = 10\frac{s+1}{100s+1}.$$

The Nyquist plot of L_o has one clockwise encirclement of $+1$, so C_o is self-optimal. So is $C_o(s) = K$ for any K in $(1, 100)$. In particular, such controllers cannot be improved upon uniformly over all frequencies.

It can be shown using the phase formula (Section 7.2) that any controller that is minimum-phase and for which L_o has a single gain crossover is self-optimal.

Proof of Theorem 1 Define

$$\Gamma_o(j\omega) := |W_1(j\omega)S_o(j\omega)|^2 + |W_2(j\omega)T_o(j\omega)|^2,$$

so that

$$\psi(C_o)^2 = \sup_\omega \Gamma_o(j\omega).$$

As we have already seen, $\Gamma_o(j\omega) = 2$. Similarly, for another controller C, define

$$\Gamma(j\omega) := |W_1(j\omega)S(j\omega)|^2 + |W_2(j\omega)T(j\omega)|^2,$$

so that

$$\psi(C)^2 = \sup_\omega \Gamma(j\omega).$$

Thus C_o is self-optimal

$$\begin{aligned}
&\iff (\forall C)\ \psi(C_o) \le \psi(C) \\
&\iff (\forall C)(\exists \omega)\ 2 \le \Gamma(j\omega) \\
&\iff \text{it is not true that } (\exists C)(\forall \omega)\ 2 > \Gamma(j\omega)
\end{aligned}$$

and C_o is uniquely self-optimal

$$\iff \text{it is not true that } (\exists C \neq C_o)(\forall \omega)\ 2 \ge \Gamma(j\omega).$$

So the theorem statement is equivalent to

$$\begin{aligned}
(\exists C)(\forall \omega)\ 2 > \Gamma(j\omega) \quad &\iff \quad (\exists C \neq C_o)(\forall \omega)\ 2 \ge \Gamma(j\omega) \\
&\iff \quad \#z(L_o - 1) \le \#p(C_o) + \#z(C_o).
\end{aligned}$$

It is convenient to turn this statement into one in terms of S_o rather than C_o. As we saw in Chapter 6, the constraints placed on S_o by the requirement that C_o achieve internal stability are

$$\begin{aligned} S_o &\in \mathcal{S}, \\ S_o &= 0 \text{ at RHP poles of } P, \\ S_o &= 1 \text{ at RHP zeros of } P, \end{aligned}$$

with appropriate multiplicity. Then S satisfies these constraints too iff it has the form

$$S = S_o + AY,$$

where A is the all-pass factor formed from the RHP poles and zeros of P, and Y is an arbitrary element of $\mathcal{S}$. It is convenient first to assume that P and C_o are biproper and have no poles or zeros on the imaginary axis, so that neither S_o nor T_o have imaginary axis zeros, and the weights are stable and biproper. Then (8.19) is equivalent to

$$\begin{gathered} (\exists Y \in \mathcal{S})(\forall \omega)\ 2 > |W_1(S_o + AY)|^2 + |W_2(T_o - AY)|^2 \iff \\ (\exists Y \in \mathcal{S}, Y \neq 0)(\forall \omega)\ 2 \geq |W_1(S_o + AY)|^2 + |W_2(T_o - AY)|^2 \iff \\ \#z(L_o - 1) \leq \#p(C_o) + \#z(C_o) \end{gathered} \tag{8.19}$$

($j\omega$ has been dropped to simplify the notation). Recall that

$$|W_1| = \frac{1}{|S_o|}, \quad |W_2| = \frac{1}{|T_o|},$$

so

$$\begin{aligned} |W_1(S_o + AY)|^2 + |W_2(T_o - AY)|^2 &= \left|1 + \frac{AY}{S_o}\right|^2 + \left|1 - \frac{AY}{T_o}\right|^2 \\ &= 2 + 2\mathrm{Re}\left(\left(\frac{1}{S_o} - \frac{1}{T_o}\right) AY\right) \qquad (8.20) \\ &\quad + \left(\frac{1}{|S_o|^2} + \frac{1}{|T_o|^2}\right) |AY|^2. \qquad (8.21) \end{aligned}$$

Thus (8.19) is equivalent to the condition

$$\begin{aligned} (\exists Y \in \mathcal{S})(\forall \omega) 0 &> 2\mathrm{Re}\,(XY) + W|Y|^2 \qquad (8.22) \\ &\text{iff} \\ (\exists Y \in \mathcal{S}, Y \neq 0)(\forall \omega) 0 &\geq 2\mathrm{Re}\,(XY) + W|Y|^2 \qquad (8.23) \\ &\text{iff} \\ \#z(L_o - 1) &\leq \#p(C_o) + \#z(C_o), \qquad (8.24) \end{aligned}$$

where

$$X := \left(\frac{1}{S_o} - \frac{1}{T_o}\right) A$$

is biproper with no imaginary poles or zeros and

$$W := \left(\frac{1}{|S_o|^2} + \frac{1}{|T_o|^2}\right) |A|^2 > 0$$

is bounded for all ω. That (8.22) implies (8.23) is immediate by inspection. We will complete the proof by first showing that (8.24) is equivalent to

$$\#z(X) \leq \#p(X) \tag{8.25}$$

and then that (8.23) $\Longrightarrow$ (8.25) and (8.25) $\Longrightarrow$ (8.22).

To see that (8.24) $\Longleftrightarrow$ (8.25) holds, note that

$$\begin{aligned} X &= \left(L_o + 1 - \frac{L_o+1}{L_o}\right) A = \frac{(L_o+1)(L_o-1)}{L_o} A \\ &= \frac{[num(PC_o)+den(PC_o)][num(PC_o)-den(PC_o)]}{num(PC_o)den(PC_o)} A. \end{aligned}$$

Now the polynomial $num(PC_o) + den(PC_o)$ has all its zeros in the left half-plane, by internal stability; and the numerator of A cancels the zeros in $num(PC_o)den(PC_o)$ coming from the RHP poles and zeros of P. Thus

$$\#z(X) = \#z[num(PC_o) - den(PC_o)] = \#z(L_o - 1)$$

and

$$\#p(X) = \#p(C_o) + \#z(C_o).$$

For (8.23) $\Longrightarrow$ (8.25), note that if the Nyquist plot of XY lies in the closed left half-plane, then in particular it does not encircle the origin. Since XY is not identically zero, by the principle of the argument

$$\#z(XY) = \#p(XY).$$

But $\#z(X) \leq \#z(XY)$ and $\#p(XY) \leq \#p(X)$.

For (8.25) $\Longrightarrow$ (8.22), note that (8.22) is equivalent to

$$(\exists Y \in \mathcal{S})(\forall \omega)\ 0 > 2\mathrm{Re}\,(XY),$$

since we can scale Y so that the quadratic term $W|Y|^2$ is negligible. We will construct a $Y \in \mathcal{S}$ such that $\mathrm{Re}(XY) < 0, \quad \forall \omega$. If $\#z(X) \leq \#p(X)$, we can write $X = X_1 X_2$, where X_1 has only RHP poles and zeros with $\#z(X) = \#z(X_1) = \#p(X_1)$, and X_2 has $\#z(X_2) = 0$ and $\#p(X_2) = \#p(X) - \#p(X_1)$. Thus both X_1 and X_2 are biproper. If

$$Y(s) = \frac{X_1(-s)}{X_2(s)},$$

then $Y \in \mathcal{S}$ and is biproper and

$$X(j\omega)Y(j\omega) = X_1(j\omega)X_1(-j\omega) = |X_1(j\omega)|^2 > 0, \qquad \forall \omega.$$

To complete the proof, we must drop the restriction that L_o is biproper and has no imaginary axis poles or zeros. This means that S_o and T_o may have imaginary zeros, and thus W_1 and W_2 may have imaginary poles. In order for (8.21) to be bounded, we must have AY share the imaginary zeros of S_o and T_o, including those at ∞.

The simplest way to proceed is to assume that A is no longer all-pass but has in addition the imaginary zeros of S_o and T_o and enough LHP poles so that A has the appropriate behavior at ∞. The location of the LHP poles is unimportant. Then

$$S = S_o + AY$$

still parametrizes all S that can arise from internally stabilizing controllers and produce a finite Γ. The proof can now proceed exactly as before. Observe that X is still biproper and has no imaginary poles or zeros, because of the construction of A. ■

Example and Implications

In the preceding subsection it was remarked that loopshaping produces self-optimal controllers. In particular, for stable plants and loopshapes with a single crossover, where $\#z(L_o - 1) = (\#$ clockwise enc. of $+1) = 1$, then the controller is self-optimal iff it has no RHP poles or zeros. For $\#z(L_o - 1) > 1$, controllers with no RHP poles or zeros are also always self-optimal. This helps make clear the conventional wisdom about why RHP controller poles and zeros are undesirable. Similar insight comes from the results on performance limitations due to RHP zeros and the integral gain-phase relations from earlier chapters.

Are there ever times when it would make sense to introduce RHP controller poles or zeros deliberately? Theorem 1 leaves open this possibility for situations where $\#z(L_o - 1) > 1$, which can occur when there are multiple crossovers.

Example To illustrate this we will reconsider the simple beam, Example 2 from Section 8.2, with P given in (8.6) and with weights from (8.3). Recall that for the noncollocated case the plant has a RHP zero at $s = 1$. Consider the controller

$$C_-(s) = 2.4\left(\frac{s-1}{s+1}\right)\left(\frac{s^2 - s + 1}{(s+0.1)(s+10)}\right). \tag{8.26}$$

A Bode plot of C_- is shown in Figure 8.25. The resulting closed-loop performance for C_- is shown in Figure 8.26, along with the performance for the optimal controller. Observe that C_- is nearly optimal. (It was actually obtained by rounding coefficients in the optimal controller to convenient values.) Also, the optimal performance of $\psi \approx 1.26$ is poorer than the optimal performance of $\psi = \sqrt{(2)}/2 \approx 0.707$ for the collocated case.

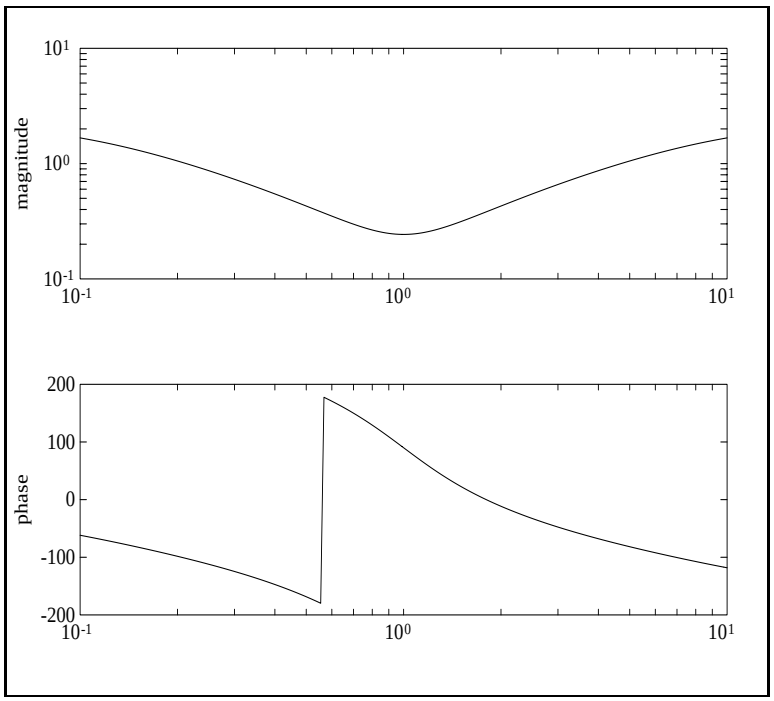

Figure 8.25: Bode plots of $|C_-|$ (upper) and $\angle C_-$ (lower).

The controller C_- has no RHP poles and three RHP zeros, so that the loop transfer function PC_- has a total of four RHP zeros. Since $\#z(PC_- - 1) = 4$, we have from Theorem 1 that this

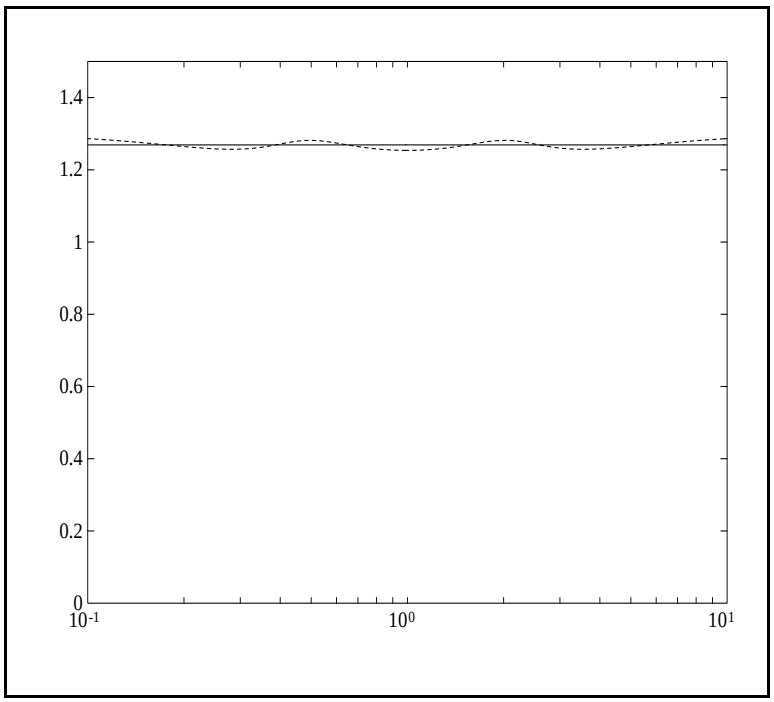

Figure 8.26: ψ for optimal C (solid) and C_- (dash).

controller is also self-optimal. It is possible to give a loopshaping interpretation of this controller, which is not much different than an all-pass. Intuitively, a good controller for this problem must have the appropriate phase at the two resonant frequencies ($\omega = 0.5, 2$) for stability, and from the arguments in Section 8.2 its gain should not deviate too greatly from 1. Thus a controller which is nearly all-pass would seem appropriate.

The ideas on dealing with RHP zeros presented in Section 8.3 are not terribly useful in this example. Since there are necessarily crossover frequencies both above and below the frequency $\omega = 1$ where the zero occurs, it is not clear how to cover this with uncertainty. The controller C_- actually places an additional three RHP zeros near this frequency. While a loopshaping methodology could potentially still apply to this example, the actual details of this controller are hardly obvious. The loopshaping methods developed in this book always involve some trial and error, but this example seems to require a great deal. This would also be true for many other problems of this complexity with RHP zeros at frequencies between multiple crossover frequencies.

This example illustrates how RHP controller zeros can be effective for problems with multiple crossovers. What about poles? Theorem 1 appears to be symmetric in the controller RHP poles and zeros, but this is somewhat misleading since RHP poles have an impact on the need for encirclements of -1 and hence on the number $\#z(PC-1)$. Nevertheless, in the problem considered in this section, with perhaps slightly different weights, there will typically be multiple crossovers and $\#z(PC-1) \geq 4$, so C can have up to a total of three RHP poles and zeros and still be self-optimal. Thus we would expect that relatively small changes in the weights could lead to controllers with a variety of RHP poles and zeros. Recall also that certain plants can only be stabilized with unstable controllers, so any problem with such a plant would necessarily have controllers with RHP poles. On the other hand, the vast majority of feedback control problems in engineering applications have a single crossover, and controller RHP poles and zeros would clearly be undesirable.

Now we return to the collocated version of this problem and use the characterization of self-

optimality from the preceding subsection to prove that the controller $C = 1$ is optimal for all physically possible values of the parameters M, I, l, l_u, and k. This is a remarkable robust performance result and does not hold in the more general noncollocated case. It illustrates why collocated control problems are so popular among researchers in control of flexible structures. We have not focused on this type of parametric uncertainty in this book, because the available results tend not to be very general. For example, the optimality of $C = 1$ for this problem depends not only on the special structure of P but also on the special structure of the performance specification. Nevertheless, the methods developed in this book can be useful in studying specific problems involving parametric uncertainty, as illustrated by this example.

To prove the optimality of $C = 1$, note that for all values of the parameters

$$P(s) = \frac{s}{Ms^2 + 2k} + \frac{l_u^2 s}{Is^2 + 2kl^2} = \frac{s\left[(I + Ml_u^2)s^2 + 2k(1 + l^2)\right]}{(Ms^2 + 2k)(Is^2 + 2kl^2)}$$

has all its poles and zeros on the imaginary axis, with poles at

$$s = \pm j\sqrt{\frac{2k}{M}}, \pm j\sqrt{\frac{2kl^2}{I}}$$

and zeros at

$$s = 0, \pm j\sqrt{\frac{2k(1 + l^2)}{(I + Ml_u^2)}}.$$

To be physically meaningful, all the parameters must be positive, and the geometry of the problem restricts the moment of inertia such that

$$0 < I < Ml^2,$$

so we have that

$$0 < \sqrt{\frac{2k}{M}} < \sqrt{\frac{2k(1 + l^2)}{(I + Ml_u^2)}} < \sqrt{\frac{2kl^2}{I}}.$$

Thus the zeros and poles alternate on the imaginary axis and

$$\mathrm{Re}P(j\omega) = 0, \qquad \forall \omega.$$

It is clear from the Nyquist diagram of P that

$$\#z(P + 1) = 0 \quad \text{and} \quad \#z(P - 1) = 4,$$

so the controller $C = 1$ is both stabilizing and self-optimal for all parameter values. Recall that the weights W_1 and W_2 that are used to define self-optimality are those that make $|W_1 S|$ and $|W_2 T|$ all-pass. Clearly, we could use weights that are a constant multiple of these as well. Thus to use self-optimality to show that $C = 1$ is optimal for

$$\psi(C) := \|(|W_1 S|^2 + |W_2 T|^2)^{1/2}\|_\infty$$

with

$$|W_1| = 0.5(|P|^2 + 1)^{1/2}, \quad |W_2| = 0.5(|P|^{-2} + 1)^{1/2},$$

we must verify that $|W_1 S|$ and $|W_2 T|$ are all-pass. But since $\mathrm{Re}P(j\omega) = 0$, $\forall \omega$, we have that

$$|P + 1|^2 = |P|^2 + 1, \qquad \forall s = j\omega,$$

and thus

$$|W_1 S|^2 = 0.25\frac{|P|^2+1}{|P+1|^2} = 0.25, \quad |W_2 T|^2 = 0.25\frac{|P|^{-2}+1}{|P^{-1}+1|^2} = 0.25,$$

as desired. This completes the proof.

What are the implications of this example and the results on self-optimality for loopshaping? Each of the design methods presented so far—shaping L, S, T, or Q—gives the designer something handy to manipulate to obtain a controller. In each case, the resulting controller will have to be examined in the closed-loop system to see if it is satisfactory—every controller results in some tradeoff between S and T, and the designer must decide if that tradeoff makes sense for a particular problem. If a reasonable tradeoff between S and T can be found by any method, and the resulting controller is self-optimal, then there is no other controller that can uniformly improve on the tradeoff—any other controller just achieves some other tradeoff. What makes self-optimality so useful is that it is very easily checked, and the loopshaping methods introduced so far generally yield self-optimal controllers.

Unfortunately, the designer may find that for some problems loopshaping does not easily lead to a reasonable tradeoff between competing performance objectives. It is for these problems that directly solving for an optimal controller is most useful. Optimal controllers are the subject of the remainder of this book.

Exercises

1. Verify the Venn diagrams in Section 8.5.
2. Prove that if $\#i(L_o - 1) \geq 1$, then C_o is self-optimal.
3. Develop notions of self-optimality that involving S and T separately, and prove results analogous to Theorem 1.

Notes and References

The problem setup in Section 8.1 is studied in much greater depth in McFarlane and Glover (1990), who develop an interesting theory of control design using a combination of loopshaping and optimality. For a recent treatment of the control of flexible structures, see Joshi (1989). Controller design by shaping Q, known in the process control literature as internal model control (IMC), is developed in detail in Morari and Zafiriou (1989). Section 8.5 is based on Lenz et al. (1988).

Model Matching

This chapter studies a hypothetical control problem called the model-matching problem which will be used in later chapters for control system design. The mathematics of interpolation theory is used to solve the model-matching problem.

9.1 The Model-Matching Problem

Let $T_1(s)$ and $T_2(s)$ be stable proper transfer functions (i.e., functions in $\mathcal{S}$). The *model-matching problem* is to find a stable transfer function $Q(s)$ to minimize the ∞-norm of $T_1 - T_2Q$. The interpretation is this: T_1 is a model, T_2 is a plant, and Q is a cascade controller to be designed so that T_2Q approximates T_1. Thus $T_1 - T_2Q$ is the error transfer function. The transfer function Q is required to be stable but not necessarily proper (this makes the problem easier). We will *assume* that T_2 has no zeros on the imaginary axis. Define the minimum model-matching error

$$\gamma_{\text{opt}} := \min \|T_1 - T_2Q\|_\infty,$$

where the minimum is taken over all stable Qs. It turns out that the minimum is achieved by virtue of the assumption on T_2; a Q achieving the minimum is said to be *optimal*.

The trivial case of the problem is when T_1/T_2 is stable, for then the unique optimal Q is $Q = T_1/T_2$ and $\gamma_{\text{opt}} = 0$. The simplest nontrivial case is when T_2 has only one zero in the right half-plane, say at $s = s_0$. If Q is stable and T_2Q has finite ∞-norm (i.e., $T_2Q \in \mathcal{S}$), then by the maximum modulus theorem

$$\|T_1 - T_2Q\|_\infty \geq |T_1(s_0)|,$$

so $\gamma_{\text{opt}} \geq |T_1(s_0)|$. On the other hand, the function

$$Q = \frac{T_1 - T_1(s_0)}{T_2} \tag{9.1}$$

is stable and yields the value $|T_1(s_0)|$ for the model-matching error. The conclusion is that $\gamma_{\text{opt}} = |T_1(s_0)|$ and (9.1) is an optimal Q, in fact, the unique optimal Q.

Example For

$$T_1(s) = \frac{4}{s+3}, \qquad T_2(s) = \frac{s-2}{(s+1)^3}$$

$\gamma_{\text{opt}} = T_1(2) = 4/5$ and the optimal Q is

$$Q(s) = -\frac{4(s+1)^3}{5(s+3)}.$$

To solve the problem in the general case we will need the mathematics developed in the next two sections.

9.2 The Nevanlinna-Pick Problem

Recall that $\mathcal{S}$ stands for the space of stable, proper, real-rational functions. Let $\mathcal{S}_c$ stand for the space of stable, proper, complex-rational functions (i.e., the coefficients are permitted to be complex numbers). For example, the function

$$\frac{(1-j)s + (2+3j)}{(0.1+j)s + (-3+j)}$$

is in $\mathcal{S}_c$ because it is proper and its pole is at $s = -0.6931 - 3.0693j$ in the left half-plane. The ∞-norm, maximum magnitude on the imaginary axis, is defined for such functions too.

Let $\{a_1, \ldots, a_n\}$ be a set of points in the open right half-plane, $\text{Re}s > 0$, and $\{b_1, \ldots, b_n\}$ a set of points in $\mathbb{C}$. For simplicity we shall *assume* that the points $a_1, \ldots, a_n$ are distinct. The *Nevanlinna-Pick interpolation problem*, or the NP problem for short, is to find a function G in $\mathcal{S}_c$ satisfying the two conditions

$$\|G\|_\infty \leq 1,$$

$$G(a_i) = b_i, \quad i = 1, \ldots, n.$$

The latter equation says that G is to interpolate the value b_i at the point a_i, or in other words the graph of G is to pass through the point (a_i, b_i). The constraints are important: G must be stable, proper, and satisfy $\|G\|_\infty \leq 1$. The NP problem is said to be *solvable* if such a function G exists. It will be convenient to write the problem data as an array, like this:

$$\begin{array}{ccc} a_1 & \cdots & a_n \\ b_1 & \cdots & b_n \end{array}$$

In fact, the NP problem is not solvable for all data. An obvious necessary condition for solvability is $|b_i| \leq 1$, $i = 1, \ldots, n$. This follows from the maximum modulus theorem: If G belongs to $\mathcal{S}_c$ and satisfies $G(a_i) = b_i$, then its magnitude equals $|b_i|$ at the point $s = a_i$, so its maximum magnitude in the right half-plane is $\geq |b_i|$ (i.e., $\|G\|_\infty \geq |b_i|$); but if it is also true that $\|G\|_\infty \leq 1$, then $|b_i| \leq 1$.

To state precisely when the NP problem is solvable, we need some elementary concepts and facts about complex matrices. Let M be a square complex matrix. Its complex-conjugate transpose is denoted by M^*. If $M = M^*$, M is said to be a *Hermitian matrix*. If M is real, it is Hermitian iff it is symmetric. It can be shown that the eigenvalues of a Hermitian matrix are all real. If M is Hermitian, it is said to be *positive semidefinite* if $x^*Mx \geq 0$ for all complex vectors x, and *positive definite* if $x^*Mx > 0$ for all nonzero complex vectors x. The notation is $M \geq 0$ and $M > 0$, respectively. It is a fact that $M \geq 0$ (respectively, $M > 0$) iff all its eigenvalues are ≥ 0 (respectively, > 0).

Example 1 The matrix

$$\begin{bmatrix} 2 & 1+j \\ 1-j & 4 \end{bmatrix}$$

is Hermitian; notice that the diagonal elements must be real. The eigenvalues are 1.2679 and 4.7321. Since these are both positive, the matrix is positive definite.

Associated with the NP problem data

$$\begin{matrix} a_1 & \cdots & a_n \\ b_1 & \cdots & b_n \end{matrix}$$

is the $n \times n$ matrix Q, whose ij^{th} element is

$$\frac{1 - b_i\overline{b_j}}{a_i + \overline{a_j}}.$$

This is called the *Pick matrix*. Notice that Q is Hermitian.

Example 2 For the data

$$\begin{matrix} 6+j & 6-j \\ 0.1-0.1j & 0.1+0.1j \end{matrix}$$

the Pick matrix is

$$\begin{bmatrix} 0.0817 & 0.0814 - 0.0119j \\ 0.0814 + 0.0119j & 0.0817 \end{bmatrix},$$

whose eigenvalues are -0.0005 and 0.1639. Since one is negative, it turns out that the NP problem is not solvable for these data.

Solvability of the NP problem is completely determined by the Pick matrix. The result is Pick's famous theorem:

Theorem 1 *The NP problem is solvable iff* $Q \geq 0$.

Pick's theorem shows that it is an easy matter to check solvability of the NP problem by computer: Input the data

$$\begin{matrix} a_1 & \cdots & a_n \\ b_1 & \cdots & b_n \end{matrix}$$

form the Pick matrix; compute its eigenvalues; see if the smallest one is nonnegative.

We saw above that a necessary condition for solvability is $|b_i| \leq 1$ for all i. So it must be that this condition is implied by the condition $Q \geq 0$. This is indeed the case: If $Q \geq 0$, then each diagonal element of Q is ≥ 0, that is,

$$\frac{1 - |b_i|^2}{2\text{Re}a_i} \geq 0.$$

Since $\text{Re}a_i > 0$, this implies that

$$1 - |b_i|^2 \geq 0$$

(i.e., $|b_i| \leq 1$).

In the next section is given a procedure for constructing a solution to the NP problem when it is solvable. The remainder of this section contains a proof of the necessity part of Pick's theorem, a

proof that illustrates in system-theoretic terms how the Pick matrix arises. A system is said to be *dissipative* if it dissipates energy—the outgoing energy (2-norm squared) is less than or equal to the incoming energy. The following proof shows that Pick's theorem says something about dissipative systems.

Since both time and frequency domains appear, the $\hat{}$-convention is in force. Also, complex-valued signals and complex-rational transfer functions are used. There is no obstacle to extending the material of Chapter 2 to the complex case.

The proof is separated into three lemmas.

Lemma 1 *Consider a linear system with input signal $u(t)$ of finite 2-norm, output signal $y(t)$, and transfer function $\hat{G}(s)$ in $\mathcal{S}_c$. If $\|\hat{G}\|_\infty \leq 1$, then*

$$\int_{-\infty}^{0} |y(t)|^2 dt \leq \int_{-\infty}^{0} |u(t)|^2 dt.$$

Proof Define a new input

$$u_1(t) := \begin{cases} u(t), & \text{if } t \leq 0 \\ 0, & \text{if } t > 0 \end{cases}$$

and let the corresponding output be $y_1(t)$. It follows from entry (1,1) in Table 2.2 that

$$\int_{-\infty}^{\infty} |y_1(t)|^2 dt \leq \int_{-\infty}^{\infty} |u_1(t)|^2 dt.$$

Since $u_1 = 0$ for positive time, this implies that

$$\int_{-\infty}^{\infty} |y_1(t)|^2 dt \leq \int_{-\infty}^{0} |u_1(t)|^2 dt$$

and hence that

$$\int_{-\infty}^{0} |y_1(t)|^2 dt \leq \int_{-\infty}^{0} |u_1(t)|^2 dt.$$

But $y = y_1$ and $u = u_1$ for negative time. ■

The second lemma shows that complex exponentials are eigenfunctions for linear systems.

Lemma 2 *Consider a linear system with transfer function $\hat{G}(s)$ in $\mathcal{S}_c$. Apply the input signal*

$$u(t) = \mathrm{e}^{at}, \quad -\infty < t \leq 0$$

with $\mathrm{Re}\, a > 0$. Then the output signal is

$$y(t) = \hat{G}(a)u(t), \quad -\infty < t \leq 0.$$

Proof Use the convolution equation: For every $t \leq 0$,

$$\begin{aligned} y(t) &= \int_0^\infty G(\tau)u(t-\tau)d\tau \\ &= \int_0^\infty G(\tau)\mathrm{e}^{a(t-\tau)}d\tau \\ &= \hat{G}(a)\mathrm{e}^{at}. \blacksquare \end{aligned}$$

The final lemma is the necessity part of Pick's theorem.

Lemma 3 *If the NP problem is solvable, then* $Q \geq 0$.

Proof To simplify notation, assume there are only two interpolation points (i.e., $n = 2$). Let $\hat{G}$ be a solution to the NP problem. For arbitrary complex numbers c_1 and c_2 apply the input signal

$$u(t) = c_1 \mathrm{e}^{a_1 t} + c_2 \mathrm{e}^{a_2 t}, \quad -\infty < t \leq 0$$

to the system with transfer function $\hat{G}$. By Lemma 2 and linearity the output signal is

$$\begin{aligned} y(t) &= c_1 \hat{G}(a_1)\mathrm{e}^{a_1 t} + c_2 \hat{G}(a_2)\mathrm{e}^{a_2 t} \\ &= c_1 b_1 \mathrm{e}^{a_1 t} + c_2 b_2 \mathrm{e}^{a_2 t}. \end{aligned}$$

Starting with Lemma 1, we get in succession

$$\begin{aligned} \int_{-\infty}^{0} |y(t)|^2 dt &\leq \int_{-\infty}^{0} |u(t)|^2 dt, \\ \int_{-\infty}^{0} |c_1 b_1 \mathrm{e}^{a_1 t} + c_2 b_2 \mathrm{e}^{a_2 t}|^2 dt &\leq \int_{-\infty}^{0} |c_1 \mathrm{e}^{a_1 t} + c_2 \mathrm{e}^{a_2 t}|^2 dt, \end{aligned}$$

and thus

$$\begin{aligned} \int_{-\infty}^{0} \Big[&\overline{c_1} c_1 (1 - \overline{b_1} b_1)\mathrm{e}^{(\overline{a_1}+a_1)t} + \overline{c_1} c_2 (1 - \overline{b_1} b_2)\mathrm{e}^{(\overline{a_1}+a_2)t} \\ &+ \overline{c_2} c_1 (1 - \overline{b_2} b_1)\mathrm{e}^{(\overline{a_2}+a_1)t} + \overline{c_2} c_2 (1 - \overline{b_2} b_2)\mathrm{e}^{(\overline{a_2}+a_2)t} \Big] dt \geq 0. \end{aligned}$$

This integral can be evaluated to give

$$\overline{c_1} c_1 \frac{1 - \overline{b_1} b_1}{\overline{a_1} + a_1} + \overline{c_1} c_2 \frac{1 - \overline{b_1} b_2}{\overline{a_1} + a_2} + \overline{c_2} c_1 \frac{1 - \overline{b_2} b_1}{\overline{a_2} + a_1} + \overline{c_2} c_2 \frac{1 - \overline{b_2} b_2}{\overline{a_2} + a_2} \geq 0,$$

which is equivalent to

$$x^* Q x \geq 0,$$

where

$$x := \begin{pmatrix} \overline{c_1} \\ \overline{c_2} \end{pmatrix}.$$

Since c_1 and c_2 were arbitrary, it must be that $Q \geq 0$. ■

9.3 Nevanlinna's Algorithm

This section presents a procedure to construct a solution of the NP problem when it is solvable. The procedure is developed inductively: First, the case $n = 1$ is solved; then the case of n points is reduced to the case of $n - 1$ points.

Let us begin by letting $\mathcal{D}$ denote the open unit disk, $|z| < 1$, and $\overline{\mathcal{D}}$ the closed unit disk, $|z| \leq 1$. A *Möbius function* has the form

$$M_b(z) = \frac{z - b}{1 - z\overline{b}},$$

where $|b| < 1$. Following is a list of some properties of Möbius functions (you should check these):

1. M_b has a zero at $z = b$ and a pole at $z = 1/\overline{b}$. Thus M_b is analytic in $\mathcal{D}$.

2. The magnitude of M_b equals 1 on the unit circle.

3. M_b maps $\mathcal{D}$ onto $\mathcal{D}$ and the unit circle onto the unit circle.

4. The inverse map is
$$M_b^{-1}(z) = \frac{z+b}{1+z\overline{b}}$$
(i.e., $M_b^{-1} = M_{-b}$). So the inverse map is a Möbius function too.

We will also need the all-pass function

$$A_a(s) := \frac{s-a}{s+\overline{a}}, \quad \text{Re}a > 0.$$

With the aid of these functions we can solve the NP problem for the data

$$\begin{matrix} a_1 \\ b_1 \end{matrix}$$

There are two cases.

Case 1 $|b_1| = 1$ A solution is $G(s) = b_1$. By the maximum modulus theorem this solution is unique.

Case 2 $|b_1| < 1$ There are an infinite number of solutions:

Lemma 4 *The set of all solutions is*

$$\{G : G(s) = M_{-b_1}[G_1(s)A_{a_1}(s)], G_1 \in \mathcal{S}_c, \|G_1\|_\infty \leq 1\}.$$

If G_1 is an all-pass function, so is G.

Proof Let $G_1 \in \mathcal{S}_c$, $\|G_1\|_\infty \leq 1$, and define G as

$$G(s) = M_{-b_1}[G_1(s)A_{a_1}(s)].$$

Thus G equals the composition of the two functions

$$\begin{aligned} s &\mapsto G_1(s)A_{a_1}(s), \\ z &\mapsto M_{-b_1}(z). \end{aligned}$$

The first is analytic in the closed right half-plane and maps it into the closed disk $\overline{\mathcal{D}}$; the second is analytic in $\overline{\mathcal{D}}$ and maps it back into $\overline{\mathcal{D}}$. It follows that $G \in \mathcal{S}_c$ and $\|G\|_\infty \leq 1$. Also, G interpolates b_1 at a_1:

$$G(a_1) = M_{-b_1}[G_1(a_1)A_{a_1}(a_1)] = M_{-b_1}(0) = b_1.$$

Thus G solves the NP problem. Moreover, if G_1 is an all-pass function, then so is $G_1A_{a_1}$, hence so is G (because M_{-b_1} maps the unit circle onto itself).

Conversely, suppose that G solves the NP problem. Define G_1 so that

$$G(s) = M_{-b_1}[G_1(s)A_{a_1}(s)],$$

that is,

$$G_1(s) = \frac{M_{b_1}[G(s)]}{A_{a_1}(s)}.$$

The function $M_{b_1}[G(s)]$ belongs to $\mathcal{S}_c$, has ∞-norm ≤ 1, and has a zero at $s = a_1$. Therefore, $G_1 \in \mathcal{S}_c$ and $\|G_1\|_\infty \leq 1$. ■

Example 1 For the interpolation data

$$\begin{matrix} 2 \\ 0.6 \end{matrix}$$

the formula in the lemma gives

$$G(s) = \frac{G_1(s)\dfrac{s-2}{s+2} + 0.6}{1 + 0.6G_1(s)\dfrac{s-2}{s+2}}.$$

The all-pass function $G_1(s) = (s-1)/(s+1)$ results in

$$G(s) = \frac{s^2 - 0.75s + 2}{s^2 + 0.75s + 2}.$$

Now we turn to the NP problem with n data points, the problem being assumed solvable, and see how to reduce it to the case of $n-1$ points. Again, there are two cases.

Case 1 $|b_1| = 1$ Since the problem is solvable, by the maximum modulus theorem it must be that $G(s) = b_1$ is the unique solution (and hence that $b_1 = \ldots = b_n$).

Case 2 $|b_1| < 1$ Pose a new problem, labeled the NP$'$ problem, with the $n-1$ data points

$$\begin{matrix} a_2 & \cdots & a_n \\ b_2' & \cdots & b_n' \end{matrix}$$

where $b_i' := M_{b_1}(b_i)/A_{a_1}(a_i)$.

Lemma 5 *The set of all solutions to the NP problem is given by the formula*

$$G(s) = M_{-b_1}[G_1(s)A_{a_1}(s)],$$

where G_1 ranges over all solutions to the NP$'$ problem. If G_1 is all-pass, so is G.

Proof G solves the NP problem iff

$$G \in \mathcal{S}_c,\ \|G\|_\infty \leq 1,\ G(a_1) = b_1,\ \text{and } G(a_i) = b_i, \quad i = 2, \ldots, n.$$

From Lemma 4, the set of all Gs satisfying the first three conditions is

$$\{G : G(s) = M_{-b_1}[G_1(s)A_{a_1}(s)], G_1 \in \mathcal{S}_c, \|G_1\|_\infty \leq 1\}.$$

Then G satisfies the fourth condition iff

$$G_1(a_i) = \frac{M_{b_1}(b_i)}{A_{a_1}(a_i)}, \quad i = 2, \ldots, n$$

(i.e., G_1 solves the NP$'$ problem). ■

It follows by induction that the NP problem always has an all-pass solution.

Example 2 Consider the NP problem for the data

$$\begin{array}{ccc} a_1 & a_2 & a_3 \\ b_1 & b_2 & b_3 \end{array} = \begin{array}{ccc} 1 & 2 & 3 \\ \frac{1}{2} & \frac{1}{3} & \frac{1}{4} \end{array}$$

The Pick matrix is

$$\begin{bmatrix} 0.3750 & 0.2778 & 0.2188 \\ 0.2778 & 0.2222 & 0.1833 \\ 0.2188 & 0.1833 & 0.1563 \end{bmatrix}.$$

The smallest eigenvalue equals 0.0004. Since this is positive, the NP problem is solvable.

A solution can be obtained by reduction to one interpolation point by applying Lemma 5 twice. First, reduce to the NP$'$ problem with two points:

$$\begin{array}{cc} a_2 & a_3 \\ b_2' & b_3' \end{array} = \begin{array}{cc} 2 & 3 \\ -0.6 & -0.5714 \end{array}$$

Here $b_i' := M_{b_1}(b_i)/A_{a_1}(a_i)$, $i = 2, 3$. Second, reduce to the NP$''$ problem with only one point:

$$\begin{array}{c} a_3 \\ b_3'' \end{array} = \begin{array}{c} 3 \\ 0.2174 \end{array}$$

Here $b_3'' := M_{b_2'}(b_3')/A_{a_2}(a_3)$.

Now solve the problems in reverse order. By Lemma 4 the solution of the NP$''$ problem is

$$G_2(s) = M_{-b_3''}[G_3(s)A_{a_3}(s)],$$

where G_3 is an arbitrary function in $\mathcal{S}_c$ of ∞-norm ≤ 1. Let's take $G_3(s) = 1$, the simplest all-pass function. Then

$$G_2(s) = \frac{1.2174s - 2.3478}{1.2174s + 2.3478}.$$

The induced solution to the NP$'$ problem is

$$G_1(s) = M_{-b_2'}[G_2(s)A_{a_2}(s)] = \frac{0.4870s^2 - 7.6522s + 1.8783}{0.4870s^2 + 7.6522s + 1.8783}.$$

Finally, the solution to the NP problem is

$$G(s) = M_{-b_1}[G_1(s)A_{a_1}(s)] = \frac{0.7304s^3 - 4.0696s^2 + 14.2957s - 0.9391}{0.7304s^3 + 4.0696s^2 + 14.2957s + 0.9391}.$$

Notice that the degree of the numerator and denominator of G equals 3, the number of data points. In general, there always exists an all-pass solution of degree $\leq n$.

In our application of NP theory to the model-matching problem, the data

$$\begin{array}{ccc} a_1 & \cdots & a_n \\ b_1 & \cdots & b_n \end{array}$$

will have conjugate symmetry; that is, if (a_i, b_i) appears, so will the conjugate pair $(\overline{a_i}, \overline{b_i})$. Then we will want the solution G to be real-rational instead of complex. Suppose that the data do have conjugate symmetry and that G is a solution in $\mathcal{S}_c$. It can be written uniquely as

$$G(s) = G_R(s) + jG_I(s),$$

where G_R and G_I both are real-rational. Then G_R belongs to $\mathcal{S}$ and is also a solution to the NP problem (the proof is left as an exercise).

Example 3 For the data

$$\begin{matrix} 5+2j & 5-2j \\ 0.1-0.1j & 0.1+0.1j \end{matrix}$$

the NP problem is solvable (the smallest eigenvalue of the Pick matrix equals 0.0051). Starting from the all-pass function 1, Nevanlinna's algorithm produces the all-pass solution

$$G(s) = \frac{(0.5268+0.1213j)s^2 - (9+j)s + (47.1073+1.1410j)}{(0.5268-0.1213j)s^2 + (9-j)s + (47.1073-1.1410j)}.$$

Let $\underline{G}$ denote the function obtained from G by conjugating all coefficients. The function G_R is then

$$G_R = \frac{1}{2}(G + \underline{G}),$$

that is,

$$G_R(s) = \frac{0.2628s^4 - 30.6418s^2 + 2217.7975}{0.2923s^4 + 9.7255s^3 + 131.9119s^2 + 850.2137s + 2220.4012}.$$

This solution is not all-pass.

9.4 Solution of the Model-Matching Problem

Now let's see how to use NP theory to solve the model-matching problem. For simplicity we will *assume* that T_2 has no repeated zeros in the right half-plane. The minimum model-matching error, γ_{opt}, equals the minimum γ such that

$$\|T_1 - T_2 Q\|_\infty \leq \gamma$$

for some stable Q. Fix $\gamma > 0$ and consider the mapping $Q \mapsto G$ defined by

$$G = \frac{1}{\gamma}(T_1 - T_2 Q).$$

If Q is stable, so is G, but the converse is not always true. A stable function G must satisfy certain conditions in order that Q be stable. To see what they are, let $\{z_i : i = 1, \ldots, n\}$ denote the zeros of T_2 in $\text{Re}s > 0$. If Q is stable, then G satisfies the interpolation conditions

$$G(z_i) = \frac{1}{\gamma}T_1(z_i), \quad i = 1, \ldots, n.$$

You can check that, conversely, if G is stable and satisfies these interpolation conditions, then Q is stable.

Therefore, γ_{opt} equals the minimum γ so that there exists a function G in $\mathcal{S}$ satisfying the conditions

$$\|G\|_\infty \leq 1,$$

$$G(z_i) = \frac{1}{\gamma} T_1(z_i), \quad i = 1, \ldots, n.$$

This is precisely a Nevanlinna-Pick problem with data

$$\begin{matrix} a_1 & \cdots & a_n \\ \gamma^{-1} b_1 & \cdots & \gamma^{-1} b_n \end{matrix}$$

where $a_i := z_i$ and $b_i := T_1(z_i)$. The associated Pick matrix equals

$$A - \gamma^{-2} B,$$

where the ij^{th} elements of A and B are, respectively,

$$\frac{1}{a_i + \overline{a_j}}, \qquad \frac{b_i \overline{b_j}}{a_i + \overline{a_j}}.$$

From Pick's theorem we can now conclude that γ_{opt} equals the minimum γ such that $A - \gamma^{-2} B \geq 0$. Both A and B are Hermitian. Furthermore, it can be proved that A is positive definite because the a_is are distinct. Such a matrix has a positive definite *squareroot* (i.e., a matrix $A^{1/2}$ satisfying $A^{1/2} A^{1/2} = A$). The inverse of this squareroot is denoted $A^{-1/2}$.

The next lemma, a simple result in matrix theory, gives an explicit way to compute γ_{opt}.

Lemma 6 *γ_{opt} equals the squareroot of the largest eigenvalue of the matrix $A^{-1/2} B A^{-1/2}$.*

Tracing backwards, we get the following procedure for solving the model-matching problem.

Procedure

Input: T_1, T_2

Step 1 Determine $\{z_i : i = 1, \ldots, n\}$, the zeros of T_2 in $\text{Re}\, s > 0$.

Step 2 Define

$$b_i := T_1(z_i), \quad i = 1, \ldots, n$$

and form the matrices

$$A := \left(\frac{1}{z_i + \overline{z_j}} \right), \qquad B := \left(\frac{b_i \overline{b_j}}{z_i + \overline{z_j}} \right).$$

Step 3 Compute γ_{opt} as the squareroot of the largest eigenvalue of $A^{-1/2} B A^{-1/2}$.

Step 4 Solve the NP problem with data

$$\begin{matrix} z_1 & \cdots & z_n \\ \gamma_{\text{opt}}^{-1} b_1 & \cdots & \gamma_{\text{opt}}^{-1} b_n \end{matrix}$$

Denote the solution by G.

Step 5 Set

$$Q := \frac{T_1 - \gamma_{\text{opt}} G}{T_2}.$$

The NP problem in Step 4 has a unique, all-pass solution. Thus, for the optimal Q the error transfer function $T_1 - T_2 Q$ equals γ_{opt} times an all-pass function.

Example 4 The procedure applied to

$$T_1(s) = \frac{s+1}{10s+1}, \qquad T_2(s) = \frac{(s-1)(s-5)}{(s+2)^2}$$

goes like this:

Step 1

$$z_1 = 1, \quad z_2 = 5$$

Step 2

$$b_1 = \frac{2}{11}, \quad b_2 = \frac{2}{17}$$

$$A = \begin{bmatrix} 0.5 & 0.1667 \\ 0.1667 & 0.1 \end{bmatrix}, \qquad B = \begin{bmatrix} 0.0165 & 0.0036 \\ 0.0036 & 0.0014 \end{bmatrix}$$

Step 3

$$\gamma_{\text{opt}} = 0.2021$$

Step 4

$$\begin{matrix} z_1 & z_2 \\ \gamma_{\text{opt}}^{-1} b_1 & \gamma_{\text{opt}}^{-1} b_2 \end{matrix} = \begin{matrix} 1 & 5 \\ 0.8997 & 0.5821 \end{matrix}$$

$$G(s) = \frac{-1.0035s + 18.9965}{1.0035s + 18.9965}$$

Step 5

$$Q(s) = \frac{0.3021s^2 + 1.2084s + 1.2084}{s^2 + 19.0308s + 1.8931}$$

9.5 State-Space Solution (Optional)

For completeness, this section presents a state-space procedure for solving the model-matching problem. The underlying theory is beyond the scope of this book.

Step 1 Factor T_2 as the product of an all-pass factor and a minimum-phase factor:

$$T_2 = T_{2ap} T_{2mp}.$$

Step 2 Define

$$R := \frac{T_1}{T_{2ap}},$$

factor R as $R = R_1 + R_2$ with R_1 strictly proper and all poles in $\text{Re}s > 0$ and $R_2 \in \mathcal{S}$, and find a minimal realization

$$R_1(s) = \left[\begin{array}{c|c} A & B \\ \hline C & 0 \end{array}\right].$$

Step 3 Solve the Lyapunov equations

$$\begin{aligned} AL_c + L_cA' &= BB', \\ A'L_o + L_oA &= C'C. \end{aligned}$$

Step 4 Find the maximum eigenvalue λ^2 of L_cL_o and a corresponding eigenvector w.

Step 5 Define

$$\begin{aligned} f(s) &= \left[\begin{array}{c|c} A & w \\ \hline C & 0 \end{array}\right], \\ g(s) &= \left[\begin{array}{c|c} -A' & \lambda^{-1}L_ow \\ \hline B' & 0 \end{array}\right], \\ X &= R - \lambda\frac{f}{g}. \end{aligned}$$

Step 6 Then $\gamma_{\text{opt}} = \lambda$ and the optimal $Q = X/T_{2mp}$.

Example For the same data as in Example 4 in the preceding section, the procedure yields the following results.

Step 1

$$T_{2ap}(s) = \frac{(s-1)(s-5)}{(s+1)(s+5)}, \quad T_{2mp}(s) = \frac{(s+1)(s+5)}{(s+1)^2}$$

Step 2

$$R(s) = \frac{(s+1)^2(s+5)}{(10s+1)(s-1)(s-5)}$$

$$A = \begin{bmatrix} 1 & 0 \\ 0 & 5 \end{bmatrix}, \quad B = \begin{bmatrix} -\frac{6}{11} \\ \frac{30}{17} \end{bmatrix}, \quad C = \begin{bmatrix} 1 & 1 \end{bmatrix}$$

Step 3

$$L_c = \begin{bmatrix} 0.1488 & -0.1604 \\ -0.1604 & 0.3114 \end{bmatrix}, \quad L_o = \begin{bmatrix} 0.5 & 0.1667 \\ 0.1667 & 0.1 \end{bmatrix}$$

Step 4

$$\lambda = 0.2021, \quad w = \begin{bmatrix} 1 \\ -0.7769 \end{bmatrix}$$

Step 5

$$f(s) = \frac{0.2231s - 4.223}{(s-1)(s-5)}, \quad g(s) = \frac{-0.2231s - 4.223}{(s+1)(s+5)}$$

$$X(s) = 3.021\frac{(s+1)(s+5)}{(10s+1)(s+18.93)}$$

Step 6

$$\gamma_{\text{opt}} = 0.2021, \quad Q(s) = 3.021\frac{(s+2)^2}{(10s+1)(s+18.93)}$$

Exercises

1. Solve the model-matching problem for

$$T_1(s) = \frac{s}{s+10}, \quad T_2(s) = \frac{s-1}{s^2+s+1}.$$

2. For the data

$$\begin{matrix} 1 & 1-j \\ j & -1+2j \end{matrix}$$

form the Pick matrix and compute its eigenvalues.

3. Find the minimum γ for which there exists a function G in $\mathcal{S}_c$ such that

$$\|G\|_\infty \leq \gamma,$$

$$G(1) = 2, \quad G(2) = 10.$$

4. Solve the model-matching problem for

$$T_1(s) = \frac{1}{s+1}, \quad T_2(s) = \frac{s^2-s+1}{(s+2)^3}.$$

5. Compute a real-rational solution to the NP problem for the data

$$\begin{matrix} 1 & 1-j & 1+j \\ 0.1 & 0.2j & -0.2j \end{matrix}$$

6. Let A and B be $n \times n$ complex Hermitian matrices with $A > 0$. Prove that $A - \gamma^{-2}B \geq 0$ iff γ^2 is $\geq$ the largest eigenvalue of $A^{-1/2}BA^{-1/2}$. (This proves Lemma 6.)

Notes and References

The NP problem is named after the mathematicians R. Nevanlinna and G. Pick, whose work dates from 1916-1919. For a complete proof of Pick's theorem together with additional references, see Garnett (1981).

In the model-matching problem, zeros of T_2 on the imaginary axis lead to boundary interpolation in the NP problem (i.e., some of a_is are on the imaginary axis). This complicates the NP problem; a reference for this case is Khargonekar and Tannenbaum (1985).

The proof of necessity in Section 9.2 is from Youla and Saito (1967), and Nevanlinna's algorithm is taken from Walsh (1969). NP theory was first used in the context of control problems by Tannenbaum (1980, 1981). The state-space procedure in Section 9.5 is from Francis (1987), which in turn is adapted from Sarason (1967) and Silverman and Bettayeb (1980).

Design for Performance

The performance criterion $\|W_1 S\|_\infty < 1$ was introduced in Section 3.4. The associated design problem is to find a proper C for which the feedback system is internally stable and $\|W_1 S\|_\infty < 1$. When does such a C exist and how can it be computed? These questions are easy when the inverse of the plant transfer function is stable. When the inverse is unstable, the questions are more interesting. The solutions presented in this chapter use model-matching theory.

10.1 P^{-1} Stable

We assume in this section that P has no zeros in $\mathrm{Re} s \geq 0$, or in other words, P^{-1} is stable. The weighting function W_1 is assumed to be stable and strictly proper. The latter condition is not too serious a loss of generality. We will see that under these conditions it is always possible, indeed quite easy, to design a proper C which is internally stabilizing and makes $\|W_1 S\|_\infty < 1$.

Let k be a positive integer and τ a positive real number, and consider the transfer function

$$J(s) := \frac{1}{(\tau s + 1)^k}.$$

Sketch the Bode plot of J: The magnitude starts out at 1, is relatively flat out to the corner frequency $\omega = 1/\tau$, and then rolls off to $-\infty$ with slope $-k$; the phase starts out at 0, is relatively flat up to, say, $\omega = 0.1/\tau$, and then rolls off to $-k\pi/2$ radians. So for low frequency, $J(j\omega) \approx 1$. This function has the useful property that it approximates 1 beside a strictly proper function.

Lemma 1 *If G is stable and strictly proper, then*

$$\lim_{\tau \to 0} \|G(1 - J)\|_\infty = 0.$$

Proof Let $\epsilon > 0$ and $\omega_1 > 0$. By the argument above regarding the Bode plot of J, if τ is sufficiently small, then the Nyquist plot of J lies in the disk with center 1, radius ϵ for $\omega \leq \omega_1$, and in the disk with center 0, radius 1 for $\omega > \omega_1$. Now $\|G(1 - J)\|_\infty$ equals the maximum of

$$\max_{\omega \leq \omega_1} |G(j\omega)[1 - J(j\omega)]|$$

and

$$\max_{\omega > \omega_1} |G(j\omega)[1 - J(j\omega)]|.$$

The first of these is bounded above by $\epsilon\|G\|_\infty$, and the second by

$$\|1 - J\|_\infty \max_{\omega > \omega_1} |G(j\omega)|.$$

Since

$$\|1 - J\|_\infty \leq \|1\|_\infty + \|J\|_\infty = 2,$$

we have

$$\|G(1 - J)\|_\infty \leq \max \left\{ \epsilon\|G\|_\infty, 2 \max_{\omega > \omega_1} |G(j\omega)| \right\}.$$

This holds for τ sufficiently small. But the right-hand side can be made arbitrarily small by suitable choice of ϵ and ω_1 because

$$\lim_{\omega_1 \to \infty} \max_{\omega > \omega_1} |G(j\omega)| = |G(j\infty)| = 0.$$

We conclude that for every $\delta > 0$, if τ is small enough, then

$$\|G(1 - J)\|_\infty \leq \delta.$$

This is the desired conclusion. ■

We'll develop the design procedure first with the additional assumption that P is stable. By Theorem 5.1 the set of all internally stabilizing Cs is parametrized by the formula

$$C = \frac{Q}{1 - PQ}, \quad Q \in \mathcal{S}.$$

Then $W_1 S$ is given in terms of Q by

$$W_1 S = W_1(1 - PQ).$$

To make $\|W_1 S\|_\infty < 1$ we are prompted to set $Q = P^{-1}$. This is indeed stable, by assumption, but not proper, hence not in $\mathcal{S}$. So let's try $Q = P^{-1}J$ with J as above and the integer k just large enough to make $P^{-1}J$ proper (i.e., k equals the relative degree of P). Then

$$W_1 S = W_1(1 - J),$$

whose ∞-norm is < 1 for sufficiently small τ, by Lemma 1.

In summary, the design procedure is as follows.

Procedure: P and P^{-1} Stable

Input: P, W_1

Step 1 Set $k =$ the relative degree of P.

Step 2 Choose τ so small that

$$\|W_1(1 - J)\|_\infty < 1,$$

where

$$J(s) := \frac{1}{(\tau s + 1)^k}.$$

Step 3 Set $Q = P^{-1}J$.

Step 4 Set $C = Q/(1 - PQ)$.

When P is unstable, the parametrization in Theorem 5.2 is used.

Procedure: P^{-1} Stable

Input: P, W_1

Step 1 Do a coprime factorization of P: Find four functions in $\mathcal{S}$ satisfying the equations

$$P = \frac{N}{M}, \quad NX + MY = 1.$$

Step 2 Set $k =$ the relative degree of P.

Step 3 Choose τ so small that

$$\|W_1 MY(1 - J)\|_\infty < 1,$$

where

$$J(s) := \frac{1}{(\tau s + 1)^k}.$$

Step 4 Set $Q = YN^{-1}J$.

Step 5 Set $C = (X + MQ)/(Y - NQ)$.

Example Consider the unstable plant and weighting function

$$P(s) = \frac{1}{(s-2)^2}, \quad W_1(s) = \frac{100}{s+1}.$$

This weight has bandwidth 1 rad/s, so it might be used to get good tracking (i.e., approximately 1% tracking error, up to this frequency). The previous procedure for these data goes as follows:

Step 1 First, do a coprime factorization of P over $\mathcal{S}$:

$$\begin{aligned} N(s) &= \frac{1}{(s+1)^2}, \\ M(s) &= \frac{(s-2)^2}{(s+1)^2}, \\ X(s) &= 27\frac{s-1}{s+1}, \\ Y(s) &= \frac{s+7}{s+1}. \end{aligned}$$

Step 2 $k = 2$

Step 3 Choose τ so that the ∞-norm of

$$\frac{100(s-2)^2(s+7)}{(s+1)^4}\left[1-\frac{1}{(\tau s+1)^2}\right]$$

is < 1. The norm is computed for decreasing values of τ:

τ	∞-Norm
10^{-1}	199.0
10^{-2}	19.97
10^{-3}	1.997
10^{-4}	0.1997

So take $\tau = 10^{-4}$.

Step 4

$$Q(s) = \frac{(s+1)(s+7)}{(10^{-4}s+1)^2}$$

Step 5

$$C(s) = 10^4\frac{(s+1)^3}{s(s+7)(10^{-4}s+2)}$$

This section concludes with a result stated but not proved in Section 6.2. It concerns the performance problem where the weight W_1 satisfies

$$|W_1(j\omega)| = \begin{cases} \dfrac{1}{\epsilon}, & \omega_1 \le \omega \le \omega_2 \\ \dfrac{1}{\delta}, & \text{else.} \end{cases}$$

Thus the criterion $\|W_1 S\|_\infty < 1$ is equivalent to the conditions

$$\begin{array}{ll} |S(j\omega)| < \epsilon, & \omega_1 \le \omega \le \omega_2 \\ |S(j\omega)| < \delta, & \text{else.} \end{array} \tag{10.1}$$

Lemma 2 *If P^{-1} is stable, then for every $\epsilon > 0$ and $\delta > 1$, there exists a proper C such that the feedback system is internally stable and (10.1) holds.* [1]

Proof The idea is to approximately invert P over the frequency range $[0, \omega_2]$ while rolling off fast enough at higher frequencies. From Theorem 5.2 again, the formula for all internally stabilizing proper controllers is

$$C = \frac{X+MQ}{Y-NQ}, \quad Q \in \mathcal{S}.$$

For such C

$$S = M(Y-NQ). \tag{10.2}$$

Now fix $\epsilon > 0$ and $\delta > 1$. We may as well suppose that $\epsilon < 1$. Choose $c > 0$ so small that

$$c\|MY\|_\infty < \epsilon, \tag{10.3}$$

[1] The assumption on P in Lemma 2 is slightly stronger than necessary; see the statement in Section 6.2.

$$(1+c)^2 < \delta. \tag{10.4}$$

Since P is strictly proper, so is N. This fact together with the equation

$$NX + MY = 1$$

shows that

$$M(j\infty)Y(j\infty) = 1.$$

Since $|M(j\omega)Y(j\omega)|$ is a continuous function of ω, it is possible to choose $\omega_3 \geq \omega_2$ such that

$$|M(j\omega)Y(j\omega)| \leq 1 + c, \quad \forall \omega \geq \omega_3. \tag{10.5}$$

The assumption on P implies that N^{-1} is stable (but not proper). Choose a function V in $\mathcal{S}$ with the following three properties:

1. VN^{-1} is proper.
2. $|1 - V(j\omega)| \leq c, \quad \forall \omega \leq \omega_3.$
3. $\|1 - V\|_\infty \leq 1 + c.$

The idea behind the choice of V can be explained in terms of its Nyquist plot: It should lie in the disk with center 1, radius c up to frequency ω_3 (property 2) and in the disk with center 1, radius $1+c$ thereafter (property 3). In addition, V should roll off fast enough so that VN^{-1} is proper. It is left as an exercise to convince yourself that such a V exists—a function of the form

$$\frac{1}{(\tau_1 s + 1)(\tau_2 s + 1)^k}$$

will work.

Finally, take Q to be

$$Q := VN^{-1}Y.$$

Substitution into (10.2) gives

$$S = MY(1 - V).$$

Thus for $\omega \leq \omega_3$

$$\begin{aligned} |S(j\omega)| &\leq c\|MY\|_\infty \quad \text{from proprty 2} \\ &< \epsilon \quad \text{from (10.3)} \end{aligned}$$

and for $\omega > \omega_3$

$$\begin{aligned} |S(j\omega)| &\leq (1+c)|M(j\omega)Y(j\omega)| \quad \text{from property 3} \\ &\leq (1+c)^2 \quad \text{from (10.5)} \\ &< \delta \quad \text{from (10.4).} \ \blacksquare \end{aligned}$$

10.2 P^{-1} Unstable

We come now to the first time in this book that we need a nonclassical method, namely, interpolation theory. To simplify matters we will assume in this section that

- P has no poles or zeros on the imaginary axis, only distinct poles and zeros in the right half-plane, and at least one zero in the right half-plane (i.e., P^{-1} is unstable).
- W_1 is stable and strictly proper.

It would be possible to relax these assumptions, but the development would be messier.

To motivate the procedure to follow, let's see roughly how the design problem of finding an internally stabilizing C so that $\|W_1S\|_\infty < 1$ can be translated into an NP problem. The definition of S is

$$S = \frac{1}{1+PC}.$$

For C to be internally stabilizing it is necessary and sufficient that $S \in \mathcal{S}$ and PC have no right half-plane pole-zero cancellations (Theorem 3.2). Thus, S must interpolate the value 1 at the right half-plane zeros of P and the value 0 at the right half-plane poles (see also Section 6.1); that is, S must satisfy the conditions

$$\begin{aligned} S(z) &= 1 \quad \text{for } z \text{ a zero of } P \text{ in } \mathrm{Re}s > 0, \\ S(p) &= 0 \quad \text{for } p \text{ a pole of } P \text{ in } \mathrm{Re}s > 0. \end{aligned}$$

The weighted sensitivity function $G := W_1S$ must therefore satisfy

$$\begin{aligned} G(z) &= W_1(z) \quad \text{for } z \text{ a zero of } P \text{ in } \mathrm{Re}s > 0, \\ G(p) &= 0 \quad \text{for } p \text{ a pole of } P \text{ in } \mathrm{Re}s > 0. \end{aligned}$$

So the requirement of internal stability imposes interpolation constraints on G. The performance spec $\|W_1S\|_\infty < 1$ translates into $\|G\|_\infty < 1$. Finally, the condition $S \in \mathcal{S}$ requires that G be analytic in the right half-plane.

One approach to the design problem might be to find a function G satisfying these conditions, then to get S, and finally to get C by back-substitution. This has a technical snag because the requirement that C be proper places an additional constraint on G not handled by our NP theory of the Chapter 9. For this reason we proceed via controller parametrization.

Bring in again a coprime factorization of P:

$$P = \frac{N}{M}, \quad NX + MY = 1.$$

The controller parametrization formula is

$$C = \frac{X + MQ}{Y - NQ}, \quad Q \in \mathcal{S},$$

and for such C the weighted sensitivity function is

$$W_1S = W_1M(Y - NQ).$$

The parameter Q must be both stable and proper. Our approach is first to drop the properness requirement and find a suitable parameter, say, Q_{im}, which is improper but stable, and then to get a suitable Q by rolling Q_{im} off at high frequency. The reason this works is that W_1 is strictly proper, so there is no performance requirement at high frequency. The method is outlined as follows:

Procedure

Input: P, W_1

Step 1 Do a coprime factorization of P: Find four functions in $\mathcal{S}$ satisfying the equations

$$P = \frac{N}{M}, \quad NX + MY = 1.$$

Step 2 Find a stable function Q_{im} such that

$$\|W_1 M(Y - NQ_{\text{im}})\|_\infty < 1.$$

Step 3 Set

$$J(s) := \frac{1}{(\tau s + 1)^k},$$

where k is just large enough that $Q_{\text{im}}J$ is proper and τ is just small enough that

$$\|W_1 M(Y - NQ_{\text{im}}J)\|_\infty < 1.$$

Step 4 Set $Q = Q_{\text{im}}J$.

Step 5 Set $C = (X + MQ)/(Y - NQ)$.

That Step 3 is feasible follows from the equation

$$W_1 M(Y - NQ_{\text{im}}J) = W_1 M(Y - NQ_{\text{im}})J + W_1 MY(1 - J).$$

The first term on the right-hand side has ∞-norm less than 1 from Step 2 and the fact that $\|J\|_\infty \leq 1$, while the ∞-norm of the second term goes to 0 as τ goes to 0 by Lemma 1.

Step 2 is the model-matching problem, find a stable function Q_{im} to minimize

$$\|T_1 - T_2 Q_{\text{im}}\|_\infty,$$

where $T_1 := W_1 MY$ and $T_2 := W_1 MN$. Step 2 is feasible iff γ_{opt}, the minimum model-matching error, is < 1.

10.3 Design Example: Flexible Beam

This section presents an example to illustrate the procedure of the preceding section. The example is based on a real experimental setup at the University of Toronto.

The control system, depicted in Figure 10.1, has the following components: a flexible beam, a high-torque dc motor at one end of the beam, a sonar position sensor at the other end, a digital computer as the controller with analog-to-digital interface hardware, a power amplifier to drive the motor, and an antialiasing filter. The objective is to control the position of the sensed end of the beam.

A plant model was obtained as follows. The beam is pinned to the motor shaft and is free at the sensed end. First the beam itself was modeled as an ideal Euler-Bernoulli beam with no damping; this yielded a partial differential equation model, reflecting the fact that the physical model of the

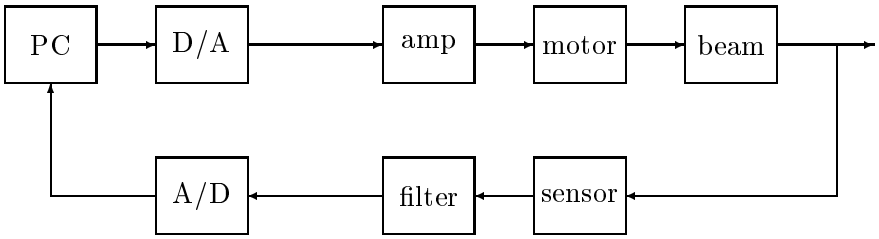

Figure 10.1: Flexible beam setup.

beam has an infinite number of modes. The model is therefore linear but infinite-dimensional. The corresponding transfer function from torque input at the motor end to tip deflection at the sensed end has the form

$$\sum_{i=0}^{\infty} \frac{c_i}{s^2 + \omega_i^2}.$$

Then damping was introduced, yielding the form

$$\sum_{i=0}^{\infty} \frac{c_i}{s^2 + 2\zeta_i \omega_i s + \omega_i^2}.$$

The first term is c_0/s^2 and corresponds to the rigid-body slewing motion about the pinned end. The second term,

$$\frac{c_1}{s^2 + 2\zeta_1 \omega_1 s + \omega_1^2},$$

corresponds to the first flexible mode. And so on. The motion was found to be adequately modeled by the first four flexible modes. Then the damping ratios and natural frequencies were determined experimentally. Finally, the amplifier, motor, and sensor were introduced into the model. The antialiasing filter was ignored for the purpose of design.

For simplicity we shall take the plant transfer function to be

$$P(s) = \frac{-6.4750s^2 + 4.0302s + 175.7700}{s(5s^3 + 3.5682s^2 + 139.5021s + 0.0929)}.$$

The poles are

$$0, -0.0007, -0.3565 \pm 5.2700j.$$

The first two poles correspond to the rigid-body motion; the one at $s = -0.0007$ has been perturbed away from the origin by the back EMF in the motor. The two complex poles correspond to the first flexible mode, the damping ratio being 0.0675. The zeros are

$$-4.9081, 5.5308.$$

Because of the zero at $s = 5.5308$ the plant is non-minimum phase, reflecting the fact that the actuator (the motor) and the sensor are not located at the same point on the beam. The procedure of the preceding section requires no poles on the imaginary axis, so the model is (harmlessly) perturbed to

$$P(s) = \frac{-6.4750s^2 + 4.0302s + 175.7700}{5s^4 + 3.5682s^3 + 139.5021s^2 + 0.0929s + 10^{-6}}.$$

A common way to specify desired closed-loop performance is by a step response test. For this flexible beam the spec is that a step reference input (r) should produce a plant output (y) satisfying

$$\begin{aligned} \text{settling time} &\approx 8\text{s}, \\ \text{overshoot} &\leq 10\%. \end{aligned}$$

We will accomplish this by shaping $T(s)$, the transfer function from r to y, so that it approximates a standard second-order system: The ideal $T(s)$ is

$$T_{\text{id}}(s) := \frac{\omega_n^2}{s^2 + 2\zeta\omega_n s + \omega_n^2}.$$

A settling time of 8 s requires

$$\frac{4.6}{\zeta\omega_n} \approx 8$$

and an overshoot of 10% requires

$$\exp\left(\frac{-\zeta\pi}{\sqrt{1-\zeta^2}}\right) = 0.1.$$

The solutions are $\zeta = 0.5912$ and $\omega_n = 0.9583$. Let's round to $\zeta = 0.6$ and $\omega_n = 1$. So the ideal $T(s)$ is

$$T_{\text{id}}(s) = \frac{1}{s^2 + 1.2s + 1}.$$

Then the ideal sensitivity function is

$$S_{\text{id}}(s) := 1 - T_{\text{id}}(s) = \frac{s(s+1.2)}{s^2 + 1.2s + 1}.$$

Now take the weighting function $W_1(s)$ to be $S_{\text{id}}(s)^{-1}$, that is,

$$W_1(s) = \frac{s^2 + 1.2s + 1}{s(s+1.2)}.$$

The rationale for this choice is a rough argument that goes as follows. Consider Step 2 of the procedure in the preceding section; from it the function

$$F := W_1 M (Y - N Q_{\text{im}})$$

equals a constant times an all-pass function. The procedure then rolls off Q_{im} to result in the weighted sensitivity function

$$W_1 S := W_1 M (Y - N Q_{\text{im}} J).$$

So $W_1 S \approx F$ except at high frequency, that is,

$$S \approx F S_{\text{id}}.$$

Now F behaves approximately like a time delay except at high frequency (this is a property of all-pass functions). So we arrive at the rough approximation

$$S \approx (\text{time delay}) \times S_{\text{id}}.$$

Hence our design should produce

$$\text{actual step response} \approx \text{delayed ideal step response.}$$

One further adjustment is required in the problem setup: W_1 must be stable and strictly proper, so the function above is modified to

$$W_1(s) = \frac{s^2 + 1.2s + 1}{(s + 0.001)(s + 1.2)(0.001s + 1)}.$$

The procedure can now be applied.

Step 1 Since $P \in \mathcal{S}$ we take $N = P, M = 1, X = 0, Y = 1$.

Step 2 The model-matching problem is to minimize

$$\|W_1 M(Y - NQ_{\text{im}})\|_\infty = \|W_1(1 - PQ_{\text{im}})\|_\infty.$$

Since P has only one right half-plane zero, at $s = 5.5308$, we have from Section 9.1

$$\min \|W_1(1 - PQ_{\text{im}})\|_\infty = |W_1(5.5308)| = 1.0210.$$

Thus the spec $\|W_1 S\|_\infty < 1$ is not achievable for this P and W_1. Let us scale W_1 as

$$W_1 \leftarrow \frac{0.9}{1.0210} W_1.$$

Then $|W_1(5.5308)| = 0.9$ and the optimal Q_{im} is

$$Q_{\text{im}} = \frac{W_1 - 0.9}{W_1 P},$$

that is,

$$Q_{\text{im}}(s) = \frac{s(0.0008s^5 + 0.0221s^4 + 0.1768s^3 + 0.7007s^2 + 3.8910s + 0.0026)}{s^3 + 6.1081s^2 + 6.8897s + 4.9801}.$$

Step 3 Set

$$J(s) := \frac{1}{(\tau s + 1)^3}.$$

Compute $\|W_1(1 - PQ_{\text{im}}J)\|_\infty$ for decreasing values of τ until the norm is < 1:

τ	∞-Norm
0.1	1.12
0.05	1.01
0.04	0.988

Take $\tau = 0.04$.

Step 4 $Q = Q_{\text{im}}J$

Step 5 $C = Q/(1 - PQ)$

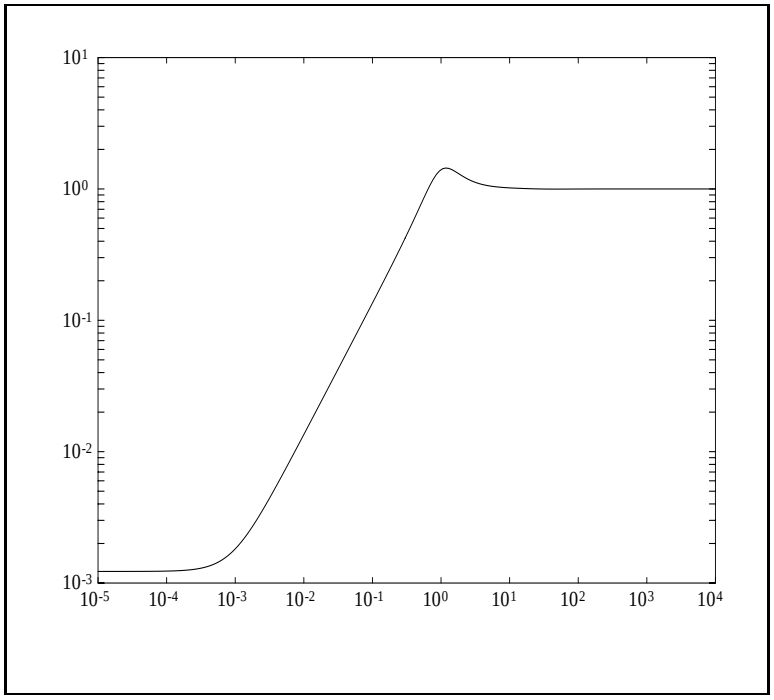

Figure 10.2: Bode plot of $|S|$.

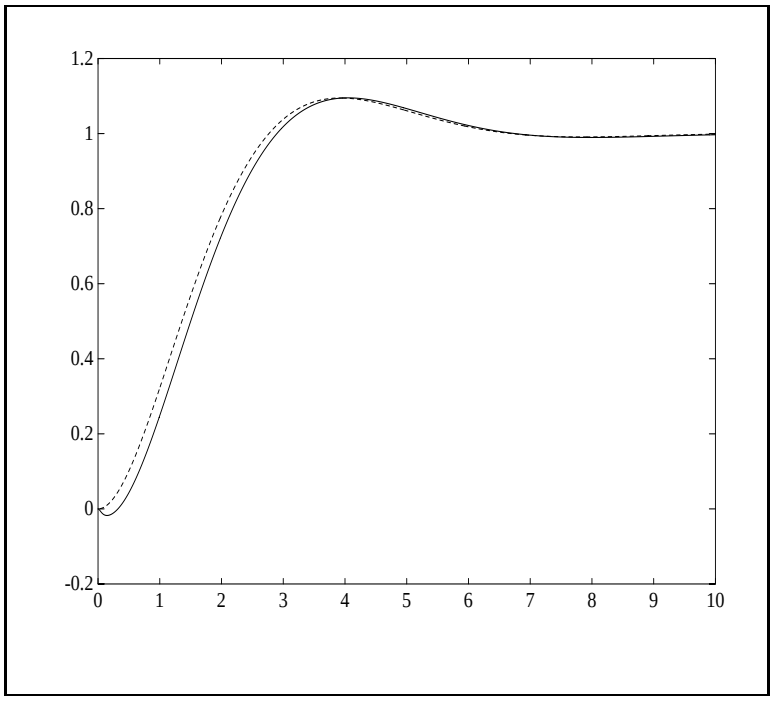

Figure 10.3: Actual (solid) and ideal (dash) step responses.

A Bode magnitude plot of the resulting sensitivity function is shown in Figure 10.2. Figure 10.3 shows the step response of the plant output together with the ideal step response (i.e., that of $T_{\rm id}$). The performance specs are met.

The design above, while achieving the step response goal, may not be satisfactory for other reasons; for example, internal signals may be too large (in fact, for this design the input to the power amplifier would saturate during the step response test). The problem is that we have placed no limits on controller gain or bandwidth. We return to this example and see how to correct this deficiency in Chapter 12.

Another disadvantage of the design above is that C is of high order. The common way to alleviate this is to approximate Q by a lower-order transfer function (it is difficult to reduce C directly because of the internal stability constraint, whereas Q only has to be stable and proper).

10.4 2-Norm Minimization

The subject of this section is minimization of the 2-norm of some designated closed-loop transfer function. As a typical case, we consider the transfer function from d to y, namely, PS. Motivation for considering the 2-norm was presented in Section 2.3. For example, if $d(t)$ is the unit impulse, then the 2-norm of $y(t)$ equals $\|PS\|_2$. Or, $\|PS\|_2$ equals the 2-norm to ∞-norm gain from d to y.

To make the problem more flexible, bring in a weighting function W—appropriate assumptions on W will be introduced as required. The problem for consideration is: Given P and W, design an internally stabilizing C to minimize $\|WPS\|_2$. The method of solution is again to parametrize all internally stabilizing Cs and then to select an optimal parameter, but now optimal for the 2-norm.

We need some preliminaries. First, let $\mathcal{S}_0$ denote the subset of $\mathcal{S}$ of all strictly proper stable transfer functions, $\mathcal{S}_0^\perp$ the set of strictly proper transfer functions analytic in Re$s \le 0$, and $\mathcal{S}_0 + \mathcal{S}_0^\perp$ the set of all sums. Thus $\mathcal{S}_0 + \mathcal{S}_0^\perp$ consists precisely of all strictly proper transfer functions with no poles on the imaginary axis. By Lemma 2.1 the 2-norm is finite for all functions in $\mathcal{S}_0 + \mathcal{S}_0^\perp$. Furthermore, every function F in $\mathcal{S}_0 + \mathcal{S}_0^\perp$ can be uniquely expressed as

$$F = F_{\rm st} + F_{\rm un}, \quad F_{\rm st} \in \mathcal{S}_0, F_{\rm un} \in \mathcal{S}_0^\perp,$$

for example, by partial fraction expansion ($F_{\rm st}$ is stable, $F_{\rm un}$ is unstable).

Pythagoras's theorem holds in this setting.

Lemma 3 *If $F \in \mathcal{S}_0$ and $G \in \mathcal{S}_0^\perp$, then*

$$\|F + G\|_2^2 = \|F\|_2^2 + \|G\|_2^2.$$

Proof

$$\begin{aligned} \|F+G\|_2^2 &= \frac{1}{2\pi}\int |F(j\omega)+G(j\omega)|^2 d\omega \\ &= \|F\|_2^2 + \|G\|_2^2 + 2\mathrm{Re}\left[\frac{1}{2\pi}\int \overline{F(j\omega)}G(j\omega)d\omega\right]. \end{aligned}$$

So it suffices to show the last integral equals zero. Convert it into a contour integral by closing the imaginary axis with an infinite-radius semicircle in the left half-plane:

$$\frac{1}{2\pi}\int \overline{F(j\omega)}G(j\omega)d\omega = \frac{1}{2\pi j}\oint F(-s)G(s)ds.$$

But the right-hand side equals zero by Cauchy's theorem. ■

For the usual representations

$$\begin{aligned} P &= \frac{N}{M}, \quad NX + MY = 1, \\ C &= \frac{X + MQ}{Y - NQ}, \quad Q \in \mathcal{S}, \end{aligned}$$

we have

$$WPS = WNY - WN^2Q.$$

So the problem reduces to: Obtain Q in $\mathcal{S}$ to minimize

$$\|WNY - WN^2Q\|_2.$$

Evidently, this is a 2-norm model-matching problem. It is much easier than the ∞-norm version.

Let us now assume that $W \in \mathcal{S}$. The idea is to factor $U := WN^2$ as $U = U_{ap}U_{mp}$. So that the minimum-phase factor U_{mp} has a stable inverse (so that we can back-solve for Q), assume in addition that W and P have no zeros on the imaginary axis. Now we shall use the fact that U_{ap} has unit magnitude on the imaginary axis as follows. For fixed Q in $\mathcal{S}$ we have

$$\begin{aligned} \|WNY - WN^2Q\|_2^2 &= \|WNY - U_{ap}U_{mp}Q\|_2^2 \\ &= \|U_{ap}(U_{ap}^{-1}WNY - U_{mp}Q)\|_2^2 \\ &= \|U_{ap}^{-1}WNY - U_{mp}Q\|_2^2 \\ &= \|(U_{ap}^{-1}WNY)_{\text{un}} + (U_{ap}^{-1}WNY)_{\text{st}} - U_{mp}Q\|_2^2 \\ &= \|(U_{ap}^{-1}WNY)_{\text{un}}\|_2^2 + \|(U_{ap}^{-1}WNY)_{\text{st}} - U_{mp}Q\|_2^2. \end{aligned}$$

Lemma 3 was used in the last equality. It is now clear that the unique optimal, generally improper Q is

$$Q_{\text{im}} = U_{mp}^{-1}(U_{ap}^{-1}WNY)_{\text{st}} = (WN^2)_{mp}^{-1}\left[(WN^2)_{ap}^{-1}WNY\right]_{\text{st}}$$

and the consequent minimum value of $\|WNY - WN^2Q\|_2$ equals $\|(U_{ap}^{-1}WNY)_{\text{un}}\|_2$. This Q_{im} must be rolled off at high frequency to get a proper suboptimal Q, just as in Section 10.1; the details are routine and are therefore omitted.

Example In this example the 2-norm of the plant output y is minimized for a unit step disturbance d. Thus $W(s) = 1/s$. A modification of the derivation above is required because this W is unstable. Take

$$P(s) = \frac{1 - s}{s^2 + s + 2}.$$

This being stable, we should take

$$C = \frac{Q}{1 - PQ}, \quad Q \in \mathcal{S}.$$

Temporarily relax the requirement that Q be proper. The function whose 2-norm is to be minimized is

$$WPS = WP(1 - PQ). \tag{10.6}$$

For this to have finite 2-norm we must guarantee that $P(1-PQ)$ has a zero at $s=0$ to cancel the pole of W; this requires $1-PQ$ to have a zero at $s=0$, that is, $Q(0)=1/P(0)=2$. The set of all stable Qs satisfying $Q(0)=2$ is

$$Q(s) = 2 + sQ_1(s), \quad Q_1 \text{ stable.}$$

Substitute this into (10.6) to get

$$WPS = T - UQ_1,$$

where

$$\begin{aligned} T(s) &:= W(s)P(s)[1-2P(s)] \\ &= \frac{(1-s)(s+3)}{(s^2+s+2)^2}, \\ U(s) &:= P(s)^2 \\ &= \frac{(1-s)^2}{(s^2+s+2)^2}. \end{aligned}$$

Then as above, the optimal improper Q_1 equals $U_{mp}^{-1}(U_{ap}^{-1}T)_{\text{st}}$, that is,

$$Q_{1im}(s) = \frac{(s^2+s+2)^2}{(s+1)^2}\left[\frac{(s+1)^2}{1-s}\frac{(1-s)(s+3)}{(s^2+s+2)^2}\right]_{\text{st}} = \frac{s^3+2s^2+2s-1}{(s+1)^2}.$$

To get a proper Q, this should be made strictly proper, so set

$$Q_1(s) = \frac{s^3+2s^2+2s-1}{(\tau s+1)^2(s+1)^2}.$$

Then

$$Q(s) = 2 + s\frac{s^3+2s^2+2s-1}{(\tau s+1)^2(s+1)^2}.$$

As $\tau \to 0$, this Q recovers optimality of $\|WPS\|_2$.

Exercises

1. Design a controller to achieve $\|W_1 S\|_\infty < 1$ for

$$\begin{aligned} P(s) &= \frac{s-1}{(s+1)^2}, \\ W_1(s) &= 0.62\frac{s^2+1.2s+1}{(s+0.001)(s+1.2)(0.001s+1)}. \end{aligned}$$

   Plot the resulting step response of the plant output.

2. Take

$$P(s) = \frac{(s-1)(s-2)}{(s+1)^3}, \quad W_1(s) = \frac{a}{100s+1}.$$

   Design a controller to achieve $\|W_1 S\|_\infty < 1$. You'll have to adjust the parameter a so that the spec is achievable. Sketch Bode plots of $|S|$, $|W_1|$, and $|CS|$.

3. Repeat with
$$P(s) = \frac{s-1}{(s-2)(s+1)}.$$

4. This problem looks at performance design with P minimum phase but having a pole on the imaginary axis. Take
$$P(s) = \frac{1}{s}, \quad W_1(s) = \frac{100}{s+1}.$$

   (a) Perturb P to $P(s) = 1/(s+\epsilon)$, $\epsilon > 0$. Find a controller C (internally stabilizing) so that $\|W_1 S\|_\infty < 1$. Let ϵ go to zero in the coefficients of C. Does the resulting C solve the performance design problem for the original P?

   (b) Factor P as
$$P = P_1 P_2, \quad P_1(s) = \frac{1}{s+1}, \quad P_2(s) = \frac{s+1}{s}.$$
   Solve the performance design problem for P_1; let C_1 be the solution. Set $C = C_1/P_2$. Does the resulting C solve the performance design problem for the original P? If so, explain why.

5. Take
$$P(s) = \frac{s-1}{(s-2)(s+1)}.$$
   Let S and T denote the sensitivity and complementary sensitivity functions. Prove that
$$\inf \|S\|_\infty = \inf \|T\|_\infty, \tag{10.7}$$
   where both infima are over all proper controllers which internally stabilize the feedback system. Hint to save you some work: The result can be proved without actually computing a coprime factorization of P.

6. Take $P(s) = 1/s^2$. By the method in the proof of Lemma 2, design an internally stabilizing C such that
$$\begin{aligned} |S(j\omega)| &< 0.05, \quad \forall \omega \leq 1, \\ \|S\|_\infty &< 1.4. \end{aligned}$$

7. Prove that if G is stable and strictly proper, then
$$\lim_{\tau \to 0} \|G(1 - J)\|_2 = 0.$$

8. Take
$$P(s) = \frac{10}{(s-1)(s+2)}.$$
   Compute an internally stabilizing C to minimize the 2-norm of the tracking error $y - r$ for r the unit step.

Notes and References

The material in Section 10.1 is drawn from Zames (1981), Bensoussan (1984), Francis and Zames (1984), and Francis (1987). In the literature the problem of minimizing $\|W_1 S\|_\infty$ is called the *weighted sensitivity problem.* Lemma 2 is from Bensoussan (1984) for P stable and Francis (1987) for the general case. Section 10.2 is based on Zames and Francis (1983), Francis and Zames (1984), and Khargonekar and Tannenbaum (1985).

There is a way to design for performance which yields a proper Q directly, but it involves boundary NP interpolation.

The technique in Section 10.4, 2-norm minimization, is also known as *minimum variance control*: If d is a zero-mean stationary random signal with power spectral density $W(-s)W(s)$, the variance of y equals exactly $\|WPS\|_2^2$. A good treatment of this subject is given in Morari and Zafiriou (1989).

Stability Margin Optimization

In Section 4.2 we looked at several measures of stability margin (e.g., gain and phase margin). In this chapter we pose the problem of designing a controller whose sole purpose is to maximize the stability margin. The maximum obtainable stability margin is a measure of how difficult the plant is to control; for example, a plant with a right half-plane pole near a zero has a relatively small optimal stability margin, and hence is relatively difficult to control.

Three measures of stability margin are treated, namely, the ∞-norm of a multiplicative perturbation, gain margin, and phase margin. It is shown that the problem of optimizing these stability margins can be reduced to a model-matching problem, as studied in Chapter 9. The reduction for gain and phase margins requires some conformal mappings, presented in Section 11.2.

11.1 Optimal Robust Stability

To establish our point of view, we begin with a general statement of the robust stability problem. Consider the usual unity-feedback system with plant transfer function P and controller transfer function C. It is hypothesized that P is not fixed but belongs to some set $\mathcal{P}$. The *robust stability problem* is to find, if one exists, a controller C that achieves internal stability for every P in $\mathcal{P}$. We would like to know two things: conditions on $\mathcal{P}$ for C to exist and a procedure to construct such C. In this generality the robust stability problem remains unsolved.

We concentrate in this section on the special case where $\mathcal{P}$ consists of multiplicative perturbations of a nominal plant P. Following Section 4.1, let $\mathcal{P}$ be the family of plants of the form $(1 + \Delta W_2)P$, where

1. P and $(1 + \Delta W_2)P$ have the same number of poles in Re$s \geq 0$.
2. $\|\Delta\|_\infty \leq \epsilon$. (In Section 4.1 we took $\epsilon = 1$.)

Here W_2 is a fixed stable proper weighting function and $\epsilon > 0$. We write $\mathcal{P}_\epsilon$ to show the explicit dependence on ϵ. Let ϵ_{sup} denote the least upper bound on ϵ such that some C stabilizes every plant in $\mathcal{P}_\epsilon$. So ϵ_{sup} is the maximum stability margin for this model of uncertainty.

The key result in Section 4.2 (Theorem 4.1) was that a controller C achieves internal stability for every plant in $\mathcal{P}_\epsilon$ iff it achieves internal stability for P and $\|W_2 T\|_\infty < 1/\epsilon$, where T is the nominal complementary sensitivity function,

$$T = \frac{PC}{1 + PC}. \tag{11.1}$$

Define

$$\gamma_{\inf} := \inf_{C} \|W_2 T\|_\infty, \tag{11.2}$$

the infimum being over all internally stabilizing controllers. Then $\epsilon_{\sup} = 1/\gamma_{\inf}$.

Proof If $\epsilon < \epsilon_{\sup}$, there exists a C internally stabilizing all of $\mathcal{P}_\epsilon$, and therefore

$$\|W_2 T\|_\infty < \frac{1}{\epsilon}.$$

This implies that $\gamma_{\inf} < 1/\epsilon$. Since ϵ could have been arbitrarily close to $\epsilon_{\sup}$, it must be that $\gamma_{\inf} \leq 1/\epsilon_{\sup}$. The reverse inequality is proved in a similar way. ■

We would like to compute $\epsilon_{\sup}$, equivalently, $\gamma_{\inf}$. Computing $\gamma_{\inf}$ reduces to a model-matching problem in the following way. As in Section 5.2, do a coprime factorization of P:

$$P = \frac{N}{M}, \quad NX + MY = 1.$$

By Theorem 5.2 the formula

$$C = \frac{X + MQ}{Y - NQ}, \quad Q \in \mathcal{S}$$

expresses all controllers achieving internal stability for the nominal plant P. Substitution of these formulas into (11.1) gives

$$T = N(X + MQ),$$

so that

$$W_2 T = W_2 N(X + MQ),$$

and hence

$$\gamma_{\inf} = \inf_{Q \in \mathcal{S}} \|W_2 N(X + MQ)\|_\infty. \tag{11.3}$$

Equation (11.3) suggests the model-matching problem of Section 9.1:

$$\gamma_{\text{opt}} = \min_{Q_{\text{im}} \text{ stable}} \|T_1 - T_2 Q_{\text{im}}\|_\infty. \tag{11.4}$$

Evidently, $T_1 = W_2 NX$, $T_2 = -W_2 NM$. So that T_2 has no zeros on the imaginary axis (an assumption in Section 9.1), we will *assume* that P has neither poles nor zeros on the imaginary axis and W_2 has no zeros on the imaginary axis. The difference between the two problems is that Q must be stable and proper in (11.3), but Q_{im} need only be stable in (11.4); the infimum in (11.3) is not achieved, while the minimum in (11.4) is achieved. Nevertheless, $\gamma_{\inf}$ equals γ_{opt}, the minimum model-matching error, a consequence of the fact that N, hence $W_2 N$, is strictly proper (Exercise 7).

The optimization problem defined by (11.3) is very much like the performance design problem in Section 10.2. The procedure there can be easily adapted to give the following one for computing $\epsilon_{\sup}$ together with a controller C which, for any $\epsilon < \epsilon_{\sup}$, achieves internal stability for all plants in $\mathcal{P}_\epsilon$.

Procedure

Input: P, W_2

Step 1 Do a coprime factorization of P: Find four functions in $\mathcal{S}$ satisfying the equations

$$P = \frac{N}{M}, \quad NX + MY = 1.$$

Step 2 Solve the model-matching problem for $T_1 = W_2NX$, $T_2 = -W_2NM$. Let Q_{im} denote its solution and let γ_{opt} denote the minimum model-matching error. Then $\epsilon_{\text{sup}} = 1/\gamma_{\text{opt}}$.

Step 3 Let ϵ be an arbitrary number $< \epsilon_{\text{sup}}$. Set

$$J(s) := \frac{1}{(\tau s + 1)^k},$$

where k is just large enough that $Q_{\text{im}}J$ is proper and τ is just small enough that

$$\|W_2N(X + MQ_{\text{im}}J)\|_\infty < \frac{1}{\epsilon}.$$

Step 4 Set $Q = Q_{\text{im}}J$.

Step 5 Set $C = (X + MQ)/(Y - NQ)$.

Example Consider the plant

$$P(s) = \frac{s-1}{(s+1)(s-p)}, \quad 0 < p \neq 1$$

with an unstable pole at $s = p$ and a zero at $s = 1$. We might anticipate some difficulty if $p \approx 1$. Suppose that the uncertainty weight is the high-pass function

$$W_2(s) = \frac{s + 0.1}{s + 1}.$$

The procedure above goes like this:

Step 1

$$\begin{aligned} N(s) &= \frac{s-1}{(s+1)^2} \\ M(s) &= \frac{s-p}{s+1} \\ X(s) &= \frac{(p+1)^2}{p-1} \\ Y(s) &= \frac{s - (p+3)/(p-1)}{s+1} \end{aligned}$$

Step 2 Factor N as $N = N_{\text{ap}}N_{\text{mp}}$ with

$$N_{\text{ap}}(s) = \frac{s-1}{s+1}, \quad N_{\text{mp}}(s) = \frac{1}{s+1}.$$

Then

$$\|W_2 N(X + MQ)\|_\infty = \|W_2 N_{\rm mp}(X + MQ)\|_\infty,$$

so an equivalent model-matching problem has $T_1 = W_2 N_{\rm mp} X$, $T_2 = -W_2 N_{\rm mp} M$, that is,

$$T_1(s) = \frac{(p+1)^2(s+0.1)}{(p-1)(s+1)^2}, \quad T_2(s) = -\frac{(s+0.1)(s-p)}{(s+1)^3}.$$

Since T_2 has only one zero in the right half-plane, namely, at $s = p$, the minimum model-matching error is (see Section 9.1)

$$\gamma_{\rm opt} = |T_1(p)| = \left|\frac{p+0.1}{p-1}\right|,$$

so

$$\epsilon_{\rm sup} = \left|\frac{p-1}{p+0.1}\right|.$$

The graph of $\epsilon_{\rm sup}$ versus p decreases monotonically as p approaches 1 from above or below. Thus less and less uncertainty can be tolerated as p approaches 1.

To proceed, let's take a particular value for p, say $p = 0.5$, for which $\epsilon_{\rm sup} = 0.8333$. The solution of the model-matching problem, $Q_{\rm im}$, satisfies

$$T_1 - T_2 Q_{\rm im} = T_1(p),$$

which yields

$$Q_{\rm im}(s) = -1.2\frac{(s+1)(s-1.25)}{s+0.1}.$$

Step 3 Set $\epsilon = 0.8$ (arbitrary) and

$$J(s) = \frac{1}{\tau s + 1}.$$

The value $\tau = 0.01$ gives

$$\|W_2 N(X + MQ_{\rm im} J)\|_\infty = 1.2396 < \frac{1}{\epsilon} = 1.25.$$

Step 4

$$Q(s) = -1.2\frac{(s+1)(s-1.25)}{(s+0.1)(0.01s+1)}$$

Step 5

$$C(s) = -\frac{(s+1)(124.5s^2 + 240.45s + 120)}{s^3 + 227.1s^2 + 440.7s + 220}$$

11.2 Conformal Mapping

For our treatment of optimal gain and phase margins, we need some preliminaries on conformal mapping.

Let $\mathcal{D}$ denote the open unit disk. Also, let $\mathcal{H}_+$ denote the open right half-plane. A well-known technique in signals and systems is to map $\mathcal{H}_+$ onto $\mathcal{D}$. One such mapping is

$$s \mapsto \frac{1-s}{1+s}.$$

This is a *conformal mapping*; that is, it is analytic in $\mathcal{H}_+$ and its inverse,

$$z \mapsto \frac{1-z}{1+z},$$

is analytic in $\mathcal{D}$. Because such a mapping exists, $\mathcal{H}_+$ and $\mathcal{D}$ are said to be *conformally equivalent*.

What proper subsets of $\mathbb{C}$ are conformally equivalent to $\mathcal{D}$? It turns out that the subsets need only be open and simply connected (i.e., have no holes)—for example, an annulus is not simply connected. This fact is known as the Riemann mapping theorem.

Example 1 Let $\mathcal{G}_1$ be the complement of the negative real axis,

$$\{s \in \mathbb{C} : s \text{ is real and } \leq 0\}.$$

It is easy to see that $\mathcal{G}_1$ is open and simply connected. We construct a conformal mapping $\phi_1 : \mathcal{G}_1 \to \mathcal{D}$ as the composition of two mappings:

$$\psi_1 : \mathcal{G}_1 \to \mathcal{H}_+, \qquad \psi_1(s) = \sqrt{s}$$

and

$$\psi_2 : \mathcal{H}_+ \to \mathcal{D}, \qquad \psi_2(s) = \frac{1-s}{1+s}.$$

Then

$$\phi_1(s) := \psi_2(\psi_1(s)) = \frac{1-\sqrt{s}}{1+\sqrt{s}}.$$

It is worth pointing out that conformal mappings are not unique, so the function ϕ_1 is just one possibility.

Example 2 Let a be a positive real number and let $\mathcal{G}_2$ be the complement of the horizontal ray from $-a$ left, that is, the complement of

$$\{s \in \mathbb{C} : s \text{ is real and } \leq -a\}.$$

The function

$$s \mapsto 1 + sa^{-1}$$

maps $\mathcal{G}_2$ conformally onto $\mathcal{G}_1$. Composing it with ϕ_1 gives

$$\phi_2(s) := \frac{1-\sqrt{1+sa^{-1}}}{1+\sqrt{1+sa^{-1}}},$$

a conformal mapping from $\mathcal{G}_2$ onto $\mathcal{D}$, taking 0 to 0.

Example 3 Let $a = a_1 + ja_2$ be a complex number in the first quadrant (i.e., $a_1, a_2 > 0$). Consider the two rays from a vertically up and from $\overline{a}$ vertically down; their union is the set

$$\{a + j\omega : \omega \geq 0\} \cup \{\overline{a} - j\omega : \omega \geq 0\}.$$

Let $\mathcal{G}_3$ denote the complement of this set. We construct a conformal mapping ϕ_3 from $\mathcal{G}_3$ onto $\mathcal{D}$ in several steps. First, the function $\psi_1(s) := s - a_1$ translates the rays to the imaginary axis. Second, $\psi_2(s) := js$ rotates them onto the real axis. Thus, $\psi_2 \circ \psi_1$ maps $\mathcal{G}_3$ conformally onto the complement of the set

$$\{s : s \in \mathbb{R}, |s| \geq a_2\}.$$

Third,

$$\psi_3(s) := \sqrt{\frac{1 - s/a_2}{1 + s/a_2}}$$

maps the latter set conformally onto $\mathcal{H}_+$. Now let's pause and see where 0 is mapped under $\psi_3 \circ \psi_2 \circ \psi_1$:

$$0 \mapsto -a_1 \mapsto -ja_1 \mapsto c,$$

where

$$c := \sqrt{\frac{1 + ja_1/a_2}{1 - ja_1/a_2}}.$$

Finally,

$$\psi_4(s) := \frac{s - c}{s + \overline{c}}$$

maps $\mathcal{H}_+$ onto $\mathcal{D}$. So a suitable ϕ_3 is

$$\phi_3 := \psi_4 \circ \psi_3 \circ \psi_2 \circ \psi_1.$$

It too takes 0 to 0.

The conformal mappings in Examples 2 and 3 both take 0 to 0, a property that will be needed in the applications to follow. This property makes them unique up to rotation. More precisely, suppose that $\mathcal{G}$ is an open, simply connected subset of $\mathbb{C}$, and ϕ_1 and ϕ_2 are two conformal mappings from $\mathcal{G}$ onto $\mathcal{D}$ taking 0 to 0; then there exists an angle α such that

$$\phi_1 = \mathrm{e}^{j\alpha}\phi_2$$

(i.e., ϕ_1 is a rotation of ϕ_2). Consequently, ϕ_1 and ϕ_2 have equal magnitudes at points of evaluation in $\mathcal{G}$; that is, for z in $\mathcal{G}$, $|\phi_i(z)|$ does not depend on the particular conformal mapping.

11.3 Gain Margin Optimization

This section continues with the robust stability problem, but now

$$\mathcal{P} = \{kP : 1 \leq k \leq k_1\}.$$

Here P is the nominal plant transfer function and k is a real gain that is uncertain and may lie anywhere in the interval $[1, k_1]$. (The family

$$\mathcal{P} = \{kP : k_0 \leq k \leq k_1\}, \quad 0 < k_0 < k_1$$

is only superficially more general; it can be reduced to the case $k_0 = 1$ by scaling.) We ask the question: How large can k_1 be but yet there exists a controller achieving internal stability for every plant in $\mathcal{P}$? Let $k_{\sup}$ denote the supremum such k_1. We'll get a formula for $k_{\sup}$ under the simplifying *assumption* that P has neither poles nor zeros on the imaginary axis.

It turns out that $k_{\sup}$ is closely related to the infimum norm of the (unweighted) complementary sensitivity function [see (11.2)],

$$\gamma_{\inf} := \inf_C \|T\|_\infty .$$

Of course, as in Section 11.1 this can be converted to a model-matching problem, an analysis of which will show that

1. $\gamma_{\inf} = 0$ if P is stable.
2. $\gamma_{\inf} = 1$ if P is unstable but minimum phase.
3. $\gamma_{\inf} > 1$ if P is unstable and non-minimum phase.

Theorem 1 *If P is stable or minimum phase, then $k_{\sup} = \infty$. Otherwise,*

$$k_{\sup} = \left(\frac{\gamma_{\inf} + 1}{\gamma_{\inf} - 1} \right)^2 .$$

Partial Proof A complete proof is fairly long, so parts will be omitted.

That $k_{\sup} = \infty$ when P is stable is trivial: Take the zero controller, $C = 0$. So we proceed under the assumption that P is unstable.

It suffices to show that there exists a C stabilizing kP for all $1 \le k \le k_1$ iff

$$k_1 < \left(\frac{\gamma_{\inf} + 1}{\gamma_{\inf} - 1} \right)^2$$

or equivalently iff

$$\gamma_{\inf} < \frac{\sqrt{k_1} + 1}{\sqrt{k_1} - 1}. \tag{11.5}$$

We will prove necessity, in three steps. Assume that such C exists.

Step 1 Since C stabilizes the nominal plant, P, it must have the form

$$C = \frac{X + MQ}{Y - NQ}$$

for some Q in $\mathcal{S}$. Fix $1 < k \le k_1$ and invoke Lemma 5.1: Since C stabilizes kP,

$$M(Y - NQ) + kN(X + MQ) \text{ is invertible in } \mathcal{S}.$$

This leads in turn to the following chain:

$$\begin{aligned}
& MY + kNX + (k-1)MNQ \text{ is invertible in } \mathcal{S} \\
\Rightarrow\ & (1 - NX) + kNX + (k-1)MNQ \text{ is invertible in } \mathcal{S} \\
\Rightarrow\ & 1 + (k-1)N(X + MQ) \text{ is invertible in } \mathcal{S} \\
\Rightarrow\ & \frac{1}{k-1} + N(X + MQ) \text{ is invertible in } \mathcal{S}.
\end{aligned}$$

Let $\overline{\mathcal{H}_+}$ denote the closed right half-plane together with the point at infinity. We conclude that the function $N(X+MQ)$ maps $\overline{\mathcal{H}_+}$ into the complement of the single point $-1/(k-1)$. Since this holds for all $1 < k \leq k_1$, $N(X+MQ)$ maps $\overline{\mathcal{H}_+}$ into the complement of the set

$$\{s \in \mathbb{C} : s \text{ is real and } \leq -a\}, \qquad a := \frac{1}{k_1 - 1}.$$

Let $\mathcal{G}$ denote this complement.

Note that $N(X+MQ)$ equals T, the complementary sensitivity function corresponding to P and C. It follows that T satisfies certain interpolation conditions [see equation (6.2)]. Let $\{p_i\}$ and $\{z_i\}$ denote the right half-plane poles and zeros of P; for simplicity, these are assumed to be distinct. Then

$$T(p_i) = 1, \quad T(z_i) = 0.$$

Step 2 As in Example 2 of the preceding section, bring in a conformal mapping from $\mathcal{G}$ onto the open unit disk, $\mathcal{D}$:

$$\phi(s) := \frac{1 - \sqrt{1 + sa^{-1}}}{1 + \sqrt{1 + sa^{-1}}}.$$

Define the function $G = \phi \circ T$. From the properties of T we get that G maps $\overline{\mathcal{H}_+}$ into $\mathcal{D}$ and

$$G(p_i) = \phi(1), \quad G(z_i) = \phi(0) = 0.$$

Step 3 The final step is to scale G: Define

$$H := \frac{1}{\phi(1)} G.$$

Then H maps $\overline{\mathcal{H}_+}$ into the disk of radius $1/|\phi(1)|$ [i.e., $\|H\|_\infty < 1/|\phi(1)|$] and

$$H(p_i) = 1, \quad H(z_i) = 0.$$

The function H is analytic in $\mathcal{H}_+$, but not necessarily real-rational because ϕ does not preserve rationality. Nevertheless, it can be proved that there exists a function, say K, which is real-rational and has the foregoing properties of H.

We can conclude that there exists a function K in $\mathcal{S}$ having the properties

$$\|K\|_\infty < \frac{1}{|\phi(1)|}, \tag{11.6}$$

$$K(p_i) = 1, \quad K(z_i) = 0.$$

These properties in turn imply that K is a complementary sensitivity function for some controller; that is, $K = N(X + MQ_1)$ for some Q_1 in $\mathcal{S}$. But then from (11.6)

$$\gamma_{\text{inf}} < \frac{1}{|\phi(1)|}.$$

It remains to compute that

$$\phi(1) = \frac{1 - \sqrt{k_1}}{1 + \sqrt{k_1}}.$$

This proves (11.5).

Notice that $k_{\sup}$ equals the value of k_1 satisfying the equation

$$\gamma_{\inf} = \frac{1}{|\phi(1)|}. \blacksquare$$

The following procedure gives a way to compute a controller that achieves an upper gain margin of k_1, any number less than $k_{\sup}$. The idea is to reverse the argument in the proof above. At a high level, the procedure is as follows:

1. Solve the model-matching problem corresponding to $\inf \|T\|_\infty$; let the solution be Q_{im}.
2. Get a suitable roll-off function J.
3. Let K be the complementary sensitivity function corresponding to the controller parameter $Q_{\text{im}}J$.
4. Set $G = \phi(1)K$.
5. Solve $G = \phi \circ T$ for T, which will be the resulting complementary sensitivity function.
6. Solve $T = N(X + MQ)$ for Q.
7. Set $C = (X + MQ)/(Y - NQ)$.

Procedure: P Unstable, Non-minimum Phase, No Imaginary Axis Poles or Zeros

Input: P

Step 1 Do a coprime factorization of P:

$$P = \frac{N}{M}, \quad NX + MY = 1.$$

Step 2 Solve the model-matching problem for $T_1 = NX$, $T_2 = -NM$. Let Q_{im} denote its solution and let γ_{opt} denote the minimum model-matching error. Then

$$k_{\sup} = \left(\frac{\gamma_{\text{opt}} + 1}{\gamma_{\text{opt}} - 1}\right)^2.$$

Step 3 Let k_1 be arbitrary with $1 < k_1 < k_{\sup}$. Set

$$J(s) := \frac{1}{(\tau s + 1)^k},$$

where k is just large enough that $Q_{\text{im}}J$ is proper and τ is just small enough that

$$\|N(X + MQ_{\text{im}}J)\|_\infty < \frac{\sqrt{k_1} + 1}{\sqrt{k_1} - 1}.$$

Step 4 Set

$$\begin{aligned} K &= N(X + MQ_{\text{im}}J), \\ G &= \frac{1-\sqrt{k_1}}{1+\sqrt{k_1}}K, \\ T &= \frac{1}{k_1 - 1}\left[\left(\frac{1-G}{1+G}\right)^2 - 1\right], \\ Q &= \frac{T - NX}{NM}. \end{aligned}$$

Step 5 Set $C = (X + MQ)/(Y - NQ)$.

Example Consider the plant

$$P(s) = \frac{s-1}{(s+1)(s-p)}, \quad 0 < p \neq 1,$$

which was studied in Section 11.1. The procedure above goes like this:

Step 1

$$\begin{aligned} N(s) &= \frac{s-1}{(s+1)^2} \\ M(s) &= \frac{s-p}{s+1} \\ X(s) &= \frac{(p+1)^2}{p-1} \\ Y(s) &= \frac{s-(p+3)/(p-1)}{s+1} \end{aligned}$$

Step 2 Factor N as $N = N_{\text{ap}}N_{\text{mp}}$ with

$$N_{\text{ap}}(s) = \frac{s-1}{s+1}, \quad N_{\text{mp}}(s) = \frac{1}{s+1}.$$

Then

$$\|N(X + MQ)\|_\infty = \|N_{\text{mp}}(X + MQ)\|_\infty,$$

so an equivalent model-matching problem has $T_1 = N_{\text{mp}}X$, $T_2 = -N_{\text{mp}}M$, that is,

$$T_1(s) = \frac{(p+1)^2}{(p-1)(s+1)}, \quad T_2(s) = -\frac{s-p}{(s+1)^2}.$$

Thus

$$\gamma_{\text{opt}} = |T_1(p)| = \left|\frac{p+1}{p-1}\right|$$

and

$$k_{\text{sup}} = \left(\frac{p+1+|p-1|}{p+1-|p-1|}\right)^2 = \begin{cases} p^2, & p \geq 1 \\ p^{-2}, & p < 1. \end{cases}$$

As with $\epsilon_{\sup}$, this function has its minimum at $p = 1$.

To proceed, let's take $p = 2$ (arbitrary), for which $k_{\sup} = 4$. The solution of the model-matching problem, $Q_{\rm im}$, satisfies

$$T_1 - T_2 Q_{\rm im} = T_1(p),$$

which yields

$$Q_{\rm im}(s) = 3(s+1).$$

Step 3 Set $k_1 = 3.5$ (arbitrary) and

$$J(s) = \frac{1}{\tau s + 1}.$$

The value $\tau = 0.01$ gives

$$\|N(X + MQ_{\rm im}J)\|_\infty = 3.0827 < \frac{\sqrt{k_1}+1}{\sqrt{k_1}-1} = 3.2967.$$

Step 4

$$\begin{aligned}
K(s) &= 3\frac{(s-1)(1.03s+1)}{(s+1)^2(0.01s+1)} \\
G(s) &= -0.9100\frac{(s-1)(1.03s+1)}{(s+1)^2(0.01s+1)} \\
T(s) &= \frac{0.0375s^5 + 3.8231s^4 + 7.3882s^3 - 0.1831s^2 - 7.4257s - 3.64}{0.0003s^6 + 0.0041s^5 + 0.1190s^4 + 0.9378s^3 + 11.1662s^2 + 19.4563s + 9.1204} \\
Q(s) &= \frac{0.0352s^4 + 3.9357s^3 + 22.1648s^2 + 59.8368s + 41.5724}{0.0003s^4 + 0.0036s^3 + 0.1116s^2 + 0.7175s + 9.6670}
\end{aligned}$$

11.4 Phase Margin Optimization

Now the family of plants to be stabilized is

$$\mathcal{P} = \left\{ \mathrm{e}^{-j\theta} P : -\theta_1 \le \theta \le \theta_1 \right\},$$

where P is the nominal plant transfer function and θ is an uncertain phase lying anywhere in the interval $[-\theta_1, \theta_1]$; θ_1 is an angle in $(0, \pi]$. Let $\theta_{\sup}$ denote the supremum θ_1 for which there exists a stabilizing controller. Under the *assumption* that P has neither poles nor zeros on the imaginary axis, a formula can be derived for $\theta_{\sup}$ in terms of $\gamma_{\inf} := \inf \|T\|_\infty$ just as in the preceding section.

Theorem 2 *If P is stable or minimum phase, then $\theta_{\sup} = \pi$. Otherwise,*

$$\theta_{\sup} = 2\sin^{-1}\frac{1}{\gamma_{\inf}}.$$

Proof The proof of Theorem 1 can be adapted with a few alterations by starting with $k = \mathrm{e}^{-j\theta}$. Again, the case that P is stable is trivial.

First, in Step 1 the appropriate set $\mathcal{G}$ is the complement of

$$\left\{ -\frac{1}{k-1} : k = \mathrm{e}^{-j\theta}, -\theta_1 \le \theta \le \theta_1 \right\}.$$

The latter set is the union of the vertical rays from

$$a = a_1 + ja_2 := \frac{1}{2} + j\frac{\sin\theta_1}{1-\cos\theta_1}$$

up and from $\overline{a}$ down. Second, in Step 2, from Example 3 of the preceding section a conformal mapping from $\mathcal{G}$ onto $\mathcal{D}$ is

$$\phi = \psi_4 \circ \psi_3 \circ \psi_2 \circ \psi_1,$$

where

$$\begin{aligned}
\psi_1(s) &= s - \frac{1}{2}, \\
\psi_2(s) &= js, \\
\psi_3(s) &= \sqrt{\frac{1 - s/a_2}{1 + s/a_2}}, \\
\psi_4(s) &= \frac{s-c}{s+\overline{c}}, \\
c &= \sqrt{\frac{1 + j/(2a_2)}{1 - j/(2a_2)}}.
\end{aligned}$$

Finally, as in the last sentence in the proof of Theorem 1, $\theta_{\sup}$ equals the value of θ_1 satisfying the equation

$$\gamma_{\inf} = \frac{1}{|\phi(1)|}.$$

So it remains to show that

$$|\phi(1)| = \sin\frac{\theta_1}{2}.$$

Elementary computations give

$$\phi(1) = -\frac{\mathrm{Im}c}{\overline{c}}, \quad |\phi(1)| = \sin\frac{\theta_1}{2}. \ \blacksquare$$

Example Consider once again the plant

$$P(s) = \frac{s-1}{(s+1)(s-p)}, \quad 0 < p \ne 1.$$

We found in the preceding section that

$$\gamma_{\inf} = \left| \frac{p+1}{p-1} \right|.$$

Therefore,

$$\theta_{\sup} = 2\sin^{-1}\left| \frac{p-1}{p+1} \right|.$$

Exercises

1. Compute ϵ_{sup} for
$$P(s) = \frac{s-1}{(s-2)(s-3)}, \quad W_2(s) = \frac{s+1}{s+100}.$$
Select some $\epsilon < \epsilon_{\text{sup}}$ and compute a robust controller.

2. Take
$$P(s) = \frac{1}{s-1}, \quad W_2(s) = \frac{as}{0.01s+1},$$
with a a positive number. Compute the least upper bound on a for which robust stability is achievable. Pick some a less than this upper bound and design a robust controller.

3. With $\gamma_{\text{inf}} = \inf \|T\|_\infty$ and P having neither poles nor zeros on the imaginary axis, prove

   $\gamma_{\text{inf}} = 0$ if P is stable,

   $\gamma_{\text{inf}} = 1$ if P is unstable but minimum phase,

   $\gamma_{\text{inf}} > 1$ if P is unstable and non-minimum phase.

4. Compute the maximum gain margin k_{sup} for
$$P(s) = \frac{s-1}{(s-2)(s-3)}.$$
Select some $k_1 < k_{\text{sup}}$ and compute a robust controller.

5. Repeat the Exercise 4 but for phase margin.

6. Recall from Section 4.2 that $1/\|S\|_\infty$ equals the distance from the critical point -1 to the nearest point on the Nyquist plot of PC, and in this way qualifies as a stability margin. The smaller $\|S\|_\infty$, the larger the stability margin. Compute $\inf \|S\|_\infty$ for the plant in Exercise 4.

7. Using the equation
$$W_2N(X + MQJ) = W_2N(X + MQ)J + W_2NX(1 - J),$$
prove that γ_{inf} in (11.3) and γ_{opt} in (11.4) are equal.

Notes and References

The problem in Section 11.1 was first solved by Kimura (1984). The gain margin problem was first solved by Tannenbaum (1980, 1981) using Nevanlinna-Pick theory. Khargonekar and Tannenbaum (1985) showed the mathematical equivalence of the problems of gain margin optimization, sensitivity minimization, and robust stabilization. Yan and Anderson (1990) considered a problem that mixes performance and gain margin.

Design for Robust Performance

This chapter presents a mathematical technique for designing a controller to achieve robust performance. Chapter 7 proposed loopshaping as a graphical method when P and P^{-1} are stable. Without these assumptions loopshaping is very awkward and the methodical procedure in this chapter can be used.

12.1 The Modified Problem

As defined in Section 4.3, the robust performance problem is to design a proper controller C so that the feedback system for the nominal plant is internally stable and the inequality

$$\| |W_1 S| + |W_2 T| \|_\infty < 1 \tag{12.1}$$

holds. Also as mentioned in Chapter 7, the exact problem as just stated remains unsolved. So we look for a nearby problem that is solvable.

We seek to replace inequality (12.1) with a tractable one. Fix a frequency and define $x := |W_1 S|$ and $y := |W_2 T|$. The region in the (x, y)-plane where $x + y < 1$ is the right-angle triangle shown here:

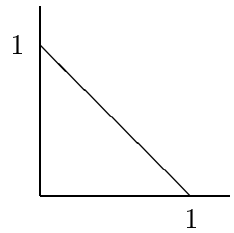

By imagining the circle with center 0, radius $1/\sqrt{2}$ you can see that

$$x^2 + y^2 < 1/2 \quad \Rightarrow \quad x + y < 1.$$

Thus a sufficient condition for (12.1) is

$$\| |W_1 S|^2 + |W_2 T|^2 \|_\infty < \frac{1}{2}. \tag{12.2}$$

In this way we arrive at the *modified robust performance problem*: Find a proper, internally stabilizing C so that (12.2) holds. This problem is a compromise; it is not exactly the problem we

would like to solve, but it is nearby and has the desirable feature of being solvable without too much difficulty.

We will solve the modified problem under the following assumptions:

1. P is strictly proper and has neither poles nor zeros on the imaginary axis.
2. W_1 and W_2 are stable and proper.
3. W_1 and W_2 have no common zeros on the imaginary axis.

Some of these assumptions could be relaxed, but with an increase in messiness.

We'll need an additional tool, covered in the next section.

12.2 Spectral Factorization

For a rational function $F(s)$ with real coefficients, let $\overline{F}$ denote the function $F(-s)$. Thus

$$\overline{F}(j\omega) = F(-j\omega) = \overline{F(j\omega)}.$$

We saw in Lemma 6.2 that, provided $F \in \mathcal{S}$, it has a factorization of the form $F = F_{\rm ap}F_{\rm mp}$. All the right half-plane zeros go into the all-pass factor, and the ones in the left half-plane or on the imaginary axis go into the minimum-phase factor. The all-pass factor has the property $\overline{F_{\rm ap}}(s)F_{\rm ap}(s) = 1$.

There is a related factorization if F has the property $\overline{F} = F$ and no zeros or poles on the imaginary axis. This means that the zeros of F form a pattern that is symmetrical with respect to both the real and imaginary axes. To see this, simply note that if z is a zero, so is $-z$ because $F(s) = F(-s)$. It follows that for every zero z in the right half-plane, the numerator of F is divisible by

$$(z - s)(z + s).$$

Similarly for the poles. Hence we can write F in terms of its gain, poles, and zeros like this:

$$F(s) = cF_1(s), \quad F_1(s) = \frac{\prod(z_i - s)(z_i + s)}{\prod(p_i - s)(p_i + s)}.$$

Note that $\{z_i\}$ and $\{p_i\}$ are the right half-plane zeros and poles. Note also that $F_1(0) > 0$. From F_1 form a function G by selecting only the factors corresponding to zeros and poles in $\mathrm{Re}s < 0$, that is,

$$G(s) := \frac{\prod(z_i + s)}{\prod(p_i + s)}.$$

Then G and G^{-1} are stable. The zeros and poles of F_1 in the right half-plane are absorbed into the function $\overline{G}$ and we have the factorization

$$F = \overline{G}cG \text{ with } G, G^{-1} \text{ stable.}$$

Finally, if $c > 0$, we define F_{sf} as

$$F_{sf}(s) := \sqrt{c}\frac{\prod(z_i + s)}{\prod(p_i + s)}$$

to get $F = \overline{F_{sf}}F_{sf}$. Since $F_1(0) > 0$, $c > 0$ iff $F(0) > 0$.

The function F_{sf}—which is like a square root of $F(s)$—therefore has the properties

$$F = \overline{F_{sf}} F_{sf} \text{ with } F_{sf}, F_{sf}^{-1} \text{ stable}$$

and is called a *spectral factor* of F. This factorization of F is called a *spectral factorization.*

An alternative characterization of the condition $\overline{F} = F$ is this: $\overline{F} = F$ iff F is a rational function in s^2.

The above is summarized as follows.

Lemma 1 *If the real-rational function F has the properties $\overline{F} = F$, no zeros or poles on the imaginary axis, and $F(0) > 0$, then it has a spectral factorization.*

Example 1 The function

$$F(s) = \frac{1}{1 - s^2}$$

can be factored as

$$F(s) = \frac{1}{1-s}\frac{1}{1+s},$$

so a suitable spectral factor is $F_{sf}(s) = 1/(1+s)$. So is $-1/(1+s)$.

Example 2 Consider the function

$$F(s) = 10\frac{4 - s^2}{25 + 6s^2 + s^4}.$$

Its poles are $\pm 1 \pm 2j$ and its zeros are ± 2. The function G is therefore

$$G(s) = \frac{2+s}{(1+2j+s)(1-2j+s)} = \frac{2+s}{5+2s+s^2}.$$

So a spectral factor is

$$F_{sf}(s) = \sqrt{10}\frac{2+s}{5+2s+s^2}.$$

Example 3 The function

$$F(s) = \frac{2s^2 - 1}{s^4 - s^2 + 1}$$

has no spectral factorization because $F(0) < 0$.

12.3 Solution of the Modified Problem

The solution of the modified problem involves transforming it into the model-matching problem of Chapter 9. Since this transformation is a little involved, it is worth describing it first on a high level, as follows.

1. We use the by now familiar factorization of all internally stabilizing controllers from Theorem 5.2. Factorize P:

$$P = \frac{N}{M}, \quad NX + MY = 1, \quad N, M, X, Y \in \mathcal{S}.$$

The formula for C is

$$C = \frac{X + MQ}{Y - NQ}, \quad Q \in \mathcal{S}.$$

In terms of Q we have

$$S = M(Y - NQ), \quad T = N(X + MQ).$$

So the modified problem reduces to this: find Q in $\mathcal{S}$ such that

$$\| |W_1 M(Y - NQ)|^2 + |W_2 N(X + MQ)|^2 \|_\infty < \frac{1}{2}. \tag{12.3}$$

Let's simplify notation by defining

$$\begin{aligned} R_1 &:= W_1 MY, \quad S_1 := W_2 NX, \\ R_2 &:= W_1 MN, \quad S_2 := -W_2 MN. \end{aligned}$$

so that (12.3) becomes

$$\| |R_1 - R_2 Q|^2 + |S_1 - S_2 Q|^2 \|_\infty < \frac{1}{2}. \tag{12.4}$$

2. Inequality (12.4) involves the sum of two squares in Q. To get closer to the model-matching problem we shall transform (12.4) so that only one square in Q appears, that is, transform it into

$$\| |U_1 - U_2 Q|^2 + U_3 \|_\infty < \frac{1}{2} \tag{12.5}$$

for suitable functions U_i, $i = 1, 2, 3$. The first two, U_1 and U_2, will belong to $\mathcal{S}$, while U_3 will be real-rational with the property $\overline{U_3} = U_3$.

3. In what follows we shall drop $j\omega$ and also introduce U_4, a spectral factor of $\frac{1}{2} - U_3$:

$$\begin{aligned} (12.5) \quad &\Leftrightarrow \quad |U_1 - U_2 Q|^2 + U_3 < \frac{1}{2}, \quad \forall \omega \\ &\Leftrightarrow \quad |U_1 - U_2 Q|^2 < \frac{1}{2} - U_3, \quad \forall \omega \\ &\Leftrightarrow \quad |U_1 - U_2 Q|^2 < |U_4|^2, \quad \forall \omega \\ &\Leftrightarrow \quad |U_4^{-1} U_1 - U_4^{-1} U_2 Q|^2 < 1, \quad \forall \omega \\ &\Leftrightarrow \quad \|U_4^{-1} U_1 - U_4^{-1} U_2 Q\|_\infty < 1. \end{aligned}$$

So the final model-matching problem is to find a Q in $\mathcal{S}$ satisfying

$$\|U_4^{-1} U_1 - U_4^{-1} U_2 Q\|_\infty < 1.$$

Now for the details. For equivalence of (12.4) and (12.5) it suffices to have the following equation hold:

$$(\overline{R_1} - \overline{R_2 Q})(R_1 - R_2 Q) + (\overline{S_1} - \overline{S_2 Q})(S_1 - S_2 Q) = (\overline{U_1} - \overline{U_2 Q})(U_1 - U_2 Q) + U_3.$$

Multiply all factors out and collect terms. The result is an identity in Q provided that the following three equations hold:

$$\begin{aligned} \overline{R_2}R_2 + \overline{S_2}S_2 &= \overline{U_2}U_2, && (12.6)\\ \overline{R_2}R_1 + \overline{S_2}S_1 &= \overline{U_2}U_1, && (12.7)\\ \overline{R_1}R_1 + \overline{S_1}S_1 &= \overline{U_1}U_1 + U_3. && (12.8) \end{aligned}$$

The idea is to get U_1 and U_2 satisfying (12.6) and (12.7), and then to get U_3 from (12.8). In fact, we can solve for U_3 right away:

$$U_3 = \frac{\overline{W_1}W_1\overline{W_2}W_2}{\overline{W_1}W_1 + \overline{W_2}W_2}. \qquad (12.9)$$

Proof From (12.7) we have

$$U_1 = \frac{\overline{R_2}R_1 + \overline{S_2}S_1}{\overline{U_2}}$$

and hence

$$\overline{U_1}U_1 = \frac{(\overline{R_1}R_2 + \overline{S_1}S_2)(R_1\overline{R_2} + S_1\overline{S_2})}{\overline{U_2}U_2}.$$

Substituting from (12.6) in the denominator gives

$$\overline{U_1}U_1 = \frac{(\overline{R_1}R_2 + \overline{S_1}S_2)(R_1\overline{R_2} + S_1\overline{S_2})}{\overline{R_2}R_2 + \overline{S_2}S_2}.$$

Using this in (12.8) gives

$$U_3 = \overline{R_1}R_1 + \overline{S_1}S_1 - \frac{(\overline{R_1}R_2 + \overline{S_1}S_2)(R_1\overline{R_2} + S_1\overline{S_2})}{\overline{R_2}R_2 + \overline{S_2}S_2}.$$

Finally, substitute into this the definitions of R_i and S_i and simplify to get (12.9). ■

Now we turn to the solution of (12.6) and (12.7). We want solutions U_1 and U_2 in $\mathcal{S}$. To see what is involved, let us look at an example.

Example 1 Suppose that

$$\begin{aligned} R_1(s) &= \frac{1}{2+s}, \quad S_1(s) = 0,\\ R_2(s) &= \frac{1}{1+s}, \quad S_2(s) = 1. \end{aligned}$$

Then equations (12.6) and (12.7) are

$$\begin{aligned} \frac{(\sqrt{2}-s)(\sqrt{2}+s)}{(1-s)(1+s)} &= \overline{U_2}(s)U_2(s), && (12.10)\\ \frac{1}{(1-s)(2+s)} &= \overline{U_2}(s)U_1(s). && (12.11) \end{aligned}$$

To satisfy (12.10), an obvious choice is the spectral factor

$$U_2(s) = \frac{\sqrt{2}+s}{1+s}.$$

But then (12.11) has the unique solution

$$U_1(s) = \frac{1}{(2+s)(\sqrt{2}-s)},$$

which is unsatisfactory, not being in $\mathcal{S}$. So as a solution of (12.10) let us take

$$U_2(s) = \frac{\sqrt{2}+s}{1+s}V(s),$$

where V is an all-pass function, as yet unknown. Again, the solution of (12.11) is

$$U_1(s) = \frac{1}{(2+s)(\sqrt{2}-s)}V(s).$$

So to get U_1 in $\mathcal{S}$ we should let V have a zero at $s = \sqrt{2}$, for example,

$$V(s) = \frac{\sqrt{2}-s}{\sqrt{2}+s}.$$

The following procedure yields functions U_1 and U_2 in $\mathcal{S}$ satisfying (12.6) and (12.7).

Procedure A

Input: R_1, R_2, S_1, S_2

Step 1 Set $F := \overline{R_2}R_2 + \overline{S_2}S_2$. Comment: F has no zeros or poles on the imaginary axis, $\overline{F} = F$, and $F(0) > 0$.

Step 2 Compute a spectral factor F_{sf} of F.

Step 3 Choose an all-pass function V such that

$$\frac{\overline{R_2}R_1 + \overline{S_2}S_1}{\overline{F_{sf}}}V \in \mathcal{S}.$$

Step 4 Set

$$U_1 := \frac{\overline{R_2}R_1 + \overline{S_2}S_1}{\overline{F_{sf}}}V, \quad U_2 := F_{sf}V.$$

Finally, the following procedure solves the modified robust performance problem.

Procedure B

Input: P, W_1, W_2

Step 1 Compute

$$U_3 = \frac{\overline{W_1}W_1\overline{W_2}W_2}{\overline{W_1}W_1 + \overline{W_2}W_2}.$$

Check if $\|U_3\|_\infty < \frac{1}{2}$, that is,

$$\left\| \frac{|W_1W_2|^2}{|W_1|^2 + |W_2|^2} \right\|_\infty < \frac{1}{2}.$$

If so, continue. If not, the problem is not solvable; stop.

Step 2 Coprime factorization of P:

$$P = \frac{N}{M}, \quad NX + MY = 1.$$

Step 3 Set

$$R_1 := W_1MY, \quad S_1 := W_2NX,$$
$$R_2 := W_1MN, \quad S_2 := -W_2MN.$$

Step 4 Apply Procedure A to get U_1 and U_2.

Step 5 Compute a spectral factor U_4 of $\frac{1}{2} - U_3$.

Step 6 Set $T_1 := U_4^{-1}U_1$ and $T_2 := U_4^{-1}U_2$. Comment: $T_1, T_2 \in \mathcal{S}$ and T_2 has no zeros on the imaginary axis.

Step 7 Compute γ_{opt}, the minimum model-matching error. If $\gamma_{\text{opt}} < 1$, continue. If $\gamma_{\text{opt}} \geq 1$, the modified robust performance problem is not solvable; stop.

Step 8 Compute Q, the solution to the model-matching problem. If Q is not proper, roll it off at a sufficiently high frequency while maintaining $\|T_1 - T_2Q\|_\infty < 1$.

Step 9 Set

$$C = \frac{X + MQ}{Y - NQ}.$$

The purpose of the next example is solely to illustrate the procedures above. It should be emphasized that the plant is very simple and the design could more easily be done using loopshaping.

Example 2 Take

$$P(s) = \frac{1}{s+1}, \quad W_1(s) = \frac{a}{s+1}, \quad W_2(s) = \frac{0.02s}{0.01s+1}.$$

The positive constant a is left unspecified at this point. In fact we will find the largest a for which the modified robust performance problem is solvable.

Step 1

$$U_3(s) = -\frac{0.0004a^2s^2}{a^2 - (0.0001a^2 + 0.0004)s^2 + 0.0004s^4}$$

The ∞-norm of U_3 is computed for selected values of a:

a	Norm
50	0.4444
52	0.4601
54	0.4757
56	0.4912
58	0.5064
60	0.5217

By interpolation, the supremum value of a for which $\|U_3\|_\infty < 1/2$ is about 57.2.

Step 2 $N = P, M = 1, X = 0, Y = 1$

Step 3

$$R_1(s) = \frac{a}{s+1}, \quad R_2(s) = \frac{a}{(s+1)^2}, \quad S_1(s) = 0, \quad S_2(s) = -\frac{0.02s}{(s+1)(0.01s+1)}$$

Step 4 Procedure A:

Step 1

$$F(s) = \frac{a^2 - (0.0001a^2 + 0.0004)s^2 + 0.0004s^4}{(1-s)^2(1+s)^2(1-0.01s)(1+0.01s)}$$

Step 2

$$F_{sf}(s) = \frac{a + bs + 0.02s^2}{(1+s)^2(1+0.01s)}$$

$$b := (0.0001a^2 + 0.04a + 0.0004)^{1/2}$$

Step 3

$$V(s) = \frac{a - bs + 0.02s^2}{a + bs + 0.02s^2}$$

Step 4

$$U_1(s) = a^2 \frac{1 - 0.01s}{(1+s)(a + bs + 0.02s^2)}, \quad U_2(s) = \frac{a - bs + 0.02s^2}{(1+s)^2(1+0.01s)}$$

Step 5

$$U_4(s) = \frac{a + cs + 0.02s^2}{\sqrt{2}(a + bs + 0.02s^2)}$$

$$c := (-0.0007a^2 + 0.04a + 0.0004)^{1/2}$$

Step 6

$$\begin{aligned} T_1(s) &= \sqrt{2}a^2 \frac{1 - 0.01s}{(1+s)(a + cs + 0.02s^2)} \\ T_2(s) &= \sqrt{2} \frac{(a + bs + 0.02s^2)(a - bs + 0.02s^2)}{(a + cs + 0.02s^2)(1+s)^2(1+0.01s)} \end{aligned}$$

Step 7 γ_{opt} is computed for selected values of a:

a	γ_{opt}
36	0.9381
37	0.9560
38	0.9742
39	0.9928
40	1.0118

So $a = 39$ is feasible, while $a = 40$ is not. Let's proceed with $a = 36$.

Step 8 The solution to the model-matching problem is

$$Q_{im}(s) = \frac{0.3317s^4 + 55.19s^3 + 2838s^2 + 64215s + 61432}{s^3 + 97.42s^2 + 3978s + 62585}.$$

This must be rolled off: Set

$$Q(s) = Q_{im}(s)\frac{1}{\tau s + 1}.$$

The value $\tau = 0.0009$ yields $\|T_1 - T_2Q\|_\infty = 0.9996$, and is therefore satisfactory.

Step 9 $C = Q/(1 - PQ)$.

The resulting Bode plots are displayed in Figure 12.1.

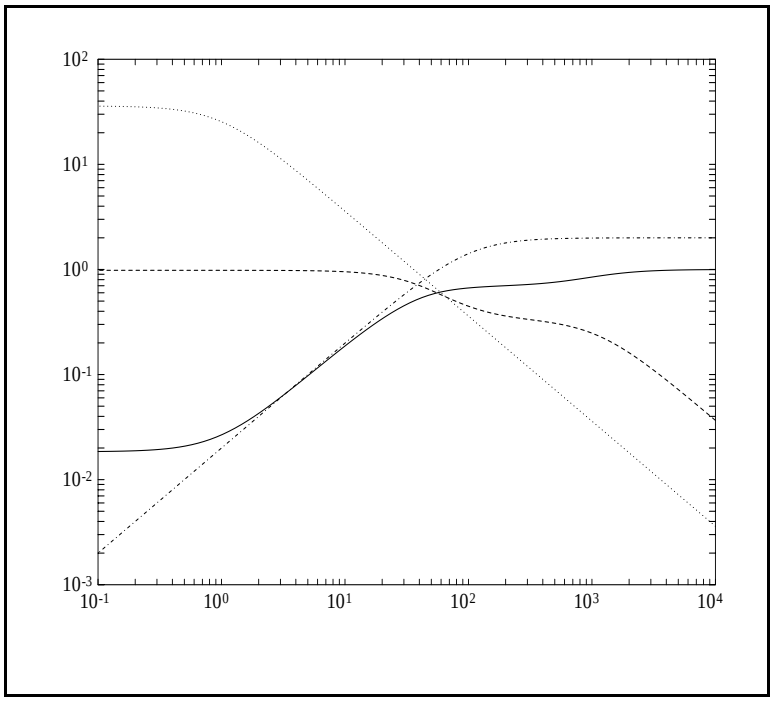

Figure 12.1: Bode plot of $|S|$ (solid), $|T|$ (dash), $|W_1|$ (dot), and $|W_2|$ (dot-dash).

12.4 Design Example: Flexible Beam Continued

In the preceding section we presented a procedure for designing a controller to achieve a tradeoff between S and T. The procedure has some appeal pedagogically, being elementary and based in

the frequency domain. However, it must be admitted that it would not be suitable even for a medium-sized problem because computations with rational functions are clumsy and numerically sensitive. Modern software for control system design is based on state-space methods, the theory behind which is beyond the scope of this book. One such software package is MATLAB with the μ-Tools Toolbox. In this section we continue the flexible beam example begun in Section 10.3. The actual computations were performed using MATLAB, so only the results are reported. Our main purpose in including this example is to discuss further the issue of weights selection, in particular, the choice of weights for time-domain specs.

Recall that the transfer function for the plant is

$$P(s) = \frac{-6.4750s^2 + 4.0302s + 175.7700}{s(5s^3 + 3.5682s^2 + 139.5021s + 0.0929)}.$$

The plant input is a voltage to a power amplifier and the output is the tip deflection of the beam. The performance specs in Section 10.3 were in terms of the unit step response:

$$\begin{aligned} \text{settling time} &\approx 8 \text{ s}, \\ \text{overshoot} &\leq 10\%. \end{aligned}$$

Using the performance weight

$$W_1(s) = \frac{0.9}{1.0210} \frac{s^2 + 1.2s + 1}{(s + 0.001)(s + 1.2)(0.001s + 1)},$$

we designed a controller achieving these two specs.

In this section we place an additional constraint, namely, an amplitude constraint on the plant input:

$$|u(t)| \leq 0.5, \quad \forall t. \tag{12.12}$$

This reflects the fact that the power amplifier will saturate if its input is outside this range. The Section 10.3 design violates this spec, the signal $u(t)$ exhibiting a very large surge over the time interval $[0, 0.03]$. No frequency-domain design procedure can treat a specification like (12.12) precisely: An amplitude bound in the time domain does not translate over precisely to anything tractable in the frequency domain. So we have to be content with a trial-and-error procedure.

Intuitively, we may have to relax the step-response spec in order to achieve (12.12); this means decreasing the gain of W_1. So let us take

$$W_1(s) = a \frac{s^2 + 1.2s + 1}{(s + 0.001)(s + 1.2)(0.001s + 1)},$$

where a is a design parameter.

The transfer function from reference input r to plant input u is CS (not T). So to achieve (12.12) it makes sense to introduce a new weight, W_3, and associated modified criterion,

$$\| |W_1 S|^2 + |W_3 CS|^2 \|_\infty < 1. \tag{12.13}$$

Although this is different from the criterion in Section 12.3, it can be handled in exactly the same way—the changes are obvious; for example, whereas in Section 12.3 we had

$$W_2 T = W_2 N(X + MQ),$$

we now have

$$W_3CS = W_3M(X + MQ).$$

The observation above, that $u(t)$ exhibits an initial large surge, suggests penalizing high-frequency control actuation by taking W_3 to be a high-pass filter, of the form

$$W_3(s) = b\frac{s + 0.01c}{s + c}.$$

The constant c was taken to be $c = 1/0.03 = 33.3$ rad/s, corresponding to the surge interval $[0, 0.03]$.

We are left with the two parameters a and b in the weights: The larger the value of a, the better the step response; the larger the value of b, the larger the penalty on control. These parameters were determined by the following iterative procedure:

1. Set $a = 0.9/1.0210$, the value for the previous design.
2. Decrease b from some starting value until (12.13) is achievable by some controller. Obtain such a controller and do a step-response simulation. Check if the specs are satisfied.
3. If necessary, decrease a and repeat Step 2.

The values $a = 0.8$, $b = 1$ were obtained, and the corresponding controller has numerator

$$1.424s^7 + 9.076 \times 10^2 s^6 + 3.141 \times 10^4 s^5 + 1.117 \times 10^5 s^4 + 9.073 \times 10^5 s^3$$

$$+1.961 \times 10^6 s^2 + 1.306 \times 10^3 s + 0.01406$$

and denominator

$$s^8 + 1.013 \times 10^3 s^7 + 1.326 \times 10^4 s^6 + 1.129 \times 10^5 s^5 + 6.326 \times 10^5 s^4$$

$$+2.348 \times 10^6 s^3 + 4.940 \times 10^6 s^2 + 3.440 \times 10^6 s + 3.435 \times 10^3.$$

The order of the controller (8) equals the sum of the orders of P, W_1, and W_3. Figure 12.2 shows the resulting Bode plots and Figure 12.3 the step responses. The specs have been met.

It is interesting to compare the step response of y in Figure 12.3 with the step response in Figure 10.3, where the control input was unconstrained: The former exhibits a pronounced initial time lag, evidently the price paid for constrained control.

Exercises

1. This exercise seeks to illustrate why minimization of the performance measure

$$\||W_1S| + |W_2T|\|_\infty \tag{12.14}$$

is harder than minimization of

$$\||W_1S|^2 + |W_2T|^2\|_\infty. \tag{12.15}$$

Consider the space $\mathbb{R}^2$ of 2-vectors $x = (x_1, x_2)$. There are many possible norms on this space; let us focus on

$$\|x\|_1 := |x_1| + |x_2| \text{ and } \|x\|_2 := (|x_1|^2 + |x_2|^2)^{1/2},$$

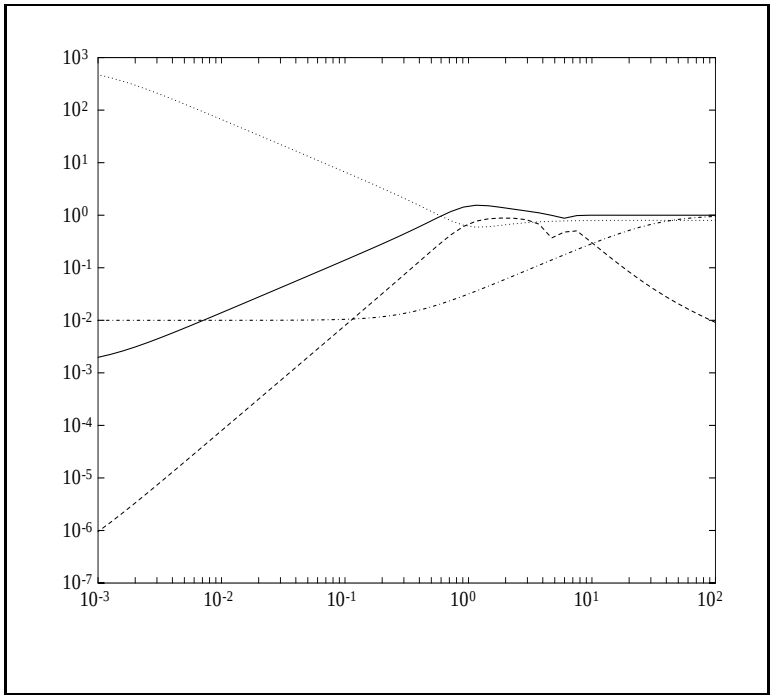

Figure 12.2: Bode plot of $|S|$ (solid), $|CS|$ (dash), $|W_1|$ (dot), and $|W_3|$ (dot-dash).

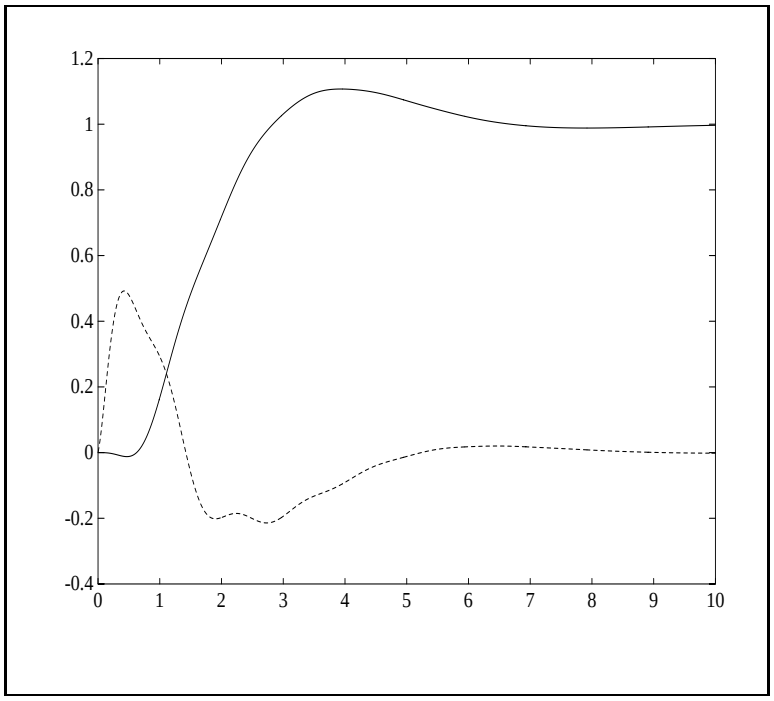

Figure 12.3: Step response of y (solid) and u (dash).

which are analogous to (12.14) and (12.15), respectively. Note that $\| \ \|_2$ is the usual Euclidean norm. Sketch the two unit balls,

$$\{x : \|x\|_1 \leq 1\}, \quad \{x : \|x\|_2 \leq 1\}.$$

To illustrate that $\| \ \|_1$ is harder to work with than $\| \ \|_2$, we will look at an approximation problem. Let $\mathcal{M}$ denote the subspace spanned by $(1, 2)$, that is, the straight line through this point and the origin. For $x = (4, 1)$, compute the vector y in $\mathcal{M}$ which is closest to x in that it minimizes $\|x - y\|_2$. Note that y equals the orthogonal projection of x onto $\mathcal{M}$. Now compute y to minimize $\|x - y\|_1$. Observe that y and $x - y$ are not orthogonal.

2. Prove directly that a necessary condition for solvability of the modified robust performance problem is

$$\left\| \frac{|W_1 W_2|^2}{|W_1|^2 + |W_2|^2} \right\|_\infty < \frac{1}{2}.$$

3. Show that

$$\| |W_1 S| + |W_2 T| \|_\infty < 1 \ \Rightarrow \| |W_1 S|^2 + |W_2 T|^2 \|_\infty < 1.$$

4. Consider the example in Section 12.3. Let $a_{\sup}$ denote the supremum value of a for which the robust performance problem is solvable. It was shown that the value $a = 39$ is feasible for the modified robust performance problem, and hence $a_{\sup} \geq 39$. Using Exercise 3, find an upper bound for $a_{\sup}$.

5. Do a loopshape design for the example in Section 12.3, trying to make a as large as possible.

Notes and References

This chapter is based on Doyle (1983) and Francis (1983). In the literature the problem of minimizing

$$\| |W_1 S|^2 + |W_2 T|^2 \|_\infty$$

over all internally stabilizing controllers is called the *mixed sensitivity problem*. It was solved (for the more general case of multivariable plants) by Kwakernaak (1985) and Verma and Jonckheere (1984). The mixed sensitivity problem is a special case of a more general ∞-norm optimization problem that is treated in Doyle (1984), Francis (1987), and Foias and Tannenbaum (1988).

References

Aubrun, J.N., K.R. Lorell, T.S. Mast, and J.E. Nelson (1987). "Dynamic analysis of the actively controlled segmented mirror of the W.M. Keck ten-meter telescope," *IEEE Control Syst. Mag.*, vol. 7, no. 6, pp. 3-10.

Aubrun, J.N., K.R. Lorell, T.W. Havas, and W.C. Henninger (1988). "Performance analysis of the segmented alignment control system for the ten-meter telescope," *Automatica*, vol. 24, pp. 437-454.

Bensoussan, D. (1984). "Sensitivity reduction in single-input single-output systems," *Int. J. Control*, vol. 39, pp. 321-335.

Bode, H.W. (1945). *Network Analysis and Feedback Amplifier Design*, D. Van Nostrand, Princeton, N.J.

Bower, J.L. and P. Schultheiss (1961). *Introduction to the Design of Servomechanisms*, Wiley, New York.

Boyd, S.P., V. Balakrishnan, C.H. Barratt, N.M. Khraishi, X. Li, D.G. Meyer, and S.A. Norman (1988). "A new CAD method and associated architectures for linear controllers," *IEEE Trans. Auto. Control*, vol. AC-33, pp. 268-283.

Boyd, S.P., V. Balakrishnan, and P. Kabamba (1989). "A bisection method for computing the $\mathbf{H}_\infty$ norm of a transfer matrix and related problems," *Math. Control Signals Syst.*, vol. 2, pp. 207-219.

Chen, M.J. and C.A. Desoer (1982). "Necessary and sufficient condition for robust stability of linear distributed feedback systems," *Int. J. Control*, vol. 35, pp. 255-267.

Desoer, C.A. and C.L. Gustafson (1984). "Algebraic theory of linear multivariable systems," *IEEE Trans. Auto. Control*, vol. AC-29, pp. 909-917.

Desoer, C.A. and M. Vidyasagar (1975). *Feedback Systems: Input-Output Properties*, Academic Press, New York.

Desoer, C.A., R.W. Liu, J. Murray, and R. Saeks (1980). "Feedback system design: the fractional representation approach to analysis and synthesis," *IEEE Trans. Auto. Control*, vol. AC-25, pp. 399-412.

Doyle, J.C. (1983). "Synthesis of robust controllers and filters," *Proc. 22nd IEEE. Conf. Decision and Control.*

Doyle, J.C. (1984). *Lecture Notes in Advances in Multivariable Control*, ONR/Honeywell Workshop, Minneapolis, Minn.

Doyle, J.C. and G. Stein (1981). "Multivariable feedback design: concepts for a classical modern synthesis," *IEEE Trans. Auto. Control*, vol. AC-26, pp. 4-16.

Enns, D. (1986). *Limitations to the Control of the X-29*, Technical Report, Honeywell Systems and Research Center, Minneapolis, Minn.

Foias, C. and A. Tannenbaum (1988). "On the four block problem, II: the singular system," *Integral Equations and Operator Theory*, vol. 11, pp. 726-767.

Francis, B.A. (1983). *Notes on $\mathcal{H}_\infty$-Optimal Linear Feedback Systems*, Lectures given at Linkoping University.

Francis, B.A. (1987). *A Course in $\mathcal{H}_\infty$ Control Theory*, vol. 88 in Lecture Notes in Control and Information Sciences, Springer-Verlag, New York.

Francis, B.A. and M. Vidyasagar (1983). "Algebraic and topological aspects of the regulator problem for lumped linear systems," *Automatica*, vol. 19, pp. 87-90.

Francis, B.A. and G. Zames (1984). "On $\mathcal{H}^\infty$-optimal sensitivity theory for siso feedback systems," *IEEE Trans. Auto. Control*, vol. AC-29, pp. 9-16.

Franklin, G.F., J.D. Powell, and A. Emami-Naeini (1986). *Feedback Control of Dynamic Systems*, Addison-Wesley, Reading, Mass.

Freudenberg, J.S. and D.P. Looze (1985). "Right half-plane poles and zeros and design trade-offs in feedback systems," *IEEE Trans. Auto. Control*, vol. AC-30, pp. 555-565.

Freudenberg, J.S. and D.P. Looze (1988). *Frequency Domain Properties of Scalar and Mulivariable Feedback Systems*, vol. 104 in Lecture Notes in Control and Information Sciences, Springer-Verlag, New York.

Garnett, J.B. (1981). *Bounded Analytic Functions*, Academic Press, New York.

Holtzman, J.M. (1970). *Nonlinear System Theory*, Prentice-Hall, Englewood Cliffs, N.J .

Horowitz, I.M. (1963). *Synthesis of Feedback Systems*, Academic Press, New York.

Joshi, S.M. (1989). *Control of Large Flexible Space Structures*, vol. 131 in Lecture Notes in Control and Information Sciences, Springer-Verlag, New York.

Khargonekar, P. and E. Sontag (1982). "On the relation between stable matrix fraction factorizations and regulable realizations of linear systems over rings," *IEEE Trans. Auto. Control*, vol. AC-27, pp. 627-638.

Khargonekar, P. and A. Tannenbaum (1985). "Noneuclidean metrics and the robust stabilization of systems with parameter uncertainty," *IEEE Trans. Auto. Control*, vol. AC-30, pp. 1005-1013.

Kimura, H. (1984). "Robust stabilization for a class of transfer functions," *IEEE Trans. Auto. Control*, vol. AC-29, pp. 788-793.

Kucera, V. (1979). *Discrete Linear Control: The Polynomial Equation Approach*, Wiley, New York.

Kwakernaak, H. (1985). "Minimax frequency domain performance and robustness optimization of linear feedback systems," *IEEE Trans. Auto. Control*, vol. AC-30, pp. 994-1004.

Lenz, K.E., P.P. Khargonekar, and J.C. Doyle (1988). "When is a controller H^∞-optimal," *Math. Control Signals Syst.*, vol. 1, pp. 107-122.

McFarlane, D.C. and K. Glover (1990). *Robust Controller Design Using Normalized Coprime Factor Plant Descriptions*, vol. 138 in Lecture Notes in Control and Information Sciences, Springer-Verlag, New York.

Mees, A.I. (1981). *Dynamics of Feedback Systems*, Wiley, New York.

Morari, M. and E. Zafiriou (1989). *Robust Process Control*, Prentice-Hall, Englewood Cliffs, N.J.

Nett, C.N., C.A. Jacobson, and M.J. Balas (1984). "A connection between state-space and doubly coprime fractional representations," *IEEE Trans. Auto. Control*, vol. AC-29, pp. 831-832.

Newton, G.C., L.A. Gould, and J.F. Kaiser (1957). *Analytic Design of Linear Feedback Controls*, Wiley, New York.

Raggazini, J.R. and G.F. Franklin (1958). *Sampled-Data Control Systems*, McGraw-Hill, New York.

Saeks, R. and J. Murray (1982)."Fractional representation, algebraic geometry, and the simultaneous stabilization problem," *IEEE Trans. Auto. Control*, vol. AC-27, pp. 895-903.

Sarason, D. (1967). "Generalized interpolation in H^∞," *Trans. AMS*, vol. 127, pp. 179-203.

Silverman, L. and M. Bettayeb (1980). "Optimal approximation of linear systems," *Proc. JACC.*

Tannenbaum, A. (1980). "Feedback stabilization of linear dynamical plants with uncertainty in the gain factor," *Int. J. Control*, vol. 32, pp. 1-16.

Tannenbaum, A. (1981). *Invariance and System Theory: Algebraic and Geometric Aspects*, vol. 845 in Lecture Notes in Mathematics, Springer-Verlag, Berlin.

Verma, M. and E. Jonckheere (1984). "$\mathcal{L}^\infty$-compensation with mixed sensitivity as a broadband matching problem," *Syst. Control Lett.*, vol. 4, pp. 125-129.

Vidyasagar, M. (1972). "Input-output stability of a broad class of linear time-invariant multivariable systems," *SIAM J. Control*, vol. 10, pp. 203-209.

Vidyasagar, M. (1985). *Control System Synthesis: A Factorization Approach*, MIT Press, Cambridge, Mass.

Walsh, J.L. (1969). *Interpolation and Approximation by Rational Functions in the Complex Domain*, 5th ed., American Mathematical Society, Providence, R.I.

Willems, J.C. (1971). *The Analysis of Feedback Systems*, MIT Press, Cambridge, Mass.

Yan, W. and B.D.O. Anderson (1990). "The simultaneous optimization problem for sensitivity and gain margin," *IEEE Trans. Auto. Control*, vol. AC-35, pp. 558-563.

Youla, D.C., J.J. Bongiorno, Jr., and C.N. Lu (1974). "Single-loop feedback stabilization of linear multivariable dynamical plants," *Automatica*, vol. 10, pp. 159-173.

Youla, D.C., H.A. Jabr, and J.J. Bongiorno, Jr., (1976). "Modern Wiener-Hopf design of optimal controllers, part II: the multivariable case," *IEEE Trans. Auto. Control*, vol. AC-21, pp. 319-338.

Youla, D.C. and M. Saito, (1967). "Interpolation with positive-real functions," *J. Franklin Inst.*, vol. 284, no. 2, pp. 77-108.

Zames, G. (1981). "Feedback and optimal sensitivity: model reference transformations, multiplicative seminorms, and approximate inverses," *IEEE Trans. Auto. Control*, vol. AC-26, pp. 301-320.

Zames, G. and B.A. Francis (1983). "Feedback, minimax sensitivity, and optimal robustness," *IEEE Trans. Auto. Control*, vol. AC-28, pp. 585-601.

Index

1-norm, 13
2-norm, 13, 16
2-norm minimization, 183
affine function, 66
algebraic constraints, 89
allowable perturbation, 46
all-pass function, 92
analytic constraints, 90
area formula, 98
asymptotic tracking, 38
autocorrelation function, 19
average power, 14

biproper, 16

Cauchy's integral formula, 90
Cauchy's theorem, 90
characteristic polynomial, 36
closed-loop poles, 36
collocated, 126
command response, 57
complementary sensitivity function, 42
computing the 2-norm, 17, 25
computing the ∞-norm, 17, 27
conformal mapping, 193
conformally equivalent, 193
conservativeness, 49
controller parametrization, 73
coprime factorization, 68
coprime functions, 68
cross-correlation function, 20
cross-power spectral density function, 20

dissipative system, 158

energy, 14
energy spectral density, 41
Euclid's algorithm, 69
exogenous input, 31

final-value theorem, 39
flexible beam, 178, 214
frequency-response experiment, 46

gain margin, 51
gain margin optimization, 195

Hermitian matrix, 157

∞-norm, 14, 16
instantaneous power, 14
internal model control, 88
internal stability, 35
interpolation constraints, 90

loop transfer function, 39
loopshaping, 105

M 0
maximum modulus theorem, 90
maximum stability margin, 189
minimum variance control, 187
minimum-phase function, 93
mixed sensitivity problem, 218
model matching, 155
model-matching error, 155
modified robust performance problem, 206
multiplicative perturbation, 46

Nevanlinna-Pick problem, 156
Nevanlinna's algorithm, 160
nominal performance, 54
noncollocated, 126
norm, 13
Nyquist criterion, 38
Nyquist plot, 38

optimal Q, 155
optimal robust stability, 189

Pareto optimal, 144
phase formula, 109
phase margin, 51

phase margin optimization, 200
Pick matrix, 157
Pick's theorem, 157
Poisson integral formula, 91
positive definite, 157
positive semidefinite, 157
potentially optimal, 144
potentially uniquely optimal, 144
power signal, 14
power spectral density, 20
proper, 16
Pythagoras's theorem, 184

ramp input, 39
relative degree, 98
Riemann mapping theorem, 193
robust controller, 50
robust performance, 54
robust stability, 50
robust stability problem, 189

self-optimal, 145
sensitivity function, 39-40
small-gain theorem, 53
spectral factor, 207
spectral factorization, 207
squareroot of a matrix, 165
stability margin, 50
stable, 16, 25
step input, 39
strictly proper, 16
strong stabilization, 78
strongly Pareto optimal, 144
structured uncertainty, 45
submultiplicative, 16
system gain, 18

total energy, 14
two-degree-of-freedom controller, 57

uniquely optimal, 144
uniquely self-optimal, 145
unity-feedback, 38
unstructured uncertainty, 45

waterbed effect, 96
weighted sensitivity problem, 187
well-posedness, 33